A Transcriptome-Level Comparison of Independently Evolved Non-Embryonic Development in Different Species of Styelidae (Tunicata)

Vitória Tobias Santos

Sorbonne Université

École Doctorale Complexité du Vivant – ED 515

Laboratoire De Biologie du Développent de Villefranche sur Mer

Regeneration Team

A Transcriptome-Level Comparison of Independently Evolved Non-Embryonic Development in Different Species of *Styelidae* (Tunicata)

Par Vitória Tobias-Santos

Thèse de doctorat en Biologie du Développement

Sous la direction du Dr. Stefano Tiozzo
Et codirection du Dr. Alexandre Alié

Présentée et soutenue publiquement le 29 Septembre 2023

Au Laboratoire de Biologie du Développement de Villefranche-sur-Mer

Devant un jury composé de :

Tiozzo, Stefano	Directeur de Recherche	Directeur de Thèse
Alié, Alexandre	Chargé de Recherche	Co-Encadrant
Furla, Paola	Professeur	Rapporteur
Brown, Federico	Professeur	Rapporteur
Ramaekers, Ariane	Maître de conférences	Rep. de l'Établissement
Sinigaglia, Chiara	Directeur de Recherche	Examinatrice
Röttinger, Eric	Directeur de Recherche	Examinateur
Amiel, Aldine	Ingénieur de Recherche	Examinatrice

”A espantosa realidade das coisas
É a minha descoberta de todos os dias.
Cada coisa é o que é,
E é difícil explicar a alguém quanto isso me alegra,
E quanto isso me basta.”

“The amazing reality of things
Is my discovery every single day.
Every single thing is what it is,
And it is difficult to explain to anyone how much it delights me,
And how much this is enough for me.”

Alberto Caeiro (Fernando Pessoa)

A espantosa realidade das coisas
The Amazing Reality of Things

Acknowledgements

I would like to start by thanking Stefano Tiozzo and Alexandre Alié for the opportunity to join this project and for their mentoring.

I want to thank my partner Roland Zimm for the companionship and all the support that helped me stay strong, inspiring me and constantly reminding me why we fell in love with science in the first place.

I am thankful for my parents, who are the primary influencers of my passion for nature. My mother taught me that girls can have all: muddy hiking boots, hands dirty of paint, a lab coat, knowing how to fix things, and being stylish. With my father, I learned that I could go anywhere and that life is too short not to try what you want.

I also want to mention my brothers and cousin, who, thanks to technology, were always present, helping me deal with the "saudade" I feel for them and making me laugh to tears.

I thank my aunts and grandma for being such an inspiration of faith, perseverance, and hardworking.

My friends Nivia, Lupis, and Rodrigo (who supplied me daily with memes) as much as the "família NUPEM-UFRJ", where I always feel at home. Here in France, I could count on the Italian trio: Alexia, Chiara, and Francesca (and the newly added Marta).

I want to thank the Regeneration Team for the friendship, help, and fruitful discussions. Thanks to Sonia, Tiphaine and especially Marie. The "Jean Maetz crew", who were my best company during the second wave of COVID and during lunchtime, especially Claire, Yas, and Catriona. Julie and Abdiel for taking me out of work for hiking and boardgames. The guys of "mezza" for the "apéros", pétanque and all bioinformatic help. The LBDV team for being so friendly and helpful, I felt very welcome. To "LauLau" and Dany for keeping my animals always in the best shape!

Lastly, thank the thesis committee and the defense jury for accepting to join and providing helpful and prolific discussions to assist me in getting the best out of this project.

Abstract

Most living animals reproduce sexually and develop from a fertilized egg, a strategy that is considered evolutionarily advantageous. However, nearly half of all animal phyla also contain species that can propagate asexually through different cloning modes such as budding, fission, or whole-body regeneration. During these processes, an adult is formed without passing through embryonic stages and are therefore referred to as "nonembryonic development" (NED). Most species of tunicates, a sister group of vertebrates, are able to reproduce asexually via various forms of NED. A recent phylogeny of the family *Styelidae* revealed two independent acquisitions of NED. *Botryllus schlosseri* and *Polyandrocarpa zorritensis* are two species that represent each of these of NED acquisitions. The former is an established laboratory model, well-studied by several groups worldwide, whereas *P. zorritensis* is a newly introduced model in our laboratory.

As I have studied both developmental and ecological aspects of asexual reproduction in *P. zorritensis*, this thesis is divided into two main projects. *P. zorritensis* is an invasive species in the Mediterranean and has colonized coastal sites that receive an influx of freshwater (i.e., harbors). Its success in colonizing these sites suggests that the animals are exposed to suitable conditions to undergo both asexual (NED) and sexual reproduction. In the first part of this manuscript, I tested the effect of different salinities on the reproductive efficiency of *P. zorritensis*. My study found that *P. zorritensis* colonies grown at lower salinities of 29 or 36 ppt showed higher rates of asexual reproduction compared to those grown at 40 ppt salinity. However, sexual reproduction did not appear to follow the same trend, with higher numbers of larvae actually observed at higher salinities. This suggests that *P. zorritensis* may have limited invasiveness in high salinity Mediterranean areas, explaining its abundance in coastal areas with significant freshwater inflow.

In the second part of my thesis, I describe and discuss an RNA-seq-based transcriptomic study of different bud stages in *B. schlosseri* and *P. zorritensis*, with comparisons to other *Styleidae*. Our preliminary results have shown that homologous genes are expressed at the onset of these convergently acquired buds. It was, therefore of particular interest to perform a large-scale comparison of gene expression in budding tissues between these two species in order to discover common genes or gene networks that are repeatedly co-opted during the

acquisition of asexual reproduction and to highlight particular genetic signatures associated with the different budding modes.

With these aims in mind, I performed a detailed differential gene expression analysis across seven developmental stages during NED in *P. zorritensis*. I found that most changes at the transcriptome level preceded changes at the morphological level, with a significant overlap in gene expression dynamics throughout all stages after the onset of epithelial swelling. The differentially expressed genes included a large set of genes that are also known to be involved in key processes of embryonic development. These results are consistent with current knowledge of histology, cell proliferation dynamics (based on publicly available data), and spatio-temporal dynamics of selected genes according to whole-mount *in situ* hybridization analysis, which I complemented with two key genes involved in bud morphogenesis. Comparison of the transcriptomic profiles with *B. schlosseri* and other *Styelidae* revealed a substantial overlap of important developmental pathways. As these data cover different types of NED, my results provide evidence for the driving hypothesis that the emergence of NED relies on homologous genetic modules that are repeatedly co-opted and rewired in different species, regardless of the nature of the budding cells and tissues.

Index

Abbreviations

AGM: aorta–gonad–mesonephros.

BN: budding nest.

CNS: central nervous system.

Ctrl: control sample

DNTA: *de novo* transcriptome assembly.

DV: double vesicle.

ECM: extra-cellular matrix.

EI: early invagination.

Fus: fusion.

GBTM: genome-based transcriptome mapping.

GRN: gene regulatory network.

***In situ* HCR:** *in situ* hybridization chain reaction.

LI: late invagination.

NED: non-embryonic development.

ONT: Oxford Nanopore Technologies.

PB: peribranchial budding.

PCA: principal component analysis.

ppt: parts per thousand.

PSw: pre-swelling.

RBH: Reciprocal BLAST best hit.

Sw: swelling.

TF: transcription factor.

VB: vascular budding.

Chapter 1 - Introduction

1.a) Sexual and Asexual Reproduction in Metazoans

Sexual Reproduction

Naturalists have analyzed the adaptive significance of sexual and asexual reproduction for a considerable time, ever since the theory of natural selection was proposed. Sexual reproduction entails genetic mixing, which in metazoans mainly happens through the union of gametes from a male and female origin, producing offspring with chromosomes from both parents (Lloyd 1980; Subramoniam 2018; Otto and Lenormand 2002; Shackelford and Weekes-Shackelford 2021). While asexual reproduction carries many advantages, sexual reproduction is still dominant. Crow (1994) proposes two main hypotheses to understand why sexual reproduction evolves. The first and oldest hypothesis suggests that sexual reproduction facilitates the production of recombinant types, which help the population adjust better to environmental changes. According to the second hypothesis, species that undergo recombination can cluster harmful mutations together and eliminate them in a single "genetic death". In contrast, asexual species can only eliminate deleterious mutations within the same genotype. Therefore, if there is a rate of one or more deleterious mutations per zygote, the species must possess an efficient mechanism to remove them.

Upon considering the costs associated with sexual reproduction, it becomes evident that there are several drawback (Lloyd 1980). Although Weisman argued that sex is a crucial element for evolution (as it provides genetic diversity that is essential for natural selection), he also acknowledged that sex is a disadvantage due to reduced reproductive rates and the need for specialized anatomical characteristics (Weismann 1889; 1892). Asexual reproduction is more efficient than sexual reproduction since the latter involves energy and resource expenditure in meiosis and syngamy processes. Additionally, the existence of separate sexes creates an additional cost for the male population, and sexual selection can result in maladapted traits and disruptive competition (Charlesworth 1980; Crow 1994). Finding a reproductive mate could be a disadvantage for sexual species living in sparsely populated or new areas (Song, Scheu, and Drossel 2011). Moreover, sexual species are more vulnerable to sexually transmitted diseases and harmful transposons (Bast et al. 2019; Dechaud et al. 2019). Finally, sexual species have a reduced capacity for short-term selection and cannot colonize

microhabitats that could be quickly inundated by hybridization or trapped in a local adaptive peak (Charlesworth 1980; Crow 1994; Engelstädter 2008).

Asexual Reproduction

Asexual reproduction is a type of reproduction that does not involve the fusion of gametes (Boyden 1954). This process is also known as clonal (De Meeûs, Prugnolle, and Agnew 2007). Asexual reproduction can be classified as gametic and agametic (Hughes 1987). Gametic asexual reproduction is commonly referred to as parthenogenesis and is generally defined by the development of a new organism from an unfertilized gamete(De Meeûs, Prugnolle, and Agnew 2007). Agametic reproduction involves the development of new individuals from somatic cells instead of gametes (Sibly and Calow 1982). At least two-thirds of metazoan phyla contain species that regularly undergo some form of agametic asexual propagation (figure 1.1), where a genotype produces an identifiable individual unit that is an exact genetic copy, making cloning a diverse and not uncommon process, as well as being well documented in soft-bodied invertebrates (Grosberg 1992; Subramoniam 2018; Hiebert, Simpson, and Tiozzo 2021).

Some annelids, as described by Giese (Giese, Pearse, and Pearse 1974), freely release clones originating from detached pieces of the parental animal body during asexual reproduction. This process is also known as self-division or propagation (Thomas Hunt Morgan 1901). External forces causing pieces to generate new clones result in the propagation phenomenon known as fragmentation. On the other hand, endogenous processes result in the propagation phenomenon known as fission (Hughes 1989; Brockes and Kumar 2008). The asexual process of a small area of the parental body sprouting and increasing in size to form a new clone is known as budding (Hughes 1989). New clones produce can be detached or stay physically connected to the parent, and their body axis is often oriented differently (Otto and Campbell 1977). In some species, clones are physically connected to the parent, exchanging metabolites and chemical signals, thus forming colonies (Mackie 1986; Hughes 1989). When physical or physiological contact ceases despite spatial proximity, it is termed as clonal aggregates (Hiebert, Simpson, and Tiozzo 2021). Throughout this thesis, agametic reproduction will be referred to as “asexual reproduction”.

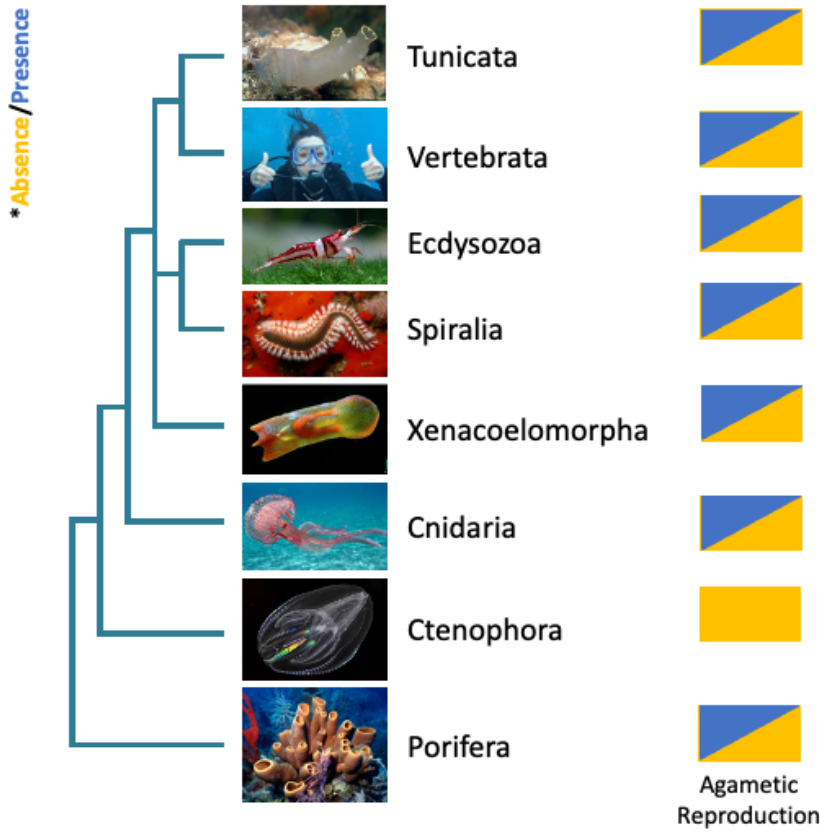

Figure 1.1: *Simplified phylogeny to illustrate the distribution of asexual reproduction (agametic reproduction) in Metazoans.*

1.b) Regeneration

Restoring lost or injured body parts is possible through regeneration, which starts from pre-existing cells or tissues. The regeneration process can be classified into different modes based on the stimuli that trigger it, the structure that can be regenerated, or the mechanisms employed in response to damage (Carlson 2011). Physiological regeneration is the natural cell turnover process that replaces worn-out or extruded body parts. This can include the regeneration of epithelial cells, erythropoiesis, as well as seasonal regrowth of structures like feathers in birds and antlers in cervids (Alvarado 2000; Price and Allen 2004; Tanaka and Reddien 2011; Chuong et al. 2012; Barker 2014) (figure 1.2). Additionally, reparative or post-traumatic regeneration occurs when tissues rebuild after being removed by self-induced amputation or external injury (Morgan 1901; Poss 2010; Kostyuchenko, Kozin, and Kupriashova 2016).

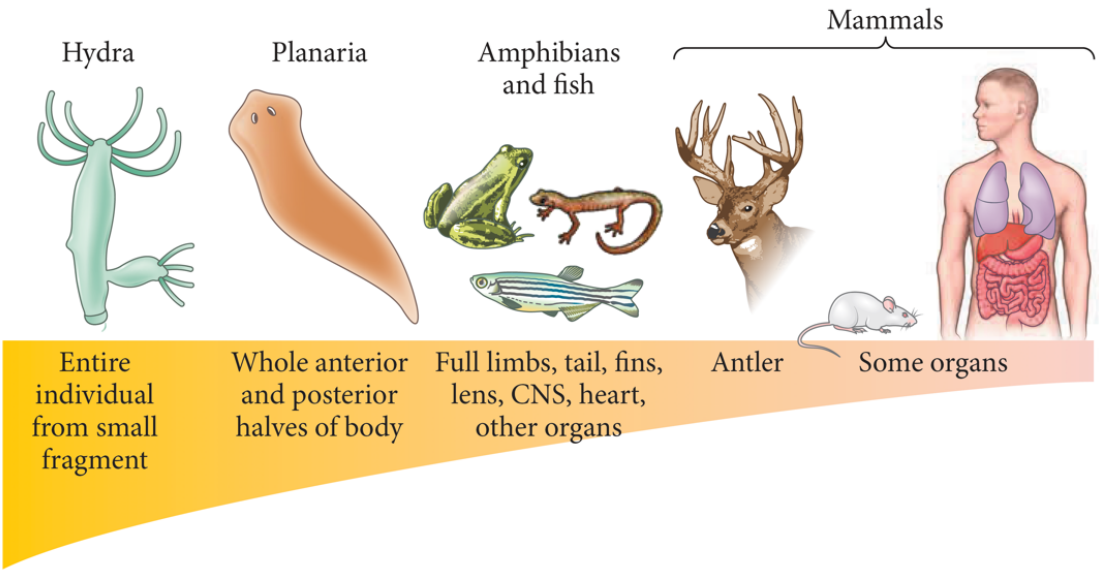

Figure 1.2: *Representative organisms and their comparative regenerative capabilities (modified from Gilbert and Barresi 2016).*

There are different levels of biological organization where regeneration can occur (Bely and Nyberg 2010; Slack 2017). These can include the cellular level, such as nerve axons (Huebner and Strittmatter 2009), the tissue level, such as the epidermis (Odland and Ross 1968), the organ level, such as the heart (Laflamme and Murry 2011), or the structural level, such as a limb (Bryant, Endo, and Gardiner 2004; Kragl et al. 2009). Sometimes, it is possible

to rebuild the entire body, starting from just a few cells or tiny fragments. This is known as whole-body regeneration (WBR), which is observed in planarians (Alvarado 2003; Gehrke and Srivastava 2016) (figure 1.3).

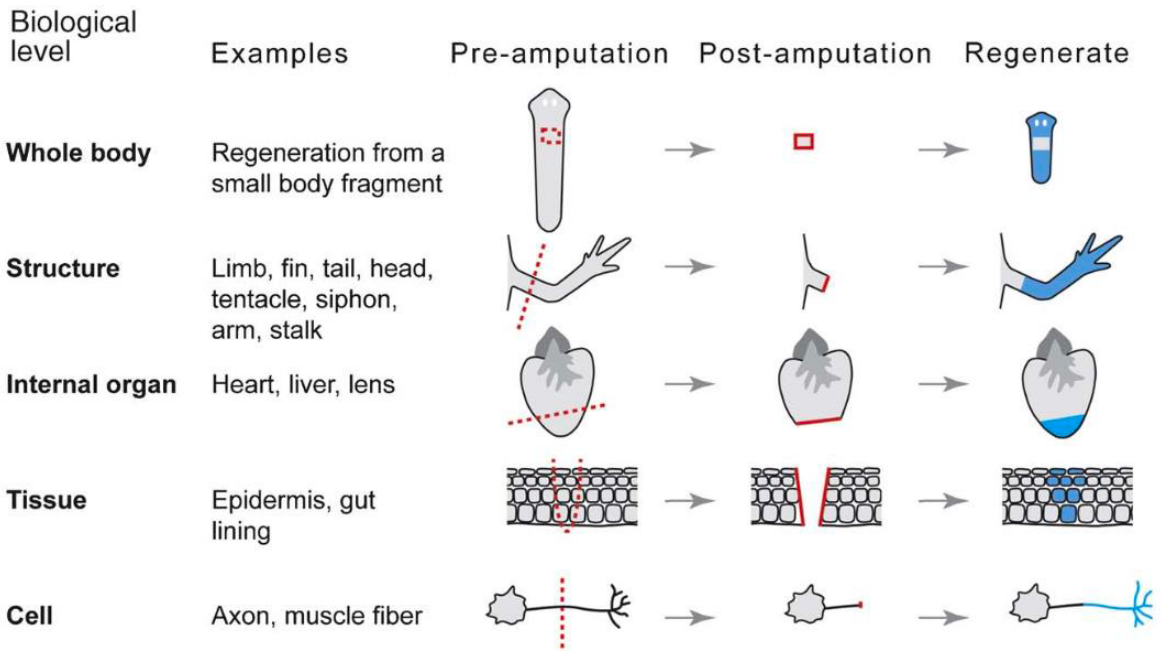

Figure 1.3: *Regeneration at different levels of biological organization. It remains unclear which aspects of regeneration are homologous across successive levels. Colony-level 'regeneration', as seen in colonial animals such as corals and ascidians, occurs through asexual reproduction rather than through the regeneration of individuals and thus is not included here. Dashed red lines indicate amputation planes; solid red lines indicate wound surfaces; blue fill indicates regenerated body parts (modified from Bely and Nyberg, 2010).*

According to Morgan (Thomas Hunt Morgan 1901), regenerative mechanisms are categorized into two groups based on cellular events that happen after an injury. He came up with the terms epimorphosis and morphallaxis. Epimorphic regeneration involves forming a structure called blastema at the injury site. The blastema comprises undifferentiated or dedifferentiated cells that migrate to the wound and grow. One example of epimorphosis is the amphibian limb regeneration (Suzuki et al. 2006) (figure 1.4.A). On the other hand, during morphallaxis, a blastema is not formed, and existing cells remodel to regenerate. An example of morphallaxis is Hydra head regeneration (Bosch 2007) (figure 1.4.B).

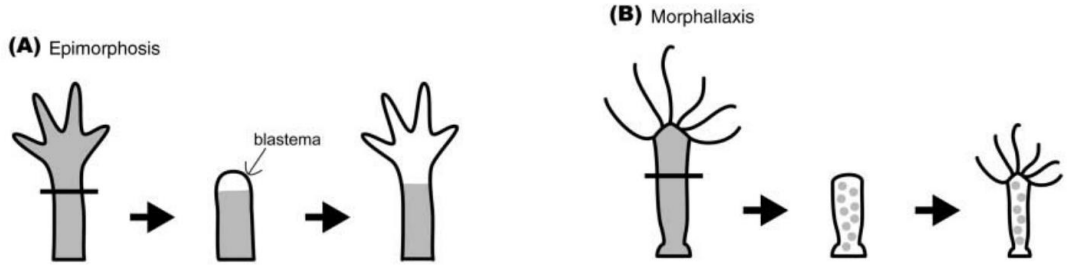

Figure 1.4: *Two examples of epimorphic and morphallactic regeneration.* ***A)*** *Limb regeneration in amphibians is a representative example of epimorphosis. In this type of regeneration, a mass of undifferentiated cells referred to as the 'blastema' is initially formed after wound healing and then blastema cells actively proliferate to restore the lost part of the amputated organ;* ***B)*** *Hydra regeneration is categorized as morphallaxis. A blastema is not formed. Direct rearrangement of pre-existing cells in the stump contributes to regeneration (modified from Agata, Saito, and Nakajima 2007).*

The distinction between the two mechanisms of regeneration, epimorphosis, and morphallaxis, is not always clear and can sometimes overlap (Agata, Saito, and Nakajima 2007; Tiozzo and Copley 2015; Pellettieri 2019). An example is the annelid *Sabella* sp., where isolated abdominal fragments can regenerate both the anterior and posterior ends (Berrill 1931; Carlson 2011). Head regeneration occurs through epimorphosis with blastema formation, while the abdominal fragments near the future head are remodeled through morphallaxis, resulting in the formation of thoracic segments (Hill 1970). The organism Hydra is often cited as an instance of morphallactic regeneration, wherein the skin cells of the parent organism are utilized and rearranged to create new tissues without the need for blastema formation. Despite the absence of blastema formation, cell division occurs during all the stages of tissue remodeling, and multipotent interstitial cells move toward the area of regeneration to aid the morphogenesis (Cummings and Bode 1984; Buzgariu et al. 2018).

The regeneration process can be broken down into several chronological steps, including wound healing, mobilization of cell precursors, and morphogenesis (Tiozzo and Copley 2015). Wound healing involves re-epithelialization, which restores damaged epithelium after an injury (Carlson 2011). This process is necessary to maintain tissue homeostasis, prevent infection and water loss, and is commonly found in various species, including mammals with limited regenerative abilities (Borena et al. 2015). In some species, wound healing is necessary to start the regenerative process. For instance, in amphibians, during limb or tail regeneration, wound healing is responsible for organizing blastema correctly (Murawala, Tanaka, and Currie 2012). Re-epithelialization features are similar in species that can regenerate and those that cannot. However, the outcome in the former

results in functional tissue, while the latter results in a scar (Bielefeld, Amini-Nik, and Alman 2013). Although wound healing and scar formation are believed to affect an animal's regenerative ability, how it happens is still unclear (Carlson 2011). Different organisms activate different cellular sources for the restoration of lost structures. According to Carlson (2011), there are three main cellular origins: dedifferentiation of mature cells in the remaining tissue, proliferation of remaining cells without dedifferentiation, and proliferation of stem cells. These progenitor cells may already exist in the damaged tissues or migrate from other sites. Multiple mechanisms can coexist in some cases, as seen during heart regeneration in zebrafish (Jopling et al. 2010; Jopling, Boue, and Belmonte 2011). After a loss, a morphogenetic event triggers the regeneration of the lost part. This process creates a new structure that is functionally identical or similar to the original one. During regeneration, developmental signals like *Wnt*, *BMP*, and *Nodal* can be utilized in various organisms, including cnidarians, planarians, and mammals (Holstein, Hobmayer, and Technau 2003; Adell, Cebrià, and Saló 2010; Clevers, Loh, and Nusse 2014).

Regeneration is a common process among metazoans but is not evenly distributed. Even within the same clade, some species can regenerate extensive body parts while others have limited regenerative abilities. Moreover, the potential for regeneration can vary based on intrinsic factors like age or size, as well as external cues like temperature or food availability (Morgan 1901; Henry and Hart 2005) (figure 1.5). The idea of regeneration as an evolutionary trait dates back to the 1890s when biologists August Weismann and Thomas Hunt Morgan debated its origins. Weismann believed it evolved as an adaptation to injuries, while Morgan argued it was a byproduct of development not necessarily linked to injuries (Weismann 1892; Morgan 1898; Esposito 2013). The concept of regeneration and its origins have been extensively studied. It has been found that certain characteristics may develop separately in different lineages. Regeneration is a complex trait that involves various cellular and molecular mechanisms, and despite its complexity, it is often simplified as a single trait and included in phylogenetic trees (Goss 1992; Tiozzo and Copley 2015). Mapping out the various regeneration mechanisms, such as identifying the cellular origin of the regenerating part and understanding the molecular mechanisms driving its development, proves to be a more complicated task. Additionally, incorporating "regeneration" into a phylogenetic tree presents broader challenges related to evolutionary biology, such as defining homology.

Nevertheless, plotting in the tree the diverse mechanisms of regeneration - like the cellular origin of the regenerating part or the molecular mechanisms driving the development - represents a more complex task. Additionally, incorporating "regeneration" into a phylogenetic tree presents broader obstacles connected to evolutionary biology, such as defining homology (Bely and Nyberg 2010).

Asexual reproduction and regeneration are closely related. Generally, species capable of asexual reproduction also have a high potential for regeneration (Alvarado 2000; Martinez, Menger, and Zoran 2005). Various forms of propagation, such as fission, strobilation, and fragmentation, can be viewed as instances of whole-body regeneration (WBR). For example, in annelids, segmentation is classified as a type of asexual reproduction since new clones are generated. However, when a separated segment regenerates its entire body, this process is called WBR (Berrill 1951). A proposed way to differentiate between WBR and asexual reproduction is by examining whether external stimuli or injury triggered the process (Alvarado 2000). In this view, the cause of fragmentation is the key factor: if it is part of the organism's life cycle, it is considered propagation/reproduction. However, if an external event causes the fragment, it is classified as WBR. Both processes result in the creation of functional clones, and they may still share certain molecular mechanisms (Martinez, Menger, and Zoran 2005). Whole-body regeneration and asexual reproduction are both forms of post-embryonic development, which means that the entire body is formed anew without the involvement of a zygote (Kostyuchenko, Kozin, and Kupriashova 2016). To highlight the mechanistic aspects of this development and its lack of a zygotic origin, the term Non-Embryonic Development (NED) has been suggested as a unifying factor for these two processes (Alié et al. 2018).

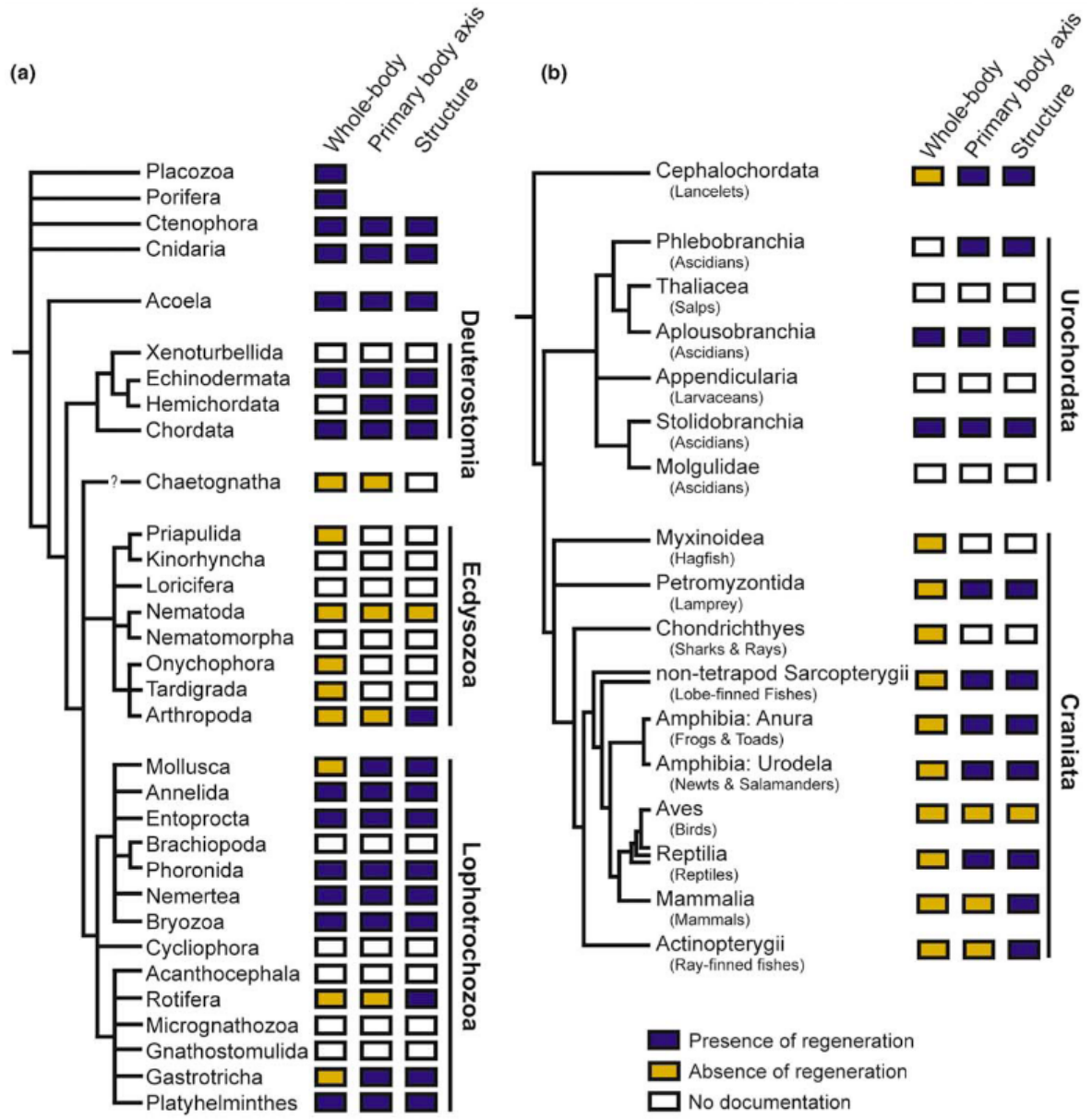

Figure 1.5: *Phylogenetic distribution of regeneration across (**A**) the Metazoa and (**B**) the Chordata. 'Presence of regeneration' indicates that at least one well-substantiated report exists for regeneration in that taxon and does not imply that all species in that taxon can regenerate. 'Absence of regeneration' indicates at least one well-substantiated report for the lack of regeneration in that taxon (and none indicating the presence of regeneration). We define 'whole-body regeneration' as the potential to regenerate every part of the body (although not necessarily simultaneously or from a tiny fragment). The ability to regenerate the primary body axis is scored independently for each taxon and does not assume the homology of body axes across or within phyla (modified from Bely and Nyberg 2010).*

1.c) Tunicates

Tunicates, also called Urochordates, are strictly marine species belonging to the subphylum of the Chordata (Delsuc et al. 2006; 2008). They are characterized by a protective sheath, called the tunic, that covers their zooids. The tunic is a synapomorphy of this subphylum and is made up of a polymer called Tunicin, which is a cellulose-like polysaccharide produced by epidermal cells. It has been suggested that tunicates acquired the ability to produce Tunicin from bacteria through horizontal gene transfer (Nakashima et al. 2004). Tunicates encompass solitary species, which reproduce exclusively sexually, and colonial species, which couple sexual and asexual reproduction, generally forming colonies (figure1.6) (Holland 2007; Manni et al. 2014).

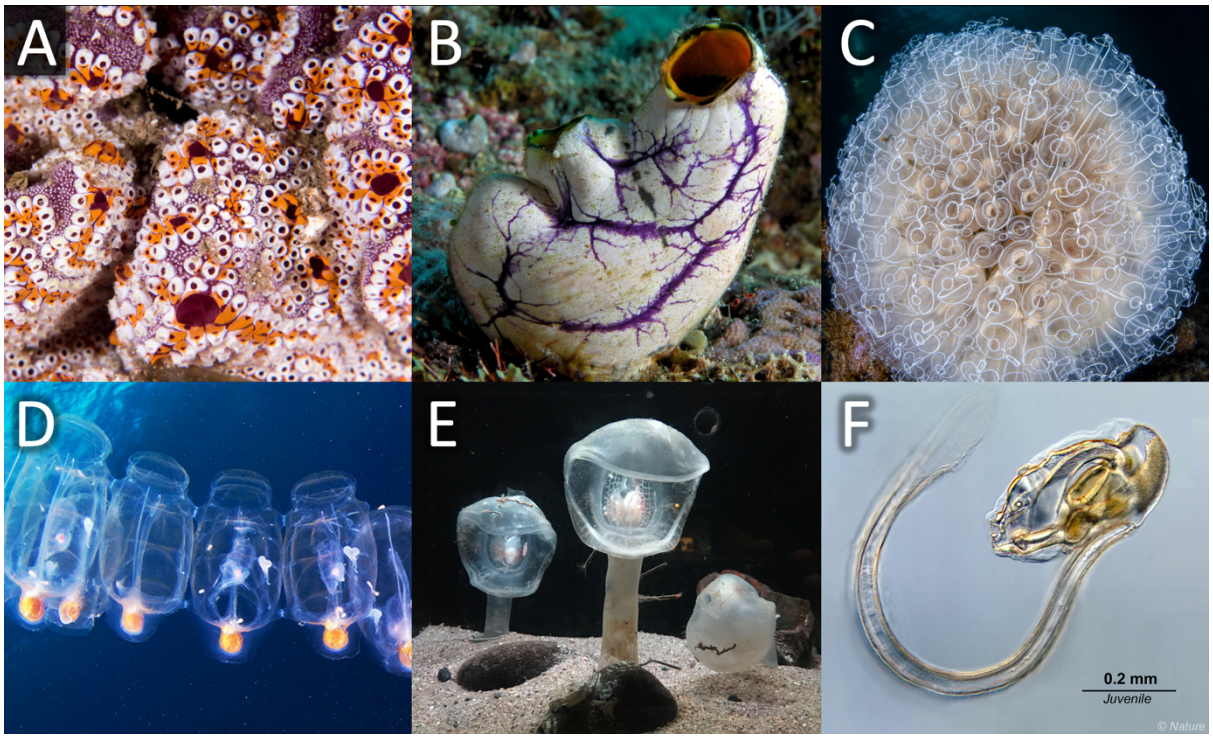

Figure 1.6: *Exemplification of Tunicates biodiversity.* ***A)*** *Botrylloides leachii, photo by John Turnbull (Flickr).* ***B)*** *Polycarpa aurata, photo by Nick Hobgood (Wikipedia).* ***C)*** *Clavelina lepadiformis, photo by Roberto Strafella (Wikipedia).* ***D)*** *Salpa fusiformis, photo by Alexander Semenov (Flickr).* ***E)*** *Megalodicopia hians, photo by Aquamarine Fukushima.* ***F)*** *Oikopleura dioica, photo by Cristian Cañestro (Holland 2007).*

Tunicates occupy various marine habitats, ranging from shallow water near shores to the open ocean and the deep sea, while remaining exclusively marine (Holland 2016). Until recently, tunicates have been divided into three classes: Ascidiacea, Thaliacea, and

Appendicularia, with over 3000 species of ascidians, about 72 species of Thaliaceans, and about 20 Appendicularians (Shenkar and Swalla 2011; Holland 2016). The first class comprises ascidians with a sessile adult; the second includes the pelagic adult of salps, doliolids, and pyrosomes. In these two types, a tadpole-like body plan is seen only in the larval stage, although some species have lost the tadpole larvae secondarily (figure 1.7). In the third type of lifestyle, observed in larvaceans, the tadpole-like body plan is retained throughout life, and the motile tail in the adult is used not only for locomotion but also for collecting food (Wada 1998). Despite being sessile as adults, most of the ascidian embryos generate a tadpole larva that exhibits characteristic chordate features such as a notochord and a dorsal, hollow nerve cord (with some exceptions in the families *Molgulidae* and *Styelidae*) (Jeffery and Swalla 1992). This is due to the repeated evolution of several features among all three ascidian suborders (Shenkar and Swalla 2011).

Tunicates are filter feeders, feeding on phytoplankton and other small particles. The water enters the branchial basket (pharynx) through an opening known as the oral (or branchial, buccal, inhalant) siphon. Multiple gill openings, called stigmata, encircle the sac-like structure known as the branchial basket. Ciliated cells are responsible for the movement of water flow in the pharynx. Water flows from the pharyngeal cavity through the stigmata and into the cloacal atrium before being expelled through the atrial (or aboral, exhalant) siphon (Petersen and Svane 2002; Petersen 2007). The endostyle, a ciliated groove that runs along the ventral side of the pharynx until the esophagus, produces the mucus to retain food particles suspended in the water flow inside the pharynx. This structure is considered homologous to the vertebrate thyroid gland (Fujita and Nanba 1971; Goodbody 1975; Ogasawara, Di Lauro, and Satoh 1999). The dorsal lamina, located in the dorsal portion of the pharynx, with its cilia, helps move food trapped in a mucus film backward towards the short esophagus to reach the stomach. The gastric epithelium, composed of different types of granulated cells, facilitates the digestion and absorption of food in the stomach. The pyloric gland, found in all species, is linked to the stomach and secretes digestive enzymes into the lumen. Undigested food particles pass through the intestine and release through the anus into the cloacal atrium. The atrial siphon carries the remaining particles along with the outgoing water flow (Goodbody 1975; Thorndyke 1977; Flood and Fiala-Medioni 1981). The heart is a tubular structure made of pericardial epithelium that beats due to muscular cells

and peristaltic waves. Pacemaker regions at both ends alternate activity, causing blood flow reversal. A sub-endostyle and a visceral vessel connect to release hemolymph in the sinus for all organs, transporting the gases in solution. Colonial tunicate species have a common extracorporeal vasculature that embeds the zooids. Radial vessels connect all the zooids and buds. These vessels terminate in sac-like structures (ampullae) responsible for the colony's adhesion and contractility (Gasparini et al. 2007; Cima, Franchi, and Ballarin 2016). The central nervous system (CNS) of ascidian larvae is on the dorsal side and is formed through neural tube closure. It is divided into different regions along the antero-posterior axis. Ascidian juveniles have an oval-shaped CNS with regional characterization. During metamorphosis, the larval tail is lost, and the CNS needs to change its innervating organs to transition smoothly from larva to adult (Sasakura and Hozumi 2018).

All ascidians have both male and female reproductive organs. However, some simultaneous hermaphrodites, like the *Ciona* genus, prevent self-fertilization by having incompatible genetic variants in their cell-surface proteins (Jiang and Smith 2005). Ascidian embryos quickly develop into tadpole larvae, with cell fates determined early on through a determinant cleavage (Jeffery and Swalla 1992). In experiments where the first two zygotic cells are separated, each cell only develops into the cells it would have formed in an intact egg (Lemaire 2009). After swimming for a few days, the larva finds a suitable surface and attaches to it using its front adhesive papillae. Its tail is absorbed shortly after, and within two days, the larva transforms into a juvenile with incurrent and excurrent siphons and two-gill slits (Berrill 1947; Durante 1991; Zega, Thorndyke, and Brown 2006; Fodor et al. 2021). Ascidians reproduce sexually, typically at regular intervals during their life span, which can be a year or more. While most solitary species release eggs and sperms, and the fecundation occurs in the water, in colonial species, embryos are often brooded inside the zooids (Nakauchi 1982; Gasparini and Ballarin 2018). Whereas the embryonic development pattern in colonial ascidians is similar to that of solitary species (Ricci, Chaurasia, et al. 2016; Ricci, Cabrera, et al. 2016; Prünster et al. 2019b; 2019a), and conserved throughout the whole class, non-embryonic development (NED) is highly variable in terms of tissue and cell origin, and early ontogenesis (Alié et al. 2021).

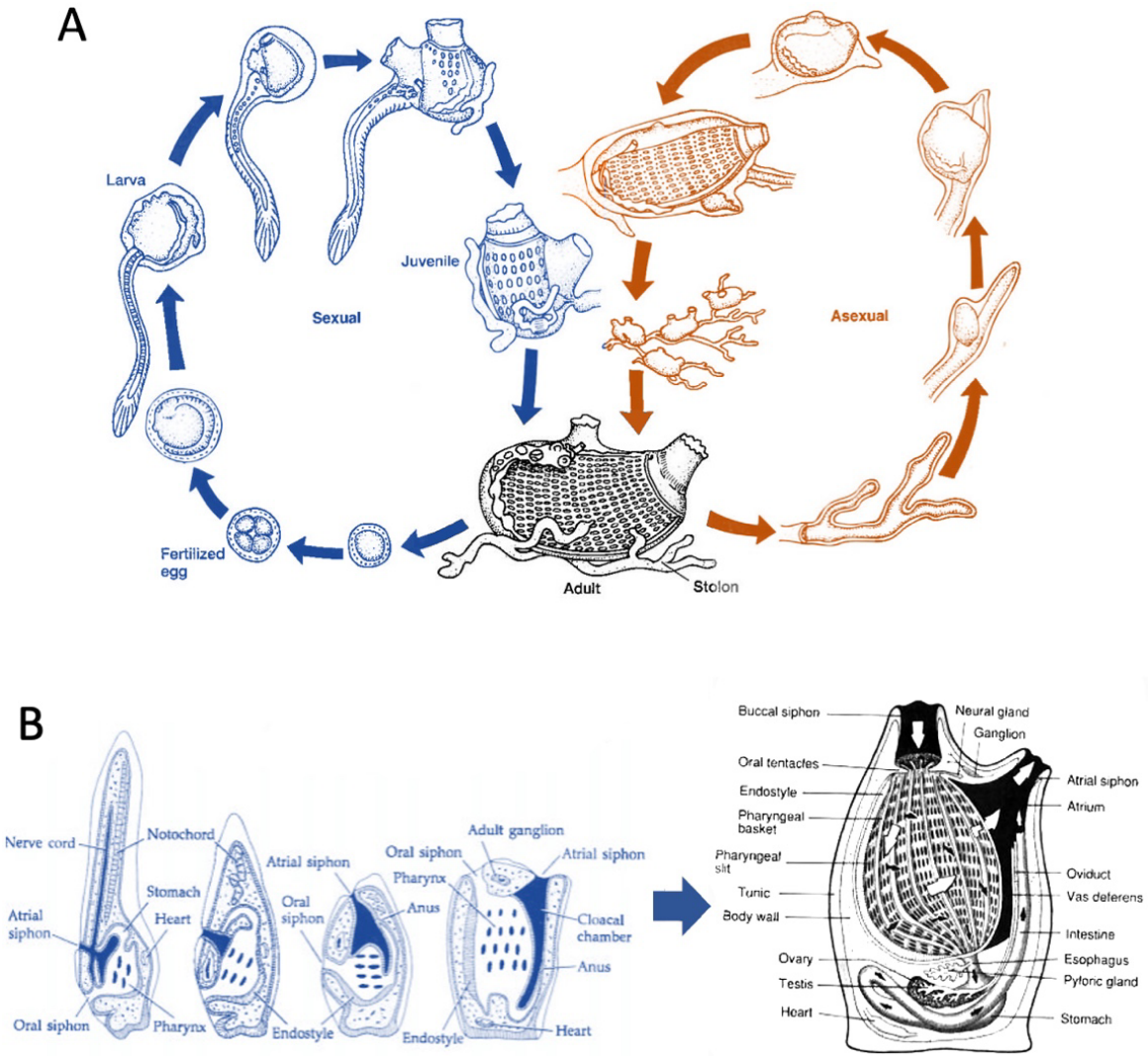

Figure 1.7: A) *Schematic representation of both ways of reproduction in Tunicates.* ***B)*** *Tunicate larvae settlement and metamorphosis in sessile animals.* ***C)*** *General example of a Tunicate adult bauplan (modified from Kardong 2019).*

Colonial tunicates undergo NED via a process called budding, where a developmental process starts from somatic cells and/or tissues and lead to the formation of a new individual. Budding is present in the four main tunicate orders: Thaliacea, Phlebobranchia, Aplousobranchia, and Stolidobranchia (figure 1.8). It is generally part of the life cycle of the colonial species, but it can also be triggered by extensive injury (Alié et al. 2018; 2021) (figure 1.8). The ability to undergo NED evolved at least seven times independently, and all budding tunicates maintain sexual reproduction and embryonic development (figure 1.7-8). Although budding originates from various cells and undergoes different ontogenesis, it can lead to similar post-metamorphic body plans. It is noteworthy that various NED processes generate

the same bauplan. Additionally, the bauplan produced by NED exhibits similarities to those generated by the embryogenesis (Alié et al. 2018; 2021). NED produces modular units known as zooids, which can form temporary or permanent colonies by remaining physically and physiologically connected to one another. Alternatively, they can form clones or clonal aggregates by staying near each other but losing their reciprocal connection (Mackie 1986; Hughes 1989; Braconnot 1970; Tiozzo and De Tomaso 2009).

While colonial species in *Doliolidae* display polymorphisms resulting in a division of labor among different modules with varying appearances (Braconnot 1970). In ascidians, the colonies are composed of identical zooids, suggesting they all contribute equally to the colony maintenance (Hiebert, Simpson, and Tiozzo 2021). Moreover, several independent evolutions have resulted in coloniality through the asexual reproduction of budding from a sexually produced zooid. In some instances, the asexually produced zooids remain closely adherent within a shared tunic, while in others, they only stay connected via narrow stolons (Hiebert, Simpson, and Tiozzo 2021; Hiebert et al. 2022). Solitary ascidians, by definition, do not form colonies. Instead, many such species tend to grow in clusters or aggregates as a consequence of gregarious settlement of larvae. Yet, these clusters do not constitute real colonies. The Thaliaceans and different taxa of colonial ascidians produce true colonies. The single modules of a colony are usually smaller than the adult of solitary species, but the entire colony can reach the size of several square meters. The degree of fusion of the zooids in a colony varies between species, forming sheet-like colonies looking like thin encrusting or massive pedunculated ones (Hiebert, Simpson, and Tiozzo 2021).

According to Berrill (Berrill 1935), colony appearance is a consequence of the distances between zooids, their number, and the distribution of extracorporeal vessels. According to Berrill, ascidian colonies can be subdivided into four major types depending on the grade of fusion (Berrill 1951): (1) zooids loosely connected at their bases by body prolongations called stolons, as in *Clavelina lepadiformis* and *Perophora viridis*. Each zooid is equipped with its own siphons and is surrounded by a separate tunic, resembling miniature solitary ascidians. Some authors call them social forms rather than colonial; (2) groups of zooids that originated by asexual reproduction but are not connected anymore, probably because their stolons degenerated after clonal propagation. Nevertheless, these clones are often densely compacted and form gregarious colonies, as in *Distomus variolosus*; (3) zooids moderately

connected to each other, sharing a common tunic (usually in the abdomen) but still presenting separate siphons, as *Diazona violacea* and *Nephtheis fascicularis*; (4) zooids strictly connected to each other and completely embedded in a common tunic; their atrial siphons coalesce into common cloacal openings, and often share an external vascular system. *Botryllus schlosseri*, *Aplidium pallidum*, and *Diplosoma listerianum* are some examples that form such intimate and very well-organized zooidal systems. The variability of zooid organization and, thus, of colony shape are ultimately the result of the mechanism adopted by their particular mode of non-embryonic development (NED).

NEDs in tunicates can also be classified based on the specific tissues and cells that trigger the budding process. A recent study used the most up-to-date phylogenetic analyses to create a comprehensive phylogenetic tree of the entire subphylum, identifying the species capable of performing NED. Colonial species capable of undergoing NED are found scattered throughout the class of Tunicata. Thus, NED appears to have independently evolved at least seven times within the three orders, involving different tissues, ontogenies, and phylogenetic relationships between solitary and colonial species (Alié et al. 2021). It has been observed that, despite the differences in cell/tissues and mechanisms involved, almost all modes of NED converge towards a conserved stage referred to as the triploblastic stage, which is characterized by the formation of a monolayered double vesicle. While the epidermis of the parental zooid always produces the outer vesicle, the inner vesicle's origin varies depending on the type of NED (Alié et al. 2021). A mesenchymal space exists between these two vesicles containing circulating mesenchymal cells, the hemocytes. After the bud reaches the double vesicle stage, the organogenesis processes are considered consistent across various NED modes. The inner vesicle undergoes folding and evagination, forming most tissues and organs of the nascent zooid, whereas the outer vesicle usually gives rise to the bud's epidermis (Tiozzo and De Tomaso 2009; Alié et al. 2021).

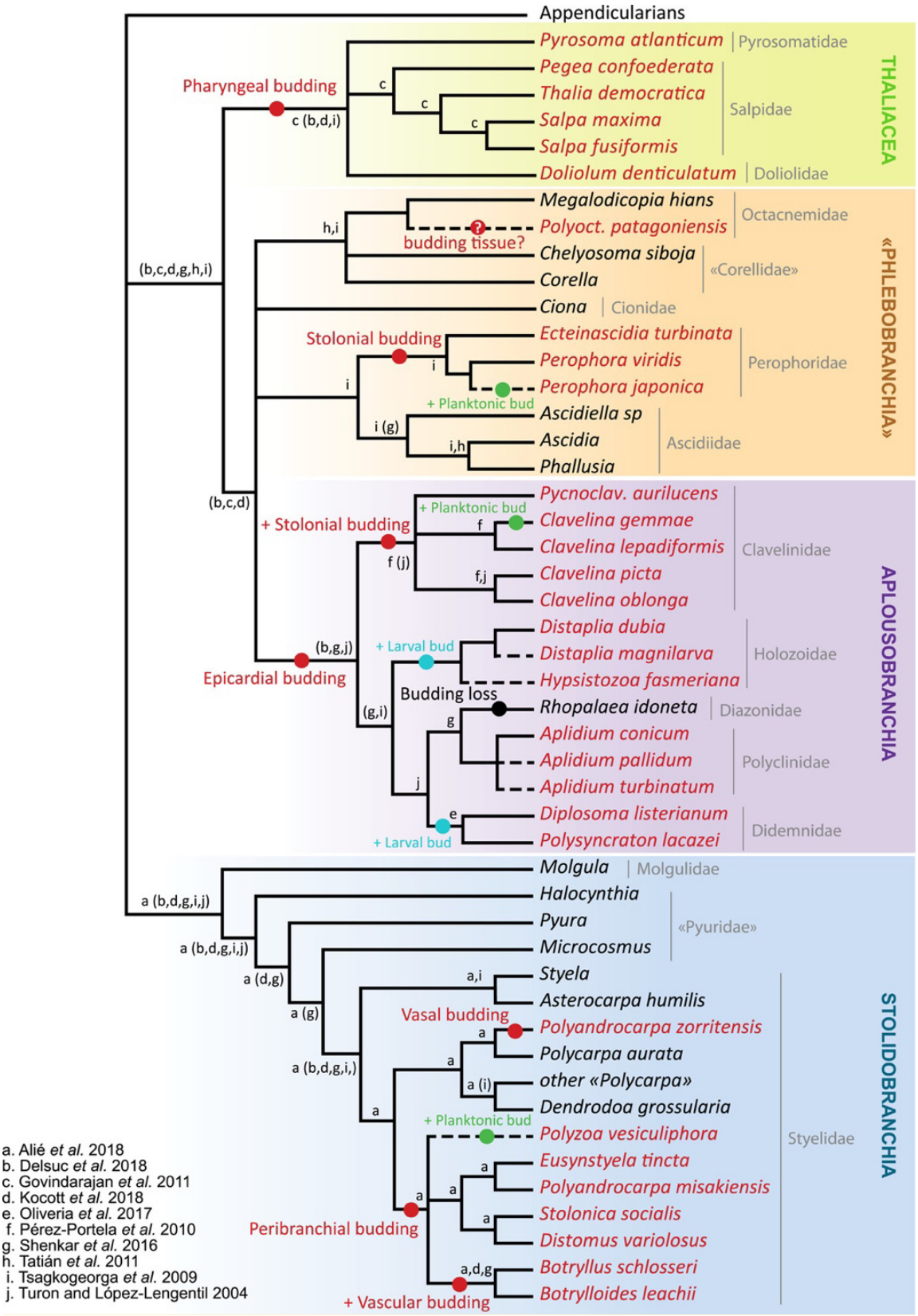

Figure 1.8: *Phylogenetic relationships between budding and nonbudding tunicates. Budding species are represented in red, nonbudding species in black. For each branch, letters refer to the studies in which this clade was retrieved, including all the represented species. Letters between parentheses refer to studies that support the corresponding clade, that is with some of the represented species and when no contradicting group were found. Species with dotted lines are positioned not based on phylogenetic studies but on classification. When a new budding mode arose in budding taxa, it's preceded by "+" (Alié et al. 2021).*

1.d) General Questions and Thesis Objectives

Colonial tunicates have acquired, during evolution, NEDs in a complex and plastic manner: while some types of NED appear to have been acquired several times independently (convergence), some species are capable of multiple modes of NED. This scenario suggests that NEDs may share histological (such as the double-vesicle stage) and transcriptomic commonalities despite their highly variable starting points. Comparing the regenerating/budding capabilities of closely related species, which belong to the same family and converge to the same bauplan, through experimental approaches, can aid in comprehending the evolution of cellular and molecular events during regeneration.

In Chapter 2, in order to improve the breeding of *Polyandrocarpa zorritensis* I studied the effect of one abiotic factor, salinity, on the asexual and sexual propagation in Polyandrocarpa zorritensis by subjecting dormant spherules to hatch and develop in different salinities based on values reported in the collecting sites where *P. zorritensis* has been reported in the Mediterranean Sea. In Chapter 3 firstly, I will report an overview of differential gene expression based on *de novo* transcriptome assembling of seven NED stages in *P. zorritensis*. Secondly, I compare two different transcriptome analyses: de novo transcriptome assembling and genome-based transcriptome mapping. Thirdly, I report differentially expressed genes that might be necessary during *P. zorritensis'* NED, and finally, I compare the differential expressed genes of *P. zorritensis* with the other four NED strategies present in the same tunicate family: *Styelidae*.

Chapter 2 - Salinity-Mediated Limitation on Asexual Growth and the Mediterranean Spread of Ascidian *Polyandrocarpa zorritensis*, a Species Introduced to the Region Decades Ago

Chapter summary

Ascidians are among the most common invasive marine invertebrates worldwide. Many non-indigenous ascidians (NIAs) species have colonized the Mediterranean Sea, particularly in anthropized coastal lagoons and harbors. Although invasive species are typically assumed to possess a broad ecological tolerance, different ascidian species exhibit variable responses to biotic and abiotic environmental stressors such as temperature and salinity. Acquiring a better understanding of the impact of such parameters on ascidian life history is crucial for predicting the invasive potential of NIAs. In this study, we investigated the impact of different salinities on the reproduction of the colonial ascidian *Polyandrocarpa zorritensis*, a species native to Peru and a very successful invader. *P. zorritensis* reproduces asexually via a peculiar form of budding named vasal budding and by producing resistant spherules that likely favored its long-distance dispersal via hull fouling. However, in striking contrast to its reported broad expansion throughout the Pacific and Atlantic coasts, its distribution across the Mediterranean Sea remains confined to a few coastal spots characterized by relatively low salinity. We measured in laboratory-controlled conditions the effect of different salinity conditions on the sexual and asexual reproduction rates of *P. zorritensis*. The rate of asexual reproduction was higher when colonies were grown at 29 or 36 ppt - corresponding to salinities where *P. zorritensis* were found - when compared to 40 ppt - a high salinity often encountered in Mediterranean marinas and harbors. These results suggest that, albeit present in the Mediterranean Sea for decades, *P. zorritensis* invasiveness may be constrained by low tolerance to high salinity in coastal environments colonized by non-indigenous invertebrates.

2.a) Introduction

Ascidians are among the most common invasive marine invertebrates worldwide (Lambert and Lambert 1998; Izquierdo-Muñoz 2009; Clarke Murray, Pakhomov, and Therriault 2011; Cardeccia et al. 2018; Ulman et al. 2017; Ulman, Ferrario, Forcada, Arvanitidis, et al. 2019). Once introduced to a new environment, non-indigenous ascidians (NIAs) have the ability to quickly propagate on hard substrates, subsequently outcompeting local species and causing alteration to the native fouling communities (Lambert 2002; Castilla et al. 2004; Bullard et al. 2007; Dias, Delboni, and Duarte 2008). Coastal anthropized environments such as harbors and lagoons are particularly prone to colonization by non-indigenous ascidians, which get mainly introduced by human-mediated vectors such as hull fouling and aquaculture activities (Lambert and Lambert 2003; Clarke Murray et al. 2014; López-Legentil et al. 2015; Ulman, Ferrario, Forcada, Seebens, et al. 2019; Nichols, Lambert, and Nydam 2023). In these semi-enclosed habitats, environmental conditions differ from the open sea from which they are separated by natural or artificial barriers, leading to short scale instability in terms of eutrophication, pollution, temperature, and salinity (Cognetti and Maltagliati 2000; Gewing, López-Legentil, and Shenkar 2017). In particular, temperature and salinity have a very strong influence on the distribution of marine species and particularly of ascidians (Dybern 1967; 1969; Sims 1984; Vázquez and Young 1996; Lowe 2002; Vázquez and Young 2005; Bullard et al. 2007; Epelbaum et al. 2009; Chebbi, Mastrototaro, and Missaoui 2010; Pineda, Turon, and López-Legentil 2012). With their limited dispersive capacity due to their biphasic life cycle, including a short-living swimming larva giving a benthic fixed adult (Carballo 2000), ascidians can not easily escape unfavorable conditions. Consequently, while successful ascidian invaders are typically recognized for their wide range of ecological tolerance (Lambert and Lambert 2003; Gröner et al. 2011; Granot, Shenkar, and Belmaker 2017; Rocha, Castellano, and Freire 2017; Platin and Shenkar 2023), NIAs can also have poor survival or reproductive outcome when they are exposed to temperature and salinity differing from their region of origin (Shenkar and Loya 2008; Lindeyer and Gittenberger 2011; Nagar and Shenkar 2016; Gewing et al. 2019). Hence, improving our understanding of the influence of environmental factors on NIA's reproduction is crucial to predict better their invasive potential (Rocha, Castellano, and Freire 2017; Platin and Shenkar 2023).

Figure 2.1: A) *Locations in the Mediterranean Sea where the presence of Polyandrocarpa zorritensis was reported (1: Turon-Pererra 1988; 2: https://doris.ffessm.fr/Especes/Polyandrocarpa-zorritensis-Polyandrocarpe-de-Zorritos-5004; 3: Brunetti 1978; 4: Tempesti et al. 2019; 5: Virgilli et al. 2022; 6: Mastrototaro et al. 2008; 7: Stabili et al. 2015). The yellow star marks La Spezia, where the samples for this study were collected;* ***B)*** *Satellite view of the Assonautica Marina in La Spezia.*

Polyandrocarpa zorritensis (Stolidobranchia: *Styelidae*) is a colonial ascidian that was first described from the coasts of Peru (Van Name 1931). Over the last few decades, *P. zorritensis* has emerged as a widely distributed non-indigenous species and is considered as an aggressive invader to temperate coastal areas (Lambert and Lambert 1998; Brunetti and Mastrototaro 2004). The first report of *P. zorritensis* outside its native range was on the Mediterranean coast of Italy (Brunetti 1978), and then later, it was also found in several Pacific and Atlantic regions, including Japan (Otani 2002; Iwasaki et al. 2004), Southern California (Lambert and Lambert 1998; Nichols, Lambert, and Nydam 2023), Hawaii (Abbott, Newberry, and Morris 1997), Galapagos Islands (Lambert 2019), the Panama canal (Carman et al. 2011), the Caribbean (Monniot 2018; Streit et al. 2021), Brazil (Millar 1958), the Gulf of Mexico (Lambert et al. 2005), Florida (Vázquez and Young 1996), and North Carolina (Villalobos et al. 2017). From 1994 to 2020, there has been a noticeable increase in the abundance of *P. zorritensis* in California marinas, accompanied by a concomitant northward expansion of the species (Nichols, Lambert, and Nydam 2023). Similarly, twenty years after its first introduction to Japan in 1991, *P. zorritensis* has become a common NIA detected over the coasts of this country (Iwasaki et al. 2004). The successful invasiveness of *P. zorritensis* has been attributed to its apparent tolerance to temperature and salinity changes (Lambert and Lambert 1998), as well as its unique mode of asexual reproduction (Brunetti and Mastrototaro 2004). During this process, the species produces resistant spherules, likely enabling long-distance human-mediated transportation and colony restoration even in the

absence of adult individuals and after prolonged periods of dormancy (Brunetti and Mastrototaro 2004; Alié et al. 2018; Scelzo et al. 2019; Hiebert et al. 2022). However, the only existing experimental study focused on the impact of low salinity on larval behavior (Vázquez and Young 1996), and therefore we have a poor understanding of the link between environmental parameters and *P. zorritensis* asexual and sexual reproduction.

Coastal lagoons, harbors, and marinas of the Mediterranean Sea are known hotspots for the entry and secondary spreading of non-indigenous invasive species (Ulman et al. 2017; Ulman, Ferrario, Forcada, Arvanitidis, et al. 2019; Ulman, Ferrario, Forcada, Seebens, et al. 2019) (Ulman et al. 2017, 2019a, 2019b). While some non-indigenous ascidians have a broad Mediterranean distribution, such as *Ascidiella aspersa*, *Styela plicata*, *Ciona robusta*, and *Pyura dura*, other NIAs originating from the Red Sea are mostly found in the eastern Mediterranean (e.g., *Microcosmus exasperatus*, *Herdmania momus*), while others are more common in the western part (e.g., *Microcosmus squamiger*) (Izquierdo-Muñoz 2009). This suggests that west-east gradients of temperature and salinity in the Mediterranean (Coll et al. 2010) may influence the distribution of non-indigenous ascidians in relation to the species-specific ecological tolerance (Shenkar and Loya 2008; Platin and Shenkar 2023). *P. zorritensis*, despite being locally abundant, is not among the most widespread Mediterranean NIAs (Izquierdo-Muñoz 2009; Cardeccia et al. 2018; Ulman, Ferrario, Forcada, Arvanitidis, et al. 2019). It was not found on the 583 vessel hulls investigated by Ulman et al. (Ulman, Ferrario, Forcada, Seebens, et al. 2019) although 71% of the boats hosted at least one NIS, and was only recorded in 1 out of the 50 marinas sampled by Ferrario et al. (Ferrario et al. 2017; Ulman et al. 2017; Ulman, Ferrario, Forcada, Seebens, et al. 2019). Furthermore, it was only present in 1 of the 32 harbors studied in northern Spain (López-Legentil et al. 2015) and is absent from NIA-rich areas along the Tunisian and Israeli coasts (Chebbi, Mastrototaro, and Missaoui 2010; Gewing and Shenkar 2017). Therefore, despite the first observation of *P. zorritensis* outside Peru being in the Mediterranean Sea (Brunetti 1978), its expansion in this area has remained relatively limited to the northern-west basins (figure 2.1.A). Notably, the salinity levels in several Mediterranean locations where *P. zorritensis* occurs are lower than the average 38 ppt of the western Mediterranean. In the Mare Piccolo of Taranto harbor (Italy) and the Thau Lagoon (France), the annual salinity values stay around 36-37 ppt (Audouin 1962; Brunetti and Mastrototaro 2004), and the Santa Carla de la Rapita harbor in the Delta del Ebro has a

low salinity due to freshwater inputs (López-Legentil et al. 2015). In La Spezia harbor, the spring salinity fluctuates between 32 and 37 ppt (Brunetti 1978), and in Livorno harbor, it ranges from 35 to 39 ppt (Tempesti et al. 2022). In this study, we investigated the influence of salinity on the reproduction of *P. zorritensis*, with a particular focus on asexual budding, analyzing in laboratory-controlled conditions the effects of different salinity values reported in regions where the species was found.

2.b) Materials and Methods

Polyandrocarpa zorritensis Collection, Identification, and Husbandry

Colonies of *Polyandrocarpa zorritensis* were collected in the harbor of La Spezia, Italy (Assonautica Benedetti, 44°06'10.7"N, 9°49'34.5"E) (figure 2.1.B). Taxonomic identification follows Van Name (1931), and molecular barcoding of colonies from La Spezia was conducted previously (Alié et al. 2018) The spherules were gently separated from the colony and stored in tanks containing seawater at 11 °C (at a salinity of 38-39 ppt) before being used for experiments. To obtain zooids used for the experiments, the spherules were transferred to water tanks containing 12 liters of artificial seawater (ASW) at 24°C, prepared with deionized water and marine salt (Red Sea Salt, Red Sea) at the desired concentration. The spherules were placed on microscope glass slides (5x7cm) at the bottom of the tanks, with 5 to 12 spherules per slide and 3 to 4 slides per tank (appendix 1). Since we observed the number of stolons to be proportional to spherule size (unpublished obs.), we took care to use spherules of similar sizes. Upon hatching, bubblers were added to oxygenate the water, animals were fed twice a day with the following mix: 15ml of live *Tisochrysis lutea*, 15ml of live *Chaetoceros gracilis*, 250µl ISO800, and 250µl of Shellfish Diet 1800 (Reed Mariculture) per tank. Water was changed every two days, temperature was maintained around 24-24,5°C and colorimetric tests (Ammonia Marine Test Kit and Nitrate\Nitrite Marine Test Kit, Red Sea) were performed on a regular basis to ensure that NH_4, NO_2, and NO_3 wastes did not reach toxic values through the experiments.

Asexual Reproduction Monitoring and Quantification

A first set of experiments was conducted on two different batches of spherules that were collected in autumn (09/05/2019 and 11/10/2022) and maintained at 11°C for 80 and 99 days, respectively. Another set of experiments was conducted on a single batch of spherules collected in winter (02/03/2022) and maintained at 11°C for 73 days and 97 days, respectively. A last experiment was conducted on spherules collected in spring (05/12/2022) and used immediately after collection. Zooids were cultivated at 22, 29, 36, and 40 ppt. Photos of the zooids were taken at regular intervals, up to 24 days after spherule seeding (appendix 2), the date from which image-based quantification of asexual reproduction

becomes complicated due to the high number of overlapping stolons, which makes the individual assignment difficult. Pictures were taken with a Canon EOS 6D camera equipped with a 100mm macro lens. Stolon bases, stolon tips, budding nests, and newly hatched zooids were quantified from pictures of the last day of each experiment using the Cell Tracker plugin on ImageJ.

Quantification of Sexual Reproduction

Sexual reproduction was evaluated by counting the number of embryos and larvae produced per zooid obtained from the autumn 2022 spherules (appendix 3). Upon having reached sexual maturity (approximately a month after spherule seeding), zooids were relaxed in seawater with Ms-222 (E10521-10G, Sigma Aldrich), then fixed in a solution of 4% paraformaldehyde diluted in ASW according to the salinity of each sample. After several days of fixation, zooids were dissected, and the number of gonads and brooded embryos in the atrial chamber were counted for each individual. We also counted the swimming larvae and the embryos accidentally released by the zooids during the 9 days preceding their fixation by visually inspecting the tanks every morning (from the time the light goes on, 8 am, to early afternoon, when they stopped releasing larvae) and before every water change. In these experiments, we raised 19 spherules at 40 ppt, 22 spherules at 36 ppt, and 20 spherules at 29 ppt (appendix 4).

Morphological Measuring, Heartbeat Rate, and Stolon Pulsation Period

The zooid size was measured using ImageJ, on the animals hatched from spherules collected in the autumn of 2022 batch, relaxed in MS-222, and before fixing. Size was measured between the tip of the inhalant siphons and the posterior-most point of the body cavity (see appendix 5 as an example). Heart and stolon beating rates were measured in an additional experiment using autumn spherules (appendix 6). Heart beating was measured visually under a stereomicroscope, thanks to the transparency of the tunic, as the number of pulsations within one minute. The stolon pulsation period was measured using timelapse imaging with a Leica M165-FC stereomicroscope equipped with a MC170-HD camera. One

picture was taken every 5 seconds, a pulsation period being the lag time until the beating tip of a stolon comes back to its initial condition (see appendix 6).

2.c) Results

The Presence of *Polyandrocarpa zorritensis* Coincides with Lower Salinity in La Spezia Marina

In 2016, we investigated several spots in La Spezia Bay, including marinas (Circolo Velico Palmito 44.086377, 9.878521; Darsena Pagliari 44.104680, 9.859106; Porto La Grazie 44.068307, 9.835713; Assonautica 44.103388, 9.82633) and open water oyster racks (44.071649, 9.857886; 44.057952, 9.842249). We only found *P. zorritensis* in the Assonautica marina (figure 2.2.A), the innermost investigated spot of the bay. From 2016 to 2023, we regularly found *Polyandrocarpa zorritensis* in this marina, usually as large aggregate colonies and/or as mats of dormant spherules on the immersed boat lines, in the proximity of a freshwater outlet (figure 2.2.A-F). In May 2016 and 2022, the species was only visible on the proximal-most pontoons of the marina, where the salinity was the lowest, i.e., 29 and 34 ppt, respectively (figure 2.2.A,D). In the autumn and winter seasons, the colonies had a wider distribution, with measured salinities ranging between 36 and 38 ppt (figure 2.2.B,C,E,F).

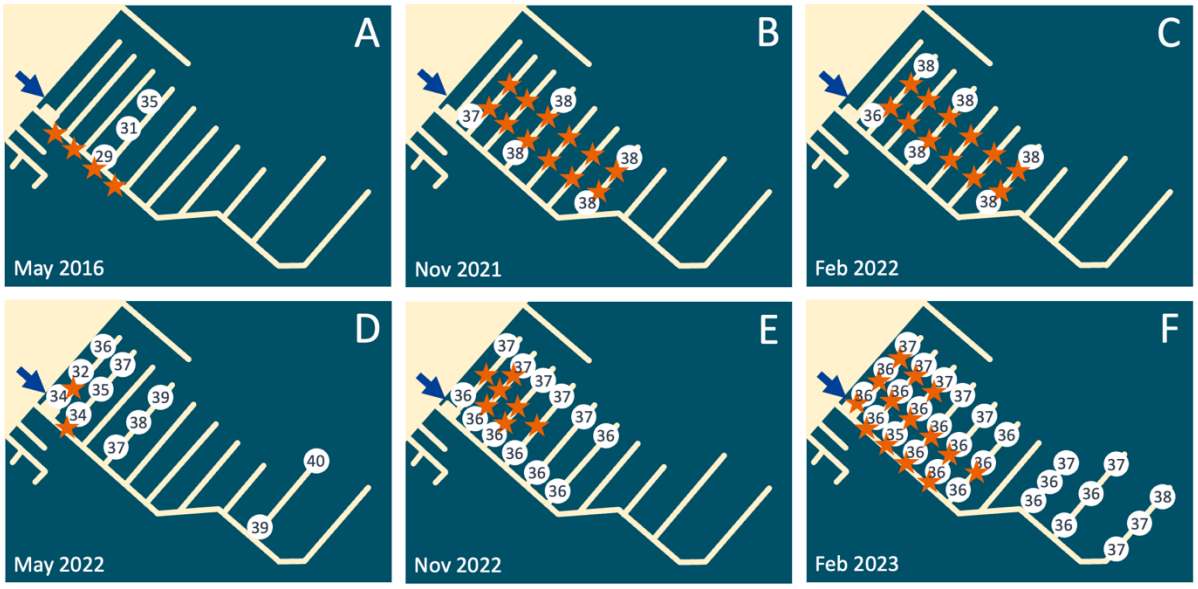

Figure 2.2: *Polyandrocarpa zorritensis presence and salinity values observed by our group in 2016, 2021, 2022, and 2023. The blue arrow indicates a freshwater influx spot in the marina. The white circles contain the salinity value (in ppt) observed in the different regions of the pontoon. The orange stars indicate the spots where P. zorritensis was found.*

High Salinity Negatively Effects the Rate of Asexual Reproduction

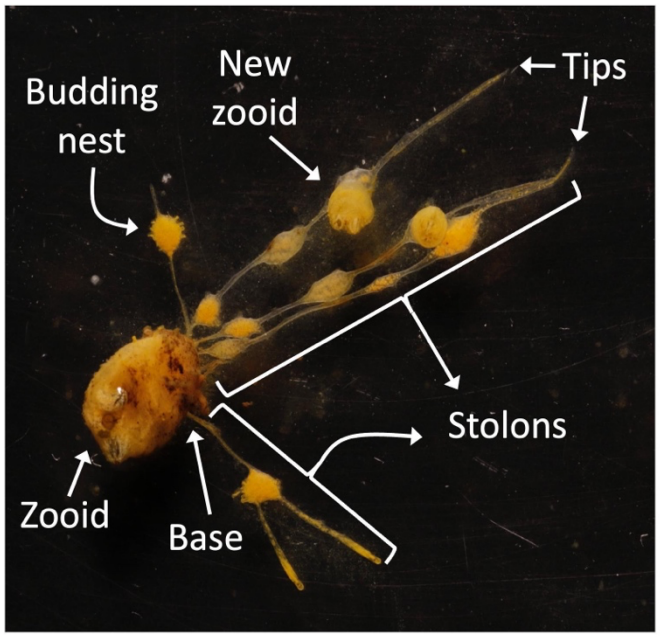

Figure 2.3: *Parameters measured for the rate of asexual reproduction. Image showing a zooid originated from a dormant spherule, indicating the base of a stolon, tips of stolons, a bud (or budding nest), and a new zooid formed from a bud.*

In order to study the effect of the observed salinity on the asexual budding in *P. zorritensis*, we quantified the production of stolons, budding nests (also called buds), and new zooids produced by individual adult zooids (illustrated in figure 2.3) cultivated at 22, 29, 36 and 40 ppt. These adults were obtained from dormant spherules collected on the field and later placed in experimental conditions in the laboratory. While not all spherules placed at 22 ppt did not hatch, every spherule in the other salinity conditions hatched after 5 to 7 days and gave rise to a functional zooid. When using spherules collected in autumn (figure 2.4.A-A") and maintained in hibernation for three months before the experiment, the salinity significantly affected the number of stolonial tips (Kruskall-Wallis p-value = 0.022) and the production of buds and new zooids (Kruskall-Wallis p-value = 0.00029). The number of stolonial tips was significantly lower at 40 than at 36 ppt (Mann-Whitney p-value = 0.0071) (figure 2.4.A'), while the number of buds and of newly born zooids were significantly lower at 40 than at 29 (p-value = 0.0099) and 36 ppt (p-value = 6.05e-5) (figure 2.4.A"). The number of stolon bases was also significantly lower at 40 ppt than 36 ppt (p-value = 0.014) and did not differ between 29 and the two other conditions (figure 2.4.A).

Experiments conducted with spherules batches collected in different seasons gave a similar, albeit less pronounced trend. When using spherules collected in winter (figure 4B-B"), the number of stolon bases and stolon tips did not differ between the three treatments (figure

2.4.B-B'), but the salinity affected the number of nests and new zooids (Kruskall-Wallis p-value = 0.035), which was lower at 40 than 29 ppt (p-value = 0.011) (figure 2.4.B"). Finally, for spherules collected in spring (Figure 4C-C"), the number of stolon bases and stolon tips did not differ between the tree treatment (figure 4.2.C-C') but the number of nest and new zooids was lower at 40 than 36 ppt (p-value = 0.037) (figure 2.4.C").

In order to estimate the yield between the somatic growth of the colony and the actual reproduction by budding, we calculated a budding index, which is the ratio between the number of nest/new zooids and the number of stolons. Regardless of the spherule batch used, the high salinity always negatively impacts this ratio (figure 2.4.D-D"). Using autumn and winter spherules, the budding index was significantly lower at 40 ppt when compared to 29 and 36 ppt (figure 2.4.D,D"), and spring spherules gave a higher index at 29 when compared to 40 and 36 ppt (figure 2.4.D').

Salinity Did Not Affect Zooid Physiology

Physiological variables reflecting the general zooid health (Dijkstra et al. 2008) were not significantly affected after exposure to the tested salinities. The average size of the zooids (figure 2.5.A), measured from the tip of the inhalant siphon to the posterior-most point of the body cavity, was 1.14, 1.24, and 1.31 cm for 50 days-old zooids grown at 29, 36, and 40 ppt respectively, with no significant impact of salinity (Kruskall Wallis p-value = 0,096). Similarly, the average heartbeats rate (figure 2.5.B) did not significantly differ between the three conditions (56, 60 and 57.2 puls.min-1 at 29, 36 and 40 ppt respectively, Kruskal-Wallis p-value = 0,26), neither did the period of stolon beating (110, 112 and 107 seconds at 29, 36 and 40 ppt respectively, Kruskal-Wallis p-value = 0,25) (figure 2.5.C). These results suggest that zooids grow at a similar rate regardless of the salinity condition and that they do not experience chronic stress significantly affecting blood circulation between adult zooids and their forming buds.

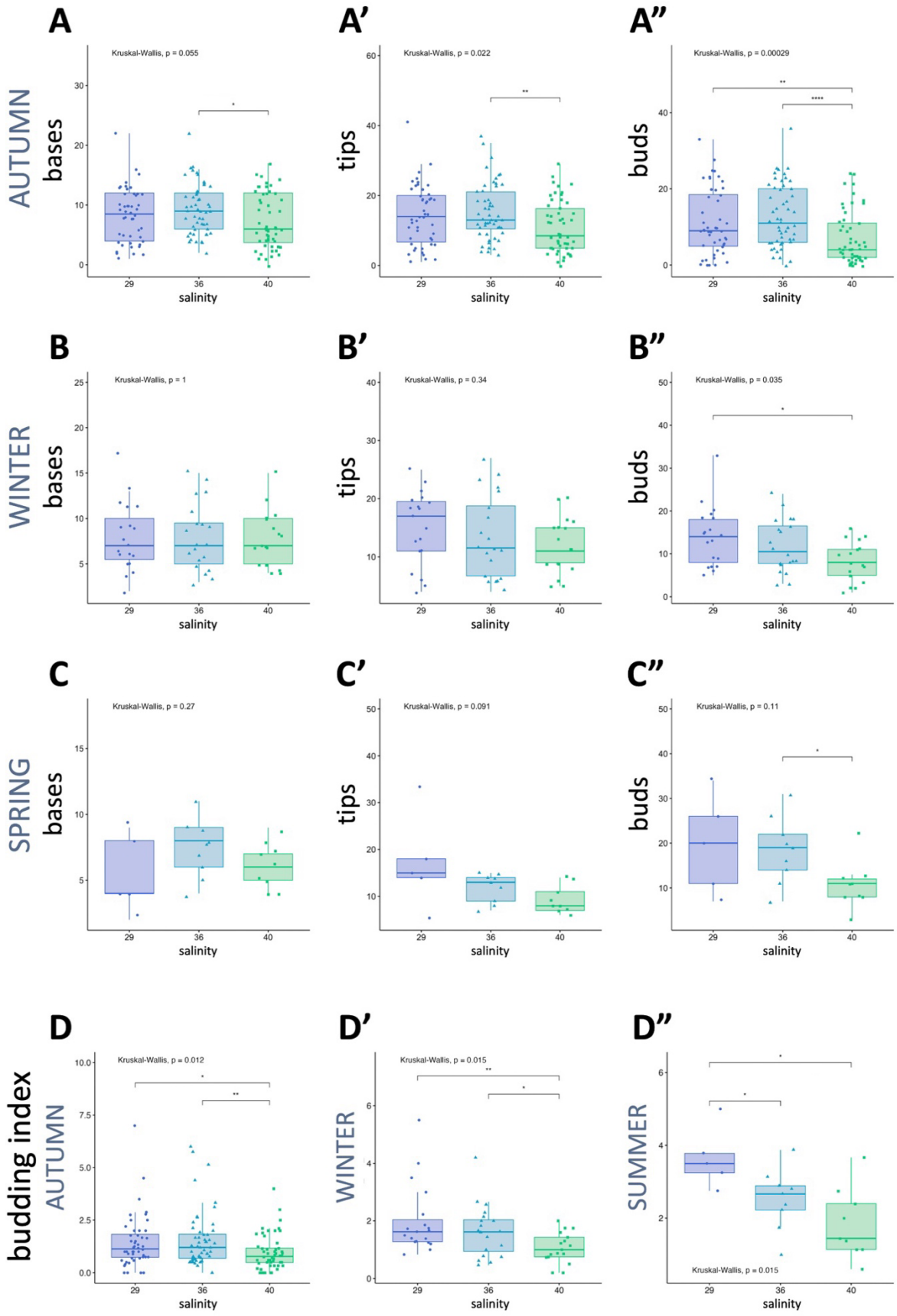

Figure 2.4: *Asexual reproduction in the three different salinities: 29, 36, and 40 ppt, measured by the production of stolons (bases), stolons ramification (tips), and buds.* ***A-A")*** *Autumn batch.* ***B-B")*** *Winter batch.* ***C-C")*** *Spring experiment.* ***D-D")*** *Budding index, i.e., the ratio of buds per stolon base.*

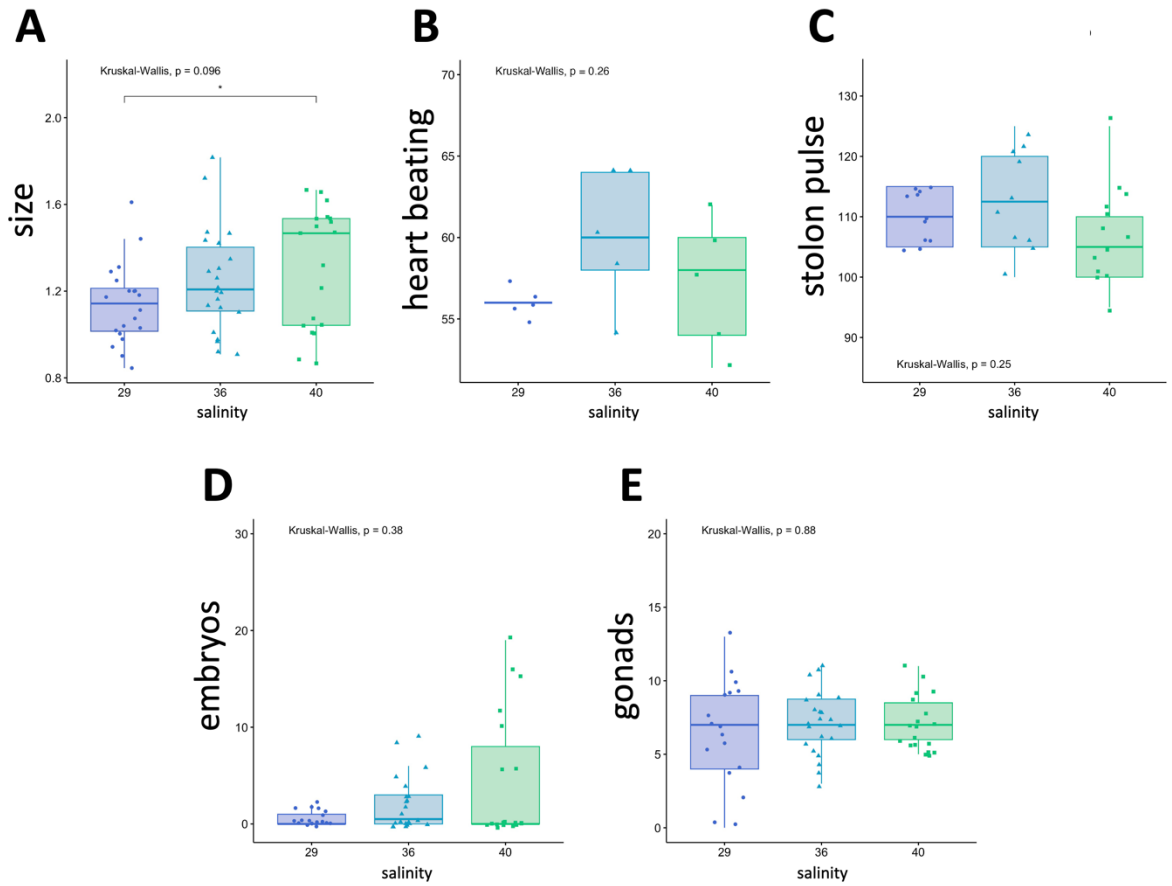

Figure 2.5: A-C) *Colony health parameters.* ***A)*** *zooid size in cm.* ***B)*** *heart beating rate (pulsation.min-1).* ***C)*** *Stolon pulsation period (time between two consecutive pulsations, in seconds).* ***D-E)*** *Influence of salinity on sexual reproduction.* ***D)*** *Number of brooded embryos per 1 month-old zooids.* ***E)*** *Number of gonads per 1 month-old zooid.*

Production of Embryos and Larvae

In order to estimate whether sexual reproduction was equally affected by the salinity, we counted the number of gonads and embryos present in the body cavity of one-month-old zooids obtained from autumn spherules (figure 2.5.D,E). The number of gonads did not significantly differ between the three conditions (figure 2.5.E). One month after spherule hatching, we counted an average of 0.50, 2.04, and 4.42 offspring per zooid at 29, 36, and 40 ppt, respectively (figure 2.5.D), with no statistical difference between the three conditions, probably due to inter-individual variance (appendix 3). However, we noticed that zooids had started to release larvae and sometimes embryos (most likely accidentally during animal manipulation) before fixation. Therefore, we also counted the larvae and embryos present in the tanks during the nine days prior to fixation (appendix 4). If we add these numbers to the offspring found in the atrial cavity, we obtain a total of 11 larva and 23 embryos released by

the 20 zooids at 29 ppt (0.24 offspring per zooid/day), 112 larvae and 37 embryos released by the 22 zooids at 36 ppt (0.73 offspring per zooid/day), and 104 larvae and 17 embryos were released by 19 zooids at 40 ppt (0.70 offspring per zooid/day). Taken together, these results do not allow us to conclude that salinity treatments significantly affect the rate of sexual reproduction but suggest that the number of offspring is approximately ten times lower at 29 ppt.

2.d) Discussion

Salinity Effect on Asexual Budding in *P. zorritensis*

Our results provide evidence that the rate of asexual reproduction, quantified by the number of blastozooids produced per oozoid 14 days after spherule hatching, decreases when *P. zorritensis* is reared at a salinity of 40 ppt compared to 29 and 36 ppt. These salinities were selected because 29 ppt is the lowest salinity at which *P. zorritensis* was found in the sampling site (La Spezia, Assonautica Marina), while 36 ppt corresponds to the average salinity in semi-enclosed basins colonized by *P. zorritensis* in the Mediterranean Sea (Tempesti et al. 2022; Brunetti and Mastrototaro 2004). 36 ppt is also close to the surface salinity along the northern Peruvian coast (Chaigneau et al. 2013), where *P. zorritensis* was originally described. Conversely, 40 ppt is commonly observed in Mediterranean marinas (Ulman, Ferrario, Forcada, Arvanitidis, et al. 2019), which serve as the primary entry point and most favorable habitat for most non-indigenous ascidians (NIAs). The number of blastozooids produced by spherules at 40 ppt compared with lower salinities in our experiments suggest that this relatively high salinity negatively impacts the asexual propagation of *P. zorritensis*.

Salinity significantly affected the budding index, i.e., the average number of buds per stolon, which was lower at 40 ppt for most comparisons (except at 36 versus 40 ppt with spring spherules, although the absence of significance may come from the low number of individuals used). The budding index was taken as an indication of the relative energy expended to somatic growth per se versus asexual replication (budding). Specifically, while salinity affected the number of buds and blastozooids in most experiments, a significant effect on stolons bases and tips was only observed for 36 versus 40 ppt with the autumn batch. It is also noteworthy that zooids raised at 40 ppt were larger than at lower salinities. Taken together, these results suggest that the animals raised at 40 ppt may allocate more energy to somatic growth and colony expansion and, conversely, less energy to asexual reproduction.

Overwintering spherules are likely to represent a seasonal population bottleneck for P. *zorritensis*. In fact, observations from March 2018 and May 2019 revealed the almost complete disappearance of *P. zorritensis* at the site of La Spezia, with only a few scattered resting spherules found attached to boat mooring lines (Hiebert et al. 2022). Similarly, in May 2022, the animals were confined to the very proximal zone (figure 2.1). This scenario is in

striking contrast with the situation in fall, during which *P. zorritensis* dominated the benthic community on the same lines, displaying dense colonies with numerous stolons and buds (see figure 5 in Hiebert et al. 2022 or figure 2 in Scelzo et al. 2019). This population dynamic suggests that a small number of spherules are sufficient to reconstitute the population. On the other hand, it also underscores that the success of spherule hatching in spring is critical for population replenishment, which heavily relies on budding (Brunetti and Mastrototaro 2004; Hiebert et al. 2022). Thus, even if they cause only a slight reduction in the rate of asexual reproduction, unfavorable conditions such as a relatively high salinity may decrease the species' fitness.

This is further supported by our observation that the influence of salinity on the budding index was particularly pronounced in colonies that originated from spring spherules. Indeed, the spring batch was the only one to exhibit a statistical difference between 29 and 36 ppt, and a budding index 2.5 times higher at 29 ppt than at 40 ppt. This may hold crucial implications for *P. zorritensis* fitness in response to salinity gradients, as the most substantial salinity gradient between proximal and distal docks in La Spezia marina (34 to 40 ppt in May 2022), as well as the lowest measured salinity (29 ppt in May 2016), were observed in spring (figure 2.2). Thus, spring spherules might be particularly sensitive to water salinity, compared to other seasons. As a result, their reproductive outcomes may be significantly influenced by strong gradients during this critical season, wherein spherules that overwintered have to replenish the population.

P. zorritensis expansion may also be limited by very low salinity. Previous findings demonstrated that exposure to salinity as low as 15 ppt for 48 hours reduced by half the number of spherules capable of hatching once returned to a higher salinity (Hiebert et al. 2022). Evidently, spherules represent a resistant form capable of coping with acute hypo-osmotic stress. However, our present results indicate that spherules cannot ensure zooid production when maintained at 22 ppt. Additionally, low salinity seems to prevent larval recruitment. Vazquez and Young (1996) studied the swimming behavior of *P. zorritensis* larvae in response to haloclines and found that larvae exhibited abnormal swimming behavior, staying at the bottom of the tank instead of swimming upward in water with a salinity lower than 26 ppt. Furthermore, through experiments involving water columns to create controlled haloclines (i.e., abrupt salinity changes between adjacent water masses),

they observed that 72% of the larvae actively escaped water of 22 ppt. Considering these findings along with our present results, it becomes evident that water with salinity as low as 22 ppt does not allow asexual reproduction and impedes larval recruitment, suggesting that *P. zorritensis* may not be able to thrive in brackish environments.

Effect of Different Salinities on Asexual Versus Sexual Reproduction

Due to the lack of a statistically significant difference in the number of embryos and larvae between the different experimental conditions, the present study does not allow us to draw a definitive conclusion on the impact of salinity on sexual reproduction. Furthermore, there was no significant difference in the number of gonads among the three treatments, but this particular trait might have limited relevance as it is a phylogenetically constrained character commonly employed for species identification (Monniot 2016). However, the number of larvae observed swimming in the tanks were approximately ten times lower at 29 ppt when compared to 36 and 40 ppt, suggesting that 36 ppt might be an ideal salinity where both asexual and sexual reproduction rates are high. Histological analyses could do further exploration of the effects of salinity on sexual reproduction to investigate gonad maturity. Additionally, other aspects related to sexual reproduction could be explored, such as the age at which zooids reach sexual maturity or the larval swimming behavior and larval recruitment under different salinities.

Decreasing asexual reproduction in *P. zorritensis*, as observed at 40 ppt, may strongly hinder its fitness, especially since sexual reproduction probably hardly compensates for reproductive success in this species. Indeed, coloniality in ascidians often coincides with zooid size reduction, ovoviviparity, and reduction in the number of embryos compared to solitary species (Berrill 1935; Svane and Young 1989; Zega, Thorndyke, and Brown 2006; Alié et al. 2018). For instance, *P. zorritensis* gonads contain relatively few eggs (Van Name 1945), each zooid bears around 20 embryos at various developmental stages (Monniot 2016), and the embryonic development in this species takes several days (personal observations). Our results also further demonstrate that *P. zorritensis* zooids release very few (less than one) larvae per day. In contrast, solitary *Polycarpa* species, which are closely related to *P. zorritensis* (Alié et al. 2018), have bigger zooids, have more and larger gonads (Van Name 1931; Vazquez, Ramos-

Espla, and Turon 1995) and can spawn several dozens of eggs weekly (Gordon et al. 2020). Additionally, internal brooders release mature lecithotrophic and low-dispersive larvae with a relatively short swimming period. For example, *P. zorritensis* larvae typically settle within minutes to a few hours post-release (Vazquez and Young 1998). In contrast, oviparous species release planktonic eggs promoting long-range dispersion by water currents (Berrill 1935; Svane and Young 1989; Havenhand 1991). For instance, *Styela plicata*, which is a solitary Stolidobranchia also very abundant in La Spezia marina, is a broadcast spawner that follows a broadcast spawning strategy, releasing floating eggs and sperm (Villa and Patricolo 2000; Crean and Marshall 2015). The fertilization of these gametes takes place externally, and the embryos undergo development outside the body for approximately 12 hours, followed by several hours before the larvae become competent to metamorphose (Yamaguchi 1975). Notably, there have been reports of solitary oviparous phlebobranchs whose larvae can survive for ten days and disperse as far as 1.5 km away (Svane and Young 1989; Havenhand 1991). In conclusion, while the colonial lifestyle is supposed to provide competitive advantages over solitary organisms because it enables indeterminate growth, colonization of complex microhabitats, or high regenerative capability (Jackson and Hughes 1985; Kott 1989; Dias, Delboni, and Duarte 2008; Hiebert et al. 2019), when a colonial ascidian such as *P. zorritensis* finds itself in an environment where asexual propagation is hindered, the relatively low production of poorly dispersal larvae may limit its ability to compete for space against other fouling benthic organisms.

Predicting *P. zorritensis* Distribution and Expansion

A finer knowledge of *P. zorritensis* ecological tolerance would be powerful to predict its invasive potential worldwide and therefore orientate conservation measures toward identified target ecosystems (Locke 2009; Nichols, Lambert, and Nydam 2023). Modeling approaches using ecological niche properties, species distribution, and ecological tolerance have been used to forecast ascidian invasion in present and future climate scenarios (Locke 2009; Epelbaum et al. 2009; Rocha, Castellano, and Freire 2017; Lins et al. 2018). These models notably demonstrated that seawater temperature and the distance from the shore are variables that strongly influence ascidians distribution. The latter is probably a proxy for other variables that are more difficult to model, such as eutrophication level, coastal

pollution, or local salinity variations (Epelbaum et al. 2009; Lins et al. 2018). To date, only one study has included *P. zorritensis* (Locke 2009), predicting its expansion toward the Canadian northern Atlantic coast, but to our knowledge, the species has not been recorded there yet. The documented impact of salinity on sexual and asexual reproduction (Vázquez and Young 1996), together with previous works demonstrating the effect of salinity and temperature stress on spherules and zooid survival (Hiebert et al. 2022), may help better prediction of *P. zorritensis* expansion in the future. Yet, a lot of work remains to better characterize the ecological tolerance range of this species. Notably, the effect of temperature on colony growth is still totally unknown.

In contrast to its Atlantic and Pacific expansion, the current distribution of *Polyandrocarpa zorritensis* in the Mediterranean Sea is confined to the Western basin. While we can speculate that the eastern basin is less suitable to *P. zorritensis* because of its generally higher salinity (Coll et al. 2010), we cannot exclude that the species has been overlooked due to particular substrate preference. The abundance of non-indigenous ascidians in coastal harbors is known to be favored by the addition of artificial substrates (e.g., concrete or plastic vertical structures), which are preferred by exotic ascidians over natural surfaces already colonized by native species (Tyrrell and Byers 2007; Ramalhosa et al. 2021). In addition, ascidian species with a wider tolerance to diverse types of substrates are more likely to successfully colonize distant regions (Granot, Shenkar, and Belmaker 2017). Surprisingly though, at each of our collection sessions in La Spezia marina, we always found *P. zorritensis* on the mooring lines but never on the vertical wall of the docks themselves, where many other species were nevertheless present (e.g., *Styela plicata*). This might explain why Ferrario et al. (2017) did not report *P. zorritensis* from the Assonautica marina, as they collected fouling species by scratching the dock walls. If this is the case, therefore, this species may have been overlooked and could be more widespread than expected in the Mediterranean Sea. Thus, in future NIA inventories, it could prove intriguing to combine ropes alongside traditional settlement plates and to position such set-up at various distances from freshwater sources when present.

2.e) Conclusion

Colonial ascidians are one of the most significant invasive species inhabiting coastal areas worldwide. Given their ecological impact, it is essential to understand the physiological limits of colonial ascidians when faced with biotic and abiotic stressors and improve our ability to forecast their dispersal and establishment in novel habitats. *Polyandorcarpa zorritensis,* a non-native species originating from South America, is a widespread invasive species in marinas along the western Mediterranean. As salinity is a critical environmental factor for several marine species, we conducted laboratory experiments to determine the correlation between the reproductive and physiological characteristics of *P. zorritensis* and varying salt concentrations. To carry out this study, we collected spherules, which are hibernation structures from which new zooids can asexually develop under increasing water temperatures, from a harbor area in western Italy. In some of those spherules, we induced the development of zooids after artificial hibernation for spherules collected before winter or immediate incubation in a laboratory tank for spherules collected in spring. Salinities were chosen so that they represented lower salinities often encountered in harbor areas (29 ppt), marine salinities typical of the natural habitat of this species in Peru (36 ppt), and higher salinities, as usually measured in the Mediterranean Sea (40 ppt).

Physiological features such as size, heartbeat, and stolon pulse rates showed no significant difference between the salinity conditions despite considerable inter-individual variation, indicating that all tested salinities allowed *P. zorritensis* to hatch and thrive. Recording parameters to assess sexual and asexual reproductive efficiency revealed an interesting contrast. No clear differences were observed in the number of gonads among zooids hatched from spherules one month ago, however, some individuals reared at higher salinities released a larger number of embryos compared to those kept at lower salinities. Conversely, we found a negative correlation between most measures of asexual success, including the number of stolon bases, where new zooids sprout, the number of stolon tips, and the number of buds along them. This correlation was either statistically significant or showed a clear and consistent trend. These results strongly suggest that higher salinities, although possibly positively affecting sexual reproduction, have a negative impact on asexual reproductive strategies. This is consistent with the observation that *P. zorritensis* is usually confined to marinas and freshwater outlets in the Mediterranean region, which includes our

collection site. This suggests that the high salt concentration outside these areas may hinder the efficient dispersion of this species. The ratio between buds and stolons serves as a measure of the efficiency of the new zooids production. It is most closely correlated with lower salinities for spherule batches collected in spring. Our findings suggest that spherules from hibernation in nature are highly vulnerable to this physiological limitation, effectively hindering further invasion into the Mediterranean. This phenomenon seems not offset by any increase in sexual offspring under higher salinity conditions, which could be a possible strategy for further dispersal in suboptimal environments. In summary, our study contributes to a better understanding of the ascidian invasion dynamics by correlating abiotic factors with the success of reproductive strategies.

Chapter 3 - Transcriptomic Comparison Among Non-Embryonic Development (NED) in *Styelids*

Chapter Summary

In this chapter, the tunicate family of *Styelidae* is used as a proxy for the entire sub-phylum to compare the transcriptomic profile of independently evolved modes of non-embryonic development, specifically budding and whole-body regeneration. The chapter is divided into three sections. The first section includes the generation of stage-specific transcriptomes covering the ontogenesis of *Polyandrocarpa zorritensis* vasal budding and the analyses of the dynamic of gene expression characterizing this type of NED. The second part compares the transcriptomic dataset of vasal budding with the other two already-described types of budding in *Styelidae*. More specifically, it compares the transcriptomes of *P. zorritensis* with those of *Botryllus schlosseri* peribranchial budding and vascular budding transcriptomes that have already been published. The third section extends the transcriptome analysis to other species of *Styelidae*, including *Botrylloides leachii* and *Polyandrocarpa misakiensis*, to gather additional information on the potential conservation of the gene set involved in the different types of non-embryonic development in ascidians.

3.a) Introduction

Many tunicate species can propagate both sexually and asexually (see Chapter 1). Through sexual development, a zygote undergoes embryogenesis and develops either directly into an adult zooid, like in some Thaliaceans, or indirectly passing through a larval stage followed by metamorphoses, like in ascidians (Shenkar and Swalla 2011; Deibel and Lowen 2012; Stolfi and Brown 2015). On the other hand, during asexual reproduction, somatic tissues start a budding process that bypasses fertilization, embryonic development, larval stage, and metamorphosis but leads to a similar adult individual (Alié et al. 2021). Through budding, a zooid gives rise to one or several genetically identical individuals, called blastozooids. In some species, blastozooids remain connected physically and physiologically to one another through the tunic and may even share a common extracorporeal vascular system, forming colonies (Alié et al. 2021; Hiebert, Simpson, and Tiozzo 2021; Hiebert et al. 2022). While embryogenesis/metamorphosis and budding initiate from different cells and unfold through different ontogenesis, the final adult bauplan is conserved between sexual and asexual reproduction (Alié et al. 2021).

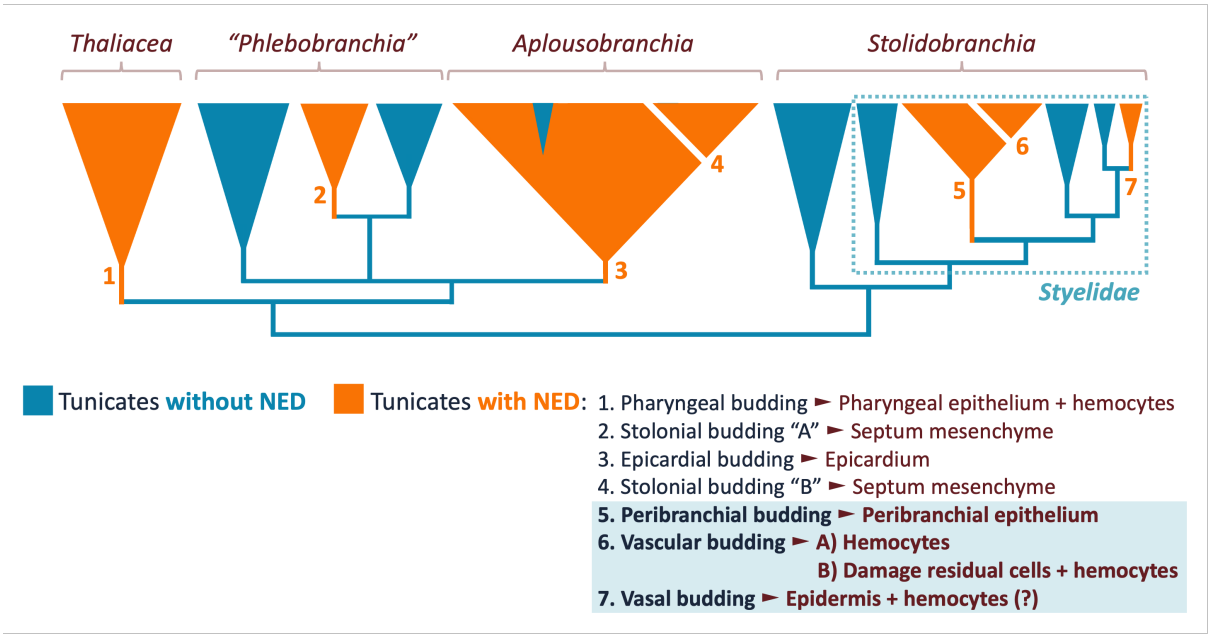

Figure 3.1: *Illustration of NED convergent evolution in Tunicates phylogeny.*

Budding (colonial) and non-budding (solitary) species are scattered across the four main orders of tunicate orders: Thaliacea, Phlebobranchia, Aplousobranchia, and Stolidobranchia. The phylogenetic distribution of colonial species clearly shows that asexual reproduction arose convergently multiple times (Alié et al. 2018; 2021). The variety of tissues and mechanisms involved in bud formation across different species further emphasizes the convergent acquisition of budding (Alié et al. 2021).

While embryonic development exhibits an extraordinary level of conservation amongst almost the majority of the main tunicate orders, budding ontogenesis involves a variety of cells and tissues even within a single order, all displaying different degrees of interaction between epithelial and mesenchymal cells (Kawamura et al. 2007; Kawamura and Sunanaga 2009; Brown and Swalla 2012; Ricci, Cabrera, et al. 2016; Scelzo et al. 2019; Ricci et al. 2022). According to Alié et al. (2021), budding in tunicates can be classified into seven distinct types, which reflect seven possible independent acquisitions, although a recent study suggests that one of them may comprise two subtypes (Ricci et al. 2022). As described in Chapter 1, almost all modes of budding converge towards a conserved stage referred to as the triploblastic stage, is characterized by the formation of a monolayered double vesicle (Alié et al. 2021). The seven budding types were classified according to the nature of the tissue giving rise to the inner vesicle, while the epidermis invariably forms the outer-most layer in every budding type:

1. **Pharyngeal budding:** like in Thaliacea. Inner tissues derive from the pharynx invagination and additional mesenchymal cell populations.

2. **Stolonial budding (type A):** Happening in *Polyoctacnemus patagoniensis* and three species of the *Perophoridae* family (*Ecteinascidia turbinata*, *Perophora viridis*, *Perophora japonica*), which are species traditionally classified in the paraphyletic "Phlebobranchia". The inner vesicle derives from hemoblasts.

3. **Epicardial budding:** All Aplousobranchia species except for the solitary *Rhopalaea idoneta*. The inner vesicle derives from the epicardium.

4. **Stolonial budding (type B):** Budding type present only in the *Clavelinidae* clade in Aplousobranchia. The inner vesicle derives from a mesenchymal septum.

5. **Peribranchial budding:** In most colonial Stolidobranchia species. The inner vesicle derives from the peribranchial epithelium.

6. **Vascular budding:** A budding type present in the sub-family *Botryllinae*. The inner vesicle derives from hemoblasts or from yet unidentified cells, depending on the species.

7. **Vasal budding:** the budding which was only observed in *Polyandrocarpa zorritensis*. The inner vesicle derives from the invagination of the epidermis.

In this manuscript, the focus will be on the NED strategies employed in *Styelid* ascidians only.

Styelids as a Model to Study Non-Embryonic Development

Non-embryonic development (NED), i.e., agametic development via budding and injury-induced whole-body regeneration (Alié et al. 2018), gives an organism the ability to replicate or restore both form and function, encompassing processes that involve fine control of cellular proliferation, cell death, cell differentiation, and cell migration. Indeed, understanding how some metazoan species can rebuild an entire body while others cannot is one of the big challenges in biology, with obvious important implications for human health and aging (Alvarado 2000; Adler and Sánchez Alvarado 2015). To better explore the very diverse forms and contexts in which NED occurs across metazoans, a comparative approach is clearly required, and the use of more than one suitable model is requisite to understand how extensive regenerative capacities have been gained and lost. Yet, the most challenging aspects of comparing phylogenetically distant metazoans models (besides the evident logistical problem of simultaneously breeding and studying multiple laboratory models) reside in the definition of homologous characters to compare between those species, as well as the establishment of cladistics frameworks for evolutionary interpretations (Tiozzo and Copley 2015; Sinigaglia, Alié, and Tiozzo 2022).

Within the tunicate family of *Styelidae,* we find solitary species, with regenerative abilities generally limited to some body structures, and colonial species able to bear different forms of NED (Alié et al. 2018). Both solitary and colonial species share comparable body plans and homologous structures (Gordon et al. 2020). The phylogeny of the family has been thoroughly reconstructed, and it shows that species like *Botryllus schlosseri* and

Polyandrocarpa zorritensis acquired NED convergently. At the same time, the absence of NED in the solitary specie *Styela plicata* is ancestral (Alié et al. 2018). This evolutionary scenario provides a special chance to compare different developmental modules, like genes, sections of GRN, or specific cell or tissue types, that regulate NED. It can help identify potential changes in gene regulatory networks and find common mechanisms that contribute to the evolution and diversification of NED. While *Botryllus schlosseri* has been routinely used in our laboratory for more than a decade and is already an emerging model for studies on NED mechanisms (Manni et al. 2019), *P. zorritensis'* NED just started to be described, yet suggesting the interplay between epithelial and mesenchymal putative stem cells (Scelzo et al. 2019).

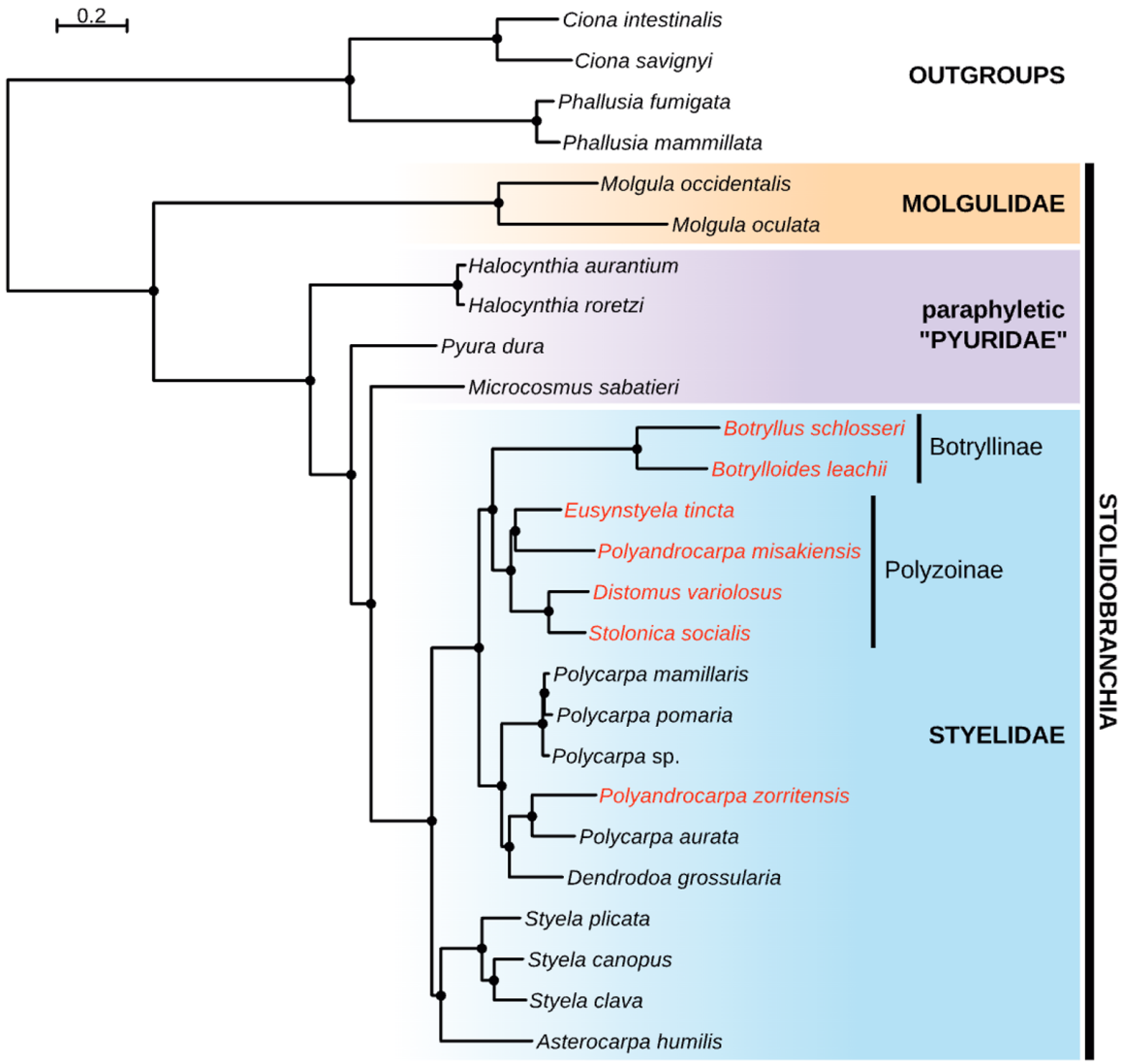

Figure 3.2: *Phylogenetic relationships between Stolidobranchia, with a focus on Styelidae (modified from Alié et al. 2018).*

Other two *Styelidae* species added to this work are *Botrylloides leachi*i and *Polyandrocarpa misakiensis*. *B. leachii* performs both vascular and peribranchial budding, and we can count on broad literature (Hyams et al. 2017; 2022; Blanchoud et al. 2017; Blanchoud, Rinkevich, and Wilson 2018) on them and publicly available transcriptome data for vascular budding (Zondag et al. 2016). *P. misakiensis* is also being used as a model in the NED context. Several papers are available on *P. misakiensis* NED (Hisata et al. 1998; Kaneko et al. 2010; Fujiwara and Kawamura 1992), and our collaborators generated a transcriptome on peribranchial budding in *P. misakiensis* for this study.

Vasal Budding in *Polyandrocarpa zorritensis*.

Vasal budding is a form of NED reported in *Styelidae*. It was recently described only in *Polyandrocarpa zorritensis* and consists of buds that emerge along the stolon (Scelzo et al. 2019) (figure 3.3). The stolon is an epithelial vessel that can reach several centimeters long, formed by an extension of the parental zooid's epidermis and covered by a thin tunic layer. Budding nests (BN) are the regions of the stolon designated for budding, with abundant vascular ampullae. They can resist adverse conditions by thickening the tunic and accumulating reserves, forming dormant spherules that can germinate under favorable conditions (Scelzo et al. 2019; Hiebert et al. 2022).

Bud development is triggered when the budding nest becomes completely isolated from the colony due to the abscission of the stolonial epidermis, cutting off hemocyte circulation between the colony and the nest. In laboratory conditions, budding can be induced by cutting the stolon with a razor blade. About 24 hours after abscission, the first signs of budding become visible: the number of ampullae (structures in the nest) decreases, and a new zooid (individual) begins to grow at the center of the nest. Within 4-5 days after abscission, all the ampullae have regressed, and two siphons open at the top of the newly formed zooid (Scelzo et al. 2019).

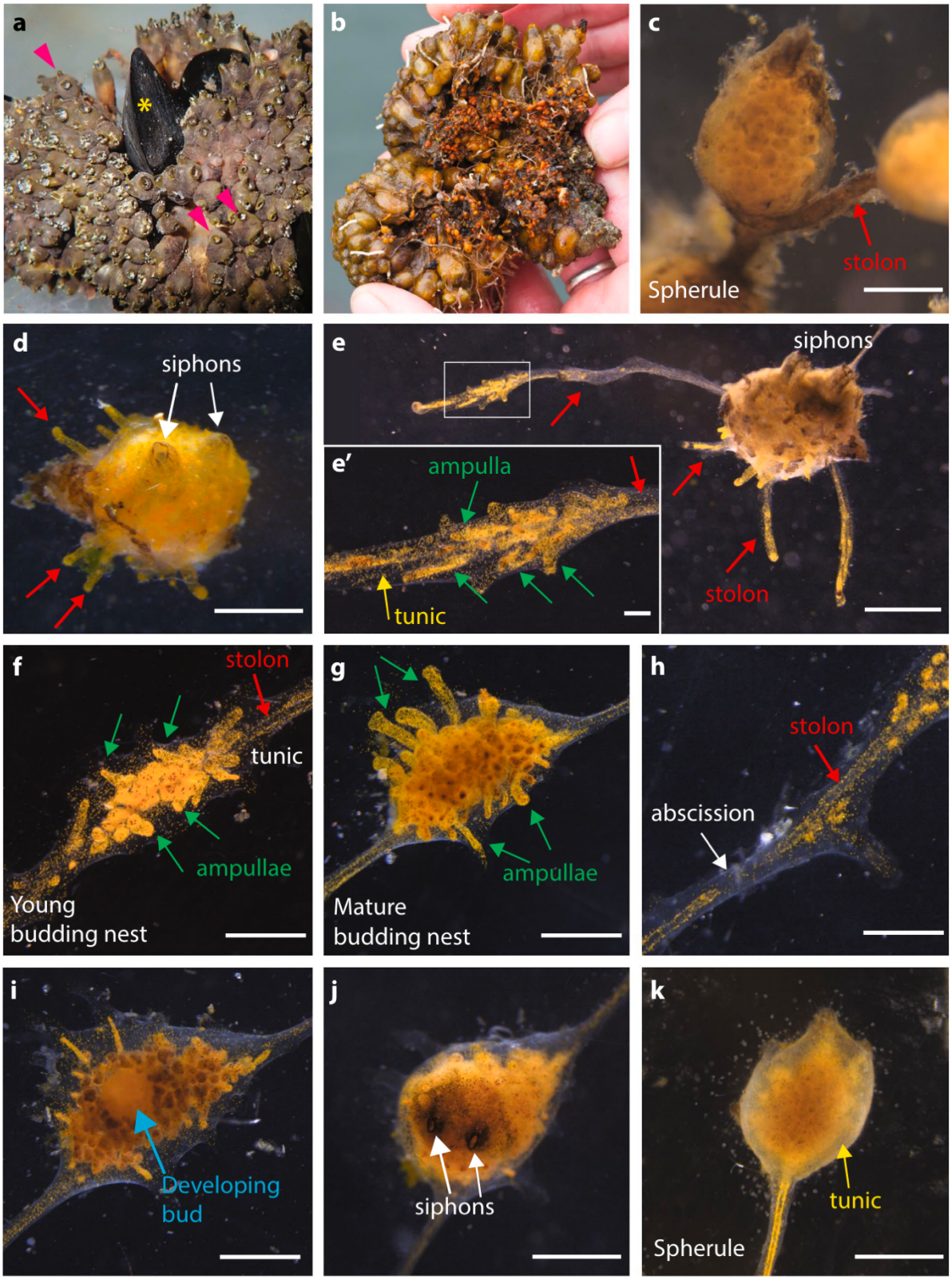

Figure 3.3: *Asexual cycle of Polyandrocarpa zorritensis in captivity.* ***A)*** *Polyandrocarpa zorritensis colony. Adult zooids can be found on other animals, such as mussels (yellow asterisk). Pink arrowheads show examples of individual zooids.* ***B)*** *Bottom side of the same colony as in* ***A****, showing the dense network of stolons and spherules.* ***C)*** *Detail of a spherule and the stolon (red arrow) connecting the spherule to the rest of the colony.* ***D)*** *One spherule one week after being transferred at 24 °C. The two siphons (white arrows) are open, and the protrusions (red arrows) that will attach to the substrate are recognizable.* ***E)*** *One completely developed zooid with several stolons (red arrows).* ***E')*** *Close-up view of one stolon: It is possible to recognize the main blood vessel (red arrow) and the ramified ampullae connected to it (green arrows), oriented in the same direction*

as the main vessel. The tunic (yellow arrow) covers the whole structure. ***F)*** *Young budding nest. The ampullae (green arrows) increased in number along the vessel (red arrow).* ***G)*** *Mature budding nest, composed of more compact ampullae (green arrows) that form a dome, highly pigmented on the top.* ***H)*** *Detail of a vessel at the abscission site (white arrow).* ***I)*** *Bud (blue arrow) developing inside the nest after abscission.* ***J)*** *Newly budded zooid with open siphons (white arrows).* ***K)*** *Spherule obtained by transferring a budding nest from 24 °C to 11 °C. (Scale bars c–e: 1 mm; e': 100 µm; f–k: 1 mm) (modified from Scelzo et al. 2019).*

During the formation of the budding nest, significant histological and cellular changes occur in the stolonial vessel and its surrounding ampullae. The epidermal cells change their shape and become roundish, connected to neighbor cells by tight junctions. The cytoplasm becomes enriched with various electron-dense bodies and granules. As the budding nest reaches a dome shape of 1-2 mm in diameter, the number and density of ampullae increase, and the central vessel and ampullae become indistinguishable from each other in histological sections. Budding nests and dormant spherules have similar histological and cytological properties. Spherules are another form the nest can transform into if abscission does not occur. After abscission, the stolonial epidermis and mesenchymal cells within the budding nest undergo cellular modifications and morphogenetic movements that eventually lead to the formation of a new individual (figure 3.3) (Scelzo et al. 2019).

The process of vasal budding involves the vascular epidermis and mesenchymal cells, leading to the formation of a new individual after abscission. The process involves four main steps: 1) Swelling, where a spherical cavity forms with polarized cells due to stolonial vessel inflation and the presence of mesenchymal hemocytes; 2) Invagination, during which epithelial folding creates two invaginations that merge to cover the epithelium; 3) Fusion, where invaginating edges unite, forming a thin cavity, and a cluster of undifferentiated hemoblasts appears; 4) Double Vesicle and Initiation of Organogenesis, where fusion results in a monolayered inner vesicle for organ formation, and the outer vesicle forms the new individual's external epidermis. Concurrently, the surrounding ampullae regress and significant ultrastructural changes occur in the ampullar epidermis (figure 3.4) (Scelzo et al. 2019).

Figure 3.4: *Early budding stages in Polyandrocarpa zorritensis.* ***A)*** *Schematic summary of vasal budding, depicting the four main steps: swelling, invagination, fusion, and double vesicle.* ***B)*** *Semi-thin section of a vasal bud at the swelling stage.* ***C)*** *Detail of the vascular epidermis on the top side (squared in* ***B****).* ***D)*** *Detail of the vascular epidermis on the bottom side (squared in* ***B****).* ***E)*** *Semi-thin section of a vasal bud at the invagination step, showing the invaginating epidermis (black arrows), the movement of the invaginating edges (pink arrows) and the part of the epidermis that goes on to form the floor of the inner vesicle (orange star).* ***F)*** *Detail of the bottle-shaped cells at the invaginating hinge points (as squared in* ***E****).* ***G)*** *Detail of*

*wedged-shaped cells at the invaginating edge (as squared in **E**). **H)** Semi-thin section of a vasal bud at the fusion step, showing the inner vesicle floor (orange star), the inner vesicle lumen (green asterisk), and the movement of the fusing borders (pink arrows). **I)**Detailed view of the inner vesicle wall. **I') ** Close-up of the cilia apex of the inner vesicle cells (as squared in **I**). **J)** Detail of hemocyte aggregate at the fusion area (as squared in **H**), showing undifferentiated hemoblasts (green arrows) and granules-containing cells (blue arrows). **K)** Semi-thin section of a vasal bud at the double vesicle stage. **L)** Detailed view of hemocytes located between the inner and the outer vesicle. **M)** Ampullar wall showing absence of cell membrane and cytoplasmic continuity between cells (pink asterisks). **N-N')** Contact between an ampullar epidermal cell and a morula cell. The blue arrow shows cytoplasmic continuity, a: ampulla, h: hemocytes, iv: inner vesicle, l: vessel lumen, m: mitochondria, n: nucleus, ov: outer vesicle, t: tunic (modified from Scelzo et al. 2019).*

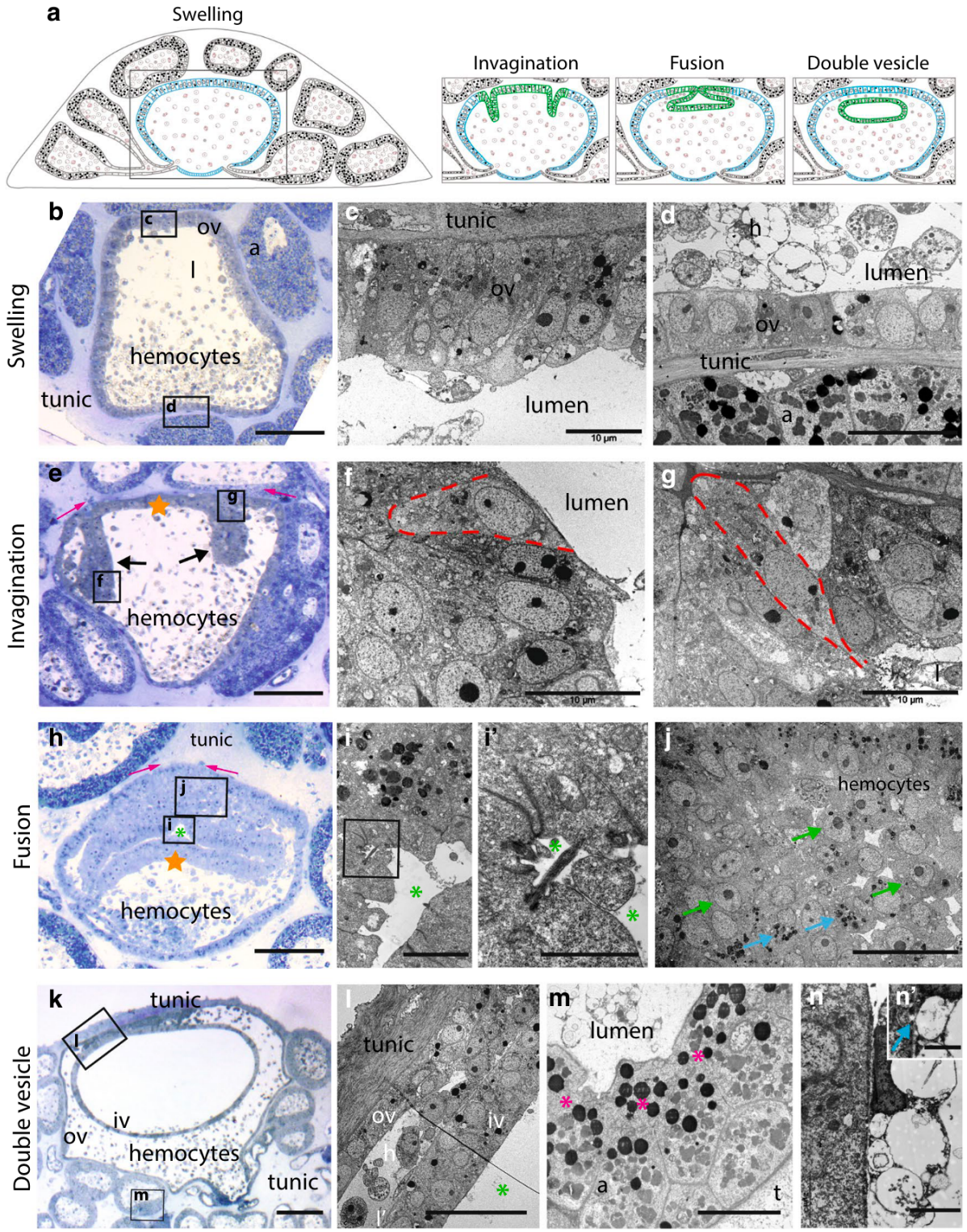

Peribranchial Budding

Most colonial *Styelidae* propagates asexually via peribranchial budding, also known as atrial, palleal, or pallial budding. Peribranchial budding arises from the peribranchial epithelium, which folds progressively and forms a hemisphere covered by the parental epidermis. The young budlet's tip then continues to invaginate, ultimately resulting in a double vesicle (figure 3.5). The peribranchial epithelium gives rise to the inner vesicle, while the outer vesicle comes from the epidermis. These two epithelial layers will trap free hemocytes (mesenchymal cells) from the vascular system. As development progresses, the epidermis develops from the outer vesicle, while most adult organs, such as the digestive tube, endostyle, central nervous system, pharynx, and peribranchial chambers, differentiate from the inner vesicle. In some species, it has been shown that the germline originates from the hemocytes (Scelzo et al. 2019).

The cell sources and the molecular mechanisms that trigger the onset of the bud still need to be fully understood. In the species *Botryllus schlosseri*, hemocytes transplantation experiments have shown that circulating putative stem cells could contribute to the development of blastozooids (Laird, De Tomaso, and Weissman 2005). However, it remains difficult to determine whether the chimerism occurs at the tissue level or is caused by contamination of donor hemocytes circulating in the complex network of hemocoel sinuses. In the same species, it has been shown that budding partially co-opts embryonic developmental genes and pathways, suggesting that peribranchial budding, at least in *B. schlosseri*, may be governed by rewiring of gene regulatory networks operating during sexual development (Tiozzo et al. 2006; Laird, De Tomaso, and Weissman 2005; Ricci, Chaurasia, et al. 2016; Ricci, Cabrera, et al. 2016; Prünster et al. 2019b; 2019a). For instance, *Botryllus schlosseri* co-opts and re-expresses transcription factors that specify the three canonical germ layers during embryogenesis in distinct and overlapping domains of the inner vesicle, indicating early cell commitment in different regions of the latter (Ricci, Cabrera, et al. 2016). Also, the nervous system and muscles co-opt neurogenic and myogenic modules from embryonic development and arise during the morphogenesis of the blastozooid (Prünster et al. 2019a, 2019b).

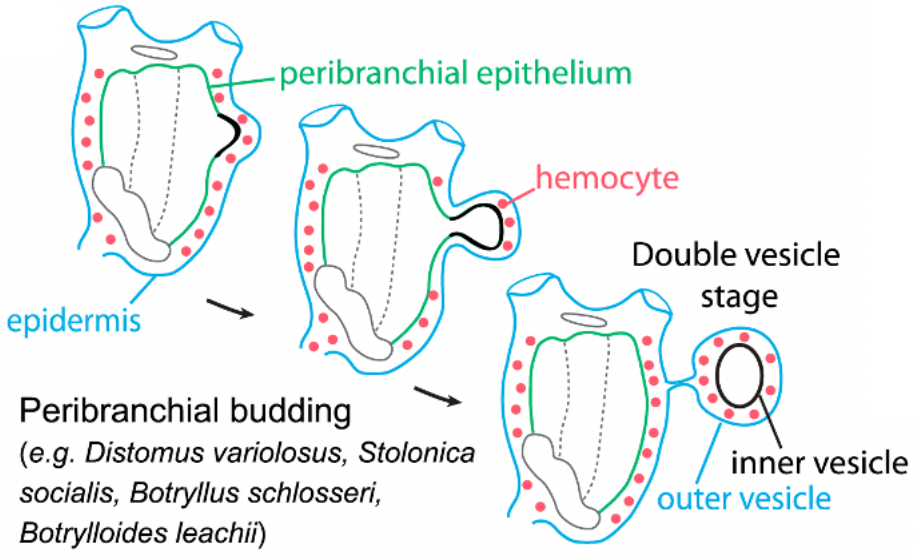

Figure 3.5: *Schematic representation of peribranchial budding at three successive stages, from peribranchial invagination to double vesicle (modified from Alié et al. 2020).*

Vascular Budding in *Botryllinae*

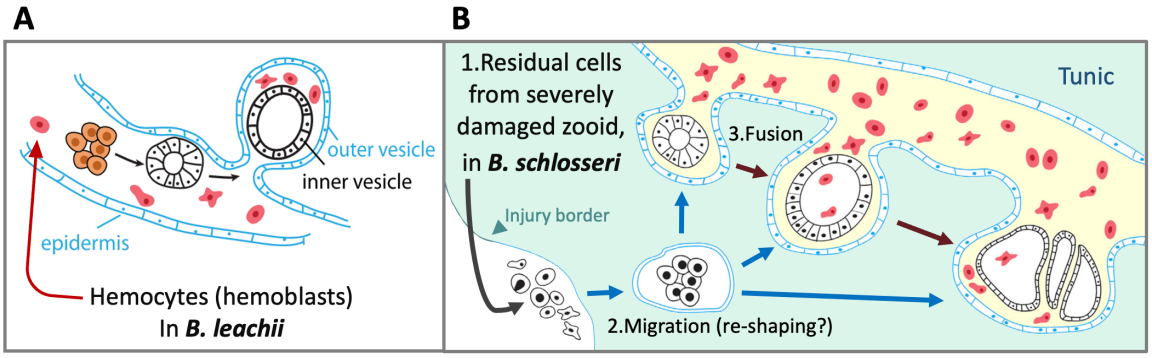

Figure 3.6: A) *Schematic representation of vascular budding at three successive stages, from hemocyte clustering to double vesicle.* ***B)*** *Scheme of vascular budding in Botryllus schlosseri (modified from Alié et al. 2020 and Ricci et al. 2022).*

The origin and early ontogenesis of vascular budding are still controversial, and the nature of the cells that initiate the process is still elusive (Voskoboynik et al. 2007; Brown et al. 2009; Sunanaga, Inubushi, and Kawamura 2010; Rinkevich et al. 2010; Nourizadeh et al. 2021; Ricci et al. 2022). Upon injury, in species like *Botrylloides leachii,* a cluster of undifferentiated hemocytes (figure 3.6.A), the hemoblasts, which express Integrin-alpha6 (IA6+) as well as other genes associated with pluripotency (*Piwi* and *Vasa*), resides in receptacles of the left vasculature, and are essential for the triggering of budding. The

beginning of the regenerative process seems to be regulated by *Notch* and *Wnt* signals (Kassmer, Langenbacher, and De Tomaso 2020). However, it is worth noting that the nature of these cells can vary between different species. In *Botrylloides leachii*, *Piwi2* and Vasa stem cell markers are expressed (Kassmer, Langenbacher, and De Tomaso 2020), whereas in *Botryllus primigenus*, Vasa and Piwi1 are not expressed in vascular buds (Kawamura and Sunanaga 2011). Additionally, in *Botrylloides violaceus*, Piwi proteins are only detected in certain peripheral cells of vascular buds (Brown et al. 2009). In a closely related species, *Botryllus schlosseri* vascular budding seems to be initiated by extravascular tissue fragments derived from the injured individuals rather than populations of IA6+ blood-borne cells (Nourizadeh et al. 2021; Ricci et al. 2022). Regardless of the cell/tissue of origin, the cell cluster forms a hollow vesicle that grows and becomes enclosed by the surrounding vasculature epithelia (Figure 3.6.B). This results in a double vesicle like the one seen during peribranchial budding. The inner vesicle will develop into future zooid organs, while the outer vesicle will become the epidermis (Ricci, Cabrera, et al. 2016). In *Botryllus schlosseri*, the expression pattern of markers of embryonic germ layer in the inner vesicle is similar to that reported in peribranchial budding. These results indicated that during both normal and injury-induced budding, a similar alternative developmental program operates via early commitment of epithelial regions (Ricci et al. 2022).

A comparative Bulk RNAseq Approach Across the Family of *Styelidae*.

The above description of the three budding types found in *Styelidae* emphasizes their mechanisms' fundamental differences and similarities. In fact, each budding mode involves different cells and tissues for the formation of the inner vesicle: the monolayered peribranchial epithelia in the case of peribranchial budding (Brown and Swalla 2012; Ricci, Cabrera, et al. 2016), mesenchymal cells or a mix of debris tissues in the case of vascular budding (Kawamura and Sunanaga 2009; Ricci et al. 2022), and a mix of vascular epidermis and mesenchymal cells in the case of vasal budding (Scelzo et al. 2019).

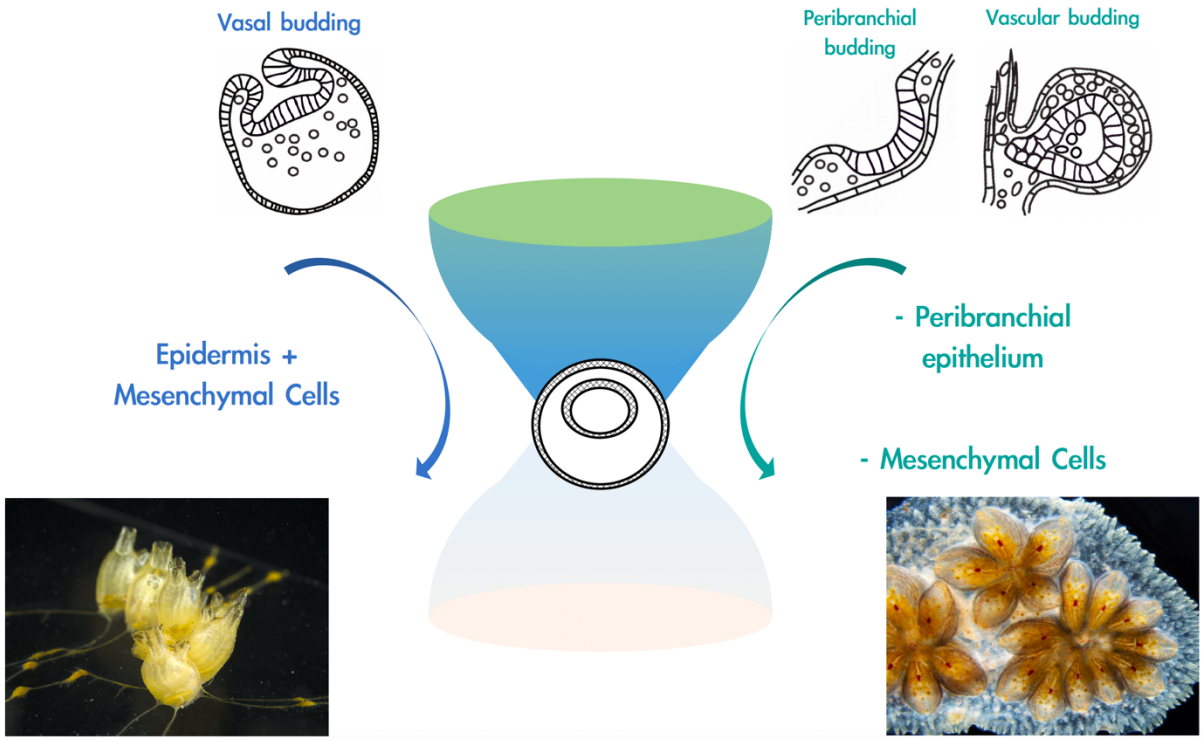

Figure 3.7: *Hourglass model for non-embryonic development, where, indifferently of the tissue and cell type source, all the NED strategies converge to a common double vesicle stage.*

Despite the different ontogenetic origins of the inner vesicle, several lines of evidence suggest that the independent acquisition of these three budding modes may result from the repeated co-option of homologous characters (Alié et al. 2018; Kassmer, Langenbacher, and De Tomaso 2019; 2020). Indeed, all three budding modes converge into a common morphogenetic stage called double vesicle (figure 3.7), the outer vesicle always being derived from the epidermis. On the molecular aspect, we found that the transcription factor *Nk4* (orthologue to the vertebrate homeobox-containing *Nkx2.5/6*) is similarly expressed in the forming inner vesicle: during vasal budding (in *P. zorritensis*) and peribranchial budding (in *B. schlosseri*), it is expressed in the early invaginating tissues, while during vascular budding (in *B. schlosseri*) it is expressed in the inner tissue aggregate (figure 3.8) (Alié et al. 2018). This was the first indication that non-homologous tissues implicated in convergently acquired budding modes may nevertheless share a common molecular identity specific to budding.

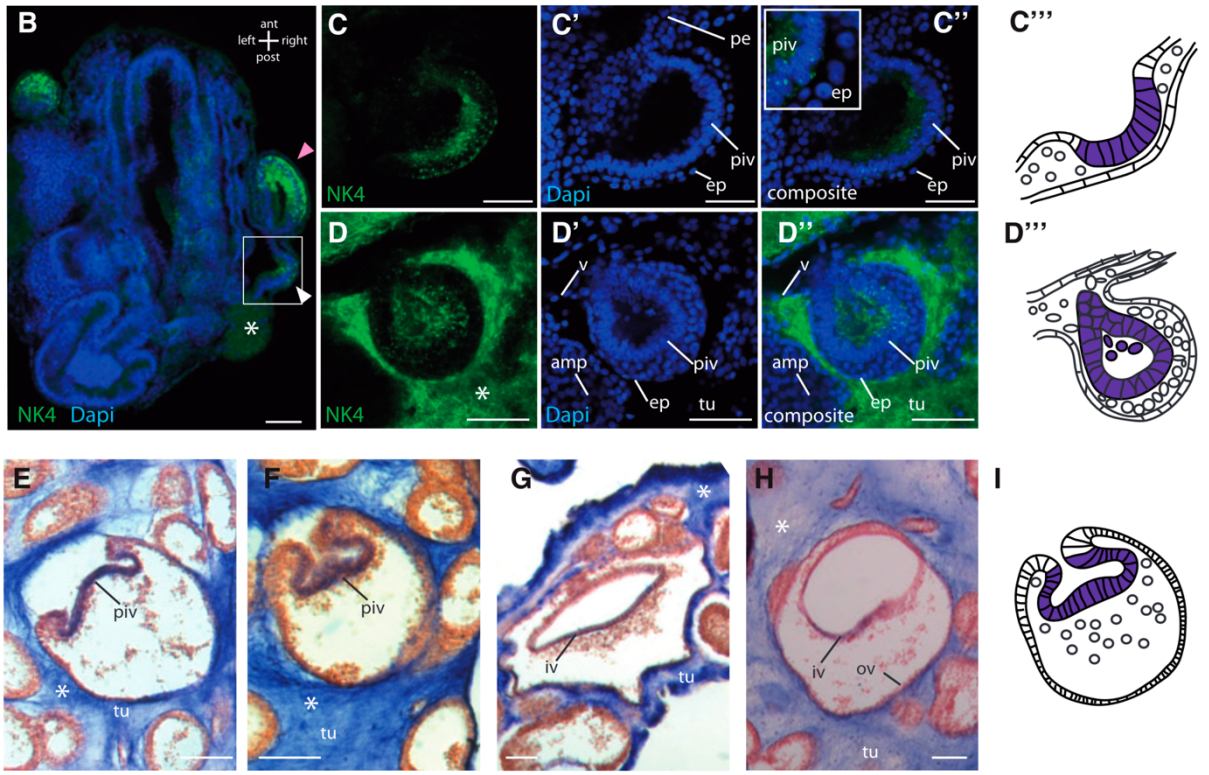

Figure 3.8: *Expression of the NK4 gene in Botryllus schlosseri and Polyandrocarpa zorritensis.* ***A)*** *Phylogenetic analysis of Nkx2.5/2.6 family members showing the orthology between B. schlosseri and P. zorritensis NK4 genes (NK4 orthology group was defined as the smallest group including Botryllus NK4, Ciona NK4, and mouse NKx2.5 and 2.6).* ***B-C'')*** *NK4 expression in peribranchial bud of B. schlosseri. In* ***B****, the zooid bears three buds at three different stages (white arrowhead shows the youngest one and the pink arrowhead shows the oldest one).* ***C–C'')*** *Close-up view of NK4 expression in the early peribranchial bud, inserted in* ***C*** *is highly magnified to show the unlabeled epidermis.* ***C''')*** *Diagram of NK4 expression in the peribranchial bud.* ***D–D'')*** *Close-up view of NK4 expression in a vascular bud at the double vesicle stage.* ***D''')*** *Diagram of NK4 expression in the inner vesicle of a vascular bud.* ***E–I)*** *Expression of NK4 in bud of P. zorritensis.* ***E)*** *Early invagination.* ***F)*** *Closure of invagination borders.* ***G)*** *Right after closure.* ***H)*** *Late double vesicle stage.* ***I)*** *Diagram showing NK4 expression in the forming inner vesicle of P. zorritensis. Asterisks show nonspecific staining in the tunic, amp: ampullae. ep: epidermis, iv: inner vesicle, ov: outer vesicle, pe: peribranchial epithelium, piv: prospective inner vesicle, tu: tunic, v: vessel (modified from Scelzo et al. 2019).*

In this chapter, I first studied the transcriptomic profile of key steps of vasal budding in *P. zorritensis*, in light of the cellular and morphological events known from previous work. I conducted two sets of analysis: a *de-novo* transcriptome approach was first used, and then when a genome of *P. zorritensis* became available, I re-analyzed the data in a genome-guided fashion. This allowed me to establish a comparison between the two approaches. Secondly, I compared these transcriptomic profiles with similar datasets for other types of budding in ascidians in order to identify molecular differences and similarities underpinning the independent evolution of NED in *Styelidae*. Finally, in the last section of this chapter, the analysis was extended to other species of *Styelids* to obtain more information on how conserved is the gene set involved in the different types of NED in ascidians.

3.b) Materials and Methods

Polyandrocarpa zorritensis Animal Husbandry

Animal rearing was performed as in Chapter Two, except for using natural seawater (NSW) instead of ASW. Dormant spherules harvested in La Spezia (44°06'12.4"N 9°49'33.0"E) were placed in tanks of approximately 10-12 liters of NSW at 24°C. For the spherule seeding, five spherules were placed on a glass slide of 5x7cm on the bottom of the water tank, using six glass slides per tank. New zooids would hatch around seven days after the seeding. The developing colonies were followed up in the tank until the sprouting of multiple budding nests (BN) from the growing stolons, upon which the colonies were harvested and processed for the experiments.

P. zorritensis Budding Tissue Live Staining

To be able to visualize the budding process inside the BN of *P. zorritensis*, I established a staining protocol in which I injected BSA 488 solution (bovine serum albumin conjugated with the fluorochrome Alexa-488 (ref. Invitrogen A13100) diluted 1:100 in PBS1X) into the stolons; this procedure had been adapted from a *B. schlosseri* protocol (Braden et al. 2014). The BSA is incorporated by some of the cells in the blood circulation as well as epithelial cells by endocytosis, and after 12 hours, the tissue morphology can be observed under fluorescent microscopy. The BSA 488 solution is injected either into the main ampulla at the tip of the stolon (active and proliferative ampulla, usually with dark cells in the tip – figure 3.1.A-A') or directly into the blood vessel (figure 3.1.C-C'). The amount of BSA 488 solution injected is not precise and varies according to the colony characteristics (blood vessel diameter, length, blood pressure, blood vessel ramification, and size of BNs). In the experiments performed in this study, the injected volume could vary between 2 and 6µl of BSA 488 solution. The injection is interrupted when all the blood circulation is fluorescent. It may be necessary to inject different stolon tips to stain a whole colony if the blood vessels of different colony sections are not connected. The pressure in which the BSA 488 solution is injected depends on the vessel's characteristics and ranges between 12 and 14 psi. Hence, it needs to be adjusted in order to facilitate dispersion within the blood circulation without leakage. The injection was performed using needles confectioned with borosilicate glass capillaries (ref.

EC164-0799, Harvard Apparatus - thin wall, with filament, 1.0mm outer diameter, 0.78 mm inner diameter, 100mm length) using a Narishige (ref. PN-31) needle puller (program: heat= 70, magnet sub= 55, magnet main= 103). The needles were backfilled with a micropipette using special tips (Microloader Pipette tip, Eppendorf, ref. 5242 956.003) for filling capillaries. The injection was performed by positioning the needle at approximately 45° (figure 3.1.B) using the microinjector Narishige (ref. IM-300).

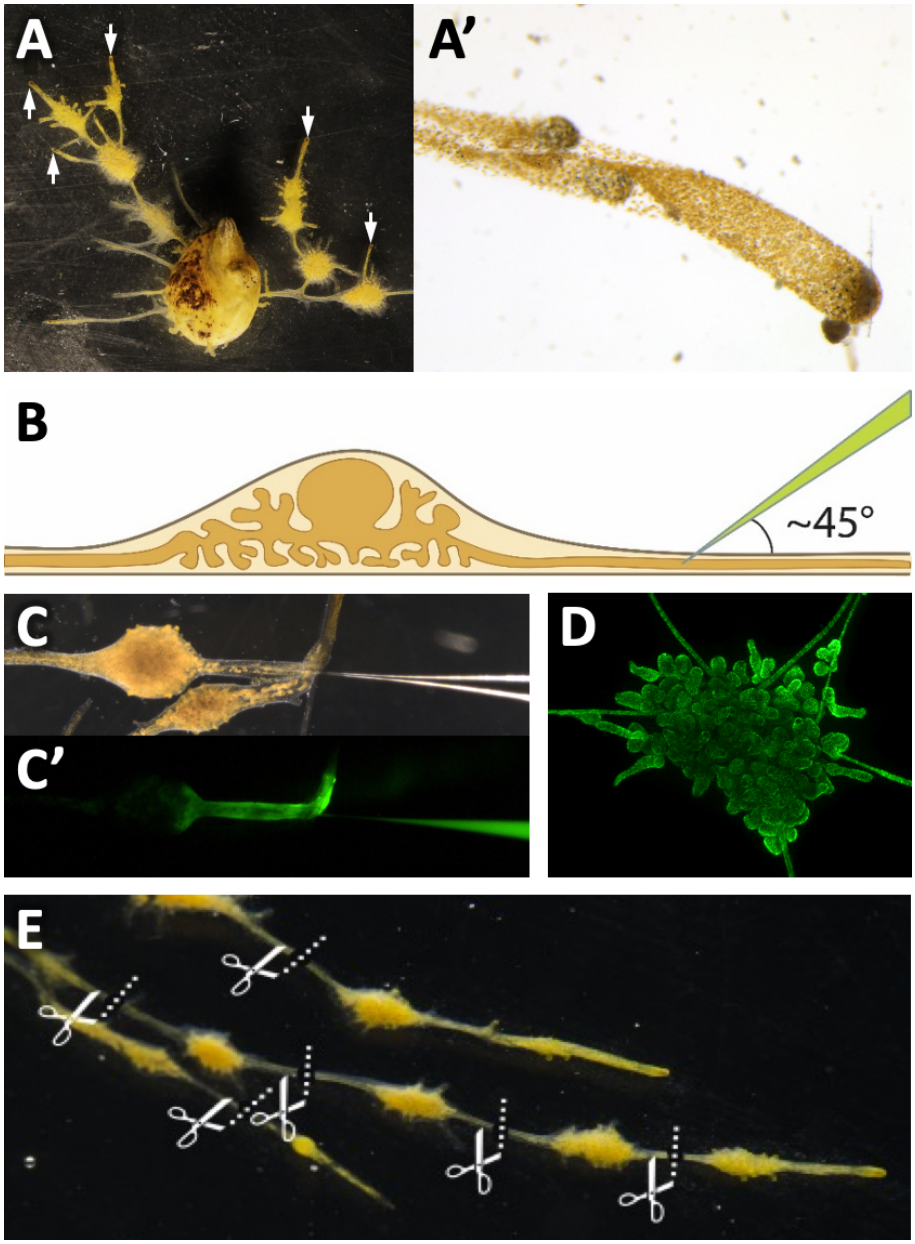

Figure 3.9: A) *Image showing a colony, with the white arrows indicating the healthy stolon tips.* ***A') B)*** *Illustration indicating how to perform the injection directly in the main blood vessel of a stolon, when injecting in the tip is not possible.* ***C-C') D)*** *Stained budding nest 12 hours after the injection.* ***E)*** *Illustration of how the stolons are cut and the budding nests are isolated for stimulating the budding.*

The colonies are observed for 24 hours after the BSA solution injection, and those BNs successfully retaining the stain will be selected for sampling. To stimulate the budding process in a BN, it is necessary to interrupt the blood circulation that connects it to the rest of the colony (figure 3.1.E). To this end, the stolons connected to BN are abscised with a syringe needle (BD Microlance 3 Needles – ref. 304000). During my first experiments, I recorded a timelapse in order to estimate the approximate budding developmental time (one photo every 3 minutes, n= 10), a useful data set for anticipating key developmental events. The animal observations and image acquisition were performed using a fluorescence stereoscope Leica (ref. M165, camera ref. MC170HD).

P. zorritensis RNA Extraction

For the RNA extraction, I collected tissues from different developmental stages containing a pool of 5 tissues per stage in each replicate (7 stages + 5 samples per stage + 3 replicates = 105 BN samples). The whole BN was harvested for the first two stages, whereas for the other 5 stages, only the budding region was dissected and processed. To dissect the budding vesicle out of the BN, a square was cut around it, leaving BN tissue equivalent to 1/3 of the vesicle's diameter around it (razor blades used for dissection: Fine Science Tools – ref. 10050-00). The dissected tissue was placed immediately into a microtube with the help of forceps (Dumont no4 – ref. 11294-00) and submerged in liquid nitrogen to be stored at -80°C until the RNA extraction (figure 3.2). At the moment of the RNA extraction, five samples belonging to the same stage were pooled together. The tissues were macerated in Lysis Buffer with the help of a plastic microtube pestle, then centrifuged for 5 seconds, after which the sample was processed according to the instructions provided by the RNA extraction kit's manufacturer (RNAqueous - Micro Total RNA Isolation Kit - Invitrogen, ref. AM1931). The extracted RNA was quantified, and its quality was assessed using the Agilent Bioanalyzer (nano-kit, ref. 5067-1511). Only the samples with RNA Integrity Number (RIN) higher than 9.8 were kept.

The isolated RNA samples were sent to NovoGene (NovoGene Company Limited – UK) in dry ice for RNA sequencing (RNAseq). The sequencing was performed on the NovaSeq 6000 platform (Illumina Inc.) using the following strategy: paired-end (PE) sequencing with a read

length of 150 bases (PE150). The quality control parameters for sequencing were set to achieve a Q30 score of at least 80% for each base, ensuring high-quality data generation.

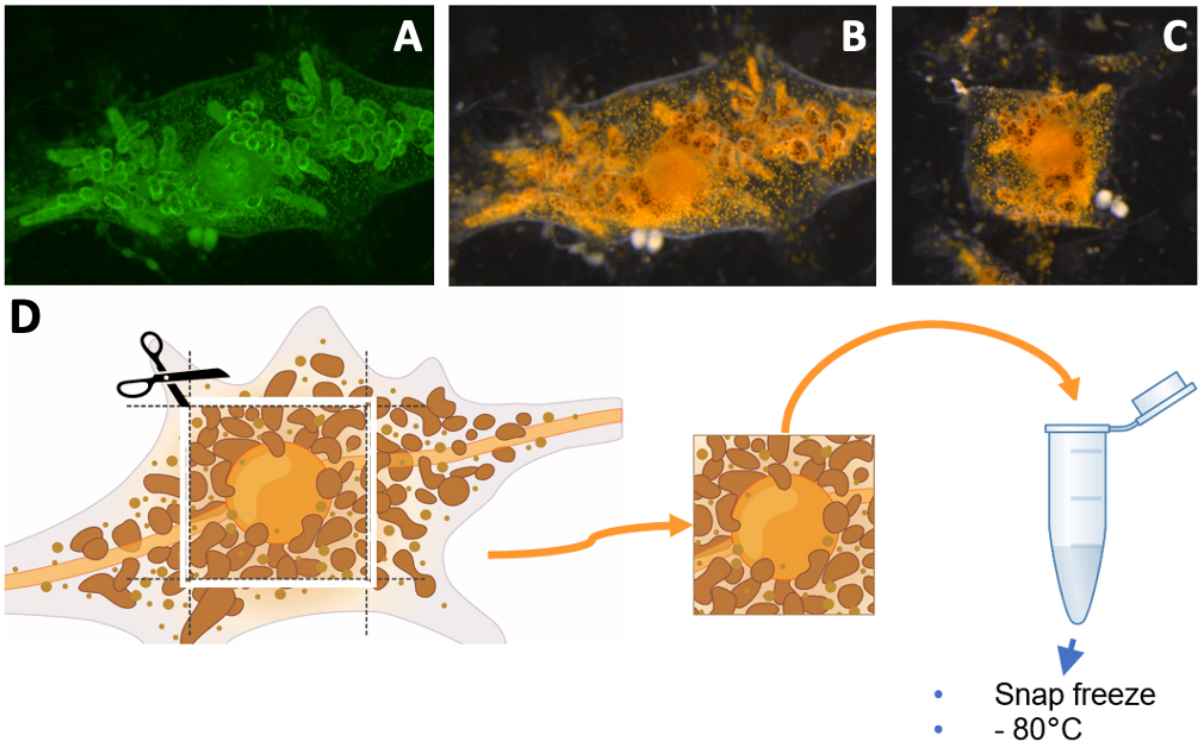

Figure 3.10: A) *Stained budding nest containing a budding vesicle.* ***B)*** *Budding nest in bright field for dissection.* ***C)*** *The dissected budding vesicle reduces in size after the dissection.* ***D)*** *Once the budding vesicle is dissected, it is immediately transferred to a sterile microtube and frozen in liquid nitrogen, being later stored at -80°C.*

P. zorritensis RNAseq Quality Control

The raw RNA sequencing data quality was assessed using the program FASTQC (version 0.11.7). FASTQC provides information on sequence quality, GC content, and potential contaminants or biases in the sequencing reads. Raw sequencing reads were trimmed to remove adapter sequences, low-quality bases, and any remaining contaminants using Trimmomatic (version 0.39). Trimmomatic employs a sliding window approach to remove low-quality bases and utilizes a trimming algorithm to remove adapter sequences.

Botryllus schlosseri, *Botrylloides leachii* and *Polyandrocarpa misakiensis* RNA-seq Raw Data Retrieval

For the comparative analyses with other *Styelidae* species, RNA-seq raw data was retrieved from previously published works from our group, provided by our collaborators, and produced by another research team. The raw data for Botryllus schlosseri peribranchial budding (PB) was produced by Ricci et al. (2016), where data was produced for two different budding stages (A2 and B2) and one control sample (Ref) using a non-budding adjacent tissue (figure 3.11). The author produced three replicates for the samples but pointed to only two as suitable for use (AS and AH). Only these two replicates were used.

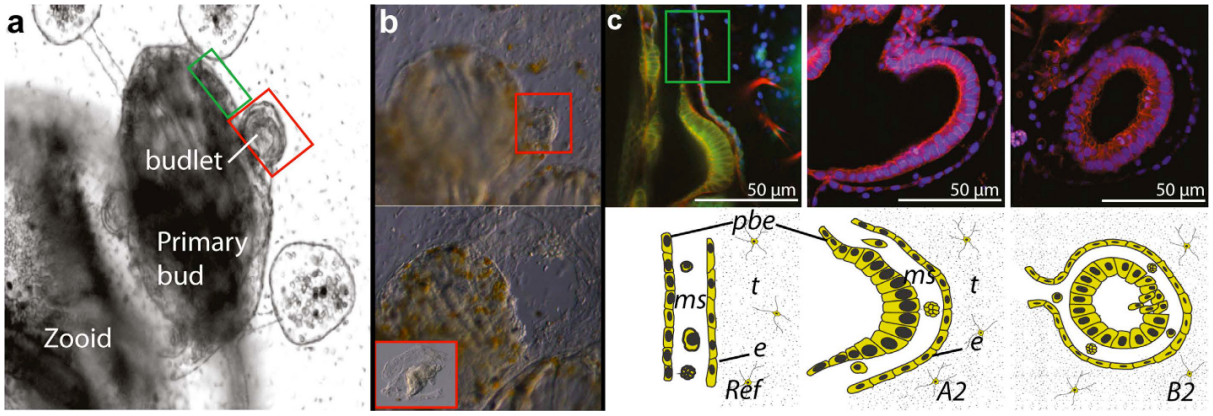

Figure 3.11: *Organization of a Botryllus schlosseri colony and blastogenic tissues.* ***A)*** *Part of a colony of B. schlosseri at stage B2 showing the emerging budlet (red frame) and neighboring non-budding tissues (green frame).* ***B)*** *Example of microsurgery performed to harvest the budlet, before (up) and after (bottom) ablation of the budlet. The red square in the bottom left corner shows the isolated budlet alone.* ***C)*** *Details of the tissues sampled for the RNAseq analyses: phalloidin and dapi staining (up), and sketches (bottom). From left to right: "Ref" (non-budding) sample, budlet stage A2, and budlet stage B2, respectively. Sampled tissues include a monolayered peribranchial epithelia (pbe), haemoblasts included in mesenchymal space (ms), a monolayered epidermis (e), and tunic (t) with embedded cells (modified from Ricci, Chaurasia, et al. 2016).*

For *B. schlosseri* was also included sequences from vascular budding (VB) extracted from the work of Ricci et al. (2022). This data comprises four regenerative stages, starting from the moment after provoking the injury (removal of all zooids and buds), in hours post-injury (hpi). These time points are 0 hpi, 6 hpi, 18 hpi, and 24 hpi. These time points cover the regeneration's start until the double vesicle stage (figure 3.12).

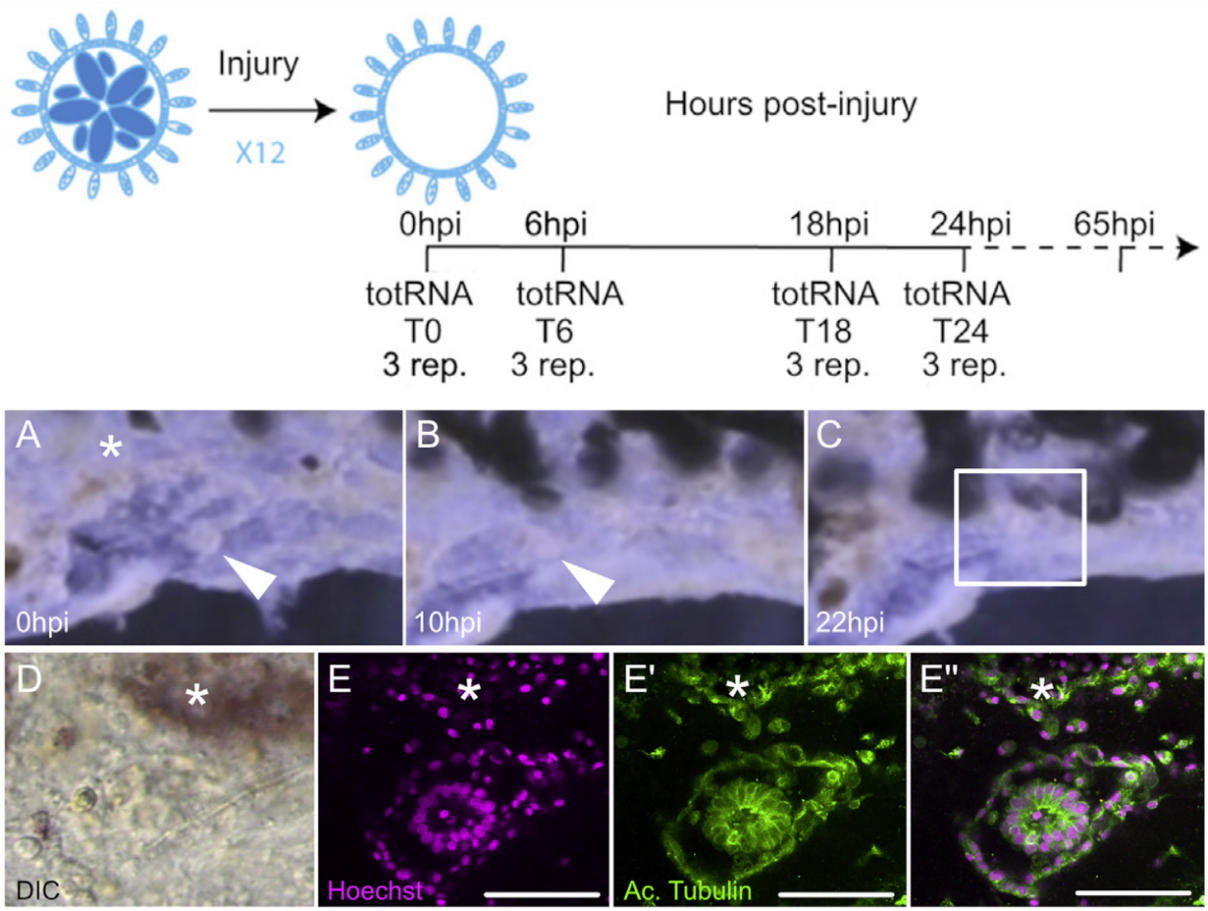

Figure 3.12: *Dynamic of the migration of extravascular tissues into the vascular network.* ***A–C)*** *Images showing the tissue left-over getting in close contact to the vasculature from* ***A)*** *0 h post-injury (hpi) to* ***B)*** *10 hpi and* ***C)*** *22 hpi.* ***D–E'')*** *Microscopic view of the areas squared in* ***C****.* ***D)*** *Transmitted light with DIC filter, the double monolayer vesicle can be seen in the tunic.* ***E)*** *Hoechst staining.* ***E')*** *Acetylated tubulin counter-staining.* ***E'')*** *Merge of* ***E*** *and* ***E'*** *(modified from Ricci et al. 2022).*

A vascular budding raw data from *Botrylloides leachi* was integrated in this study too. This data was obtained from the work of Zondag et al. (2016) and comprises one control sample (where the whole colony was sequenced, stage A) and six regenerative stages (stages 0 to 5, figure 3.13), from the moment after injury until the formation of new and active zooid (0 hpi to 216 hpi). This data does not posse replicates.

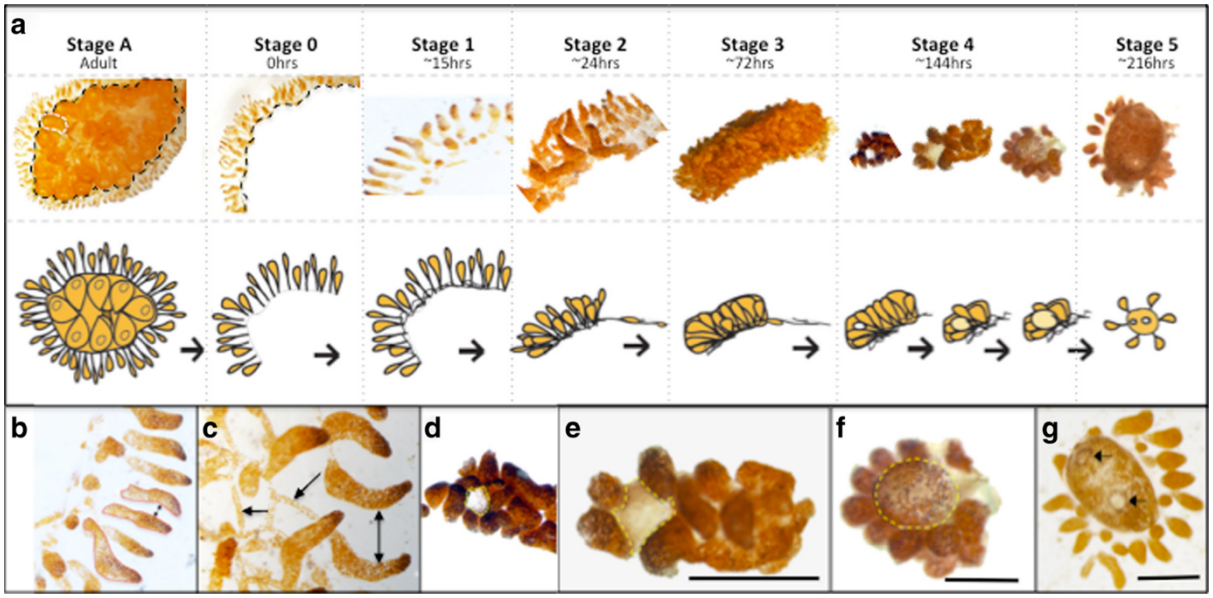

Figure 3.13: *Staging scheme used for WBR in B. leachi.* ***A)*** *Stage A: B. leachi colony prior to dissection. Black dashed line indicates the dissection sites. Stage 0: Marginal ampullae at 0 h, directly after dissection from the zooids. Black dashed line indicates dissection site. Stage 1: New vascular connections formed between ampullae, creating the beginning of a new circulatory system. Stage 2: Marginal ampullae starting to condense together, creating a compact network of blood vessels within the tunic matrix. Stage 3: Further condensing of the blood vessels. Stage 4: Formation of small transparent vesicle (regeneration niche) in the middle of the condensed blood vessels. The regeneration niche continues to expand in size, gaining pigmentation and ultimately forming the new adult. Stage 5: A fully developed zooid capable of filter feeding forms ~ 8 days.* ***B)*** *Higher magnification image of the terminal ampullae at Stage 0. Red line surrounding individual ampullae and double arrow indicating space between two ampullae. This distance inversely correlates with the time it takes the vascular tissue to reach Stage 3.* ***C)*** *Same as* ***B****, with arrows pointing at blood vessels connecting individual ampullae to one another.* ***D-F)*** *Higher magnification images of Stage 4. Yellow line surrounding the regeneration niche that grows to form the new adult.* ***G)*** *Adult zooid capable of filter feeding. Arrows indicating the two siphons present (atrial and peribranchial siphons). Scale bar represents 0.5 mm (modified from Zondag et al. 2016).*

Lastly was incorporated the peribranchial budding data obtained by our collaborators at the Fujiwara Lab (Kochi University). Asexual strains of *Polyandrocarpa misakiensis* were cultured on glass plates in culture boxes settled in the Uranouchi inlet near the Usa Marine Biological Institute, Kochi University. For RNA extraction, 40 growing buds of 4-6 mm long, 40 developing buds, 20 juvenile zooids, and five adult zooids from glass plates were collected. We extirpated growing buds from adult zooids using razor blades and allowed them to develop for two days to obtain developing buds. Pre-budding stage individuals were considered juvenile zooids, while budding stage individuals with all protruding buds removed were considered adult zooids. Total RNA was extracted from growing buds (GB), 2-day-developing buds (DB), juvenile zooids (JZ), and adult zooids (AZ) (figure 3.14), respectively, using the NucleoSpin RNA kit (Macherey-Nagel, Inc, PA, USA). No replicates were processed in this sample preparation. The RNA samples' qualities were assessed as for *P. zorritensis* and they were sequenced using the same parameters.

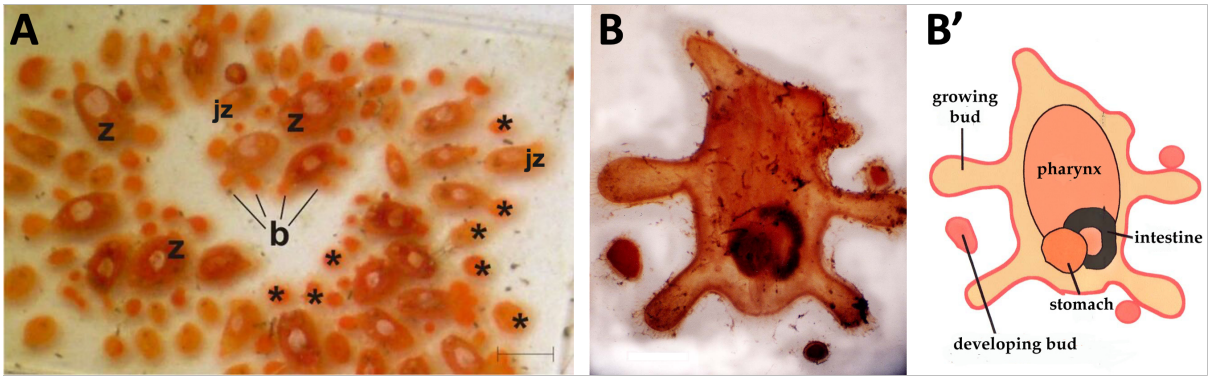

Figure 3.14: A) *Colony of P. misakiensis. Adult zooids (**z**) bear many buds (**b**). Developing buds are indicated by asterisks. And juvenile zooids marked by **jz**. Bar = 0.5 mm (modified from Ballarin and Kawamura 2009) .* ***B)*** *A ventral view of Polyandrocarpa misakiensis. The adult animal is about 1 cm-long. The branchial sac (pharynx), stomach and intestine are seen. The growing bud is an outgrowth of the parental body wall. The bud separates from the parent and starts cell differentiation and morphogenesis to reconstruct a new individual.* ***B')*** *Schematic representation of **B**. Images from Fujiwara's Lab.*

Polyandrocarpa zorritensis, Botryllus schlosseri, Botrylloides leachii and *Polyandrocarpa misakiensis De Novo* Transcriptome Assembly

The trimmed reads from each sample were used for *de novo* transcriptome assembly using Trinity (version 2.15.1). Trinity combines the reads from multiple samples to generate a comprehensive transcriptome assembly. It employs a three-step process: Inchworm, Chrysalis, and Butterfly (Trinotate), to perform the de Bruijn graph-based assembly. The assembled transcriptome was subjected to open reading frame (ORF) prediction using Transdecoder (version 5.5.0). Transdecoder identifies potential coding regions within the assembled transcripts and predicts the corresponding protein sequences. CD-HIT-EST (version 4.8.1) was employed to reduce redundancy and cluster similar transcripts. CD-HIT-EST groups highly similar sequences into clusters based on a specified sequence identity threshold, thereby reducing computational complexity. The resulting representative sequences from each cluster were used for downstream analysis.

Mapping and Differential Gene Expression (DGE) Analysis with *De Novo* Assembly

To determine gene expression levels, the quantification of transcript abundances was carried out using Kallisto (version 0.46.0), a tool known for its efficient pseudo-alignment-based approach to rapidly estimating transcript levels. By employing pseudo-alignment,

Kallisto effectively maps the reads to their respective transcripts, facilitating a robust assessment of gene expression levels. The output from Kallisto is assembled in a matrix where each row contains the expression values of each stage and every replicate, and the first column contains the sequence identifier (ID).

The data obtained from Kallisto contains the expression values for transcripts. To quantify gene expression, all the expression values of transcripts originating from the same gene were summed up, and the sequence ID kept was the one referring to the gene number. DESeq2 (version 1.38.3) was employed to investigate differential expression between the samples, which is a widely used software tool in RNAseq analysis. DESeq2 leverages a negative binomial distribution model suitable for count-based data such as RNAseq reads. By fitting this statistical model to the count data, DESeq2 identifies genes that display significant differences in expression levels across the samples. The output generated by DESeq2 provides a detailed list of genes that exhibit differential expression. Alongside these gene identifiers, the output also provides statistical significance measures, which help ascertain the reliability of the observed differences in expression. Additionally, DESeq2 supplies fold change values, which indicate the magnitude of change in gene expression between the compared samples.

Transcriptome Functional Annotation

For the transcriptome's functional annotation, Trinotate (version 2.15.1) was used. Trinotate is a comprehensive software suite for functional annotation and analysis of transcriptomic data, particularly *de novo* transcriptome assemblies. Trinotate employs tools like TransDecoder to identify potential protein-coding regions within transcript sequences, forming the basis for subsequent homology searches and functional annotations. During the homology search, Trinotate compares the predicted proteins against publicly available protein databases using BLAST (or DIAMOND) algorithms, identifying similarities to known proteins and transferring functional annotations from well-characterized proteins to the novel transcript sequences. Additionally, Trinotate enhances functional annotation by analyzing the predicted proteins to search for conserved protein domains and functional motifs. This analysis utilizes databases such as Pfam, SMART, or InterProScan, allowing

researchers to infer potential functions based on the presence of specific domains. The Gene Ontology (GO) module of Trinotate was not employed.

P. zorritensis Clustering and Gene Ontology Enrichment

For K-Means clustering, iDEP 1.1 was utilized to identify distinct expression patterns among the genes in our dataset. iDEP (Integrated Differential Expression and Pathway analysis - http://bioinformatics.sdstate.edu/) is a user-friendly web-based tool for analyzing high-throughput omics data, such as RNA-seq and microarray. For this analysis, the input data was the same gene expression matrix as the one used for the DESeq2 analysis, with the gene IDs being replaced by their respective gene names provided by Trinotate. The data was preprocessed, filtering out lowly expressed genes, and the Transcripts Per Million (TPM) values were normalized with log transformation for variance stabilization. The K-Means algorithm was then applied with appropriate parameters to identify optimal gene clusters. Interactive visualizations like heatmaps and scatter plots in iDEP 1.1 were used to interpret the clustering results. For GO term enrichment analysis, iDEP 1.1 was used to determine overrepresented biological processes, molecular functions, or cellular components among the gene clusters identified by K-Means. This involved selecting gene sets from the clusters, statistical testing using hypergeometric or Fisher's exact test, and multiple testing corrections to control for false discovery rate. Enriched GO terms and associated statistics were visualized through interactive bar plots or network diagrams in iDEP 1.1. The results from both clustering and GO term enrichment analyses were further interpreted to gain insights into the biological functions associated with different gene expression patterns. Normalized expression values were extracted for the genes per cluster and plotted using gnuplot for better visualization.

P. zorritensis and *B. schlosseri* Genome Assembly and Annotation

In the process of constructing a genome assembly pipeline, a combination of different sequencing technologies and assembly methods were employed. This entailed merging reads from the HiFi (long high-fidelity, PacBio - Pacific Biosciences of California, Inc.) sequencing platform with reads from both ONT (Oxford Nanopore Technologies, PLC) long-read sequencing and Illumina short-read sequencing (Illumina, Inc.).

HiFi is a type of sequencing technology known for producing high-fidelity reads. ONT is a sequencing technology that offers long-read lengths, which can be particularly helpful in spanning repetitive regions of genomes. Illumina sequencing produces shorter reads but with high accuracy.

The initial stage of the assembly involved solely the use of HiFi reads, which were processed using the Hifiasm assembler (version 0.18.2-r467). Hifiasm is designed to efficiently assemble genomes using the high-fidelity reads from HiFi sequencing. After this, the assembly's completeness was gauged using the Kat completeness metric (version 2.4.2).

To refine the assembly, ONT reads were incorporated. After adding the ONT reads, the haplotypes were purged, a process that removes redundant sequences arising from the diploid nature of genomes. Two distinct methods were utilized: the first is Purge Dups (v0.0.3) method, which identifies and removes haplotigs, which are alternative sequences of the same region in diploid genomes. It also helps in resolving overlapping contigs; The second is Purge Haplotigs (version 1.1.2), which seeks to identify pairs of contigs that are syntenic, meaning they have the same or very similar gene order.

For the scaffolding process, which involves arranging contigs in the right order and orientation, the ntLink program was used (version 1.3.8). This method capitalizes on both HiFi and ONT reads for lightweight mapping. Furthermore, to improve the quality of the assembled data, the HyPo program was employed (version 1.03). With this program was used a combination of HiFi and Illumina reads to polish and refine the genome assembly.

After the genome was assembled, it was annotated using the program Repeat Modeler2 (version 2.0.3), which identifies repeat sequences present in the genome, and after it was used the program Repeat Masker (open-4.0.6), which identified the repetitive sequences which were annotated and masked to prevent interference in subsequent analyses. Next, the program STAR aligner (version 2.7.10b) was used for this purpose. It aligned transcripts using the output from the HyPo polishing method, and RNAseq reads. The final genome annotation was carried out using Braker3 (version 3.0.2), an automated tool that predicts genes in eukaryotic genomes.

Lastly, to ensure quality and completeness at every step of the assembly and annotation process, BUSCO analysis was undertaken. BUSCO offers a standardized approach to quickly

assess the quality and completeness of genomic and transcriptomic data. It gives insights into the proportion of essential genes captured in the assembled or annotated genome, indicating its accuracy. This procedure was performed to assemble *Polyandrocarpa zorritensis* and *Botryllus schlosseri* genomes.

P. zorritensis and *B. schlosseri* Genome-Based Transcriptome Mapping

As mentioned above, the genome was first annotated using the Braker3 software. This program automates the process of genome annotation by combining two other tools: GeneMark-ET and AUGUSTUS. It particularly uses both ab initio gene prediction and evidence-based gene prediction to give more reliable results. For the alignment of RNA-Seq reads to the reference genome, HISAT2 was employed (version 2.0.1). HISAT2 stands for Hierarchical Indexing for Spliced Alignment of Transcripts and is specifically designed for aligning RNA-Seq reads. It is efficient and can align reads from spliced transcripts. Post-mapping, the quality of the alignment was inspected using SAMtools (version 1.17). SAMtools is a suite of programs for interacting with high-throughput sequencing data in SAM and BAM formats. It was used here to filter and ensure the quality of aligned reads. In addition, SAMtools was utilized to sort the BAM files, which arranges records in the BAM file based on the reference position. Following the alignment and quality check, StringTie (version 2.2.1) was utilized to estimate transcript abundances. StringTie is a tool that assembles RNA-Seq aligned reads into potential transcripts and then estimates their abundance. It does this efficiently and can work with even very low coverage samples. To detect genes that are differentially expressed across different conditions or treatments, DESeq2 was employed as described above.

Functional Annotation with Blast2GO and eMapper

The gene sequences obtained from the gene annotation were preprocessed by first performing a BLASTn (nucleotide-nucleotide Basic Local Alignment Search Tool) against the local database, using an appropriate E-value threshold for significance (standard values from the program Blast2GO, version 6.0). The BLAST results were imported into the Blast2GO software, and filtering criteria were applied to retain significant hits based on E-value, percent identity, and alignment length. The filtered BLAST hits were mapped to Gene Ontology (GO)

terms using Blast2GO's GO mapping functionality. Functional annotations were assigned to the query sequences based on the obtained GO terms, with each functional assignment annotated with an appropriate evidence code. Annotation validation was conducted using additional tools like InterProScan, and statistical analyses were performed to assess the distribution of GO terms and gain insights into the functional profiles of the annotated sequences (Conesa et al. 2005). Gene Ontology enrichment analysis was carried out to identify significantly enriched or overrepresented functional categories. Visualization techniques, such as graphs, charts, and tables, were used to interpret the results obtained from the functional annotation and analysis. The results of the functional annotation and analysis were summarized in a clear and concise manner as a “csv” format table.

In parallel, it was performed a functional annotation with eMapper (EggNOG-mapper v2.0) which starts with the identification of orthologous genes. eMapper leverages advancements in the eggNOG orthology resource to facilitate quicker and more efficient annotation of novel sequences using pre-established sequence profiles and orthology assignments. This tool is optimized for large datasets from genomes and transcriptomes and employs a multi-step process including sequence mapping, orthology assignment, and functional annotation, using HMMER or DIAMOND for matching and drawing data from a vast collection of Orthologous Groups. This ensures annotations are derived from the most relevant taxonomic sources, and users can even refine their results for increased reliability, drawing upon a wealth of curated functional descriptors (Cantalapiedra et al. 2021). The two functional annotations were merged to complement each other’s results in a single table.

In situ Hybridization Chain Reaction (HCR)

The colonies were maintained as described above, and to avoid any unspecific staining and fluorescence background, no BSA+Alexa488 was injected, the stage sampling was performed based on the developmental time identified with the timelapse imaging solely and later confirmed post-dissection. All the parts of the colony that are not desired (i.e., zooids, stolons without BN, BN without bud) before fixation. The remaining tissue is circulated with a lipid pen (PAP pen, Sigma Aldrich, ref. Z377821-1EA), and PFA 4% (in PBST1x) is added until the tissue is completely covered and left for pre-fixing for 30 minutes in a closed chamber.

After two cuts are made lateral to the vesicle and perpendicularly to the main blood vessel passing through the BN. And the sample is left fixing for one hour in the closed chamber. After this step, a cut is made in the same sense as the previous ones, dividing the vesicle into two halves and left fixing it for more 30 minutes. At the end of this step, the sample is carefully removed from the slide with the help of a razor blade, collected with forceps, and transferred to a microtube with PFA4% (in PBST1x) to continue fixation overnight, at 4o, under soft agitation (forceps and blades Ref).

On the following day, the samples are washed four times with PBST1x (15 minutes each wash, at RT, soft agitation) and after being transferred gradually to methanol 100% (methanol 25, 50, 75% in PBST1x + one wash with methanol 100%, 15 minutes of incubation each, at RT, soft agitation) and kept in methanol 100% to be stored at -20C until further use. RNA protect (1:500 – ref) was added to all the solutions used in this process (PFA, PBST, and methanol).

Prior to hybridizing, the samples were gradually transferred from methanol 100% back to PBST1x. The probes synthesis and in situ hybridization were performed according to the standard whole-mount protocol from Molecular Instruments (HCR™ RNA-FISH Protocols - generic sample in solution), with a few changes: tRNA (0.1 mg/ml – Torula Yeast RNA, Thermo Scientific Chemicals, ref. J23551.Q5) and Salmon sperm (100 µg/mL – Invitrogen ref. 15632011) were added to the Hyb solution, and all the incubations were performed under soft agitation. In the last wash to remove the hairpins, was added DAPI (10 µl/ml – Invitrogen, ref. D3571) and incubated for 15min, followed by three washes of 15 minutes each with PBST1x. To mount, all the PBST1x was removed and replaced by glycerol 50% in PBS1x, and the samples were mounted on a microscopy glass slide and covered with a cover slip. Four layers of eyelet adhesives were used as spacer between the slide and the cover slip to not smash the sample and to not let the mounting media leak. The gene sequences used to synthesize the probe and the pool of probes can be found in appendix 7.

Orthologues Assignment with OrthoVenn

OrthoVenn3 is a tool designed for comprehensive comparative genome analysis, allowing to discern evolutionary relationships and genetic variations across different species based on protein sequences. Each species protein sequences in Fasta format were uploaded

in the OrthoVenn3 website (https://orthovenn3.bioinfotoolkits.net/). OrthoVenn3 produces outputs such as Venn Diagrams for smaller species sets and UpSet tables for larger sets. Powered by the OrthoFinder2 tool, OrthoVenn3 identifies orthologous clusters, offering visualization options through UpSet and Venn diagrams. All the parameters were kept as the program's standards (Sun et al. 2023).

DEG Comparative Visualization Using Heatmap

In order to compare gene expression profiles across species, transcripts were normalized using Z-scores. This means, the raw expression values were subtracted from the average expression value and this difference was then divided by the standard deviation. To automatize this step, a Fortran code was used. Next, were extracted the candidate genes that were present in the overlapping result from OrthoVenn and a matrix was built. The samples with replicates were averaged among them and the final matrix was uploaded in the online program Heatmapper, using the option of expression heatmap with standard pre-set parameters (http://www.heatmapper.ca/expression/).

Protein Alignment and Phylogeny

Protein phylogeny examines the evolutionary relationships of species or genes by comparing amino acid sequences. The protein sequences were retrieved from our transcriptome assemblies' pipelines for the *Styelidae* species of interest, and the sequences for the other species were extracted from NCBI (the reference codes for these proteins are present in their phylogeny in appendices 8, 9, 10, 11, and 12). The program of choice for performing the alignment was Unipro UNIGENE, where the workflow involves using MAFFT option, a fast and precise Multiple Sequence Alignment program, to align these sequences, using the following parameters: Gap opening penalty of 1.53. Once aligned, PhyML, known for its speed and accuracy, is utilized to construct a phylogenetic tree representing these relationships. This construction employs the BioNJ algorithm, Blosum62 as substitution model, empirical equilibrium frequencies, estimated proportion of invariable sites, estimated gamma shape parameter, and a bootstrap value of 1000 for reliability. After building the tree, it's visualized using TreeViewer for interpretation.

3.c) Results and Discussion

In vivo BSA Labeling Allowed Identifying Seven Budding Stages

In vivo BSA labeling allowed the identification of seven budding stages. A previous study defined four main morphological changes during vasal budding based on histological analyses: swelling, invagination, fusion, and double vesicle. The same study also reported at which respective time after the triggering of budding each of those developmental stages was observed (Scelzo et al. 2019). Yet, inter-individual variations of the timing of the developmental events during the budding process exist, and, therefore, the different developmental stages could only be precisely attributed after fixation and subsequent histological observations of each specimen. Using the BSA-Alexa488 labeling protocol allowed following in vivo the unfolding of vasal budding and reproducibly selecting seven stages that start from the moment the budding process is activated until the formation of the inner vesicle (figure 3.15.B). These seven stages were then chosen for RNA extraction/sequencing: Control, resting nest (**Ctrl**): comprising BNs in which budding had not been stimulated yet; Pre-swelling (**PSw**): a nest that was harvested three hours after budding stimulation; Swelling (**Sw**): when the vesicle formed in the main blood vessel of the BN is conspicuously spherical; Early Invagination (**EI**): after the swelling stops, the cells in the upper portion of the vesicle undergo a morphological change and become columnar. The borders of this columnar area start to invaginate by apicobasal constriction, thus delineating an invagination circle (Scelzo et al. 2019); Late Invagination (**LI**): the vesicle continues invaginating and, therefore, the diameter of the invagination circle decreases. We attributed the late invagination stage to the budding process from the moment the diameter of the invagination circle went below 50% of the initial diameter of the invaginated tissue; Fusion (**Fus**): at the end of invagination the folding borders meet and fuse; Double Vesicle (**DV**): the fusion will result in a smaller vesicle inside the initial vesicle, and then, this inner will swell to subsequently start the organogenesis process (figure 3.15.A). The DV stage was collected before any mark of organogenesis was visible. For each stage, 3 replicates consisting of five pooled buds were collected.

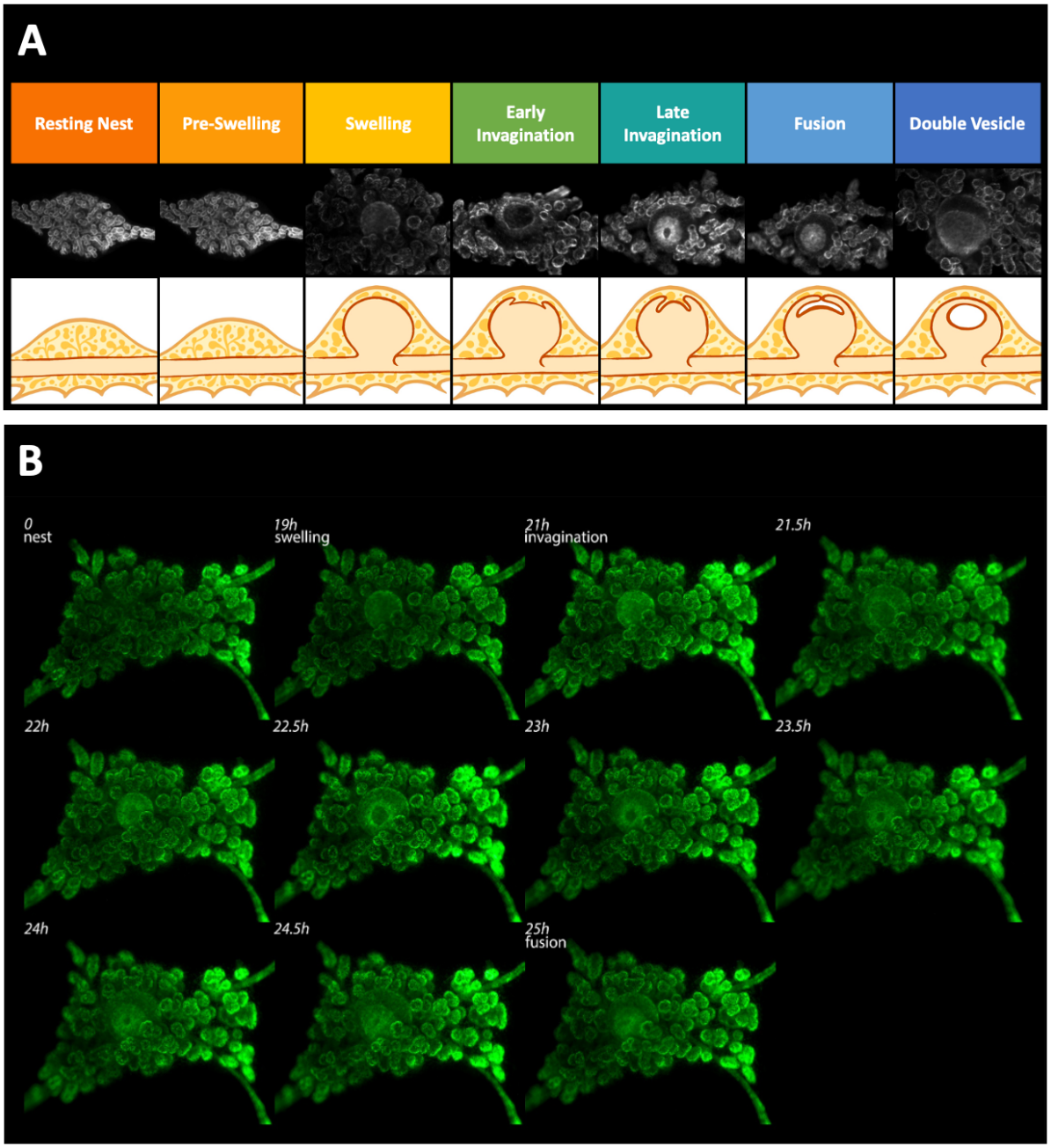

Figure 3.15: A) *Seven stages selected for transcriptome synthesis.* ***B)*** *Time-lapse imaging of the vasal budding development with approximated hours between each stage.*

P. zorritensis De Novo Transcriptome Assembly and Mapping

The result's quality was verified using the program FastQC, and all samples had scores higher than 20 and had a total number of sequences > 27 × 10^6 (Figure 3.16). Low-quality reads were removed using the program Trimmomatic, thus reducing the number of reads by 25-30% and increasing the quality score to above 36. Initially, no genome of *P. zorritensis* was

available, so these reads were assembled *de novo* using Trinity, which predicted 283,181 contigs (putative transcripts) corresponding to 178,951 putative genes (GC: 42.23%). The assembly completeness was assessed with BUSCO, resulting in 96.8% of complete matches, containing 77.5% doubly mapped contigs and 19.3% singly mapped contigs, suggesting a high level of redundancy. TransDecoder was employed for predicting open reading frames (ORFs) within the assembled transcripts. The analysis resulted in 112,755 contigs containing predicted ORFs. The complete matches were reduced to 95.8%, and the doubly mapped contigs to 66.4%. Then, I used CD-HIT-EST to collapse redundant sequences in the transcriptome assembly, which resulted in 30,662 putative genes (non-redundant sequences) and 48,345 contigs, with GC content of the collapsed transcriptome of 43.83%. This step reduced the doubly mapped contigs to 5.7%.

The transcript expression levels were quantified using Kallisto, and each sample's TPM values were pulled together in a single matrix. When reads map to several contigs (e.g., several isoforms from the same gene), Kallisto estimates (using an Expected-maximization procedure), to which contig the reads most likely belong (Deschamps-Francoeur et al. 2020). Therefore, the TPM expression values of all transcripts belonging to the same gene were summed to calculate the gene expression instead of its transcripts' expression. In parallel, the sequences obtained with TransDecoder were used for the transcriptome functional annotation using the program Trinotate and the output from the BLAST module was used in the next steps (figure 3.16).

P. zorritensis DEG Based on *De Novo* Transcriptome Assembling (DNTA)

The differential gene expression was calculated with DESeq2, and it showed through principal component analysis (PCA) and heat mapping (figure 3.17) that the data cluster in three main groups: Control (Ctrl) replicates, pre-swelling (PSw) replicates, and another compact cluster comprising all the other later stages. In this latter cluster, the swelling (Sw) replicates groups close to one another, and in the heatmap, they form a separate cluster on their own.

De novo transcriptome assembly

1. FastQC + Trimmomatic

Example: Ctrl 1

Before Trimmomatic

Measure	Value
Filename	Ctrl_1_1.fq.gz
Total Sequences	27627252
Sequences flagged as poor quality	0
Sequence lengh	150
%GC	43

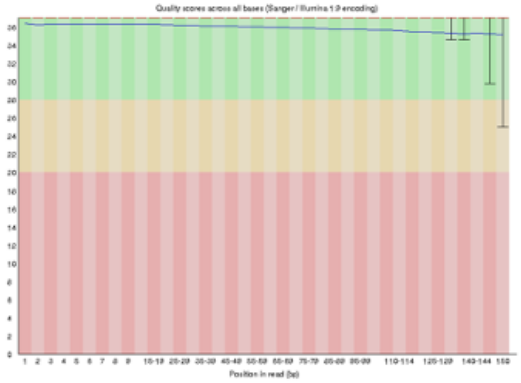

After Trimmomatic

Measure	Value
Filename	Ctrl_1_1_paired.fq
Total Sequences	20211621
Sequences flagged as poor quality	0
Sequence lengh	75-150
%GC	43

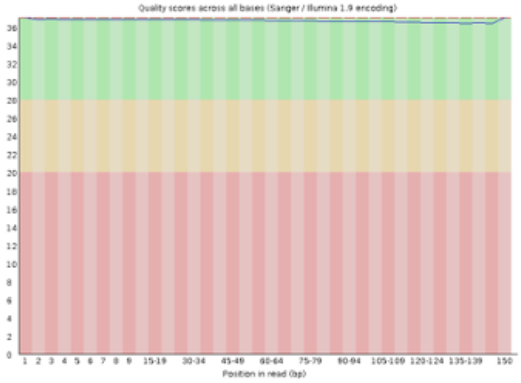

1. Total Sequences > $27^{\wedge}10^{6}$ (score higher than 24)
2. Removal of low quality reads – 25-30% (final score higher than 36)

2. Trinity → Transcriptome assembly

"Genes" = 178951 | Transcripts = 283181 | GC: 42.23%
Busco: C:96.8% [S:19.3%, **D:77.5%**], F:1.5%, M:1.7%, n:954

3. TransDecoder → Transcripts prediction

Contigs = 112755
Busco: C:95.8% [S:29.4%, **D:66.4%**], F:1.9%, M:2.3%, n:954

4. CD-HIT-EST → Collapses redundancy

"Genes" = 30662 | Contigs = 48345 | GC: 43.83%
Busco: C:95.7% [S:90.0%, **D:5.7%**], F:1.9%, M:2.4%, n:954

5. Kallisto ↴

Transcripts expression

6. Trinotate ↴

Functional annotation

7. DESeq2 → Differential transcript expression (DTE)

8. iDEP → k-Means clustering and GO term enrichment

Figure 3.16: *De novo transcriptome assembly to differential expression analysis pipeline.*

The DESeq2 output identified 7812 (of 30662) genes being differentially expressed in at least one of the seven budding stages. In order to gather more information on the genes and indirectly on the pathways that are up- or downregulated during *P. zorritensis'* vasal budding, I conducted multiple pairwise comparisons between the seven budding stages. Important differences in gene expression were observed in all comparisons with respect to the control. Comparisons to Ctrl yielded 927 upregulated and 557 downregulated DEGs for Sw, 341 upregulated and 449 downregulated DEGs for PSw, 1048 upregulated and 647 downregulated DEGs for LI, 1051 upregulated and 665 downregulated DEGs for Fus, 1093 upregulated and 661 downregulated DEGs for EI, and 1087 upregulated and 713 downregulated DEGs for DV (Figure 3.18).

The comparison between PSw and other stages also yielded a large number of DEGs. PSw showed 689 upregulated and 454 downregulated DEGs compared to Sw. When compared to LI, PSw exhibited 865 upregulated and 606 downregulated DEGs. Similarly, PSw showed 932 upregulated and 612 downregulated DEGs compared to Fus, and 927 upregulated and 613 downregulated DEGs compared to EI. In the comparison between PSw and DV, 978 DEGs were upregulated, and 683 DEGs were downregulated.

Comparing Sw to stages other than Ctr and PSw did not yield a high number of DEGs. When compared to LI, Sw exhibited 11 upregulated and 10 downregulated DEGs. Sw showed 52 upregulated and 29 downregulated DEGs compared to Fus and 23 upregulated and 24 downregulated DEGs compared to EI. In the comparison between Sw and DV, 81 DEGs were upregulated, and 27 DEGs were downregulated.

All the later stages resulted in significant numbers of DEGs compared to Ctrl and PSw stages. There were no DEGs between those later stages, except between DV and EI (only 9 DEGs) and between Fus and EI (only 2 DEGs).

This result emphasizes what had been apparent in the PCA and heatmap analyses, namely a higher difference in DEGs between the initial stages before the initiation of the budding (Ctrl and PSw) and the later stages when the budding becomes visible (Sw to DV). It also shows that despite their distance from the remainder of the stages, there are still more DEGs between Ctrl and PSw than in any comparison among the later stages. To obtain more information on the composition of the DEGs between the budding stages, I performed a GO term enrichment for Biological Processes.

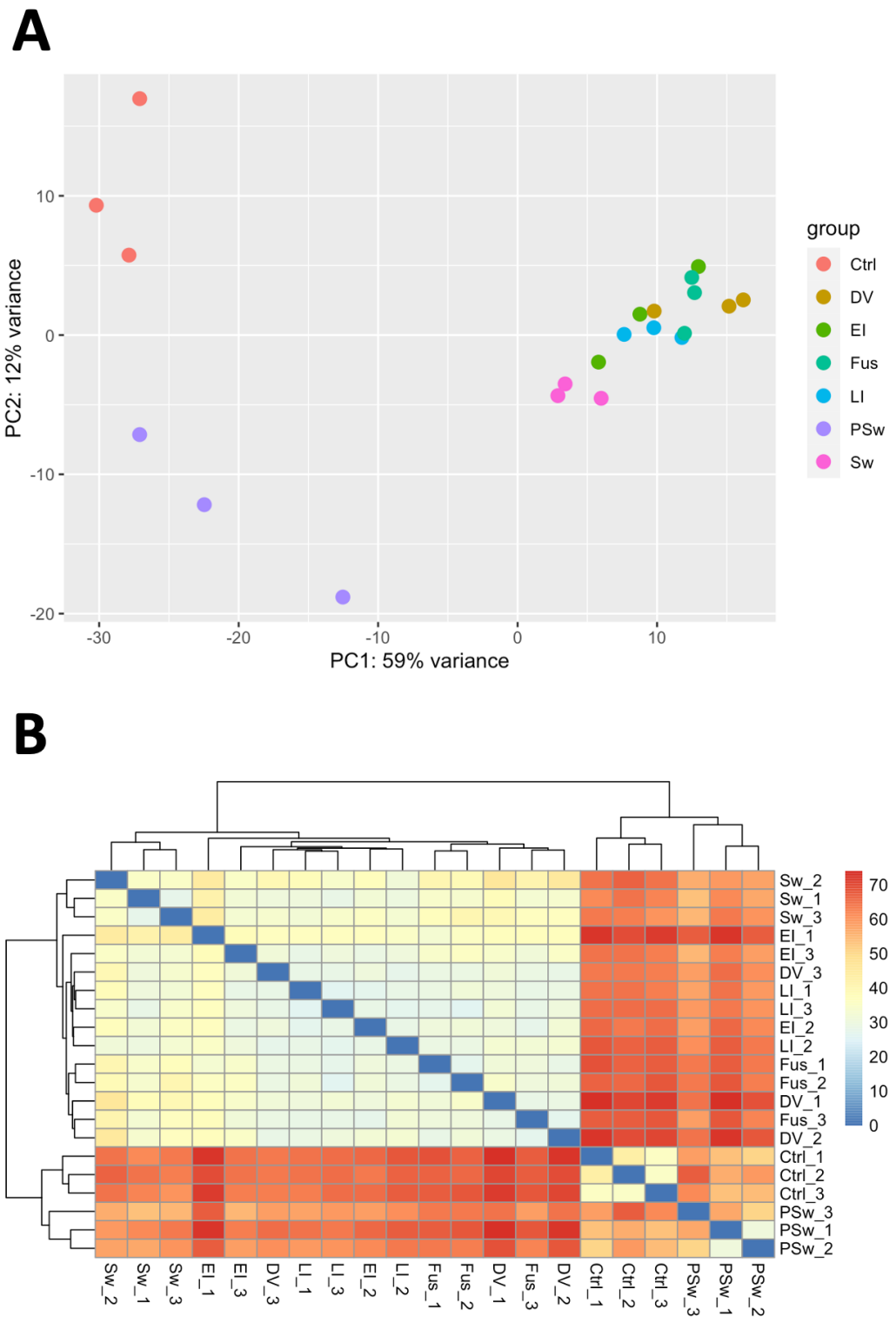

Figure 3.17: A) *PCA showing the distribution of the transcriptome data and its clustering by similarity.* ***B)*** *Heatmap showing the clustering of the samples by their similarity.*

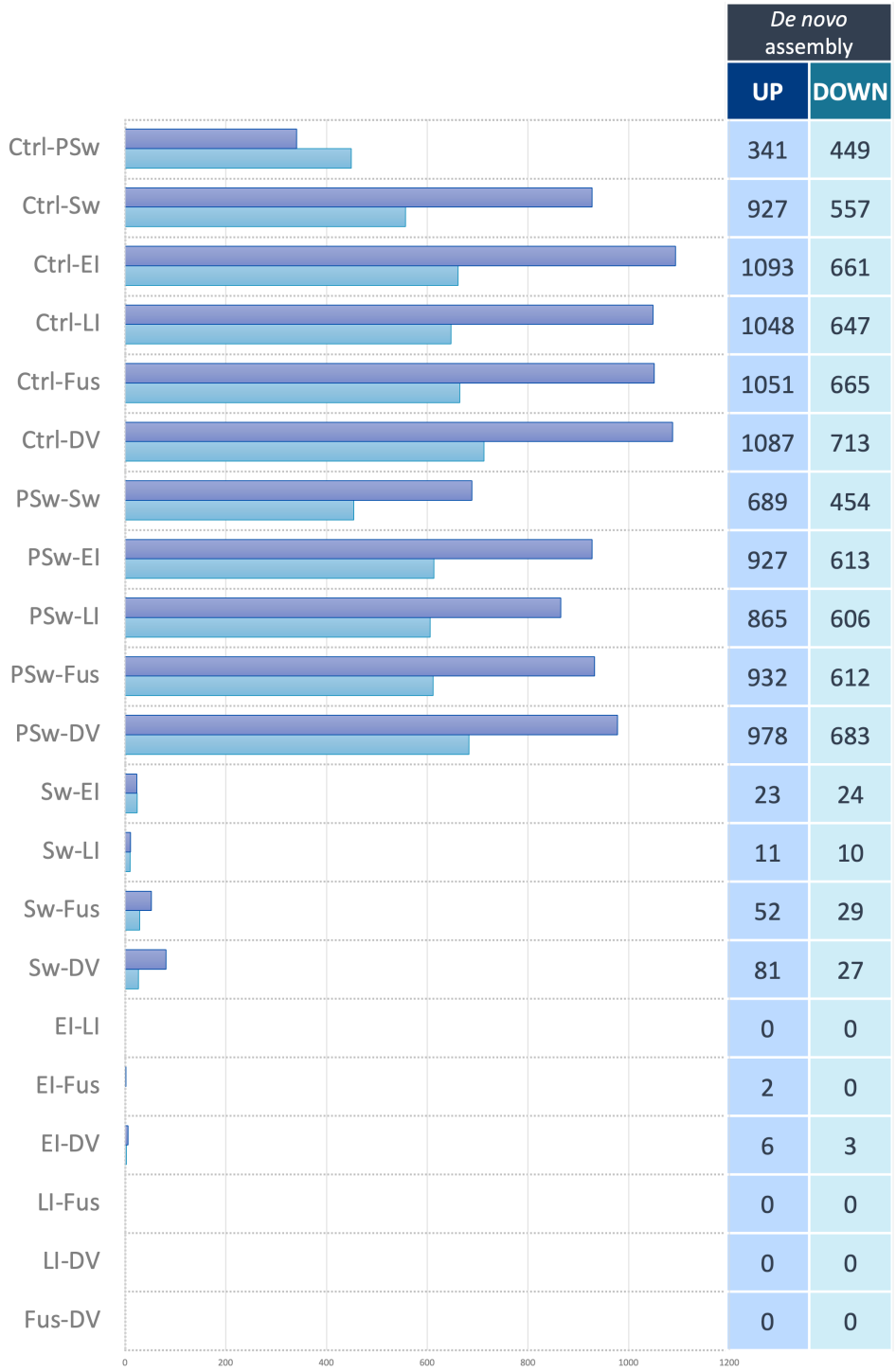

Figure 3.18: *Pairwise gene differential expression comparison showing the number of up and downregulated genes.*

The GO term enrichment analysis conducted on the DEGs resulting from comparing Ctrl and Sw revealed several biologically significant terms associated with the genes upregulated at the swelling stage (figure 3.19). One prominent enriched GO term was "DNA replication," indicating that during Sw, increased activity in the machinery responsible for copying and

duplicating DNA molecules may be triggered. This suggests potential cellular proliferation and replication processes taking place and is consistent with the previous observation that vasal budding is accompanied by a burst of cell proliferation starting from the late swelling stage (4-18 hours post-abscission) in the mesenchymal as well as in the epidermal cells of the growing vesicle (Scelzo, Lebel et al. in preparation). Another enriched term at the swelling stage was "cell differentiation", which highlights the potential for cells to change their structure and function in response to the budding stimulus. This finding correlates with histological observations according to which the main vessel is initially made of homogenous epidermal flat cells before they undergo heterogeneous modifications such as apicobasal elongation and constriction, ciliogenesis, and likely mesenchymal-epithelial transition, overall increasing cell type diversity, complexity and functionality (Scelzo et al. 2019).

Additionally, the term "animal organ morphogenesis" was enriched in swelling. These processes are involved in shaping and forming organs during animal development. This term suggests that important tissue and cell rearrangements occur in the early stages of Sw, driving the differentiation and organization of specific organs or tissues. Finally, "embryonic morphogenesis" also appeared among the GO terms enriched between Ctrl and swelling. This annotation designates the process that involves the formation of distinct structures and body patterns during early embryogenesis. Therefore, this suggests an overlap in the pathways recruited for body patterning during embryogenesis and vasal budding. As we will see below in more detail, many developmental transcription factors are upregulated as early as the swelling stage in *P. zorritensis*. This was somehow unexpected because their orthologues in *B. schlosseri* were shown to be expressed later from the double vesicle stage to later organogenesis (Ricci, Cabrera, et al. 2016; Prünster et al. 2019b; 2019a). This difference could account for the fact that vasal budding in *P. zorritensis* is fundamentally different from peribranchial budding in *B. schlosseri*. Later, the inner vesicle derives from the peribranchial epithelium, while the outer vesicle does not play any role in the inner organogenesis. In contrast, in *P. zorritensis*, the inner vesicle derives from the outer vesicle by invagination on one side, and, therefore, the outer vesicle patterning may play a central role in bud morphogenesis.

Another aspect worth highlighting is the fact that contrary to intuition, the largest shift in DEGs is revealed to happen before tissue morphogenesis becomes visible on a histological

level. However, this may simply reflect that morphogenetic processes need to be prepared and that, therefore, the synthesis of key proteins required for cell and tissue changes necessarily precedes key developmental processes.

GO enrichment – Biological Process

Ctrl X Sw		
Upregulated		
Adj.Pval	*Fold*	*Pathway*
0.0006	7.2	Negative regulation of neuron differentiation
0.000617	12.6	DNA unwinding involved in DNA replication
0.00113	4.2	Regulation of neuron differentiation
0.00154	2	Animal organ morphogenesis
0.00154	12.9	Regulation of DNA-templated DNA replication initiation
0.00154	2.5	Negative regulation of cell differentiation
0.00154	2.9	Gland development
0.00275	2.2	Positive regulation of cell differentiation
0.00275	8.9	Neuron fate specification
0.00305	2.4	Embryonic morphogenesis

Figure 3.19: *Biological Process Gene Ontology terms enriched between the Ctrl and Sw stages.*

In this study, I conducted a comprehensive analysis of gene expression changes across the seven budding stages. To this end, I listed all genes that, based on the previously described DESeq2 analysis results, showed differential up- or down-regulation in any pair of stages. This pairwise comparison provides information on gene expression dynamics for specific developmental time windows, ranging from small intervals between neighboring stages to larger intervals between extreme stages during the budding process.

Clustering by Expression Profile Highlights Six Transcriptional Dynamics

The previous step provided information on pairwise comparison between specific stages. However, to visualize the whole dynamics of gene expression during these seven stages, a clustering approach was employed to obtain a more comprehensive view of the genes' expression profiles throughout the budding process. Specifically, the k-Means clustering method within the iDEP 1.1 online program was used. This approach organized the

genes into distinct clusters based on their expression patterns. The program determined the number of clusters by calculating the k-means elbow plot, a graphical tool used to determine the optimal number of clusters (k) for the k-means clustering algorithm. The k-means algorithm is an unsupervised clustering technique used to partition data into k clusters based on their similarity. The goal of the elbow plot is to find the value of k that strikes a balance between minimizing the within-cluster variance and avoiding overfitting or underfitting the data. It assisted in identifying six ideal clusters, labelled from A to F, to categorize the genes based on their expression profiles. (figure 3.20).

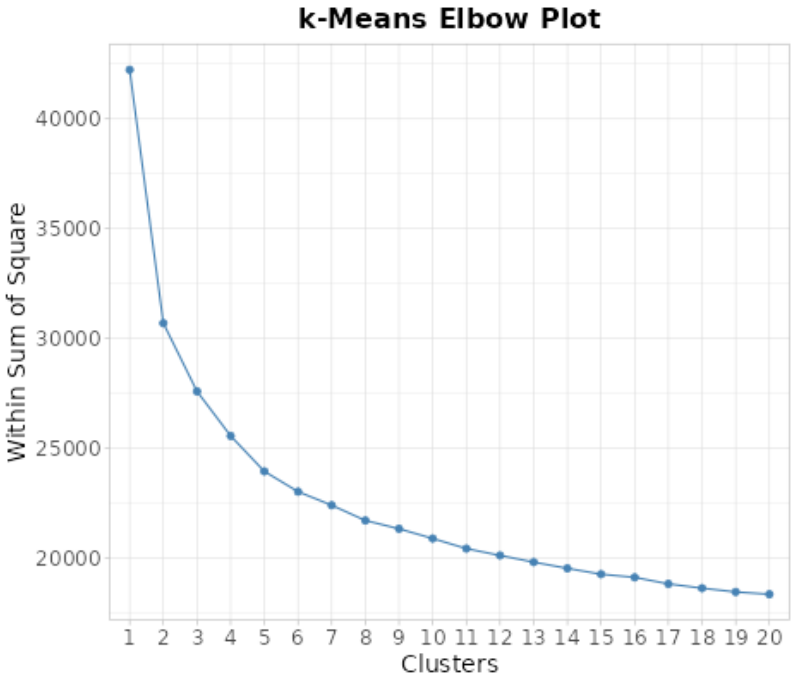

Figure 3.20: *Elbow plot for estimation of k-Means clusters.*

By clustering the genes with the k-means clustering algorithm, I could discern distinct gene expression patterns across the seven budding stages. Each cluster represents a group of genes with similar expression profiles (figure 3.21). I then crossed this result with the DESeq2 list and retrieved the DEGs present in each cluster. I decided to narrow down the list of genes to focus my investigation. For each cluster, I focus on genes considered fundamental during early embryogenesis and identified as DEGs during the budding process in *P. zorritensis*. This list contains genes involved in antero-posterior/dorso-ventral axis patterning, segmentation, gastrulation, and germ layer specification.

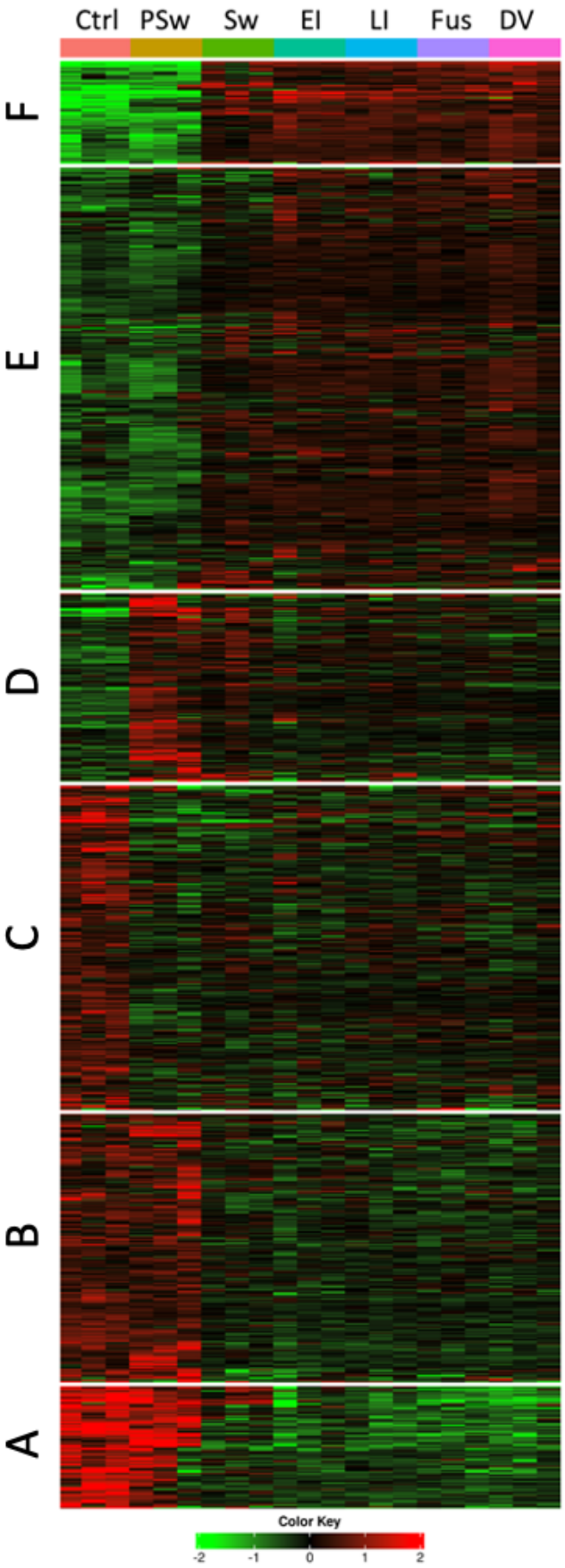
Ctrl
PSw
Sw
EI
LI
Fus
DV
F
E
D
C
B
A
Color Key
-2
-1
0
1
2

Figure 3.21: *Heatmap of genes identified in the de novo assembly that are expressed during different stages of NED in P. zorritensis, with colors referring to their respective normalized expression values. The genes form six major clusters (as resulting from the K-Means clustering algorithm), according to their temporal expression profiles.*

The rationale behind starting the investigation with these early development candidate genes is due to the fact that these genes are known to play fundamental roles during the early stages of embryogenesis, and they have well-documented functions in other organisms across the metazoan phylogeny (Kimelman and Martin 2012). By examining and utilizing the existing data on their roles across different organisms, we can gain a deeper understanding of their potential involvement in NED in *P. zorritensis*. Since the budding development process stems from tissues that have already undergone differentiation, a comprehensive study of these pivotal developmental genes will likely reveal the specific mechanisms used during the budding phase (Di Maio et al. 2015; Ricci, Cabrera, et al. 2016; Prünster et al. 2019b). The expectation is that studying the functions of these set of developmental genes will offer a glimpse into how budding development is orchestrated, potentially recapitulating key signaling pathways and co-opting gene regulatory networks utilized during embryogenesis. Each cluster is composed of several genes related to various processes.

It is important to clarify that the genes' names here presented for *P. zorritensis* are based on the annotation result. Functional annotation tools like Trinotate, eMapper, and BLAST2GO are primarily designed to detect functional annotations based on sequence similarity or domain/motif analysis. While they can provide valuable information about orthologues, homologues, and isoforms, they might not detect gene duplications and paralogues. Further analysis, based on the phylogenetic relationship, is required to infer the precise annotation for each gene. The potential function of some of these genes and their possible role in NED will be discussed in the next sub-chapter (page 100).

The clusters “A” and “B” contain all genes upregulated during Ctrl and PSw but downregulated once the bud enters the swelling stage. The cluster “A” displays several GO terms about biological processes as enriched. The “Adenylate Cyclase-Modulating G Protein-Coupled Receptor Signaling Pathway” is a fundamental mechanism for cells to respond to extracellular signals involving GPCRs (G Protein-Coupled Receptors) and influencing processes like proliferation, differentiation, and migration. “Cellular amino acid metabolic processes” are vital for the synthesis and breakdown of amino acids, which are crucial for cellular growth

and development. Similarly, the “alpha-amino acid metabolic process” is directly related to protein synthesis and energy production. The "response to chemical" and "response to organic substance" GO terms encompass cellular reactions to chemical stimuli, including cell signaling responses. “Cell adhesion” involves cells attaching to each other or the extracellular matrix, also cell migration. The “small molecule metabolic process” is essential for energy production, signaling, and generating cellular building blocks. “Regulation of multicellular organismal processes” refers to the coordination of cellular activities at the organismal level, but is relatively unspecific. Lastly, the “cellular modified amino acid metabolic process” involves modified amino acid metabolism, which can function in cellular signaling and regulation, acting as signaling molecules or post-translational modifications of proteins.

Overall, the enriched GO terms appear to be centered around aspects of cell metabolism, with the exception of cell adhesion, which mediates tissue cohesion (or its changes). They may reflect normal housekeeping functions as would be expected during the Ctrl stage, i.e., before the onset of budding is triggered at all. In the successive stages, such housekeeping functions may, then, be reduced at the expense of developmental functions (Weiße et al. 2015). On the other hand, amino acid metabolic processes may be relevant in the preparation of protein synthesis, as would be expected around the initialization of the budding process, mainly during the PSw stage.

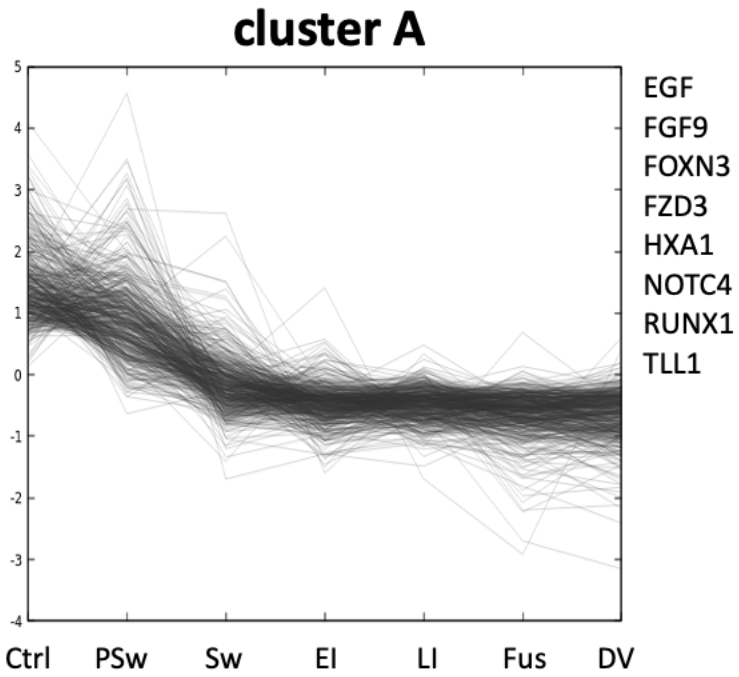

GO enrichment by cluster: Biological Process (*de novo* transcriptome assembly)		
Cluster A		
Adj.Pval	*Fold*	*Pathway*
4.38E-04	4.7	Adenylate cyclase-modulating G protein-coupled receptor signaling pathway
9.11E-04	4.1	Cellular amino acid metabolic process
9.11E-04	4.7	Alpha-amino acid metabolic process
1.08E-03	1.6	Response to chemical
1.58E-03	2.1	*Cell adhesion*
1.58E-03	1.9	Small molecule metabolic process
3.07E-03	1.6	Response to organic substance
5.04E-03	1.7	Regulation of multicellular organismal process
7.02E-03	4.2	Cellular modified amino acid metabolic process
1.04E-02	2.5	G protein-coupled receptor signaling pathway

Figure 3.22: *Genes expression profile and GO term enrichment for Biological processes for cluster F. DEG candidate genes that were found in this cluster are listed.*

The cluster "B" showed enrichment in the following GO terms: "mRNA metabolic processes" involve the synthesis, modification, and degradation of messenger RNA (mRNA), which carries genetic information for translation into proteins. "RNA processing" includes splicing, capping, and tailing of precursor RNA to generate mature RNA, ensuring correct functional forms during development. "Transcription initiation from RNA polymerase II promoter" tightly regulates gene activation and repression, directing cell fate determination and tissue differentiation. "Ribonucleoprotein complex assembly" ensures proper RNA transport and localization, contributing to spatiotemporal gene expression regulation. Additionally, "ribonucleoprotein complex subunit organization" maintains functional integrity. "DNA-templated transcription initiation" controls specific gene expression for cell differentiation and tissue formation. mRNA processing further refines gene regulation by modifying precursor mRNA to produce mature mRNA. "Protein-containing complex organization" and "assembly" are crucial for diverse cellular processes in development, including cell signaling and gene regulation. Finally, "transcription preinitiation complex assembly", involving regulatory proteins at gene promoters, precisely activates and silences genes during different developmental stages. Similar to cluster "A", this cluster appears to encompass mainly basic cellular functions, mostly enriched for transcription regulation. Again, this may reflect a need to increase protein production at the onset of budding or simply basic housekeeping. On the other hand, some key developmental pathways, such as Wnt, Fgf,

Bmp, and Notch, appear enriched, potentially suggesting the onset of morphogenetic processes (Steventon et al. 2009; Stuhlmiller and García-Castro 2012).

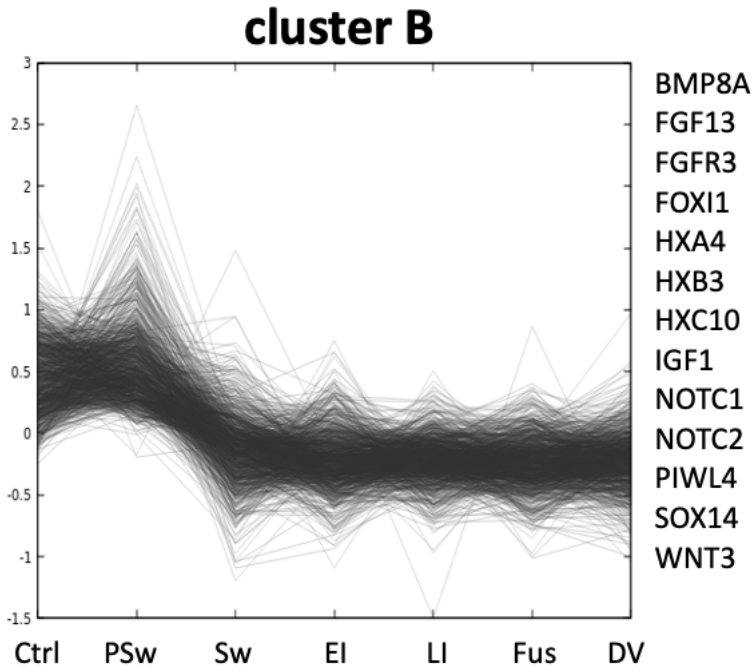

GO enrichment by cluster: Biological Process (*de novo* transcriptome assembly)

Cluster B

Adj.Pval	*Fold*	*Pathway*
1.84E-04	1.4	MRNA metabolic process
5.62E-04	1.3	RNA processing
1.01E-03	1.9	Transcription initiation from RNA polymerase II promoter
1.01E-03	1.7	Ribonucleoprotein complex assembly
1.01E-03	1.7	Ribonucleoprotein complex subunit organization
1.07E-03	1.8	DNA-templated transcription initiation
1.07E-03	1.4	MRNA processing
1.07E-03	1.2	Protein-containing complex organization
1.07E-03	1.3	Protein-containing complex assembly
1.19E-03	1.9	Transcription preinitiation complex assembly

Figure 3.23: *Genes expression profile and GO term enrichment for Biological processes for cluster F. DEG candidate genes that were found in this cluster are listed.*

In the cluster "C", the enriched GO terms identified were: "Transport" processes facilitate the movement of molecules and ions within and between cells, distributing essential nutrients, signaling molecules, and regulators necessary for cell differentiation, proliferation,

and tissue formation. “Autophagy”, a regulated process, degrades and recycles cellular components, sculpting tissues and eliminating defective cells during development. Precise cellular localization ensures correct spatial organization, essential for tissue morphogenesis and differentiation (“Establishment of localization”). “Processes utilizing autophagic mechanisms” selectively remove unwanted cellular components, influencing cell fate and tissue homeostasis. “Vesicle-mediated transport” delivers proteins, lipids, and signaling molecules to specific cellular compartments, which are critical for cell polarity, tissue patterning, and developmental regulation. “Macroautophagy” aids in cellular remodeling and differentiation by removing unnecessary components and maintaining homeostasis. “Catabolic processes” provide energy and building blocks for growth, and sodium ion transport regulates cell volume, membrane potential, and tissue morphogenesis. “Endocytosis” internalizes molecules and regulates cell signaling and surface receptors, influencing tissue remodeling. The “regulation of transport” processes is essential for orchestrating cellular movements, tissue patterning, and cellular polarity during development.

This cluster appears to be less well-defined than most of the others, featuring substantial activation only in the Ctrl stage and may, therefore, be less insightful with respect to the budding process. In line with this, most GO terms are important for cell metabolism and tissue homeostasis. Nevertheless, a few prominent “classic” developmental genes are enriched, among them are *Bmp1*, which in vertebrates regulates extracellular matrix formation (Vadon-Le Goff, Hulmes, and Moali 2015); *Bmp3*, playing roles in tissue development and homeostasis (Sánchez-Duffhues et al. 2015; Kumar and Nandhini 2018); and *Bmp6*, which contributes to neural development and tissue regeneration (Tomizawa et al. 1995; Vukicevic and Grgurevic 2009). *Dll4* is essential for cell fate determination, affecting tissue and organ formation (Pellegrinet et al. 2011), while *Dlx1* plays a vital role in CNS development (J. de Melo et al. 2003). *Egr2* regulates nervous system functioning and musculoskeletal development (Nagarajan et al. 2001). *Fgfr1* mediates growth factor signaling during organ development (Brewer et al. 2015). *Fzd10* is crucial in *Wnt* signaling for tissue patterning (Matos et al. 2020), and *HoxA7* regulates the tissue differentiation (Zha, Wang, and Di 2020). *Notch3*'s cell communication is vital for tissue formation (Hosseini-Alghaderi and Baron 2020), *Smad7* is a key player in *Tgfβ* signaling for cell growth and differentiation

(Han et al. 2006; Yan, Liu, and Chen 2009). Tll2's metalloprotease activity is crucial for tissue remodeling (Swanson et al. 2009).

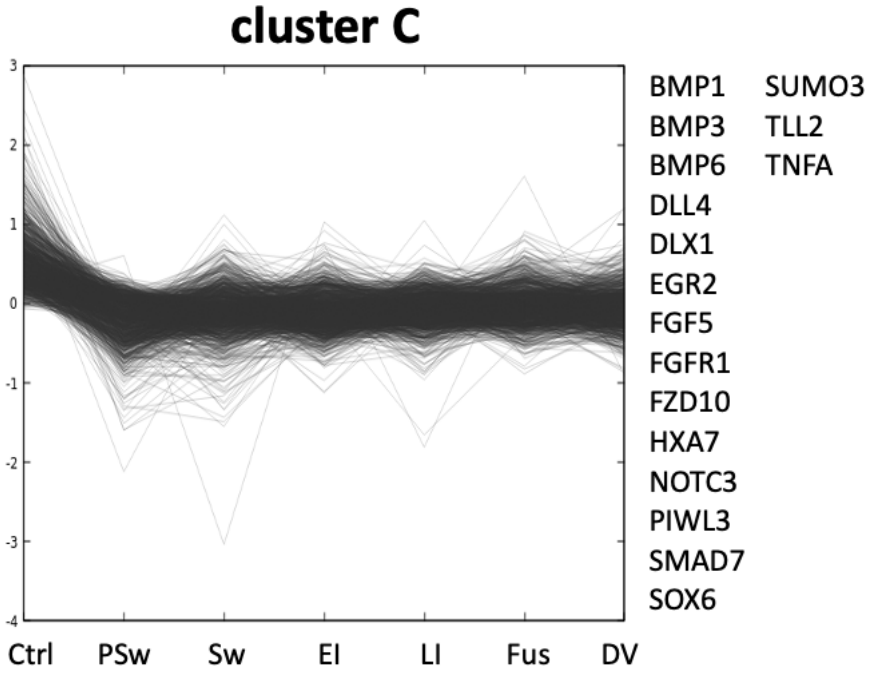

GO enrichment by cluster: Biological Process (*de novo* transcriptome assembly)

Cluster C

Adj.Pval	*Fold*	*Pathway*
3.23E-05	1.4	Transport
1.57E-04	2	Autophagy
1.57E-04	1.3	Establishment of localization
1.57E-04	2	Process utilizing autophagic mechanism
1.60E-04	1.6	Vesicle-mediated transport
2.95E-04	2.3	Macroautophagy
2.12E-03	1.4	Catabolic process
2.47E-03	3.6	Sodium ion transport
2.66E-03	1.9	Endocytosis
2.71E-03	1.5	Regulation of transport

Figure 3.24: *Genes expression profile and GO term enrichment for Biological processes for cluster F. DEG candidate genes that were found in this cluster are listed.*

Cluster "D" features the following enriched GO terms are: During development, "organophosphate metabolic processes" are crucial for synthesizing, breaking down, and regulating compounds containing phosphate groups, essential for biomolecule formation like nucleotides and phospholipids, necessary building blocks for DNA, RNA, and cell membranes.

Phosphorylation, a key aspect, controls cell signaling, influencing developmental processes like cell differentiation, tissue morphogenesis, and organ formation. Additionally, “transmembrane transport” is vital, facilitating the movement of substances across cellular membranes and supporting cell growth and differentiation by facilitating nutrient, ion, and signaling molecule uptake into developing tissues. “Ion transport” is essential for neural and muscle development, establishing ion gradients and membrane potentials critical for nerve signal transmission and muscle contraction during embryogenesis. “Ion transmembrane transport”, focuses on ion movement across cellular membranes, playing a crucial role in nerve impulse transmission, muscle contraction, and other vital cellular activities necessary for proper development. Another cluster whose enriched GO terms, although their enrichment is not even very high, point to homeostasis. Among the enriched genes that are part of the cluster, *Bmp* and *Wnt* feature prominently, such as *Bmp4* and *Bmp5*. In vertebrates, *Bmp4* plays key roles in embryonic development, including mesoderm induction which forms structures like muscles and bones, establishes the dorsoventral (back-belly) axis, influences limb outgrowth at the apical ectodermal ridge, aids in the formation of organs like the eyes, heart, and lungs, and participating in bone formation and osteoblast differentiation. On the other hand, *Bmp5* is vital for skeletal development, especially in bone and cartilage formation, impacts neural cell differentiation, and collaborates with other *Bmp*, such as *Bmp4* and *Bmp7*, in various developmental processes (De Robertis and Kuroda 2004; Mizutani and Bier 2008); *Wnt4* which plays diverse roles, e.g., in kidney, sex determination, and mammary gland development (Jeays-Ward et al. 2003). Besides a few others that are reported to be involved in axis development, i.e., *FoxH1* and *Nodal* (Pogoda et al. 2000; Yamamoto et al. 2001; Hirokawa et al. 2006). This may suggest that, while simple homeostatic processes still predominate, some central mechanisms of early development might become active during the stage of PSw.

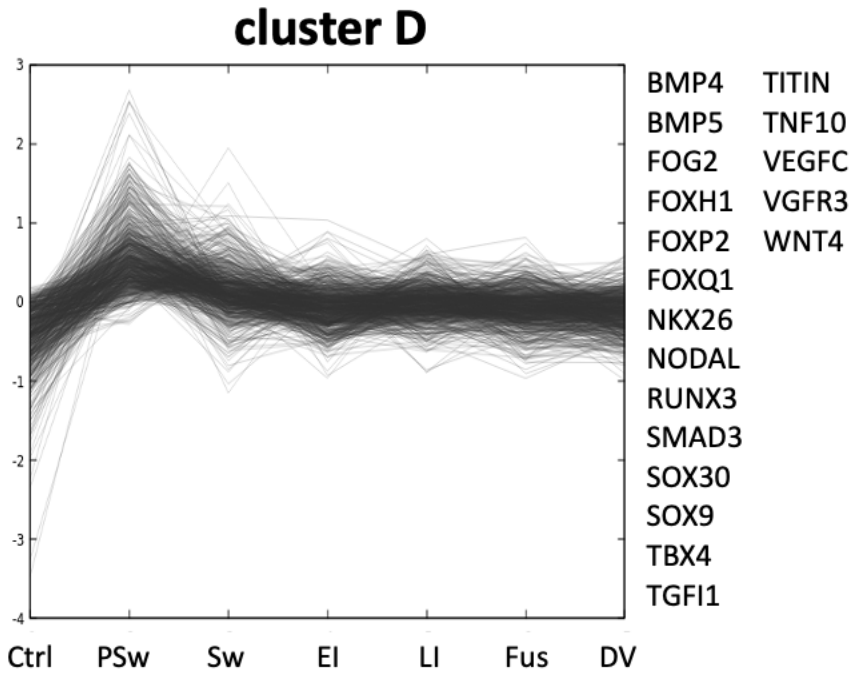

GO enrichment by cluster: Biological Process (*de novo* transcriptome assembly)		
Cluster D		
Adj.Pval	*Fold*	*Pathway*
1.18E-02	1.7	Organophosphate metabolic process
2.44E-02	1.8	G protein-coupled receptor signaling pathway
2.44E-02	1.6	Transmembrane transport
2.64E-02	1.6	Ion transport
2.93E-02	1.2	Transport
2.93E-02	1.7	Ion transmembrane transport

Figure 3.25: *Genes expression profile and GO term enrichment for Biological processes for cluster F. DEG candidate genes that were found in this cluster are listed.*

In the cluster "E" these GO terms were found enriched: "NcRNA metabolic processes", regulating gene expression and cellular functions, while "NcRNA processing", ensuring proper folding and functionality of non-coding RNA molecules critical for cell specification and organogenesis; "ribosome biogenesis", providing an adequate supply of ribosomes for protein synthesis during rapid cell growth; "rRNA processing", enabling the formation of functional ribosomes for efficient translation of proteins; "rRNA metabolic processes", supporting ribosomes with necessary components for optimal protein translation; "ribonucleoprotein complex biogenesis", crucial for diverse roles in gene regulation, RNA transport, and signaling during development; "RNA processing", influencing RNA diversity and stability, contributing to cell fate determination and tissue-specific functions; "chromosome

organization", arranging and "compacting chromosomal DNA" to impact gene regulation and cell differentiation; "DNA metabolic processes", ensuring accurate transmission of genetic information during replication, repair, and recombination, critical for cell proliferation, tissue growth, and organ development; and "chromosome segregation", occurring during cell division to maintain genomic stability and prevent developmental abnormalities and genetic disorders. This cluster shows GO term enrichments that point to increases in transcription and cell division, both relevant for increased morphogenesis. Key morphogenesis genes, such as members of the *Shh* family, *Wnt*, several homeobox transcription factors, and genes essential for cell differentiation, such as *Gata* and *Smad2* support this notion.

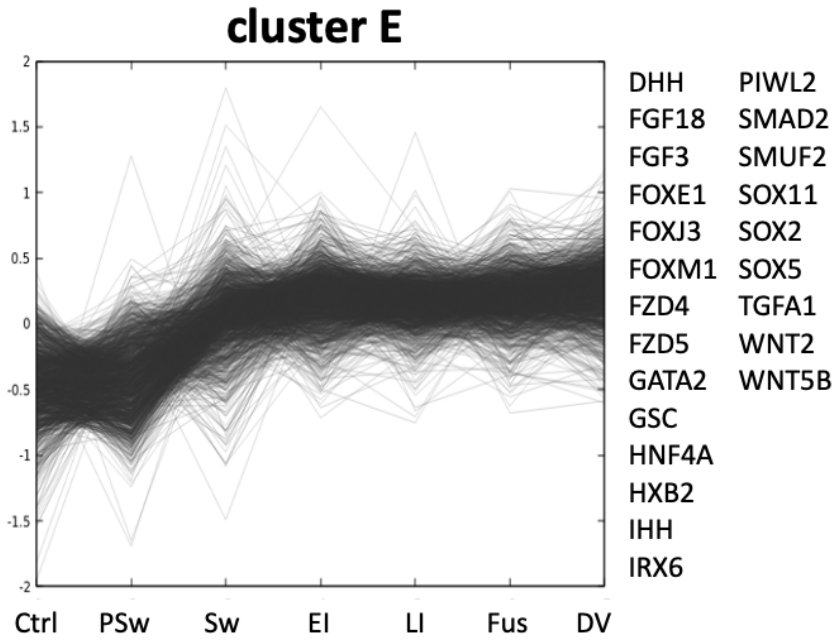

GO enrichment by cluster: Biological Process (*de novo* transcriptome assembly)

Cluster E

Adj.Pval	*Fold*	*Pathway*
1.97E-12	2.3	NcRNA metabolic process
4.40E-12	2.4	NcRNA processing
4.40E-12	2.7	Ribosome biogenesis
1.85E-11	2.8	RRNA processing
1.87E-11	2.8	RRNA metabolic process
2.36E-09	2.2	Ribonucleoprotein complex biogenesis
2.28E-08	1.8	RNA processing
1.42E-07	1.7	Chromosome organization
9.73E-06	1.6	DNA metabolic process
1.56E-05	2.1	Chromosome segregation

Figure 3.26: *Genes expression profile and GO term enrichment for Biological processes for cluster F. DEG candidate genes that were found in this cluster are listed.*

In the cluster "F" the following GO terms are enriched: "System development" involves the formation and maturation of complex systems like the nervous, cardiovascular, respiratory, and digestive systems, crucial for coordinating body functions. "Animal organ development" leads to the creation of distinct organs, such as the heart, liver, kidneys, and lungs. "Axon guidance" ensures precise connectivity between developing neurons, establishing functional neural circuits in the nervous system. "Sensory organ development" forms structures like eyes, ears, nose, and taste buds, enabling organisms to perceive and respond to the environment. "Neuron projection guidance" focuses on the outgrowth and navigation of axons and dendrites, creating neural networks for information processing. "Anatomical structure morphogenesis" shapes organs, tissues, and body parts through cell proliferation, migration, and differentiation, creating diverse body structures. "Animal organ morphogenesis" involves cellular and molecular interactions, driving tissue differentiation and growth to form fully functional organs. "Tissue morphogenesis" structures tissues through cell differentiation, proliferation, and migration, generating functional tissues with specific properties. "Tissue development" encompasses the growth and differentiation of various tissue types, essential for proper organ functioning and overall body homeostasis. Overall, this cluster contains the highest amount of enriched GO terms that clearly point to developmental processes on the tissue and organ level, which are expected to occur after the PSw stage. The fold changes of these enrichments are substantial, too. Among the upregulated genes, we tend to find many, particularly transcription factors, involved in organogenesis and later development, such as *Fox* and *Gata6* (Morrisey et al. 1998; Hanashima et al. 2004), while there are fewer "early developmental" genes than in the previous cluster (i.e., *Dll* and *Wnt*). This seems to fit coarsely with the shape of the expression of this cluster, once this cluster is mainly composed of genes that will keep upregulated until later stages.

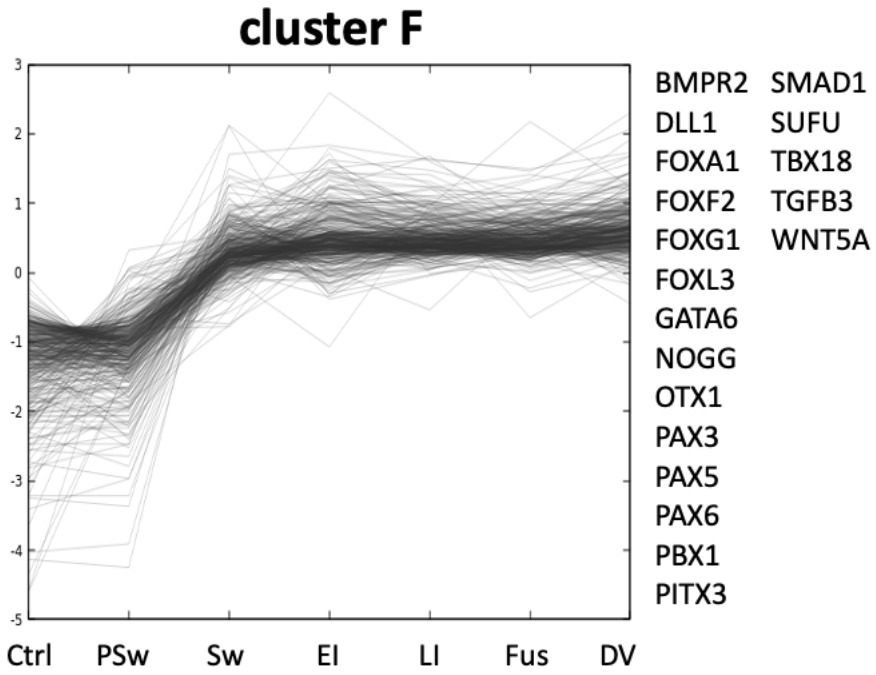

GO enrichment by cluster: Biological Process (*de novo* transcriptome assembly)		
Cluster F		
Adj.Pval	*Fold*	*Pathway*
1.27E-06	2	System development
2.06E-06	2.1	Animal organ development
6.81E-06	7.4	Axon guidance
6.81E-06	4.4	Sensory organ development
6.81E-06	7.4	Neuron projection guidance
7.28E-06	2.2	Anatomical structure morphogenesis
1.77E-05	3.1	***Animal organ morphogenesis***
4.62E-05	3	Cell adhesion
4.62E-05	3.7	Tissue morphogenesis
8.38E-05	2.4	Tissue development

Figure 3.27: *Genes expression profile and GO term enrichment for Biological processes for cluster F. DEG candidate genes that were found in this cluster are listed.*

Genome-based Transcriptome Mapping (GBTM) and Comparison with DNTA

When I generated the transcriptome for the seven NED stages in *Polyandrocarpa zorritensis*, no reference genome was available. As a result, all analyses were conducted using *de novo* transcriptome assembly. While useful, this method has limitations, including potential challenges in accurately identifying transcript isoforms, alternative splicing, and lowly expressed genes (Lee, Na, and Park 2021; Oomen et al. 2022). However, more recently,

a collaboration with the Flot Lab (ULB) has led to the sequencing and partial assembly of a reference genome for *Polyandrocarpa zorritensis*. The new reference genome allowed to use a different approach for the analysis of the collected transcriptomes: mapping the transcriptome to this new reference genome.

Mapping the transcriptome to the reference genome provided several advantages. For instance, this approach offers higher accuracy than *de novo* transcriptome assembly, ensuring precise alignment of reads to the genome and resolving issues such as fragmented contigs and isoform redundancies. Reference genome-based mapping enables the discovery of novel transcripts not present in existing annotations by analyzing unmapped reads or regions with low coverage. Utilizing the same reference genome ensures consistent and comparable results across experiments, as they all measure against a common standard. In contrast, *de novo* assembly, or assembling a genome from scratch, can produce variable outcomes based on the chosen settings, the quality and quantity of the RNA sequenced data, and the specific assembly software or algorithms used (Clarke et al. 2013).

The genome assembly pipeline was conceived and run by our collaborator (Flot Lab, ULB), combining HiFi, and Oxford Nanopore Technologies (ONT) long-reads with Illumina short-reads (see Material and Methods). The initial assembly using only HiFi reads and Hifiasm assembler resulted in a genome size of 424,323,369 bp, with an N50 value of 1,657,153 bp, and a total of 829 contigs. The assembly completeness was evaluated using the Kat completeness metric, which yielded a score of 59.17%. Additionally, the BUSCO analysis indicated that 92.6% of the expected genes were found in the assembly, with 84.1% classified as complete single-copy genes, 8.5% as complete duplicated genes, 3.7% as fragmented genes, and 3.7% as missing genes.

To improve the assembly further, reads obtained using the ONT were incorporated, and two different haplotype purging methods were applied. First, the "Purge_dups" step was performed to remove haplotigs and resolve contig overlaps. This process resulted in a reduced assembly size of 375,785,810 bp, an N50 value of 1,863,282 bp, and a total of 490 contigs. The Kat completeness score slightly decreased to 51.47%, and the BUSCO analysis indicated that 92.4% of the expected genes were present, with 90.6% complete single-copy genes, 1.8% complete duplicated genes, 3.7% fragmented genes, and 3.9% missing genes. The second haplotype purging step, "Purge_haplotigs," aimed to identify pairs of contigs that are

syntenic. After this step, the assembly size was further reduced to 364,995,275 bp, with an N50 value of 1,913,193 bp and a total of 397 contigs. The Kat completeness score was similar to the previous step, at 50.54%, and the BUSCO analysis showed 92.4% of the expected genes present, with 90.7% complete single-copy genes, 1.7% complete duplicated genes, 3.7% fragmented genes, and 3.9% missing genes.

To scaffold the assembly, the ntLink method was employed, using both HiFi and ONT reads for lightweight mapping. The final scaffolded assembly had a size of 364,798,430 bp, an N50 value of 14,178,783 bp, and a total of 106 contigs. The Kat completeness score was 50.41%, and the BUSCO analysis yielded 92.4% of the expected genes, with 90.7% complete single-copy genes, 1.7% complete duplicated genes, 3.7% fragmented genes, and 3.9% missing genes. Additionally, the assembled data was polished using the HyPo method, which combined HiFi and Illumina reads. The polished assembly had a size of 364,761,307 bp, an N50 value of 14,177,737 bp, and a total of 106 contigs. However, the polishing process resulted in a slightly decreased Kat completeness score of 49.61%. The BUSCO analysis showed 92.5% of the expected genes present, with 90.8% complete single-copy genes, 1.7% complete duplicated genes, 3.6% fragmented genes, and 3.9% missing genes.

Following genome assembly, the genome annotation process was conducted through a series of steps. Repeat identification was performed using Repeat Modeler2 and repeat annotation/masking was carried out using Repeat Masker. Transcripts alignment was performed using STAR, incorporating the HyPo output and RNAseq reads. Genome annotation was achieved using Braker 3, resulting in the identification of 17,126 genes and 21,451 transcripts.

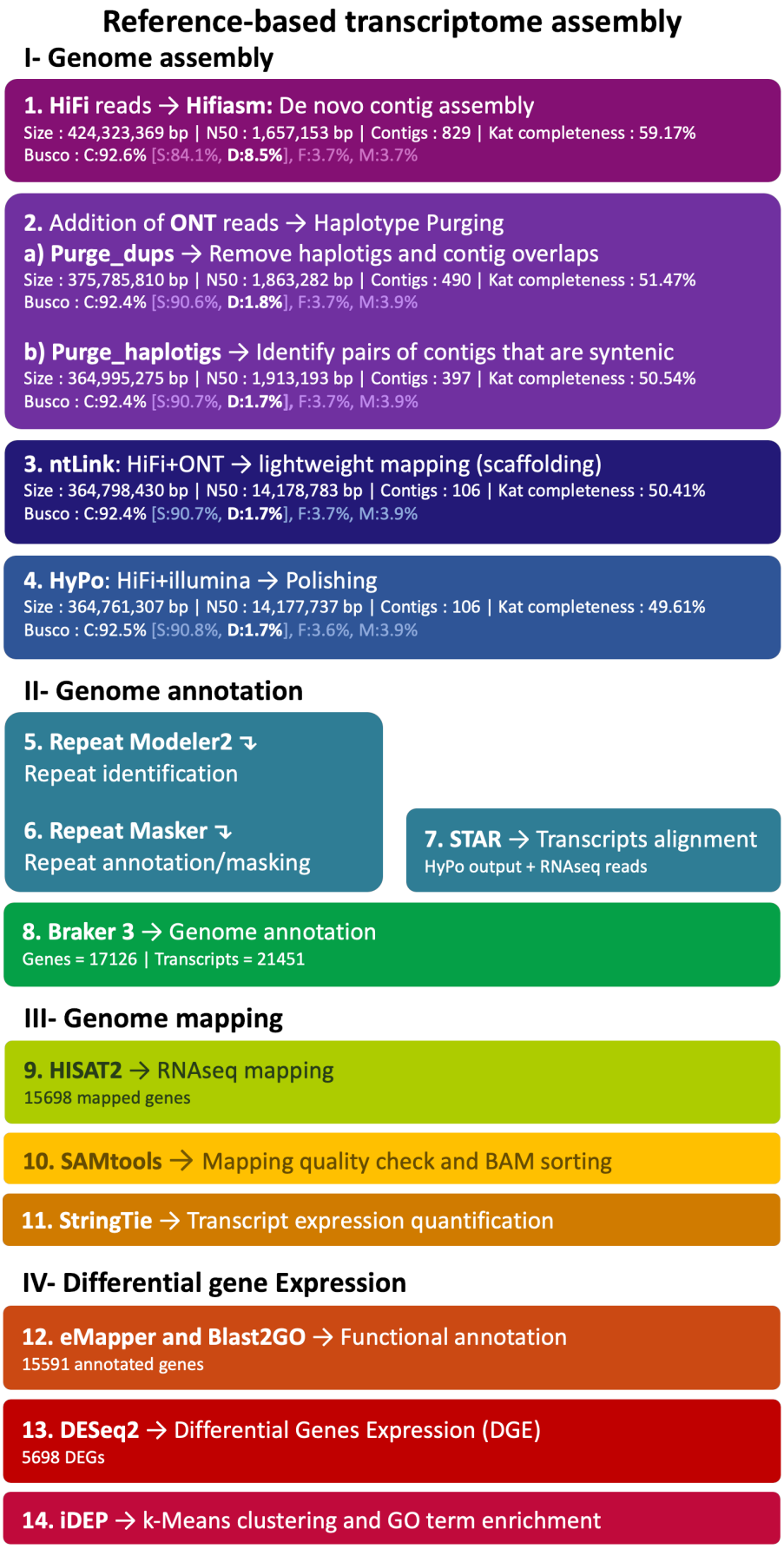

Figure 3.28: *Genome-based mapping pipeline and scores of each step.*

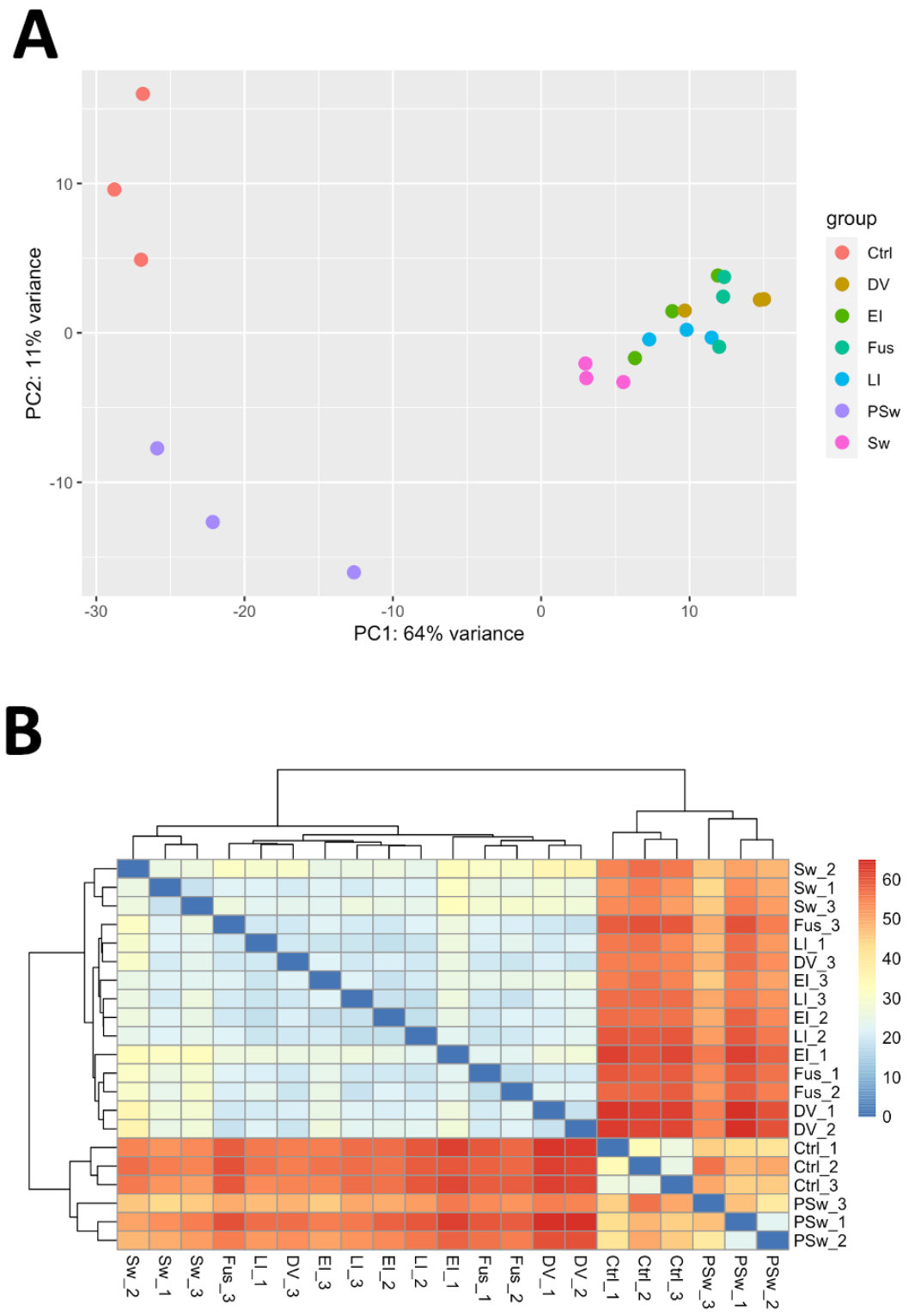

Figure 3.29: *DESeq2 initial analysis. A) Principal Component Analysis (PCA) of the differentially expressed genes in the de novo assembly as revealed by the DESeq2. Only the first two principal components are plotted, with colors attributed according to the different NED stages. All later stages cluster together, while the first two stages form two isolated clusters that are separated from the remainder. B) Heatmap of pair-wise comparisons between all conditions (all stages and replicates) based on the same dataset. Color hues and branch lengths of the juxtaposed dendrograms indicate pair-wise distances.*

The initial steps of DESeq2 analysis performed a PCA and heatmap plotting which were very similar to the one obtained from the *de novo* analysis, with a difference in the plot scale that might be justified by the difference in the matrices' sizes (the denovo matrix contains approximately the double of genes). The DESeq2 analysis revealed that 5698 genes showed differential expression in at least one of the seven budding stages of *P. zorritensis*, a value not much lower than the one obtained with the *de novo* assembly output. To gain a better understanding of which genes and pathways are up or downregulated during the NED process, it was performed a DGE pairwise comparison between two budding stages was performed before. This result showed that the number of genes being up and downregulated is also very similar to the result obtained from the *de novo* assembly analysis.

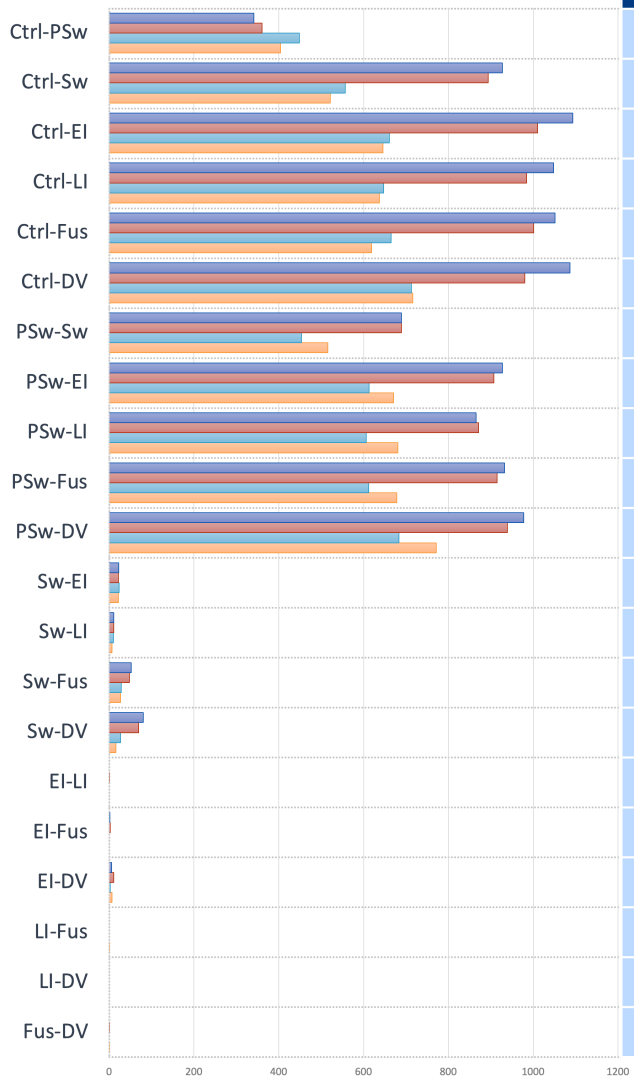

	De novo assembly		Genome-based analysis	
	UP	DOWN	UP	DOWN
Ctrl-PSw	341	449	361	404
Ctrl-Sw	927	557	894	522
Ctrl-EI	1093	661	1010	646
Ctrl-LI	1048	647	984	637
Ctrl-Fus	1051	665	1001	619
Ctrl-DV	1087	713	980	716
PSw-Sw	689	454	689	516
PSw-EI	927	613	907	671
PSw-LI	865	606	871	681
PSw-Fus	932	612	915	678
PSw-DV	978	683	939	771
Sw-EI	23	24	22	22
Sw-LI	11	10	11	7
Sw-Fus	52	29	48	27
Sw-DV	81	27	70	16
EI-LI	0	0	1	0
EI-Fus	2	0	3	0
EI-DV	6	3	11	7
LI-Fus	0	0	0	1
LI-DV	0	0	0	0
Fus-DV	0	0	1	1

Figure 3.30: *Comparison of the number of up- and downregulated DEG in both analyses: DNTA and GBTM. Bar lengths correspond to numbers of DEG between the respective pairs of stages.*

To verify if the differentially expressed genes composition of the two DESeq2 outputs (*de novo* assembly and genome-based mapping) was also similar, the proteins sequences for the genes present in both outputs were compared against each other using the tool OrthoFinder (inside the OrthoVenn online program) to identify how much the two outputs overlap. The result produced 3521 clusters that had at least one protein sequence either from the *de novo* analysis or from the genome-based analysis and the overlap in DEGs was composed of 4812 genes from the *de novo* analysis and 4660 from the genome-based analysis. Of the 3521 clusters, 2529 were composed of a single copy gene (protein) from each analysis.

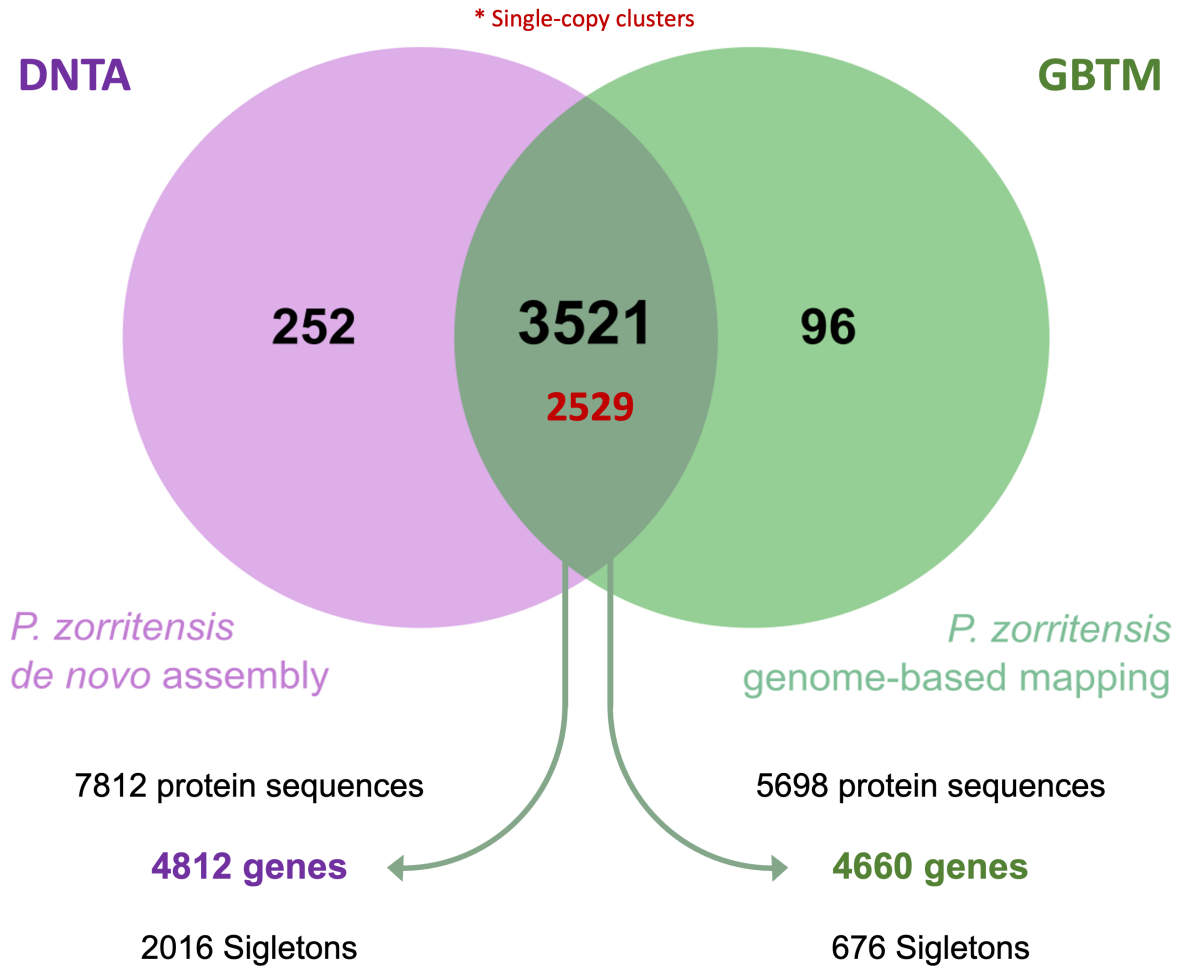

Figure 3.31: *General overlap of protein sequences referent to DEG in DNTA and GBTM analyses in P. zorritensis.*

The functional annotation was conducted using eMapper and Blast2GO, resulting in a total of 15,591 genes functionally annotated. This annotation was added to the expression matrix used as input for DESeq2 analysis and was used for k-Means clustering and GO term enrichment analysis were conducted using iDEP, the same way as it was performed with the *de novo* assembly analysis data. An elbow plot was done, suggesting 6 k-Means clusters, labelled from 1 to 6. The k-Means clustering resulted in clusters with expression profiles similar to those from the *de novo* analysis.

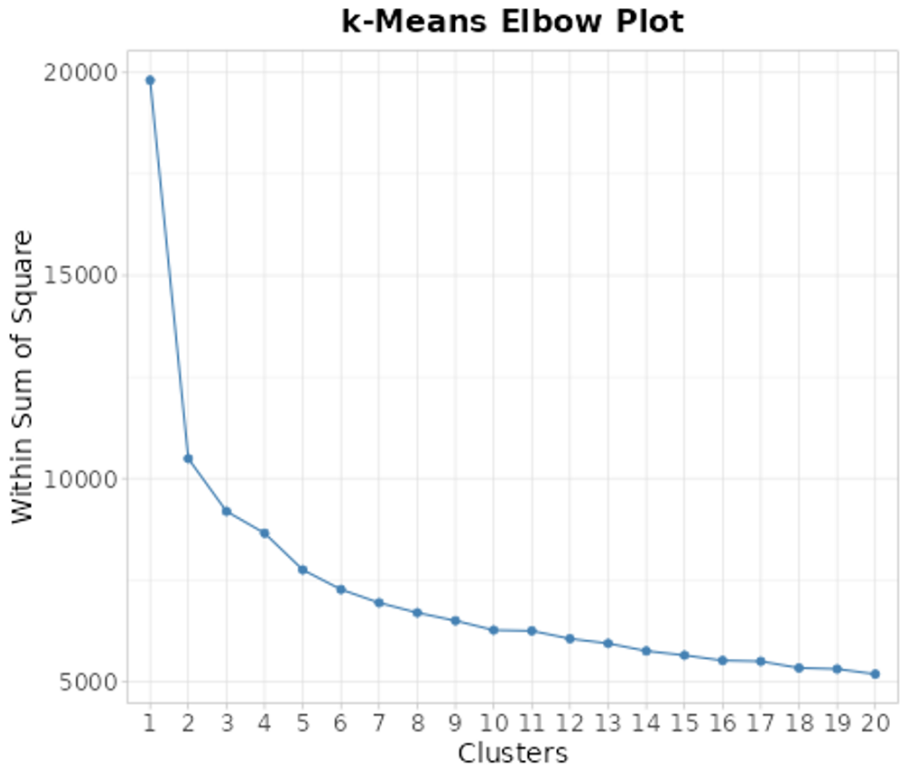

Figure 3.32: *Elbow plot for determining the number of k-means clusters for the GBTM expression.*

Figure 3.33: *Heatmap of genes identified in the GBTM that are expressed during different stages of NED in P. zorritensis, with colors referring to their respective normalized expression values. The genes form six major clusters (as resulting from the K-Means clustering algorithm), according to their temporal expression profiles.*

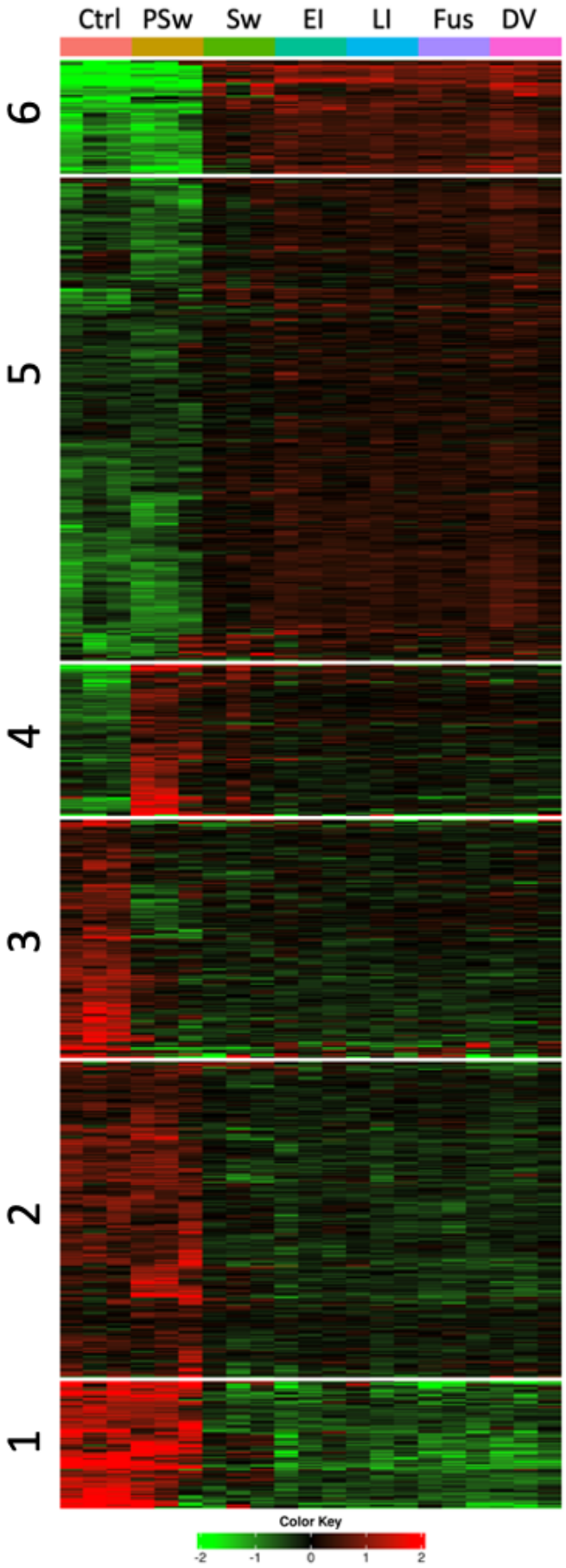
Ctrl
PSw
Sw
EI
LI
Fus
DV
6
5
4
3
2
1
Color Key
-2
-1
0
1
2

In cluster 1 genes were found that are upregulated between Ctrl and PSw but downregulated during budding (Sw to DV). This cluster was only enriched for the Biological Process GO term “cell adhesion”. This term was also enriched in the cluster “A” of the *de novo* assembly analysis, which is a cluster with a very similar expression pattern to this one. In this cluster were presents the following genes of interest: *Fgf9*, *Runx1*, and *Tll1*, which were also present in the DNTA, but also the genes *Bmp1*, *Fos*, and *Titin*. *Bmp1* was found in cluster “C”, and *Titin* was found in cluster “D” in the DNTA. The gene *Fos* (proto-oncogene - Protein c-Fos) is involved in cellular events like cell proliferation, differentiation, and survival, and it can also be involved in the loss of cell polarity and epithelial-mesenchymal transition (Fialka et al. 1996).

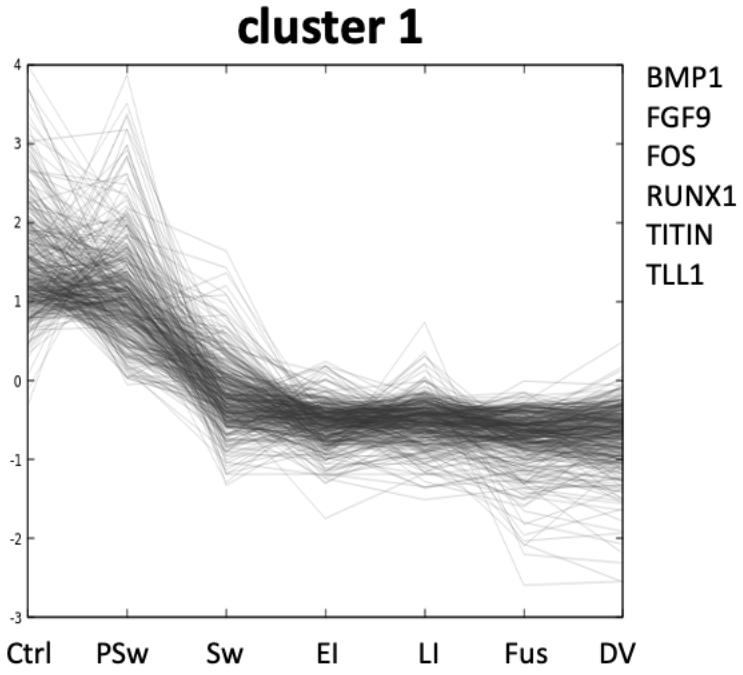

Figure 3.34: *Temporal expression profiles of genes comprised in cluster 1.*

In cluster 2 are genes that are upregulated between Ctrl and PSw and downregulated in the following stages. In this cluster, the enriched GO terms are: “response to chemical” and “response to organic substance,” which were reported in cluster “A” in the DNTA, “G protein-coupled receptor signaling pathway”, which was also present in the cluster “D” in the DNTA. "Response to amphetamine" and "Response to amine," respectively, influence neuronal activity and neurotransmitter release, impacting neural circuit formation, synaptogenesis,

and plasticity. Additionally, the GO term "Modulation of chemical synaptic transmission" governs the precise control and adjustment of neurotransmitter release, reception, and regulation at neuronal synapses, establishing functional neural circuits and shaping neuronal connection strength. In parallel, "Negative regulation of transport" mechanisms during development inhibit or attenuate molecular and cellular component distribution, ensuring accurate delivery to intended destinations at the appropriate times, thereby preventing aberrant development and maintaining cellular homeostasis. The GO terms "Regulation of trans-synaptic signaling" and "Trans-synaptic signaling" are vital in coordinating neuronal activity and forming functional neural circuits, with precise regulation being essential for proper neural connectivity and supporting learning and memory functions. Furthermore, the GO term "Regulation of biological quality" is involved in controlling overall biological system quality, including developmental processes, by ensuring cellular and organismal structures and functions meet specific criteria for proper development and homeostasis, including critical quality control processes for proteins, organelles, and cellular structures, ultimately contributing to normal development and overall health.

In cluster 2 were also found the genes: *HoxA4*, *Notch1*, *Notch2*, *Piwl4*, and *Sox14* were also present in cluster “B” in the DNTA. *HoxA4* is involved in directing anterior-posterior patterning and neural development in vertebrates (Hubert and Wellik 2023). In the DNTA, the genes EGF and *Notch4* were also present in cluster “A” and *FoxP2* was present in cluster “D”. Cluster 2 also contained the genes: FGFR2, which encodes a receptor crucial for fibroblast growth factors (FGFs) that play important roles in cell growth, differentiation, and tissue patterning, particularly essential for bone and central nervous system development (Brewer et al. 2015). IGF1 codes for insulin-like growth factor 1, promoting cell growth, proliferation, and differentiation in various tissues, including muscle and bone (Laron 2001). *Nfkb1* encodes a subunit of *NF-κB* protein complex, regulating immune and inflammatory responses, along with cell survival and apoptosis during development (Liu et al. 2017). *Tbx6*, a transcription factor important for the segmentation and differentiation of the axial skeleton, including vertebrae and ribs (Yasuhiko et al. 2006). Lastly, *TgfA* codes for transforming growth factor alpha, a protein from the *Egf* family, contributing to cell proliferation, tissue differentiation, and morphogenesis throughout development (Kumar, Bustin, and McKay 1995).

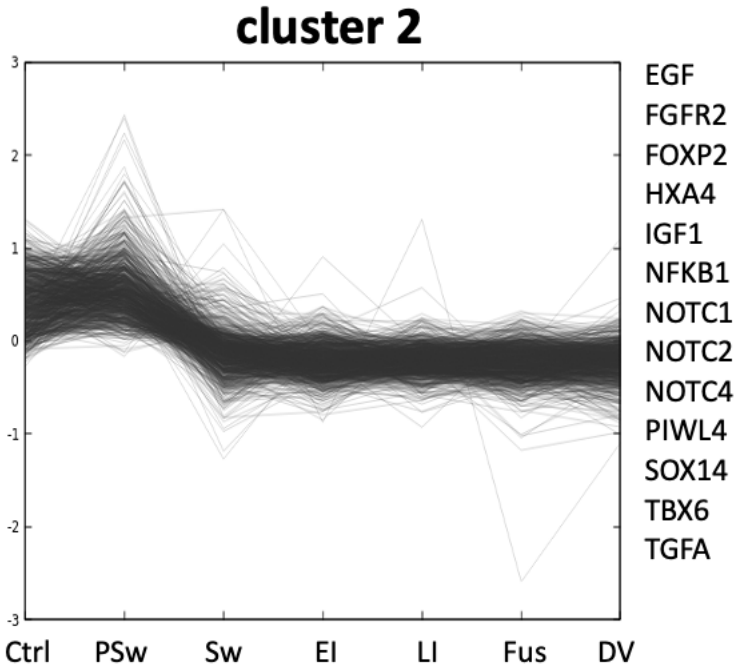

GO enrichment by cluster: Biological Process (*de novo* transcriptome assembly)		
Cluster 2		
Adj.Pval	*Fold*	*Pathway*
1.59E-02	1.9	G protein-coupled receptor signaling pathway
1.59E-02	1.3	Response to chemical
1.74E-02	5.5	Response to amphetamine
1.74E-02	4.7	Response to amine
1.74E-02	2	Modulation of chemical synaptic transmission
1.74E-02	2	Negative regulation of transport
1.74E-02	2	Regulation of trans-synaptic signaling
1.74E-02	1.8	Trans-synaptic signaling
2.31E-02	1.3	Response to organic substance
2.31E-02	1.3	Regulation of biological quality

Figure 3.35: *Temporal expression profiles of genes comprised in cluster 2 with the main GO terms enriched within this cluster.*

In the cluster 3 is mainly composed of genes that are downregulated when the budding is activated (PSw) and remain downregulated during all the following stages. This cluster is enriched in the GO terms “animal organ morphogenesis” and “anatomical structure morphogenesis” which were reported in the cluster “F” in the DNTA. The cluster “C” is also enriched in the terms: Heart looping involves a complex transformation of the heart tube, ensuring proper orientation and alignment of heart chambers and blood vessels for efficient cardiovascular function. Catabolic processes break down complex molecules, providing essential energy and building blocks for cellular activities during embryogenesis. Tube

development plays a fundamental role in forming organs like the nervous and respiratory systems through shaping and elongating cylindrical structures. Epithelial morphogenesis organizes tissue layers with specific functions as cells rearrange, change shape, and migrate. Determining heart left/right asymmetry is tightly regulated, positioning heart structures correctly to prevent congenital heart defects. Embryonic heart tube morphogenesis remodels the heart tube into distinct cardiac chambers, valves, and blood vessels. Mammary gland development, starting in embryogenesis and continuing postnatally, involves branching, alveoli formation, and cell differentiation for lactation and nourishing offspring. Cellular catabolic processes maintain cellular homeostasis, removing damaged or unnecessary components through apoptosis, ensuring proper tissue sculpting during embryonic development and the formation and functioning of organs and systems.

The cluster 3 also contained the genes *Fgfr1* (Fibroblast Growth Factor Receptor 1) codes for a crucial receptor protein involved in developmental processes, including cell proliferation, migration, and differentiation. It is vital for developing tissues and organs like the brain, limbs, and skeleton, and mutations can lead to disorders like craniosynostosis and skeletal dysplasia (Brewer et al. 2015). *FoxP3* (Forkhead Box P3) encodes a transcription factor critical for the differentiation and function of regulatory T cells (Tregs), maintaining immune system balance and preventing autoimmune disorders like IPEX syndrome (Ramsdell and Ziegler 2014). *Fzd7* (Frizzled 7) codes for a receptor protein that mediates *Wnt* signaling, crucial for cell fate determination, tissue patterning, and organogenesis during development (Winklbauer et al. 2001). *Wnt1* (Wingless-Type MMTV Integration Site Family, Member 1) codes for a secreted signaling protein important in various developmental processes, particularly in early midbrain patterning (Kimelman and Martin 2012). The genes *Bmp3* and *Dlx1* were also present in cluster "C" in the DNTA, which was a cluster with the same expression profile as this one. The gene *Wnt3* was reported in the cluster "B" in the DNTA, while *Wnt5B* was reported as upregulated in the DNTA (cluster "E"). *Wnt5B* is involved in the regulation of intracellular signal transduction, including its effects on both the non-canonical (β-catenin-independent) and canonical *Wnt* signaling pathways (β-catenin dependent) (Perkins et al. 2022).

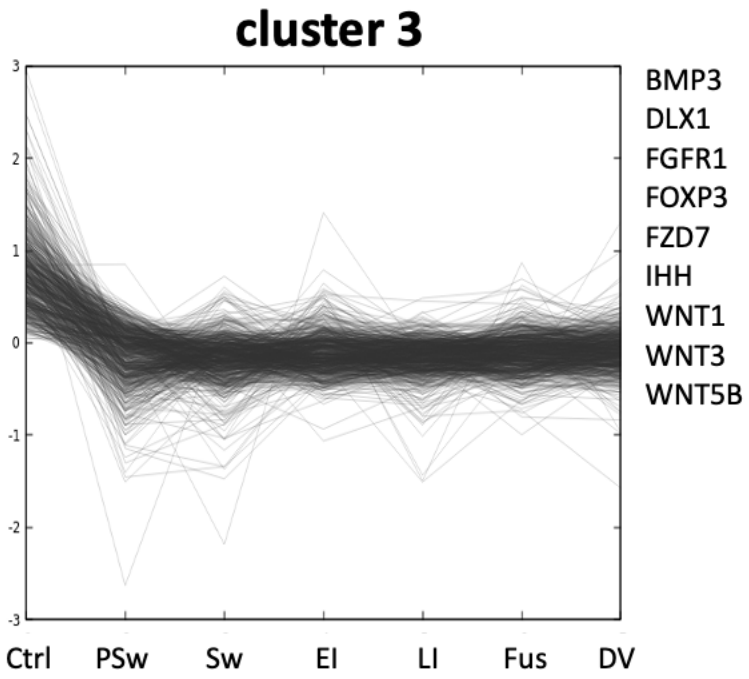

GO enrichment by cluster: Biological Process (*de novo* transcriptome assembly)		
Cluster 3		
Adj.Pval	*Fold*	*Pathway*
1.21E-02	4.2	Heart looping
1.21E-02	1.5	Catabolic process
1.21E-02	1.8	Animal organ morphogenesis
1.21E-02	1.8	Tube development
2.45E-02	2.1	Morphogenesis of an epithelium
2.45E-02	3.8	Determination of heart left/right asymmetry
2.66E-02	1.4	Anatomical structure morphogenesis
2.90E-02	3.6	Embryonic heart tube morphogenesis
2.90E-02	3.1	Mammary gland development
2.90E-02	1.5	Cellular catabolic process

Figure 3.36: *Temporal expression profiles of genes comprised in cluster 3 with the main GO terms enriched within this cluster.*

The cluster 4 contains genes with a peak of expression only during the PSw stage, these genes did not display any specifically enriched GO term. Inside this cluster were present the genes *Fgfr3*, which regulates cell growth and differentiation, particularly in skeletal development (Brewer et al. 2015). *Fog2* is vital for heart development and normal cardiac structures. *FoxH1* acts as a key regulator in early embryonic development and mesoderm formation. *FoxP4* participates in lung and neuronal development, as well as speech and language development. *FoxQ1* is involved in epithelial development and tissue homeostasis, and also plays a role in cancer progression (Shimeld, Degnan, and Luke 2010). *Hnf4A* is

expressed in the liver and regulates hepatic function and metabolism (DeLaForest et al. 2011). *Lbx1* is crucial for limb and neural development (Müller et al. 2002). *Sox9* is involved in sex determination and skeletal development (Marshall and Harley 2000). *Tgfi*1 is induced by *Tgf-beta* signaling and participates in cell growth, differentiation, and immune response (Miyazono 2000). *Tnf10* is a member of the *Tnf* superfamily, regulating immune responses, inflammation, and cell death (Falvo, Tsytsykova, and Goldfeld 2010). *VegfC* is a critical regulator of lymphangiogenesis and angiogenesis, forming lymphatic and blood vessels, respectively (Joukov et al. 1997).

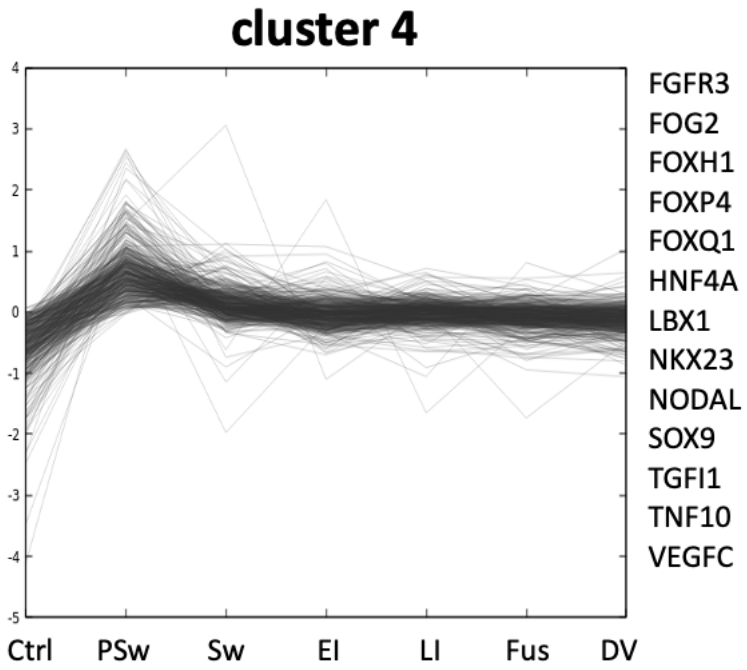

Figure 3.37: *Temporal expression profiles of genes comprised in cluster 4.*

The cluster 5 presented not only a expression curve similar to the one in the cluster "E" in DNTA, but also the majority of enriched GO terms were the same. Many of the candidate DEG were also common to the DNTA cluster "E", except for few ones like *Bmp10*, *Gli2* which is involved in embryonic cell differentiation and patterning (Pan et al. 2006), *HoxA3* triggers cell migration in both endothelial and epithelial cells, thus enhancing angiogenesis and wound healing (Mace et al. 2005), *Pax5* controls B-cell differentiation and function (Cobaleda et al. 2007), *Pbx1* influences limb development (Capellini et al. 2006), *Piwl1*, *Tbx1* is crucial for the formation of various structures derived from pharyngeal arches (Zhang et al. 2005), *Tll2*, *Vgfr1*

is critical for angiogenesis, tissue repair, and nerve regeneration (Guaiquil et al. 2016) and *Wnt6* is involved in nervous system and limb development through the *Wnt* signaling pathway (Schubert et al. 2002).

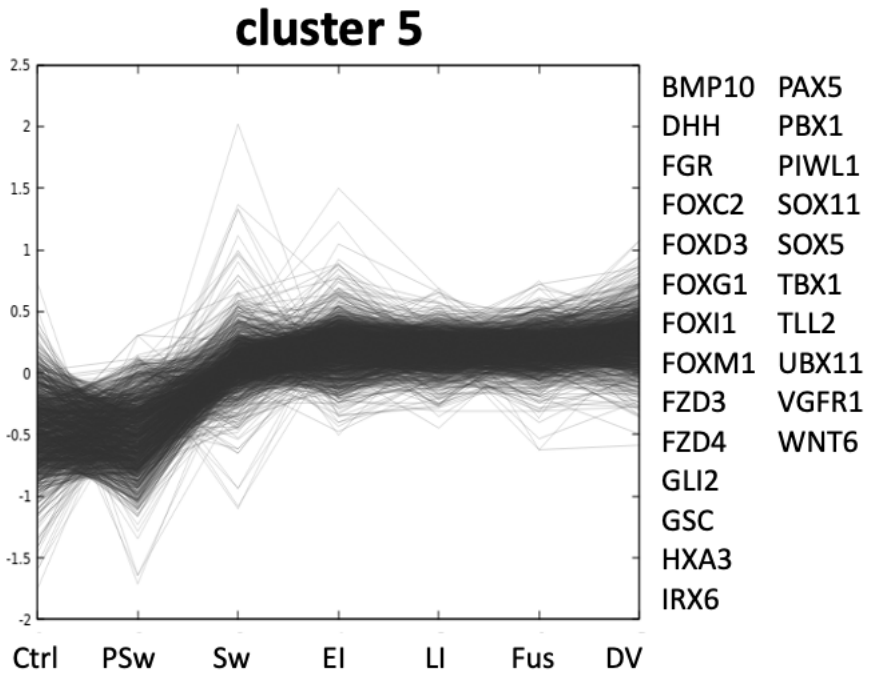

GO enrichment by cluster: Biological Process (*de novo* transcriptome assembly)		
Cluster 5		
Adj.Pval	*Fold*	*Pathway*
4.63E-22	2	***RNA processing***
3.44E-20	2.4	***Ribonucleoprotein complex biogenesis***
6.11E-15	2.3	***NcRNA processing***
6.11E-15	2.5	***Ribosome biogenesis***
6.03E-14	2.6	***RRNA processing***
5.24E-13	2.5	***RRNA metabolic process***
8.94E-12	2	***NcRNA metabolic process***
1.13E-09	1.6	***Chromosome organization***
1.21E-09	2	MRNA processing
3.03E-07	1.7	MRNA metabolic process

Figure 3.38: *Temporal expression profiles of genes comprised in cluster 5 with the main GO terms enriched within this cluster.*

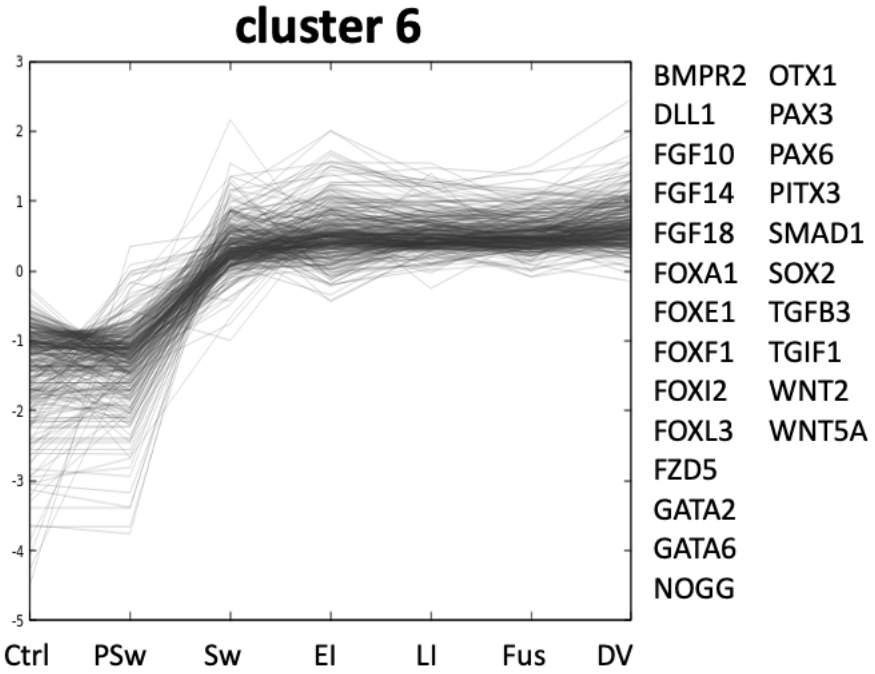

GO enrichment by cluster: Biological Process (*de novo* transcriptome assembly)		
Cluster 6		
Adj.Pval	*Fold*	*Pathway*
2.01E-05	2.3	Chromosome organization
2.40E-05	3.4	Regionalization
2.40E-05	8	DNA replication initiation
2.40E-05	2.3	Animal organ morphogenesis
6.89E-05	3.4	Urogenital system development
6.89E-05	2.9	Pattern specification process
9.16E-05	2.2	Mitotic cell cycle
9.96E-05	7.6	Regulation of DNA-templated DNA replication
1.25E-04	3.4	Renal system development
1.54E-04	2.5	Vasculature development

Figure 3.39: *Temporal expression profiles of genes comprised in cluster 6 with the main GO terms enriched within this cluster.*

The cluster 6 comprises genes that are upregulated when the Sw starts and remain upregulated during the rest of budding development. This cluster contains genes like: *Otx1* specifies the anterior regions of the embryo, critical for brain and sensory organ formation (Simeone et al. 1993). *Pax3* regulates neural crest cells, muscle, and CNS development (Monsoro-Burq 2015). *Pax6* is a master regulator in eye development and (Kamachi et al. 2001). *Pitx3* is crucial for dopaminergic neuron differentiation in the midbrain (Smidt, Smits, and Burbach 2004). *Fgf18* is involved in skeletal development (Haque, Nakada, and Hamdy 2007). *Smad1* regulates cell growth and mesoderm development (Furtado et al. 2008). *TgfB3*

influences palate, lung, and tissue development (Yang and Kaartinen 2007). *Tgif1* modulates *Tgf-β* signaling and CNS development (Powers et al. 2010).

This cluster is also enriched for different GO terms, like: “Chromosome organization” which involves spatial arrangement and maintenance of chromosomes, playing a role in cell division and differentiation. “Regionalization” refers to specifying embryonic tissues or regions, establishing different body segments. “Animal organ morphogenesis” was also detected in cluster “F” in the DNTA. “Pattern specification” establishes spatial patterns and structures in tissues and organs. “Vasculature development” creates blood vessels for tissue perfusion during development.

Clustering Comparisons Between GBTM and DNTA

To compare the equivalence of the clusters’ compositions between both analyses (DNTA and GBTM) not only in expression profile but also in gene composing them, the list of genes present in each cluster was compared using a simple Venn Diagram to visualize how much each analyzed clusters overlap in their composition. In the DNTA, cluster “A” consisted of 461 unique gene names, while in the cluster “1”, there were 360 genes. There was an overlap of 140 genes between them two. Cluster “B” had 709 genes in the DNTA and 427 in the cluster “2” of the GBTM, with 225 genes overlapping. For cluster “C”, there were 1012 genes in the DNTA and 891 in the GBTM cluster “3”, with 312 genes matching. The cluster “D” had 1223 genes in the DNTA and 672 in the GBTM in the cluster “4”, with an overlap of 256 genes. In the cluster “E”, there were 1590 genes in the DNTA and 1363 in the cluster “5” of the GBTM, with 633 genes overlapping. Lastly, cluster “F” had 387 genes in the DNTA and 321 in the GBTM cluster “6”, with 174 genes common between both clusters (figure 3.40).

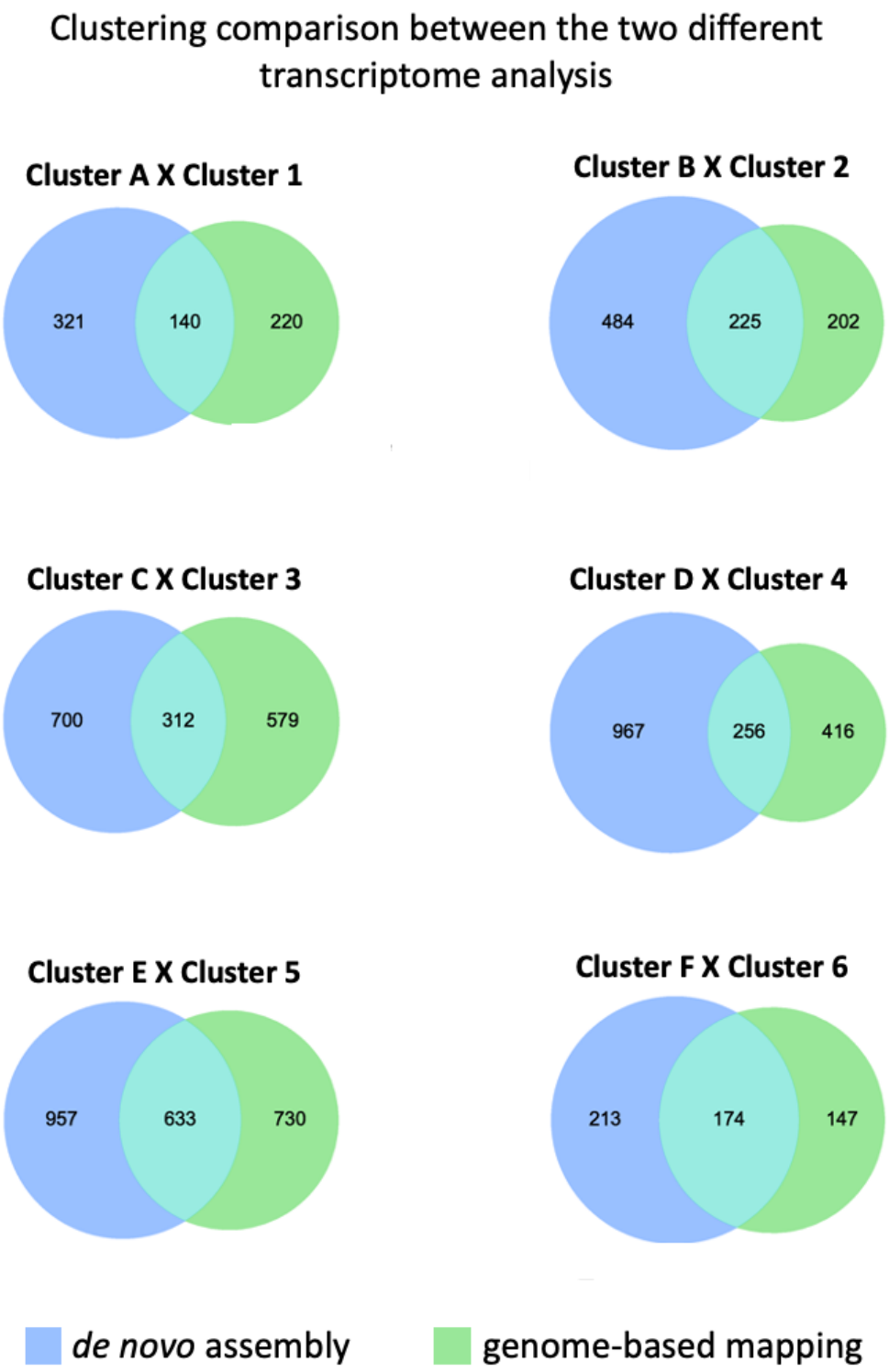

Figure 3.40: *Cluster gene composition comparison between DNTA and GBTM analyses.*

The DEG included in the same clusters in both GBTM and DNTA, have revealed, among others, a number of genes that have been reported as involved in different developmental processes, such as *Bmp*, *Tll*, *Dll*, *Notch*, *Irx6*, *Hh*, *Nk4*, *Gata*, *Wnt*, *Runx*, *Piwl* and *Gsc*. For these

selected candidates, in the following paragraphs, I highlighted some of the most important features, discussing their distinct roles in animal and ascidian developmental processes:

Bmp/Tll

Bmp (Bone Morphogenetic Proteins) are key members of the transforming growth factor-β (*Tgf-β*) superfamily, pivotal for various cellular processes in embryonic development, such as differentiation, proliferation, and apoptosis, with a marked role in organogenesis, bone formation, and limb patterning (Cadigan and Nusse 1997; Wodarz and Nusse 1998; Nusse 2005). While, Tolloid-like proteins (*Tll*) are metalloproteinases responsible for modulating several matrix molecules and signaling proteins, including B*mp*. *Tll* regulates *Bmp* signaling by controlling *Bmp* ligand availability and activity (Vadon-Le-Goff, Hulmes, and Moali 2015). *Bmp* interacts with extracellular proteins like *Chordin* and *Noggin*, which, in turn, act as *Bmp* inhibitors, thereby controlling their own activity. These antagonists bind *Bmp*, preventing their receptor interaction and thus inhibiting *Bmp* signaling. *Tll* counteract this negative feedback by cleaving chordin, increasing *Bmp* binding to their receptors, and consequently activating *Bmp* signaling, which ensures apt temporal and spatial modulation during the development (Troilo et al. 2015). This interplay is evident in the dorsal-ventral patterning of embryos like in *Xenopus* and zebrafish, where *Tll* facilitate ventral *Bmp* signaling by cleaving dorsally produced *Chordin*, establishing a dorso-ventral *Bmp* activity gradient that is instructive for subsequent development and tissue differentiation (Muraoka et al. 2006). Furthermore, *Bmp* reciprocally influences the expression of *Tll* and its antagonists, setting up feedback mechanisms that increase the precision of developmental patterning. In essence, *Bmp* and *Tll* have a symbiotic relationship critical for the nuanced regulation of developmental signaling pathways, orchestrating precise cellular processes and tissue organization (Vadon-Le-Goff, Hulmes, and Moali 2015).

Bmp1, part of cluster 1, was found to be downregulated at the onset of the budding process. *Bmp3,* part of cluster 3, shows a similar dynamic. Conversely, *Bmp10*, part of cluster 5, increases its activity after the PSw stage. The *Bmp* inhibitor *Noggin*, part of cluster 6, exhibited a similar expression profile.

The clusters 1, 2, 3 and 4 contain genes that are downregulated either after the Ctrl or PSw stages and genes that show a peak of expression only at PSw (clusters 1 and 4), i.e., genes whose activity is restricted to early stages or downregulated at the beginning of the budding process. The *Bmp1* orthologue was found in cluster 1. In vertebrates, *Bmp1* regulates extracellular matrix formation (Vadon-Le-Goff, Hulmes, and Moali 2015). *Bmp1* proteins can help release *Bmp2* and *Bmp4* from chordin, generating the *Bmp* signaling gradients that are instructive for the development of the dorsal-ventral axis during embryogenesis (Ge and Greenspan 2006). At the 32-cell stage, *Bmp* can be found in the majority of vegetal cells in *Ciona intestinalis*, *Phallusia mammilata*, and *Halocynthia roretzi* (Darras and Nishida 2001; Fiuza et al. 2020). However, it is limited to the anterior endodermal cells at the 64- and 112-cell stages. While the inhibition of *Bmp* signaling following overexpression of *Chordin* or *Noggin* does not affect gastrulation, it does prevent the development of sensory head pigment cells (Darras and Nishida 2001; Fiuza et al. 2020). In the ascidian *Polycarpa mytiligera* *Bmp1*-expressing cells were detectable in the tunic matrix (which resembles the extracellular matrix) in the region of an injury prior to regeneration (Hendin et al. 2022). *Bmp1* is also detected in the primary budding in *B. schlosseri* marking cells committed to the germ line (Rosner et al. 2013). The *Bmp* antagonist *Noggin* is found as DEG, upregulated during later budding stages (cluster 6). This gene was first discovered in *Xenopus* and it produces a polypeptide that can stimulate the development of neural tissues while inhibiting *Bmp*, which leads to the formation of dorsal structures. Although the role of *Noggin* in neural induction in ascidians is not yet fully understood, its consistent expression in the neural folds and nerve cord of *C. intestinalis* suggests that it plays a similar role in neural tube closure (Imai et al. 2004) as in vertebrates. Furthermore, the orthologue of *Bmp10* was found upregulated in a similar manner as *Noggin*, which in vertebrates is involved in heart development (Choi et al. 2023). In *C. intestinalis*, it was described as upregulated together with other genes involved in cardiovascular development, suggesting a conserved role, although its precise function in tunicates is still unclear (Matsubara et al. 2021). Apart of the three *Bmp* orthologues cited above, it was also identified *Bmp2/4*, *Bmp5/6/7/8*, *Bmp11* and other two *Bmp* proteins which the homology was not clear (figure 3.41, full phylogeny in the appendix 8).

Bmp orthologues might be involved in the reorganization of the ECM surrounding the vesicle to allow the vesicle swelling, patterning the budding vesicle into specific domains,

delimitating the portion of the vesicle which will suffer the invagination and later activating downstream TFs (i.e., *Gata*) to orchestrate different organs formation.

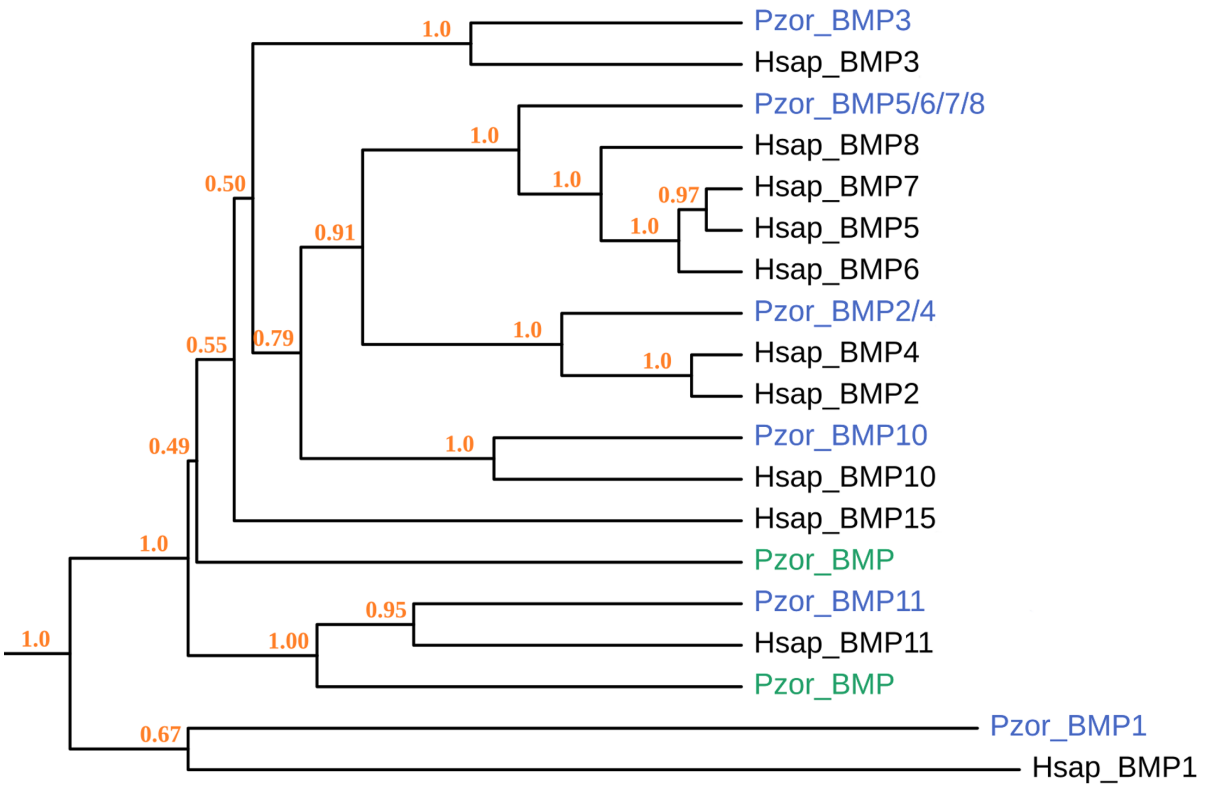

Figure 3.41: *Simplified phylogenetic analysis of BMP genes from species Polyandrocarpa zorritensis and Homo sapiens. The tree reveals evolutionary relationships among various BMP genes. Bootstrap values, given at the nodes, indicate the confidence of each branching event (orange).*

In the cluster 1, it was also found *Tll1* downregulated after the PSw stage. Conversely, *Tll2*, part of cluster 5, was upregulated after PSw. The *Tll* gene encodes Tolloid-like proteins, *Tll1* and *Tll2*, in vertebrates. These metalloproteinases are vital in embryogenesis, especially in shaping the dorso-ventral body axis and tissue patterns by modulating the *Chordin-Bmp* signaling pathway. They control *Bmp* activity by cleaving *Chordin*, which releases *Bmp* to signal and determine cell fates. This modulation is also key in influencing neural tissue development and possibly impacting the heart and cartilage formation (Vadon-Le-Goff, Hulmes, and Moali 2015). A study found that in *Botryllus schlosseri*, *Tll1* was expressed in testes and localized to maturing eggs (Rodriguez et al. 2014), suggesting a role in balancing *Bmp* during germ cell development and differentiation (Rosner et al. 2013).

Delta (*DLL*) and *Notch*

Dll is part of cluster 6, meaning it is upregulated from the PSw until DV stages. Notch 1, 2, and 4 are found in cluster 2; they are downregulated after PSw. Delta is a membrane-bound ligand of the Notch receptor, crucial for various developmental processes in vertebrates (Parks et al. 2000). Upon binding, Delta triggers the release of the Notch intracellular domain, which in turn activates or represses downstream gene expression. As both *Delta* and *Notch* are membrane-bound, their signaling can lead to lateral inhibition, ensuring different cell fates among neighboring cells, for instance, during neurogenesis, where *Notch* signaling plays a role in choosing neurons in neurogenic areas of the developing neural plate (Appel, Givan, and Eisen 2001). By virtue of this juxtacrine mechanism, it is essential for demarcating boundaries in tissues, guiding angiogenesis by determining roles of endothelial cells at the onset of vessel formation, and influencing organ development, such as in the heart and the pancreas (Nijjar et al. 2002). In adult tissues, this signaling remains vital for stem cell maintenance and tissue homeostasis, impacting T-cell development and bone remodeling (Pasini et al. 2006; Louvi and Artavanis-Tsakonas 2006; Pellegrinet et al. 2011). In *Ciona*, the *Delta2/Notch* pathway plays a role in determining both the lateral and medial fates within the neural plate. While a lateral inhibition function of *Notch* signaling during neurogenesis has not been studied in the central nervous system of *Ciona* (Pasini et al. 2006), it actively participates in selecting epidermal sensory neurons within the dorsal and ventral midline neurogenic regions of the larval tail epidermis (Hudson, Lotito, and Yasuo 2007). *Notch* and *Delta* were also found as highly expressed in the blastema during siphon regeneration in *C. intestinalis* and as upregulated during WBR in *Botrylloides leachii* (Rinkevich, Rinkevich, and Reshef 2008; Hamada et al. 2015). It is possible that *Delta* and *Notch* are acting during *P. zorritensis* budding by initially establishing the domain of the future nervous system and later also participating in the pre-setting of organogenesis.

Iroquois (*Irx6*)

The Iroquois homeobox (*Irx*) genes are part of the evolutionarily conserved family of homeobox genes, essential for the formation of body plans during embryonic development in animals. Specifically, in vertebrates, *Irx* genes play multiple roles (Cavodeassi, Modolell, and Gómez-Skarmeta 2001). They are crucial for heart development, with different *Irx* genes

expressed in distinct heart compartments, determining and maintaining cardiac regions' identity. They participate in neural development, assisting in the regional specification of the neural plate that forms the central nervous system and can influence the creation of particular neural structures. In the eye, *Irx* genes are instrumental in retinal cell differentiation and patterning, ensuring proper retinal organization. These genes also have a role in the segmentation of early vertebrate embryos, helping establish the anterior-posterior axis. They are involved in skeletal muscle differentiation, influencing muscle fiber patterning during embryogenesis, and are essential for limb development and patterning, defining specific limb regions and ensuring the proper formation of structures like fingers and toes. The function of *Irx* genes can differ based on the species and developmental context, and they often collaborate with other genes and signaling pathways in their developmental roles (Cavodeassi, Modolell, and Gómez-Skarmeta 2001; Gómez-Skarmeta and Modolell 2002).

In *B. schlosseri*, *IrxB* expression has been reported from the double vesicle stage. During that stage, it delineated the place where the future dorsal tube began forming from a thickening of the inner vesicle's epithelium. In subsequent stages, *IrxB* expression appears to become restricted to a central section of the dorsal tube (Prünster et al. 2019a). These results seem to suggest a role in differentiating the anterior-posterior axis of the embryo. Based on the function of *Irx6* in vertebrates and in the ascidian *B. schlosseri* (*IrxB*), it is possible to hypothesize about it being involved in the patterning of bud's dorsal region and later participates in heart and nervous system development once it keeps upregulated until the DV stage (cluster 5).

Hedgehog (*Hh*)

Desert Hedgehog (*Dhh*), belonging to cluster 5, is found to be upregulated after the PSw stage. HH, on the other hand, is part of cluster 3, i.e., it is downregulated between Ctrl and PSw and remains downregulated. *Gli2*, a TF downstream of *Hh* is found in cluster 5, which means it is upregulated after the PSw stage. The *Hedgehog* pathway in vertebrates is integral to embryonic development, which primarily comes down to three central proteins: *Sonic hedgehog* (Shh), *Indian hedgehog* (Ihh), and *Desert hedgehog* (*Dhh*), with *Shh* being the most representative. It plays a crucial role in tissue patterning during early embryogenesis, such as in the neural tube, limbs, somitogenesis, and organogenesis, being involved in lung, pancreas,

and liver development (Ingham and Placzek 2006; Choudhry et al. 2014). Furthermore, it influences cell differentiation and proliferation (Carballo et al. 2018). When *Hedgehog* ligands bind to *Patched1* (*Ptch1*) receptors, it activates a pathway that involves the Smoothened protein and *Gli* transcription factors in a messenger cascade within the cell. Intricate feedback mechanisms, mainly via *Ptch1*, ensure its fine-tuned regulation (Warzecha et al. 2006; Briscoe and Thérond 2013; Fernandes-Silva, Correia-Pinto, and Moura 2017).

In *Ciona intestinalis*, *Hh1* was found as an evenly distributed maternal transcript in fertilized eggs and early embryos, while *Hh2* was found to be zygotically expressed in the tailbud stage, with its transcript being restricted to the ventral nerve cord (Takatori, Satou, and Satoh 2002). At the larval stage, *Gli* was expressed in the endoderm's central part and visceral ganglion, while HH2 was expressed in cells adjacent to the *Gli* expression domain (Tariqul-Islam et al. 2010). In *B.schlosseri*, *Hh* appears expressed in stem cells that show migration towards developing buds between stages A1 and A6 (Kowarsky et al. 2021). As mentioned above, two genes for hedgehog were found in *P. zorritensis* (figure 3.38, fully detailed tree in appendix 9), one being *Hh* (*Ihh* in cluster 3) and *Dhh* (present in cluster 5).

During NED, the role of *Hh* may differ from its function in embryogenesis. Some tissues may downregulate *Shh* to prioritize other pathways vital for regeneration. This downregulation can prevent the re-specification of tissues, especially since *Shh* defines tissue types during embryogenesis. Factors like feedback inhibition due to high *Hedgehog* pathway activity, cell cycle regulation needs, shifts in the local microenvironment, and potential tissue damage responses might influence this reduction in *Shh* expression (that can explain *Hh* downregulation in cluster 2) (Torok et al. 1999). Additionally, while its expression may initially decrease, SHH might become more active in later regeneration stages. Moreover, *Shh*'s interactions with other pathways, such as *Wnt*, *Fgf*, and *Bmp*, can impact its activity (Kucerova et al. 2012). Most of these genes are upregulated during *P. zorritensis* budding. In other hand there is *Dhh* being upregulated after PSw, until the DV stage. This might be related with HH roles in axis patterning, patterning the tissue together with other pathways (i.e., *Wnt*, *Bmp*, *Fgf*, *Gli*) to orchestrate organogenesis.

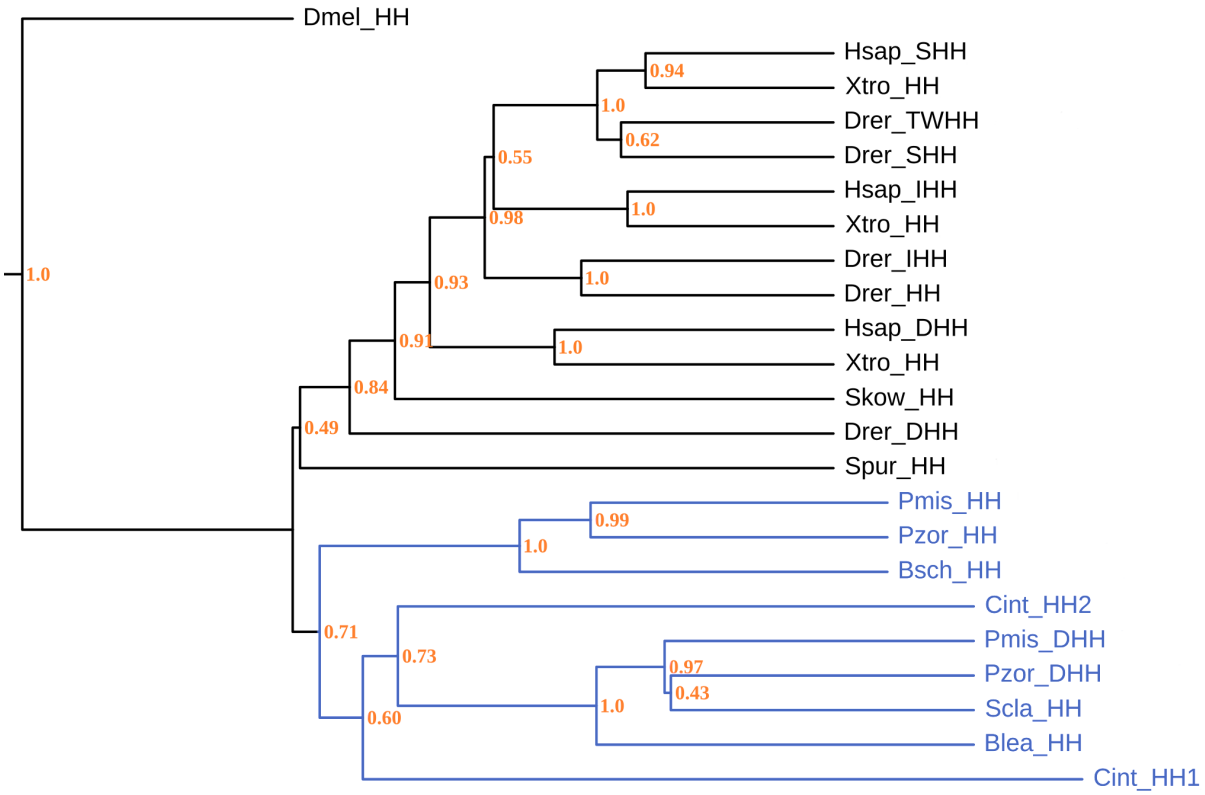

Figure 3.42: *Phylogenetic tree depicting relationships among Hedgehog (HH) gene sequences across diverse organisms, primarily vertebrates. The tree showcases the evolutionary dynamics of HH genes, including SHH, IHH, and DHH, among species. Bootstrap values, given at the nodes, indicate the confidence of each branching event (orange).*

NK4

Nk4 is the *C. intestinalis* homologue of *Nkx2-5/tinman*, a homeobox protein controlling cardiac development in vertebrates, and has been implicated in regeneration processes throughout ascidians. This may be mainly due to its important role in promoting the expression of *GataA* by antagonizing the action of *Tbx1* (Wang et al. 2013). *Nk4* expression is displayed across the ventral epidermis as well as the anterior trunk endoderm between the neurula stage and metamorphosis of the tailbud larva. Like in vertebrates, *Nk4* is pivotal for the specification of the heart precursors (Wang et al. 2013).

During the early stages of *B. schlosseri* and *P. zorritensis* regeneration, *Nk4* expression was described in the bud area where the inner vesicle would form. In the case of peribranchial budding, it was described to be expressed in the thickened, evaginating epithelium. Upon formation of the inner vesicle, the expression territory of *Nk4* would become restricted to the anterior-right side. The expression territory in *B. schlosseri* vascular budding would be the developing inner vesicle. Finally, in the vasal budding process of *P. zorritensis*, the first

instances of *Nk4* expression would become visible from the time of epithelial invagination, distinguishing the *Nk4*+ invaginating part of the epithelium from the non-invaginating part (Alié et al. 2018).

While the expression of *Nk4* (*Nkx2.3/2.5/2.6* in vertebrates) in *P. zorritensis* had been reported previously, it was utilized as a control due to its significance in this context and the fact that this in situ technique had not been employed before in *P. zorritensis* (Alié et al. 2018). The Sw stage was included during the experiment, which was not studied in the work of Alié et al. (2018). Notably, during this stage, the *Nk4* expression domain has the shape of a spherical cap in the upper region of the outer vesicle, probably where invagination is set to occur (Figure 3.43). At a later stage, *Nk4* is expressed in the whole invaginating region and then later in the newly formed inner vesicle, after which it seems to get restricted to a portion of the older vesicle (Alié et al. 2018), before the organogenesis starts.

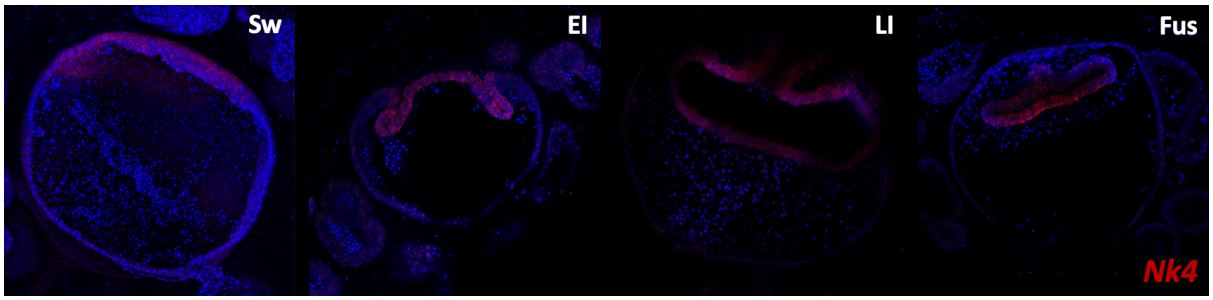

Figure 3.43: *in situ hybridization for NK4 in Polyandrocarpa zorritensis.*

Wnts

Wnt proteins in vertebrates use three main signaling pathways: the Canonical (*Wnt*/*β-catenin*) pathway which regulates gene transcription, the Planar Cell Polarity (PCP) pathway influencing cell orientation and movement, and the *Wnt*/Ca2+ pathway that affects intracellular calcium levels and cellular functions (Kühl et al. 2000). These pathways are central to various developmental processes in embryogenesis, including axis formation, gastrulation, neural development, limb development, organogenesis, somitogenesis, and stem cell maintenance (together with *Notch*) (Reya and Clevers 2005; Duncan et al. 2005). Furthermore, *Wnt* signaling interacts with other pathways and is regulated by external

inhibitors like sFRPs and DKKs, ensuring proper developmental coordination (Sharma et al. 2015).

In adult organisms, stem cells are responsible for tissue homeostasis and regeneration. The *Wnt* pathway is crucial in preserving the undifferentiated status of stem cells and regulating their ability to self-renew in various tissues, including the skin, intestine, and hematopoietic system, which is pivotal for repair responses such as tissue regeneration. Injuries or diseases that cause tissue damage often trigger regenerative responses (Whyte, Smith, and Helms 2012). The *Wnt* pathway is activated during these regenerative processes. In animals like axolotls, which can regenerate lost limbs, *Wnt* signaling is activated and is essential for successful regrowth. After partial hepatectomy, the liver can regenerate, and *Wnt* signaling has been shown to play a role in this process. The cyclic growth of hair follicles is regulated by *Wnt* signaling (Wang, Etheridge, and Wynshaw-Boris 2007). While mammals, including humans, have limited capacity for neural regeneration, the *Wnt* pathway has been implicated in neurogenesis, axonal growth, and neural plasticity (Gao et al. 2021).

The importance of *Wnt* for regeneration processes may lie in its short signaling distance which may associate stemness of a cell with its distance respective to the niche where *Wnt* is produced via paracrine signaling. This may contribute to controlling the amount of cells participating in organ regeneration and thus guide morphogenesis in a spatial and quantitative manner (Millar et al. 1999). However, the decision on the future cell fate may be made through different pathways, such as *Delta/Notch* which has been suggested to act in concert with *Wnt* (Collu, Hidalgo-Sastre, and Brennan 2014). Conversely, depletion of *Wnt* signal in a stem cell niche may trigger local differentiation (Clevers, Loh, and Nusse 2014; Gao et al. 2021).

Wnt have been described from studies in several ascidian species. First, in *Halocynthia roretzi*, *Wnt5a* is required for specifying muscle cell types during myogenesis. The finding that, unlike in *C. intestinalis*, *Halocynthia* does not require Nodal signaling in addition, provides evidence of significant diversification of developmental mechanisms among ascidians (Tokuoka, Kumano, and Nishida 2007). More relevant for the study of NED, *Wnt* seems to be pivotal for the early steps in bud morphogenesis in *B. schlosseri*. It was shown that an ectopic increase of *Wnt* activity may result in the formation of additional budlets, and duplication of the AP axis. *Wnt* can also induce changes in polarity on the cellular level, for instance within

the atrial epithelium of the inner vesicle of the primary bud. Consistently, the place within the peribranchial epithelium that experiences thickening is also the area of particularly strong Wnt expression. Additional roles for *Wnt* signaling in this species have been suggested for angiogenesis, vascular development, and germ cell proliferation and migration. In *C. intestinalis*, *Wnt* signaling has also been associated with gastrulation, germ layer specification, and metamorphosis, but, like in *B. schlosseri*, appears to be critical for endoderm formation and polarization of the embryo body axis (Di Maio et al. 2015). Taken together, *Wnt* may be critical for at least two developmental functions consistently between species: First, as a way to control local stem cell balance, and second, to coordinate polarity both on the cellular and tissue level.

Runx/runt

Runx is present in cluster 1, being downregulated at the start of the budding process. In vertebrate embryogenesis, *Runx* genes play pivotal roles: *Runx1* is essential for hematopoiesis, particularly in the formation of hematopoietic stem cells in the AGM (aorta–gonad–mesonephros) region and T-cell development in the thymus. *Runx2* is crucial for osteogenesis. These genes also influence neurogenesis, with specific roles in the development of dorsal root ganglion neurons (Kramer et al. 2006). Additionally, they are implicated in chondrocyte differentiation (cartilage formation), gut development by *Runx3*, and the evolution of various sensory neurons. These functions, complex and varied, are part of intricate regulatory networks and may differ across vertebrates (Mevel et al. 2019; Srivastava 2021). *Runt* has been shown to have important roles in planarian regeneration (Wenemoser et al. 2012). *Runt* expression is also upregulated in sea star larval regeneration (Cary et al. 2019). Furthermore, homologs of these genes have also been implicated in regeneration in varied contexts in vertebrates. *Runx* transcription factors are involved in repair and regeneration processes in many tissues, including upregulation upon myopathic damage (Srivastava 2021).

While only single *Runx* proteins are known from the non-vertebrate chordates (*Branchiostoma floridae, B. lanceolatum,* and *Ciona*), there are three human paralogs (*Runx* 1–3), which cluster together on the tree (figure 3.44, detailed phylogeny in appendix 10). This is not surprising given that two rounds of whole genome duplication are known to have

occurred early in vertebrate evolution, prior to the divergence of the ray-finned fishes from the lobe-finned fishes (Sullivan et al. 2008). In *B.schlosseri*, *Runx* expression was documented within the developing buds, with expression domains becoming increasingly spatially restricted, starting from a ubiquitous expression in the secondary bud to the junction area between the primary and secondary bud (Langenbacher et al. 2015). *Runx* is downregulated when Sw starts in *P. zorritensis* NED. The role of *Runx* in this context might be involved in maintaining tissue homeostasis, recruiting cells to the swelling region, and activating cell division and cell proliferation, allowing the tissue to reorganize for budding (Hughes and Woollard 2017).

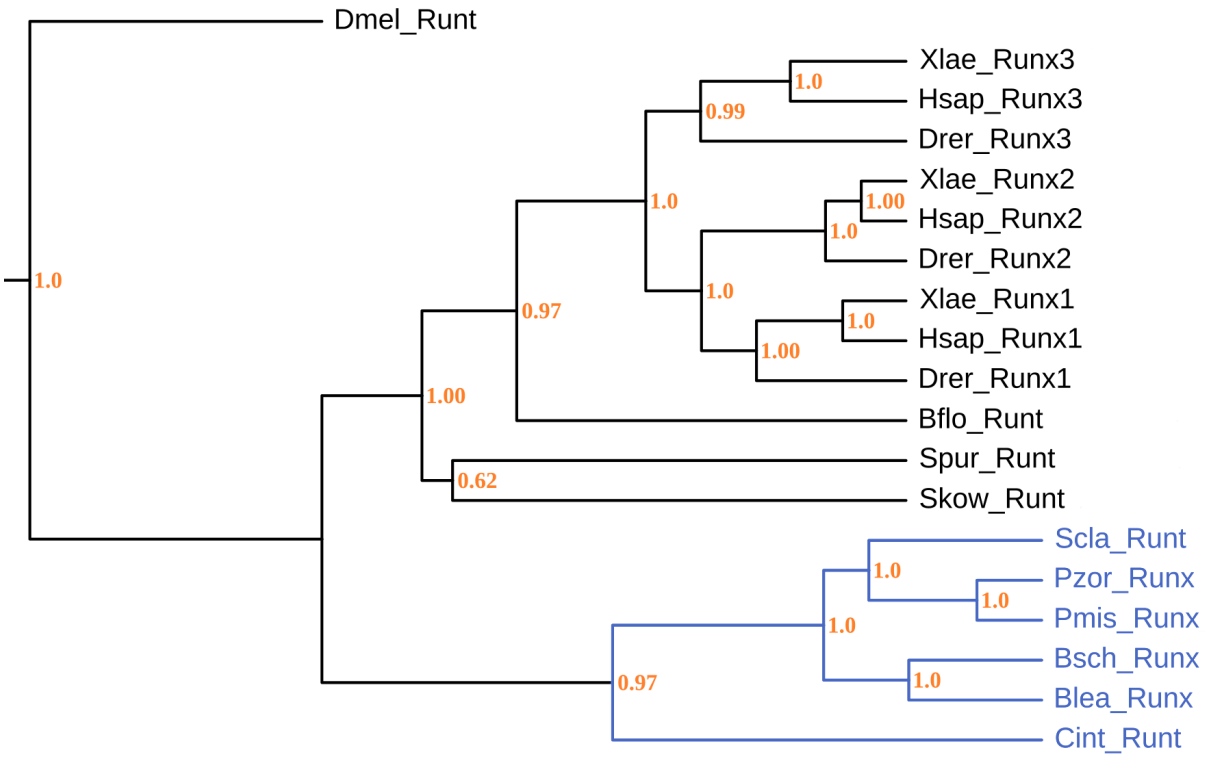

Figure 3.44: *Phylogenetic tree representing evolutionary relationships among 'Runx/runt' genes across various species. Notably, genes from 'Xlae', 'Hsap', and 'Drer' species form distinct, closely related clades for Runx3, Runx2, and Runx1, highlighting their recent shared ancestry. Ascidians form another clade, a sister one, contain only one Runx. 'Dmel' serves as a more distantly related outgroup. Bootstrap values, given at the nodes, indicate the confidence of each branching event (orange).*

Piwi-Like

Piwl1 (*PiwlA*) is present in cluster 5, meaning that it is upregulated after the PSw stage. *Piwl4* is present in cluster 2, being downregulated after the PSw stage. Ascidians *Piwl* is *Piwl1*

according to the phylogeny. Both *Piwi-like* (*Piwl*) and *Argonaute* (*Ago*) proteins play roles in small RNA-guided gene regulation in vertebrates. *PIWL* proteins, in partnership with *Piwi*-interacting RNAs (piRNAs), are predominantly active in germ cells in order to ensure genomic stability by silencing transposons, potentially playing roles in genomic imprinting and stem cell maintenance. On the other hand, *AGO* proteins, associated with small interfering RNAs (siRNAs) or microRNAs (miRNAs), are integral to the RNA interference pathway and influence gene expression during vertebrate embryogenesis, including promoting cell differentiation, morphogenesis, and maintaining stem cell pluripotency (Höck and Meister 2008; Darricarrère et al. 2013).

PIWI-like protein 1 (*PIWL1*), known as *HIWI* in humans, is part of the *PIWI* protein family and plays a crucial role in germline development, stem cell self-renewal, and genome defense. It operates primarily via the small RNA-mediated gene silencing pathway, preventing genomic mutations during embryogenesis. Furthermore, *Piwl1* maintains germline stem cells and ensures proper spermatogenesis. This protein family also influences the epigenetic landscape (particularly by repressing transposable elements) and has emerging roles in early embryogenesis and protection against DNA damage (Lee et al. 2006; Lim et al. 2013).

Piwi has been documented to be involved in the development and regeneration of different ascidian species. In *Botrylloides leachii*, Piwi starts being expressed in cells lining vascular epithelia that, upon activation, are mobilized for incipient WBR. Those cells were reported to undergo morphological changes, proliferate and differentiate. Regeneration arrests upon knockdown of *Piwi* revealed that this protein is not only a marker of cells recruited for WBR but is crucially involved in orchestrating this process (Rinkevich et al. 2010).

Another study showed Piwi expression in germline cells, and a cell population in the hemocoel and tunic vessels in *Botryllus primigenus*, suggesting a role in somatic stem cell maintenance. However, hemoblasts that were involved in vascular bud formation did not exhibit *Piwi* expression (Sunanaga, Inubushi, and Kawamura 2010). Conversely, in *B. violaceus*, small clusters of *Piwi+* hemoblasts were described as aggregating and present in bud development until the early vesicle stages (Kassmer, Langenbacher, and De Tomaso 2020). *Piwi+* cells have also been documented as surrounding regenerating tissues, but not within the differentiating tissues themselves (Brown et al. 2009). Although it has not been shown now exactly those cells participate in the regeneration process, *Piwi* expression

appears to be pivotal for stem cell recruitment and differentiation in the early bud formation. Apart of *Piwl1*, I have identified possibly two orthologues of *Ago*, one that in the phylogeny clusters together with the vertebrates *Ago* and one outside this clade (figure 3.45, detailed tree in appendix 11).

Figure 3.45: *Phylogenetic tree of Argonaute and Piwi-like proteins from various organisms. The tree illustrates the evolutionary relationships and divergence among the proteins, with branch lengths representing evolutionary distances. Bootstrap values, given at the nodes, indicate the confidence of each branching event (orange). Notably, Argonaute proteins and Piwi-like proteins form two distinct clades.*

Goosecoid

Goosecoid (*Gsc*) is part of cluster 5, which means that it becomes upregulated during budding after the PSw stage. In *Xenopus laevis*, the *Gsc* gene plays a crucial role in the formation of Spemann's Organizer, which prevents *Bmp4* from turning the ectoderm into epidermis in the embryo's future head region. By inhibiting *Wnt8* and *Bmp4,* Spemann's

Organizer ensures normal anterior development (Yao and Kessler 2001). *Gsc* is expressed twice during embryogenesis: first during gastrulation and then during organogenesis. During gastrulation, high concentrations of *Gsc* are found in the dorsal mesoderm and endoderm. Later, *Gsc* expression is confined to the head region (Yamada et al. 1995). In *Xenopus*, cells that express *Gsc* become the pharyngeal endoderm, the mesoderm of the head, the ventral skeletal tissue of the head, and the notochord (De Robertis et al. 1992). The gene's role is evolutionarily conserved across vertebrates. Abnormalities in its function can disrupt gastrulation and, in some cases, induce secondary body axes (Cho et al. 1991; Ulmer et al. 2017).

In *B. schlosseri* embryogenesis, *Gsc* was described as ubiquitously expressed during early stages until the neurula stage, with expression domains to be localized in the neck and head domains of the tailbud. In NED, *Gsc* expression was found in the double vesicle, with later restriction to the dorsal epithelium. Overall, a similarity to the spatiotemporal expression dynamics of *Gsc* in vertebrates has been stated (Imai et al. 2004; Ricci, Cabrera, et al. 2016). During *P. zorritensis*, it is possible that *Gsc* is acting modulating *Bmp* and *Wnt* during the regions patterning of the Sw vesicle and later is involved in the organogenesis, participating in the nervous system and pharyngeal basket development.

Gata

GataA (*Gata4/5/6*) and *GataB* (*Gatat1/2/3*) are found in cluster 6, meaning they are upregulated after the PSw stage. The family of *Gata* transcription factors are crucial in the development of vertebrates during embryogenesis. *Gata1* is pivotal for hematopoiesis, notably in erythropoiesis and megakaryopoiesis, with mutations causing blood disorders like thalassemia (Yu et al. 2002). *Gata2* is vital for hematopoietic stem cells development and maintenance, with mutations leading to immunodeficiency and leukemia (Katsumura et al. 2018). *Gata3* governs T-lymphocyte development and is central in the development of the inner ear and kidney structures; mutations result in hypoparathyroidism and deafness (Lemos and Thakker 2020). *Gata4* is central to cardiac development and the formation of liver, gut, and gonads, with mutations causing congenital heart defects (Garg et al. 2003). *Gata5*, although less studied, is linked to cardiac development, and mutations are associated with heart diseases (Haworth et al. 2008). Lastly, *Gata6* is crucial for lung and pancreas

development, with mutations causing pancreatic agenesis and heart defects (Morrisey et al. 1998; Patient and McGhee 2002; Collin, Dickinson, and Bigley 2015; Kang et al. 2018). Ascidians have two *Gata* genes: *GataA*, functionally equivalent to *Gatat4/5/6* of vertebrates, and *GataB*, equivalent to *Gata1/2/3* in vertebrates (Ragkousi et al. 2011) (figure 3.46, see appendix 12 for complete phylogeny).

The suppression of ectoderm fates in *Ciona intestinalis* is achieved by antagonizing the maternal *GataA* function. This function is necessary for the initial specification of "naïve" ectoderm and also for neural induction at a later stage (Rothbächer et al. 2007). The gene *GataA* is present in heart progenitor cells and the adjacent endoderm. Repression of endodermal *GataA*'s function leads to endoderm morphogenesis disruption (Ragkousi et al. 2011). In *Botryllus schlosseri*, the *Gata4/5/6* gene is active in the ventrolateral region of the branchial chamber, which is where the heart muscle develops (Ricci, Cabrera, et al. 2016). *GataA* expression was also found during peribranchial budding in a group of cells in the posterior half of the inner vesicle during stage B1. As the development of the budlet progressed, the expression was limited to a smaller patch of 10-15 cells. During the transition to stage C1/C2, the gut rudiment formed and *GataA* signal was detected as it elongated to form the digestive tract. *GataA* expression was then limited to the stomach rudiment and not present in the intestine and its associated glands. *GataA* transcripts were also detected in cells where heart organogenesis occurs and in follicle cells surrounding mature oocytes (Ricci, Cabrera, et al. 2016). Ricci et al. (2016) also reported GataA expression during vascular budding in *B. schlosseri.*

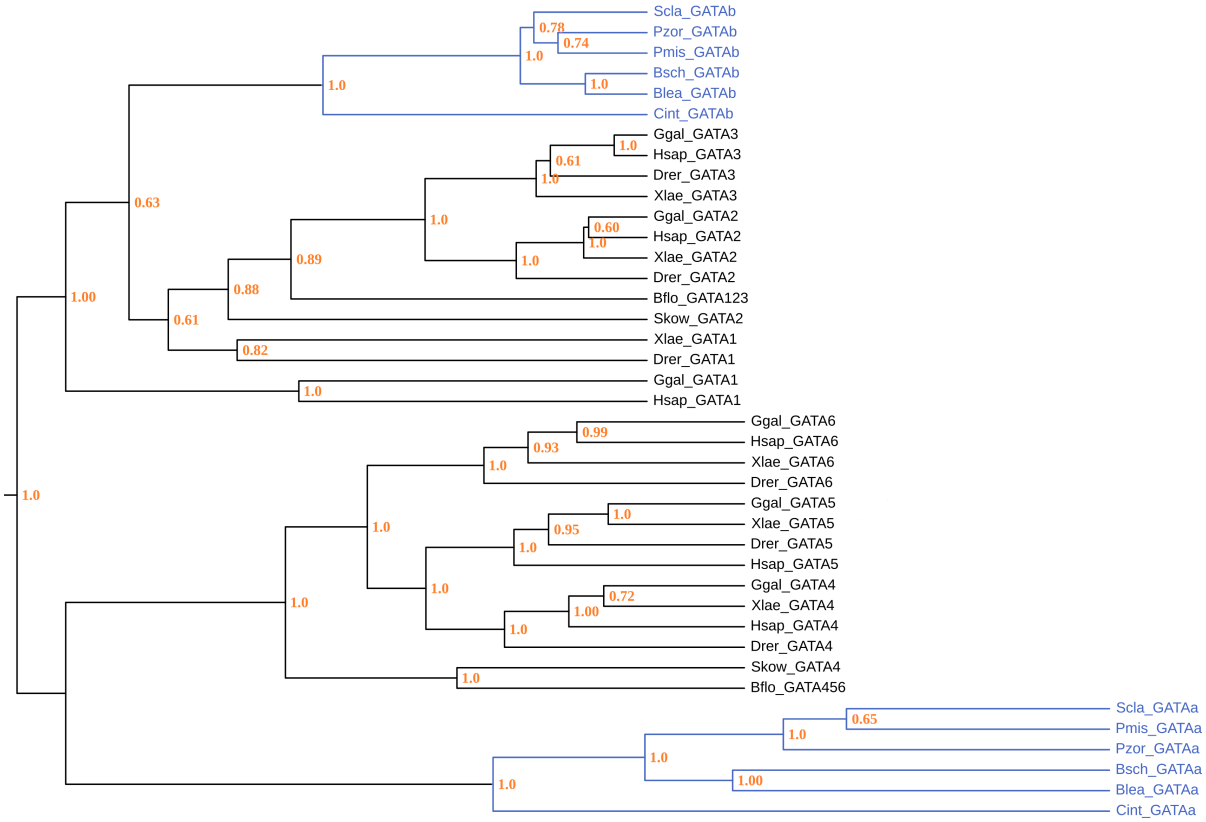

Figure 3.46: *Phylogenetic relationships of GATA transcription factors across multiple species, including chicken (Ggal), human (Hsap), African clawed frog (Xlae), zebrafish (Drer), the lancet (Bflo, a hemichordate (Skow) and the ascidians Ciona intestinalis, Styela Clava, Polyandrocarpa zorritensis, Polyandrocarpa misakiensis, Botryllus schlosseri, and Botrylloides leachii. The tree reveals evolutionary branching patterns of the GATA1 through GATA6 gene families, with bootstrap values, given at the nodes, indicate the confidence of each branching event (orange).*

To be able to compare the spatio-temporal *GataA* expression dynamics between NED in *Botryllus schlosseri* and *Polyandrocarpa zorritensis*, I performed an *in situ* hybridization study across all developmental budding stages. The *in situ* HCR for *GataA* showed expression in the upper portion of the outer vesicles of *P. zorritensis*. During the EI stage, *GataA* displayed a strong expression in a ring pattern in the lowest portion of the invagination fold. As development progressed to the DV stage, *GataA* was expressed in a small region in the lower part of the inner vesicle. Subsequently, in the later stages of early organogenesis, *GataA* expression was observed in the ventral region of the branchial folds. Upon the formation of the gut, *GataA* exhibited expression in both the mouth and gut regions (Figure 3.47). The dynamic expression changes of *GataA* in different bud regions and during various stages of development indicate its involvement in regulating tissue differentiation and morphogenesis. Overall, the expression pattern of *GataA* observed in *P. zorritensis* is reminiscent of the one previously described in *Botryllus schlosseri*. In line with my observations in the former species,

Bsch-GataA is also expressed in the forming inner vesicle and restricted to the posterior territory before and during the formation of the gut primordium (Ricci, Cabrera, et al. 2016). This suggests that *GataA*, similarly to *Nk4*, might have been convergently co-opted to pattern the inner vesicle from its formation to the onset of organogenesis. *In situ* hybridization of *GataA* at the swelling stage of *P. zorritensis* would be necessary to confirm that the expression of this gene remains undetectable at the swelling stage, as suggested by the transcriptomic profile of cluster 6.

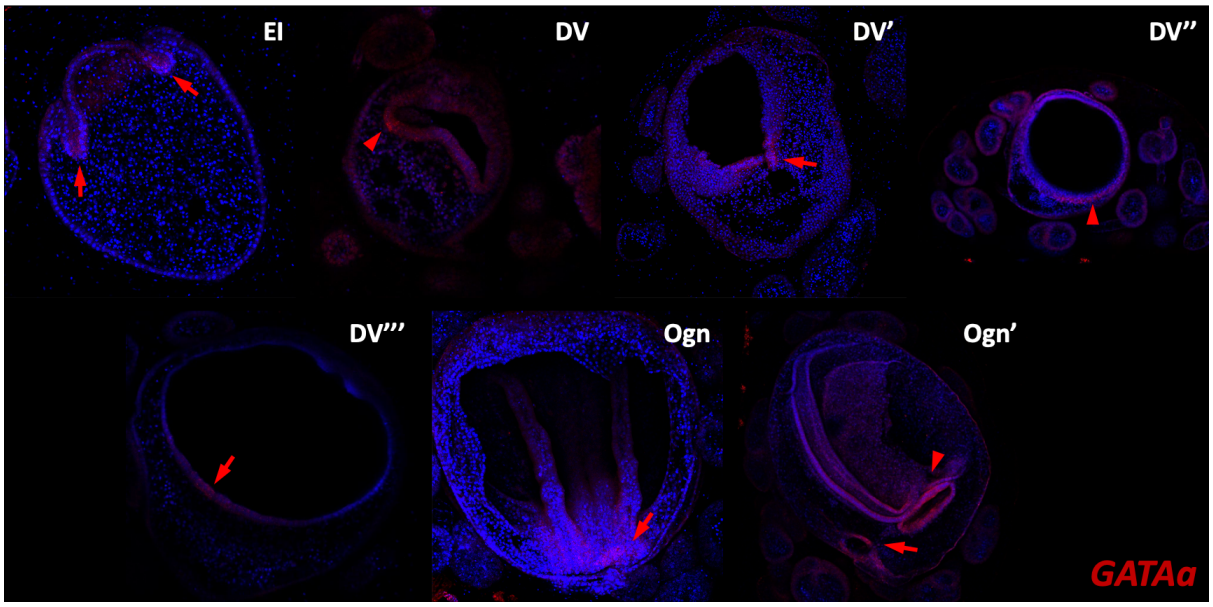

Figure 3.47: *In situ hybridization for GATAa in Polyandrocarpa zorritensis. Red arrows indicate the localized expression during NED.*

In *B. schlosseri*, *GataB* was not found expressed in the early stages of vascular budding, while vascular buds at stage 5 clearly express *GataB* in the epithelia lining the vascular endothelium along the sides of the vascular bud. In addition, it was found to be expressed in the peribranchial epithelia, serving as a marker of ectodermal identity. Furthermore, a peak of *GataB* expression was observed precisely in the region where new budlets will originate (Ricci, Cabrera, et al. 2016).

Transcriptome Comparisons Among *P. zorritiensis* Vasal Budding, *B. schlosseri* Peribranchial Budding, and Vascular Budding

Among the family of *Styelidae*, we can identify at least three independently evolved types of NED (Alié et al. 2018). In order to search for molecular players shared and not shared among the three NED types, the transcriptomic dataset of *P. zorritensis'* vasal budding presented above has been compared with two published *Botryllus schlosseri* transcriptome datasets, one encompassing three early stages of peribranchial budding (Ricci, Chaurasia, et al. 2016) and one encompassing four stages of vascular budding (Ricci et al. 2022). The reference genome used for the transcriptome mapping was generated by Tiozzo's Lab in collaboration with Flot's Lab, following the same strategy used for *P. zorritensis* genome. The whole pipeline used for mapping and analyzing the transcriptomes is the same also used for *P. zorritensis* (appendices 13 and 14).

Transcriptomes comparisons

To extract a list of common differentially expressed genes during NED in the two species, *P. zorritensis* and *B. schlosseri*, I first identified orthologous genes using the program OrthoFinder inside the online program OrthoVenn. A total of 9700 orthogroups were identified, of which 6565 were found to be single-copy clusters, i.e., they contain only one single gene per species (no paralogues). 750 orthogroups contained DEGs present in the output of both species from DESeq2 analysis, among which 494 were single-copy orthogroups (figure 3.48).

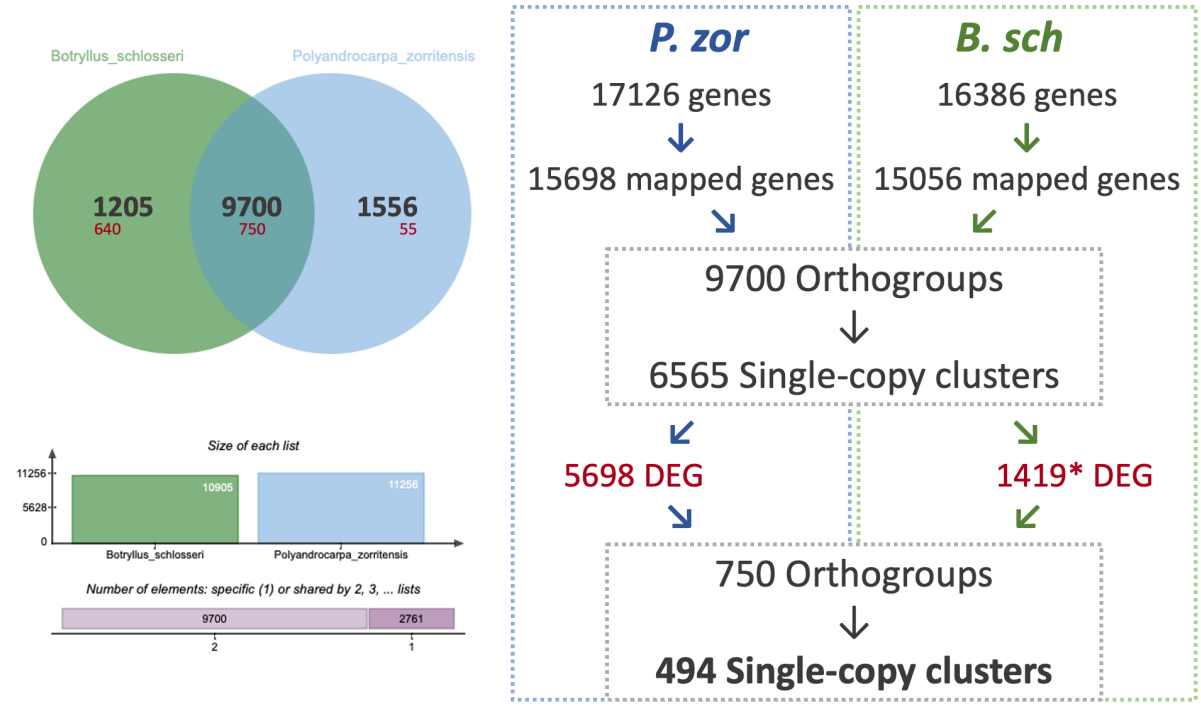

Figure 3.48: *Quantitative comparison of genes and DEG between B. schlosseri and P. zorritensis. On the left side, the numbers of shared and not shared orthogroups are depicted. On the right side, a workflow chart illustrates the analysis steps leading to the isolation of 494 single-copy clusters among the shared DEG.*

To facilitate comparative analysis, the expression values from the three transcriptome sets (*P. zorritensis* vasal budding, *B. schlosseri* peribranchial, and vascular budding) were normalized to the same scale. The replicates were averaged, and the final expression values were used to construct an expression matrix. Utilizing this matrix, I generated a heatmap to identify NED stages with similar expression profiles. The heatmap analysis revealed two main groups: one encompassing all control stages from the three NED types and another group comprising the remaining NED stages. Within this latter group, peribranchial and vasal budding are grouped together, excluding vascular budding (Figure 3.49).

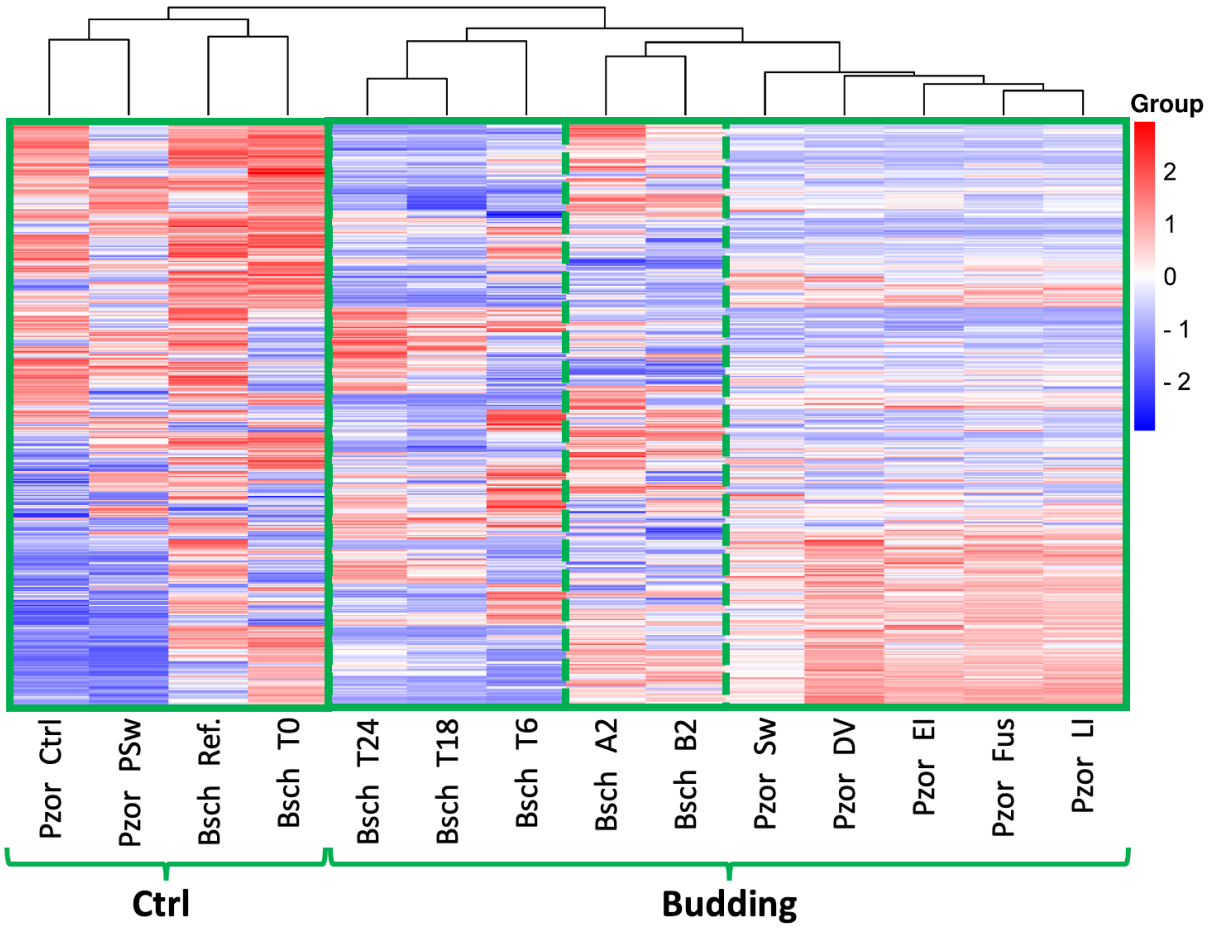

Figure 3.49: *Heatmap of normalized stage-wise expression values of genes that are expressed during different NEDs in two different species, during P. zorritensis vasal budding (Pzor), B. schlosseri vascular budding (Bsch T0, T6, T18 and T24), and B. schlosseri peribranchial budding (Bsch Ref, A2, B2). With the help of the dendrogram, groups of similar expression profiles across species, stages, and budding types are identified.*

Although the clusters appear still rather heterogeneous within, they allow a coarse quantitative comparison between the NED. First, it can be seen that the initial stages of all these three NED clusters together, irrespective of the species or the specific process, suggest the involvement of developmental processes that may be general and not process-or species-specific. One might speculate that this is because mechanisms such as stem cell activation, proliferation, and early differentiation are needed in any developmental process. This conclusion is intriguing since in *P. zorritensis*, the initial stages of budding encompass more dynamic gene expression changes than later stages. It is also interesting since one might have, intuitively, expected larger differences between the earlier stages in light of the different origins of the tissue that the budding starts from. Second, the separation between whole-body regeneration and asexual reproduction in *B. schlosseri* suggests that the later stages of

those two NED may either have diverged early within *Styelidae* or that substantial co-option of pathways and developmental mechanisms between *B. schlosseri* and *P. zorritensis* asexual reproduction has taken place. Otherwise, clustering would have been expected to have followed taxonomic clades.

Among these 494 genes, I focused on the developmental genes that were previously pre-selected in the *P. zorritensis* analysis. The genes I retrieved from this filtration process were: *Piwl1*, *Tshr*, *FoxA1*, *FoxG1*, *FoxH1*, *Wnt5B*, *Runx1*, *Tll1*, *Tll2*, *Notch2*, *Hnf4A*, *Sox11*, and *Gsc*. Interestingly, none of the selected genes exhibited a consistent expression profile across the control stages compared to the other budding stages. These genes showed up or downregulation in the control stages relative to the other budding stages. Some genes displayed a partially similar pattern between the two budding types. For instance, the gene *Runx1* was found to be lowly expressed in all peribranchial budding stages of *B. schlosseri*. However, in the vascular budding of *B. schlosseri* and vasal budding of *P. zorritensis*, it exhibited an upregulation in the control stage and a downregulation during the subsequent budding stages. Similarly, the genes *Notch2* and *Hnf4a* shared similar expression profiles in peribranchial and vasal budding. *Notch* and *Hnf4A* were downregulated in the control and upregulated during the budding stages. On the other hand, the gene *FoxH1* displayed a common expression pattern between the two budding types in *B. schlosseri*. It showed an upregulation in the initial budding stages and a downregulation in the later budding stages (Figure 3.50).

Despite these few instances of similarity, for most of the genes in the list, no conserved or clear expression pattern emerged. This observation could be attributed to factors such as the quality and coverage of transcriptomes for the stages and intermediate stages or the possibility that these specific genes may not be responsible for the comparability among the different budding types.

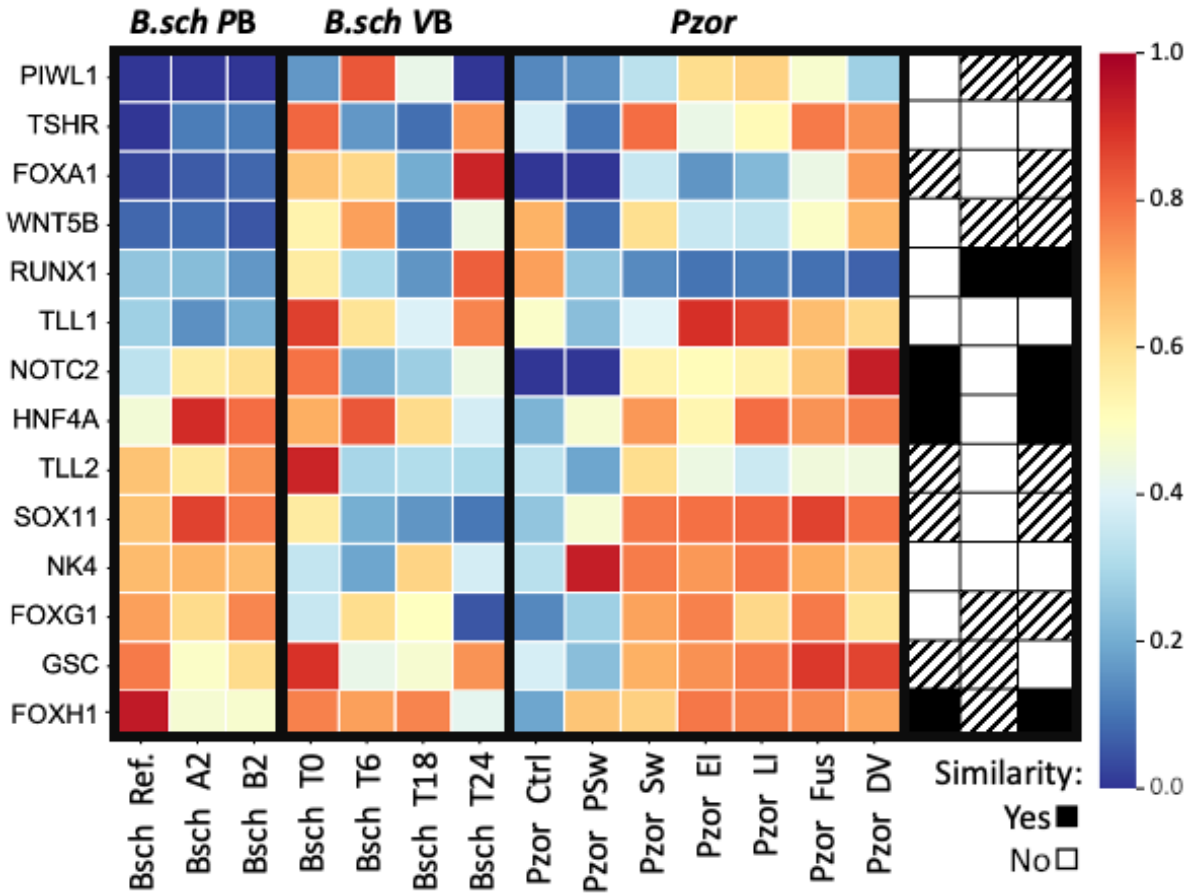

Figure 3.50: *Coarse comparison of temporal gene expression profiles of selected developmental genes between different species and budding types (PB: peribranchial budding, VB: vascular budding). Colors represent relative gene expression between no expression and maximum expression. Overall similarity was assigned on a qualitative base (left column: B.sch PB, central column: B.sch VB, right column: P.zor).*

NED Transcriptome Comparison: Within Other *Styelidae* Species

The comparison of genes expressed during NED was expanded to the other *Styelidae* *Botrylloides leachii* and *Polyandrocarpa misakiensis*. The data incorporated for *B. leachii* was previously published by Zondag et al. (2016), and the transcriptome data for *P. misakiensis* was processed following the same protocol used for *P. zorritensis,* and the *de novo* assembly scores can be found in the appendix section (appendix 17).

To identify the genes in *B. leachii* and *P. misakiensis* whose expression during budding were shared with *P. zorritensis* and *B. schlosseri* DEGs, a processing pipeline was performed similarly to the previous sub-chapter. In the first step, the proteins sequences obtained from the *de novo* assembly of *P. misakiensis* and *B. leachii*, together with the proteins' sequences

obtained in the *P. zorritensis* and *B. schlosseri* genomes, were clustered in orthogroups. The output provided 7388 orthogroups with at least one protein sequence of each species (figure 3.51). In the second step, only the single-copy clusters which included the DEG in *P. zorritensis* and *B. schlosseri* were filtered, resulting in 253 clusters. In these clusters the following candidate genes were found: *Fgfr1*, *Fos*, *FoxG1*, *FoxH1*, *Gsc*, *Hnf4*, *Hox4*, *Nk4*, *Runx*, *Tll2*, and *Tshr*.

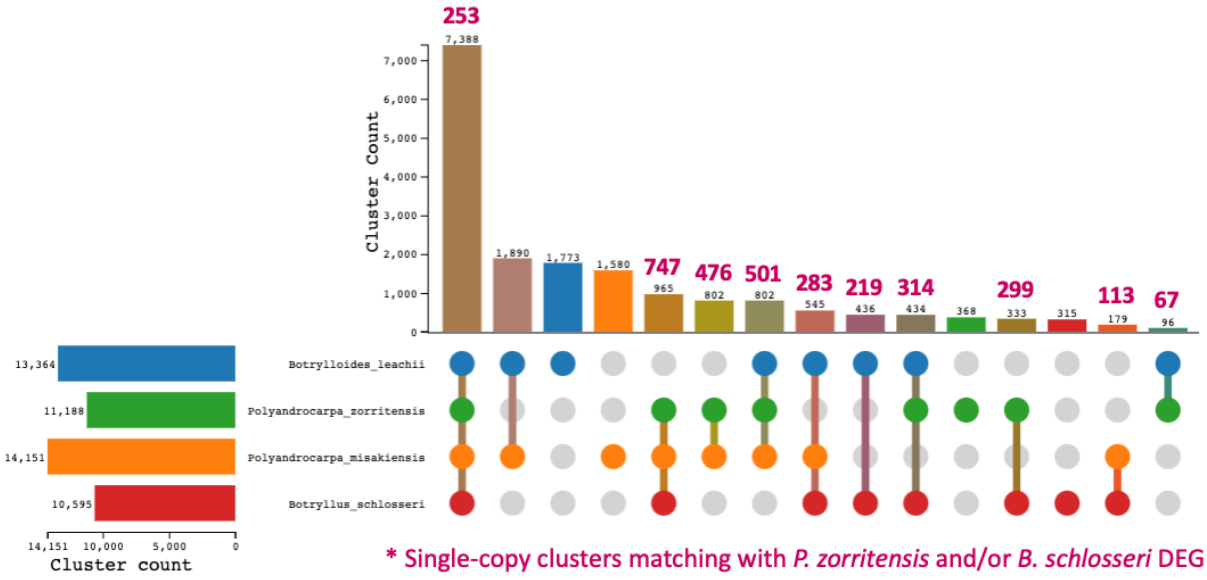

Figure 3.51: *Quantitative comparison of gene clusters and single-copy DEG shared between four different species.*

The OrthoFinder also outputted single-copy clusters covering only two or three species. However, this result only points to the fact that these 253 genes are commonly expressed among the four species. When trying to compare the expression profiles across species, the result was similar to the one observed by comparing only *P. zorritensis* and *B. schlosseri*, meaning there is no clear conserved expression profile among the different types of budding for the genes I selected (figure 3.52). For some of them, focusing on the interval between NED start until double vesicle (see Materials and Methods for staging information), it is possible to establish a correlation, for example, *Hox4* in *P. zorritensis*, *B. schlosseri* VB, and PB and *B. leachii* being downregulated; *Runx* is downregulated during budding development in the five NED examples studied; *Hnf4* is upregulated during budding in all the examples, with exception of *B. schlosseri* PB; *Nk4* is upregulated during the budding development in all the examples;

Gsc is upregulated during budding *P. zorritensis, P. misakiensis,* and *B. leachii* but downregulated in *B. schlosseri* VB; *Fgfr1* is upregulated in *B. schlosseri* VB, *P. misakiensis* and in *B. leachii*, however, it is downregulated in *P. zorritensis*.

To better compare the expression of these genes across different NED strategies and species, a spatial expression pattern characterization using *in situ* hybridization can provide further insights, potentially unraveling more nuanced regulatory mechanisms and interactions during the various budding stages. Another consideration is that this result provided a good approximation but has the limitation that two of the NED data do not have replicates (*B. leachii* and *P. misakiensis*), meaning that the expression dynamics of some of the genes may be either even more similar or more different than NED in *P. zorritensis* and *B. schlosseri*.

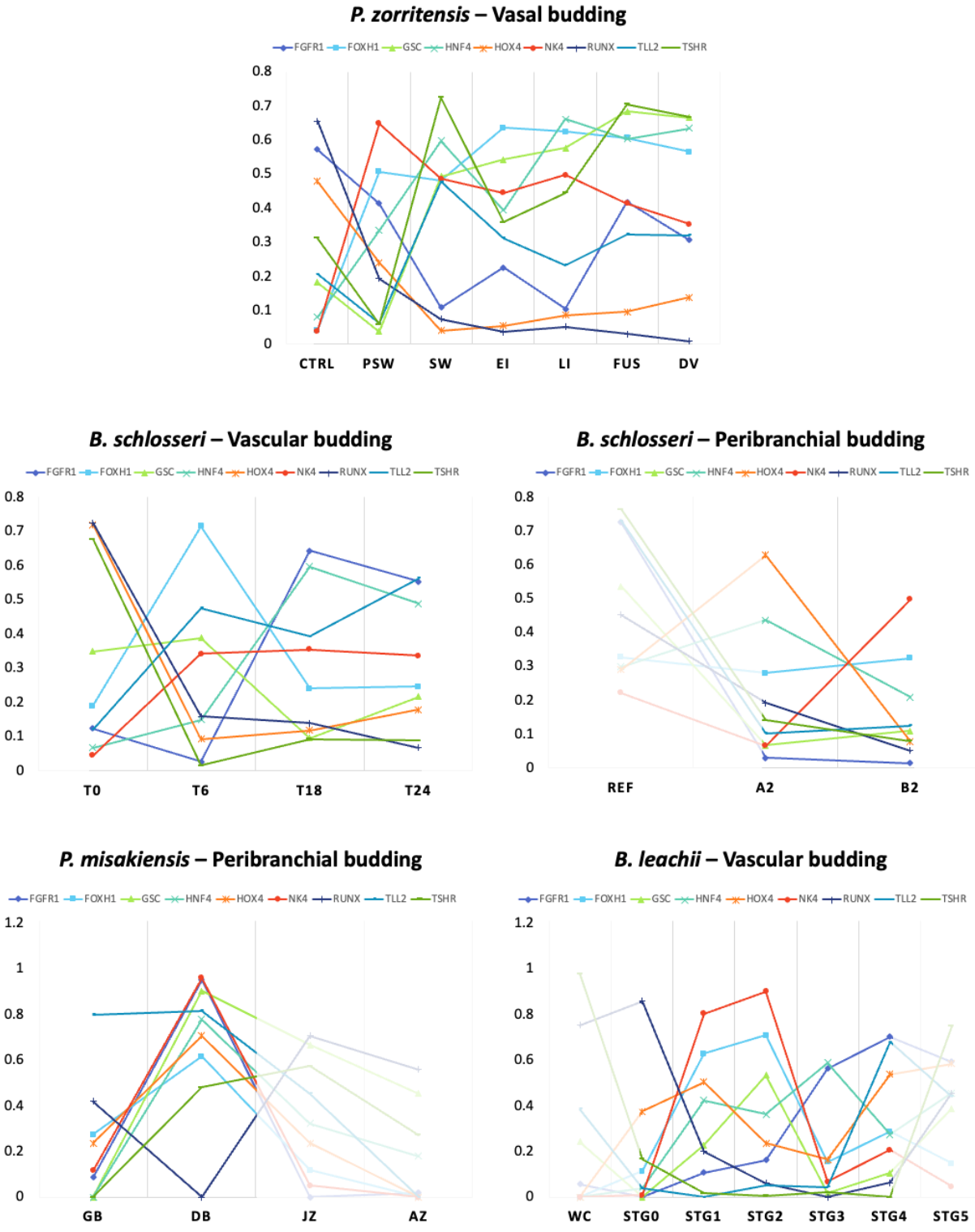

Figure 3.52: *Expression profiles of candidate genes filtered from the orthogroups single-copy clusters across different species. In the Y axis are the expression values, normalized (0-1), and in the X axis are the NED developmental stages.*

3.d) Conclusion

Development is the process that reconstructs functional organisms (or organs) from simpler starting conditions. These starting conditions can be the fusion of gametes, usually referred to as sexual reproduction leading to a stereotypical form of embryonic development. On the other hand, development can start asexually from diploid, adult structures, which can be called non-embryonic development (NED) because it does not go through typical embryonic stages. This latter mode of development is common in ascidians, particularly in the family *Styelidae*, where previous studies have found that NEDs have undergone plastic and partly independent evolution. Different tissues can give rise to NED, and this is highly species-dependent. Therefore, elucidating the developmental mechanisms underlying different types of NEDs in ascidians may help to understand their extant diversity as well as their evolution.

Here, I chose a comparative approach based on transcriptomic and some histological data, which allows us to find quantitative patterns of developmental genes, pathways, and GRNs that are dynamically involved in different stages of NEDs. First, I used the vasal budding process in *Polyandrocarpa zorritensis* in which I characterized seven developmental stages: Control, Pre-Swelling, Swelling, Early Invagination, Late Invagination, and Double Vesicle. The last stage, in which a completely closed inner vesicle forms, seems to be common to different NEDs. For analysis, I extracted RNA from *P. zorritensis* buds at each of those stages. While a suitable genome to guide the assembly of the transcriptome became available in the later stages of this project, I first had to identify differentially expressed genes (DEG) between the stages using *de novo* assembly and DeSeq2. This yielded over 7800 DEGs representing more than 25% of all expressed bona fide genes. Using principal component analyses, I found that the transcriptomes of the seven NED stages fell into two main clusters: a cluster the first two stages (Control and Pre-Swelling), which encompass developmental events before histological changes become apparent in the tissues, and the remainder of stages. While there was still a significant number of DEGs between the control and pre-swelling stage, there were only very few DEGs between the later stages. Within the DEGs, I found several GO terms enriched, including DNA replication, neuronal differentiation, cell differentiation, and morphogenesis, suggesting the onset of developmental dynamics. I also clustered genes by expression profile and identified several classic developmental gene families and pathways whose expression was upregulated after the onset of NED. These included members of *Wnt*,

Bmp, the *Hh* family, *Notch*, *Gsc*, *Fgf*, *Pax*, *Fox*, and several markers of cell differentiation such as *Gata* and *Piwi*. Consistent with this, early stages were enriched for GO terms specifying cell metabolism, RNA processing, and chromosomal organization as enriched, whereas genes upregulated at later stages were enriched for GO terms such as development, tissue, and organ morphogenesis. These results suggest that most developmental pathways are active before morphological changes become manifest. The genome-guided transcriptome assembly gave very similar results from around 5700 genes.

As a control, I tested the spatial expression dynamics of *Nk4* and *GataA* throughout the vasal budding process using in situ hybridization. This experiment confirmed a very similar expression pattern to Botryllus schlosseri, suggesting that very similar genetic mechanisms have been convergently co-opted in the two clades.

To compare different NEDs in different species from a transcriptomic perspective, I used transcriptome data from *P. misakiensis*, *Botryllus schlosseri*, which has two different modes of NED (vascular and peribranchial), and *Botrylloides leachii*. A comparison between *P. zorritensis* and the two budding modes of *B. schlosseri* revealed a separate clustering of the two NEDs of *B. schlosseri* and no clustering by species. A gene-wise comparison identified common developmental genes such as *Wnt5B*, *Piwl1*, *Gsc*, *Hnf4A*, *Notch2*, *Nk4*, *Runx1*, *Sox11*, and several *Fox* members but failed to find consistent expression profiles between the NEDs, suggesting complex developmental dynamics. In other words, either the actual expression profiles of those genes are too dynamic to yield comparable stage-wise profiles, or the topology of specific gene regulation happens to have evolved fast even between related species. A broader comparison between all species mentioned above showed that a much larger proportion of the expressed genes are common to all species. Overall, this study demonstrated, from a quantitative perspective, the dynamic nature of the mechanisms underlying NEDs and that there are commonalities even between independently acquired budding strategies. However, a closer comparison between temporal and spatial changes in gene expression and tissue changes will be necessary for a mechanistic understanding of these complex processes.

Given the large number of differentially expressed genes that are known from other developmental processes, it is tempting to compare their expression in NED with their

functions in embryonic development. This is not a straightforward task as many of these developmental genes are involved in many different functions.

Gastrulation is a key event during early embryogenesis in nearly all animals, during which the initial monolayer of multipotent blastula cells becomes a multilayered embryo. These layers then, correspond to the different germ layers that will give rise to the subsequent cell lineages that will eventually form the organs. Thus, a tight control of this process is crucial for successful development. A number of studies in Phallusia and Ciona have identified several *Fgf, FoxD, Bmp, Nodal, Tolloid,* all of which were also found on the list of differentially expressed genes during NED, as key morphogens involved in the invagination of the prospective endoderm during ascidian gastrulation (Imai et al. 2004; Hudson and Yasuo 2005; Hudson, Lotito, and Yasuo 2007; Fiuza et al. 2020). Suggesting a high degree of conservation, most of these signaling pathways, *Nodal, Fgf, Bmp*, and also *Wnt*, are known from vertebrate gastrulation (Ciruna and Rossant 2001; Von Der Hardt et al. 2007; Heisenberg and Solnica-Krezel 2008; Luxardi et al. 2010; Fiuza et al. 2020). Since the problem of germ layer separation also arises in the context of NED, it is not surprising that some of the key gastrulation pathways are also active. Furthermore, gastrulation involves cell rearrangement mechanisms (such as apical constriction and baso-lateral shortening leading to invagination, intercalation etc.) that may also be central to other developmental mechanisms. For instance, Nodal has been shown to be critical in the transition between apical constriction and apico-basal shortening (Fiuza et al. 2020). Thus, some of these "gastrulation genes" might be considered more as markers of basic cell behaviors and tissue-level changes and are therefore likely to be recruited during a variety of developmental processes, both embryonic and in NED.

Another gene that is central to the orchestration of early vertebrate development is *Goosecoid*. It has been shown, first in *Xenopus*, that ectopic expression of this homeobox factor is sufficient to induce the establishment of the body axis if ectopically expressed, thus mimicking the proposed activity of a Spemann organizer. Cell populations expressing *Gsc* are then specified to differentiate into pharyngeal endoderm, head mesoderm, and notochord tissues. *Gsc* expression is in turn controlled by dorsal (Wnt) and ventral (FGFs) factors (Eddy M. De Robertis et al. 1992). Since *Gsc*, along with *Wnt* and *Fgf*, is expressed during *P. zorritensis* NED, it can be speculated that it may represent a hallmark of active axis specification and tissue differentiation.

In general, several of the pathways found to be differentially expressed in NED are known to be involved in basic tissue and lineage specification. For instance, *Noggin, Nodal*, *Bmp* and *Fgf,* which are downstream of b-Catenin in pre-gastrulation and early gastrulation stages, are critical for mesenchymal induction (Bertrand et al. 2003; Imai et al. 2004). It has also been shown that mesenchymal specification by different *Fgf* are essential for prospective notochord formation in Ciona (Hudson, Lotito, and Yasuo 2007). Since NED can originate from different tissue contexts, it is necessary to recruit developmental mechanisms that can form ontologically distant tissues *de novo*. Thus, reactivating pathways that were central to the specification of their major germ layers and their derived cell types during embryonic development may be an evolutionarily simple strategy to address this problem.

The formation of the neural plate is one of the first steps in the development of the central nervous system (CNS). In ascidians, it involves a stereotypical geometric patterning of cells that serve as precursors for different neural cell lineages, requiring very precise developmental control at the level of each cell. These includes the Nodal, Delta/Notch pathway, which are critical for establishing lateral inhibition and single-cell boundaries, and the FGF signaling pathway, which ensure a transversal antero-posterior gradient (Hudson, Lotito, and Yasuo 2007). The same signaling pathways have been reported to be upregulated during NED. It is very likely that a similar mechanism is recruited during NED in a functional CNS, and therefore a precise patterning process is indispensable for any whole-body formation process. The involvement of *Fgf* (in concert with *Wnt*) in the establishment of a posterior identity in prospective neural tissue in the late vertebrate gastrula suggests a high degree of conservation of the processes involved in early chordate neurogenesis (Gamse and Sive 2000).

Although this exercise is inevitably speculative, it can generate hypotheses that may provide a starting point for future follow-up experiments. In general, such a comparison is also hampered by the fact that there appears to be no substantial difference in gene expression profiles between the Swelling and Double Vesicle stages. This can be interpreted in two ways.

First, most of the changes in gene expression, which are indicative of changes in cell and tissue behaviors, occur at the very beginning of NED, with later stages contributing only to growth and minor changes. If this view is correct, then a more refined staging between the

Control and Swelling stages is needed to be able to discern a temporal sequence of expression of developmental genes. Conversely, studies quantifying transcriptome dynamics during limb regeneration in axolotl and amphipods do not suggest a significant decrease in gene expression changes over time (Li et al. 2021; Sinigaglia et al. 2022). However, limb regeneration and NED in ascidians may not be comparable at all, and thus propagating gene expression dynamics in the former may not be informative for understanding NED.

Alternatively, gene expression may continue to undergo dynamic changes but be restricted to specific cell populations. Hence, dilution from the rest of the tissue with no or constant gene expression may render any signal of local expression change negligible or indistinguishable from background noise. Thus, a single-cell or tissue-specific approach may be required to detect such signals. Again, this view, seems plausible given the increasing compartmentalization and lineage specification during the later stages of NED. It would be analogous to the later stages of development when regionalized and organ-specific patterning follows early embryogenesis with embryo-wide expression patterns. Yet, a strong regionalization of embryogenesis at the end of the Swelling stage seems to be quite early.

Overall, this comparison shows striking similarities between NED and early development. I think is not surprising, since the main task, the reconstruction of a stereotypical adult, is ultimately the same. Despite the obvious differences at the onset of both types of development (embryonic and non-embryonic), it makes sense that the pathways and mechanisms involved in development would be redeployed. The recruitment of developmental modules that are normally active during embryonic development also follows an evolutionary logic, since recycling of developmental modules is a fast way to generate functional NEDs. If such a scenario is evolutionarily easy to achieve, it could explain the plastic evolution of NEDs in *Styelidae* as well as the multitude of different strategies. Thus, a more detailed analyses of the similarities and differences between embryonic and different non-embryonic developmental strategies in ascidians may be a promising strategy to decipher how development evolves, and why this evolution seems to allow different reproductive strategies to emerge more easily in some clades but not in others.

Chapter 4 - Conclusion

Conclusion

In order to predict how species can thrive in different habitats, it is highly informative to assess the interaction between environmental conditions and their reproduction. This is why, in this thesis, I first examined how salinity levels affect the reproductive strategies of a known invasive ascidian species, *P. zorritensis*. The results provide valuable insights into the impact of a key environmental factor on the production of asexual and sexual offspring. They reveal the complexity of the relationship between external factors and internal life-history decisions and suggest that there is an optimal range of salinities where asexual reproduction takes place most efficiently. Although sexual reproduction is a central life-history process and as such not strictly dependent on the water salinity, it may not be sufficient to compensate for the negative effects of extreme salinities on the efficiency of asexual reproduction.

Many colonial ascidians are interesting models for understanding the evolutionary history of ascidians and their success in colonizing new environments, due to their ability to perform different reproductive strategies, including sexual reproduction, different modes of asexual reproduction (budding) and hibernation stages (Jenner and Wills 2007; Sommer 2009). Understanding the underlying mechanisms that govern the decisions to initiate these different phenomena requires further investigation. This study also complements the previous work on *P. zorritensis* (Hiebert et al. 2022), which highlights the importance of overwintering spherules in replenishing populations and considers the possibility that the survival of dormant forms could be a bottleneck for annual population growth. Considering the fact that colonial ascidians are sessile organisms that will lose the ability of locomotion upon larval settlement, adapting to changing environmental conditions can take place in three different ways. First, asexual reproduction will clonally expand the size of an existing colony, which is an efficient way of taking advantage of locally favorable environmental conditions. Second, sexual reproduction allows dispersal owing to larval motility. While this mode of the reproduction will contribute to the success of a residual population independently of the environmental conditions, it offers a way to stray away from local conditions that do not favor colony growth. Third, transient unfavorable conditions, such as seasonal shifts in environmental factors, can be circumvented by forming dormant stages that

retain the ability to regenerate a functional individual once the conditions start improving (Hiebert et al. 2022). Overall, my study supports this interpretation of a linkage between environmental conditions and a selective reproductive response, but future studies are needed to elucidate how these decisions are made on a developmental-metabolic level.

Predicting the success of invasive species as a function of environmental parameters is central to understanding how ecosystems evolve in light of a changing climate and direct or indirect anthropogenic interchange of species. The chapter 2 of this thesis stresses the significance of recognizing the environmental and developmental boundaries of the species under investigation, such as a range of salinities. Although such preferences may change during evolution, there appear to be, even for relatively tolerant or generalist species, salinity thresholds under which their efficiency of reproduction will diminish.

The research also brings attention to how anthropically modified coastal regions can locally lead to increased invasiveness, selectively boosting the success of asexual reproduction. Conversely, such insight may allow predictions about where an invasive population is most likely to start thriving and suggests strategies to selectively curb invasion success. Specifically, it helps understand how specific human activity types will affect coastal ecosystems. Therefore, it is crucial to adopt a holistic conservation approach that takes into account both natural and human-influenced factors impacting the reproductive strategies of marine invertebrates.

Development is a complex process that, among others, requires precise regulation of gene expression in time and space to create distinct tissues and organs, which is true for both sexual and asexual modes of reproduction. Since both modes result in the same, conserved, adult bauplan, elucidating how different NED strategies converge into a common stage, namely the double-vesicle stage, is all the more fascinating. However, the complexity of development stems from the fact that genes interact in networks which, together and dynamically, will change the expression of specific effector proteins locally, making a causal association of specific genes with functions a challenging enterprise. Recent advances in transcriptomics have enabled researchers to investigate differences in gene expression patterns across various organisms in a sufficiently fine-tuned manner. My research has, specifically, explored ascidian non-embryonal development (NED) and how gene expression dynamics contribute to this intricate process.

In the second part of my thesis, I aimed to improve our understanding of how NED developed in colonial *Styelidae.* To this end, I explored the process of vasal budding in *P. zorritensis* with respect to the molecular regulation of morphogenesis, differentiating key developmental stages which I analyzed further using transcriptomics and spatio-temporal expression patterns of key morphogens. This effort resulted in a comprehensive, high-quality transcriptome, serving as a molecular guide to decipher the complex genetic dynamics that regulate vasal budding.

During the subsequential analysis, I found that most of the changes in gene expression occur at the early stages of vasal budding, even before the visual onset of histological changes. This came, *prima facie*, as a surprise, and prevented a direct association between visual changes in the tissue and the transcriptomic level. However, as the genetic processes underlying vasal budding are finely orchestrated and involve synchronized communication between various molecular players to ensure its successful initiation and progression, it can be expected that most of the gene expression changes are performed before major tissue rearrangements take place. In other words, it is likely that gene regulatory dynamics unfold to initialize subsequent developmental steps and be maintained in a stable state during the tissue changes that are observed. The alternative scenario, concomitant gene expression and morphological changes might be overall less robust and prone to environmental influences (Salazar-Ciudad and Jernvall 2004). Besides, the maintained expression of key effector genes will continue to promote cell differentiation and tissue morphogenesis, even if this is not reflected in expression changes *per se* that would be recorded by transcriptome analysis. Another possible explanation of the conspicuous lack of differential gene expression past the PSw and Sw stages might be that important changes of gene expression become increasingly restricted to specific cell populations (which may be a common trend in animal development, cf. Salvador-Martínez and Salazar-Ciudad 2015), which would lead to an overall dilution of the signal the differential gene expression analysis is capable of detecting. Taken together, my analysis shows a high concentration of gene expression dynamics at the very onset of development, which might be a more general feature and could be interpreted in terms of developmental robustness, but comparative studies would be needed to corroborate such a hypothesis.

Transcriptomic technologies allow the detection of the molecular players of the networks that control developmental processes which ultimately drive the cellular events during vasal budding. Interestingly, my analysis revealed that many genes and regulatory gene cascades (pathways) with well-defined roles in embryogenesis are also involved in vasal budding during NED, suggesting repurposing for budding processes that are part of ascidian life cycles. Many of those genes are part of conserved genetic toolkits whose functions have been well described throughout ascidian development, and, in some cases, metazoan. For instance, *Nk4* in *C. intestinalis* is equivalent to *Nkx2-5/tinman*, a vital protein in vertebrate cardiac development and ascidian regeneration. It indirectly promotes *GataA* expression, vital for heart precursor specification . *Nk4* is expressed in the ventral epidermis and anterior trunk endoderm (Wang et al. 2013). In *B. schlosseri* and *P. zorritensis* regeneration, *Nk4* is expressed in bud areas, inner vesicles, and invaginating epithelia. In *P. zorritensis, Nk4* expression during the Sw stage suggests a role in epithelial invagination (Alié et al. 2018). Iroquois (*Irx6*) genes are essential for body plan formation throughout vertebrates, and in *B. schlosseri*, *IrxB* expression is linked to dorsal tube development, indicating involvement in anterior-posterior axis differentiation (Cavodeassi, Modolell, and Gómez-Skarmeta 2001; Gómez-Skarmeta and Modolell 2002; Prünster et al. 2019a). Runx genes, crucial in vertebrate hematopoiesis, are downregulated at budding onset. In *B. schlosseri*, *Runx* is expressed in developing buds, potentially contributing to tissue reorganization (Langenbacher et al. 2015). Goosecoid (*Gsc*), upregulated during budding, plays roles in vertebrate head development (De Robertis et al. 1992). In *B. schlosseri*, *Gsc* expression mirrors vertebrate patterns, suggesting involvement in nervous system and pharyngeal basket development (Imai et al. 2004; Ricci, Cabrera, et al. 2016). *GataA/B*, crucial in vertebrate development, are upregulated post-PSw stage. GataA's roles in ascidians include heart development, endodermal morphogenesis, and digestive tract formation (Rothbächer et al. 2007; Ragkousi et al. 2011). In *B. schlosseri*, *GataA* is expressed in ventrolateral regions, during peribranchial and vascular budding, and in cells associated with heart organogenesis (Ricci, Cabrera, et al. 2016). It has to be cautioned that, despite these and other examples, a functional account of key pathways during NED is crucial for any more specific hypotheses, yet my observations and speculations may provide a starting point for future evo-devo research.

Amongst those molecular toolkits, I identified homologues of several pathways that are involved in developmental processes and well-defined roles in early tissue morphogenesis, such as cell differentiation, tissue patterning, gastrulation, neurulation (in vertebrates) and specific organogenesis, although it still needs to be tested to which extent their function has been retained. The diversity in gene expression patterns highlights the complexity of these processes and suggests the various ways in which NEDs in different species navigate the intricate landscape of embryonic development. My analysis highlights the conservation of fundamental developmental processes and deepens our understanding of the organization and evolution of regeneration processes, across diverse biological contexts. Furthermore, it underscores the evolutionary continuity in the orchestration of developmental events, providing insight into the general principles of evo-devo such as homology on several levels, developmental drift, developmental modularity and innovations.

The identification of key developmental pathways among the set of differentially expressed genes during NED suggests that developmental processes tend to be based on the modular recruitment and adoption of elementary morphogenetic mechanisms into a network orchestrating whole-body morphogenesis, which would provide a way for evolution to assemble and re-assemble developmental processes, including ascidian NEDs.

The research included in my thesis provides a comprehensive transcriptome of *P. zorritensis* vasal budding, shedding light on the temporal dynamics, and evolutionary relationships. These insights enhance our understanding of developmental biology and pave the way for future studies on the molecular processes acting in ascidian life cycles.

NED is widespread among colonial ascidians, with different types of NED (characterized by the specific tissue that gives rise to a new individual via budding), suggesting a dynamical evolution of budding modes. This fact allows us to compare the development of NED both between different species and between different budding modes, to understand key evo-devo questions: how did these complexes, yet heterogeneous, modes of asexual reproduction emerge multiple times in evolution? What are the commonalities and differences in developmental mechanisms that orchestrate NEDs? Is this pattern of dynamic evolution in line with homology or convergence hypotheses of the origination of NEDs?

To contribute to answering these relevant questions, I conducted a comparative analysis of gene expression dynamics between two ascidian species, *P. zorritensis* and *B.*

schlosseri, taking advantage of transcriptomic data. Despite different staging systems and significant differences in overall gene expression patterns, I found that a significant number of differentially expressed genes were shared between the two species.

The discovery of shared gene expression patterns between two distantly related ascidian species, despite significant differences in gene expression dynamics, raises important questions about the functional significance of these shared genetic signatures. One possibility is that these shared genes may play a key role in conserved developmental pathways, suggesting deep homology. Alternatively, they may reflect the specific developmental roles of mechanisms central to NEDs, suggesting convergent evolution or convergent recruitment of developmental pathways with specific functions. Investigating these questions is critical for unravelling the mysteries of ascidian evolution and the adaptive significance of shared genetic elements in the context of the evo-devo of diverse budding processes.

Since *B. schlosseri* uses two different modes of NED, and *P. zorritensis* uses a third one, I was able to examine differences in gene expression between those. Intriguingly, gene expression patterns in vasal and peribranchial budding were found to be more similar across different ascidian species than between the two distinct budding types within *B. schlosseri,* according to the different tissues that were involved. This is even more surprising, as both NEDs are believed to have emerged independently in the two species, respectively. This interesting finding suggests that developmental mechanisms may tend to be recruited in a specific manner depending on the particular anatomical contexts of each type of budding, indicating a tissue-specific, rather than a species-specific, co-option of genetic programs.

This study revealed that the interplay of genes and pathways with important roles during embryogenesis in the context of ascidian budding is not limited to a single species but also extends to tissue-specific intricacies within a species. This finding highlights the complexity of ascidian developmental biology and offers opportunities for more targeted investigations into the molecular mechanisms behind tissue-specific gene expression and the specific ways evolutionary forces dynamically shape these intricate genetic networks.

These observations of gene and pathway recruitment in NED reveal an interesting insight: developmental pathways may be, generally, adapted in a tissue-specific manner. This means that specific tissues have the property, or ability, to adjust their gene expression programs to best suit their particular functions. This type of flexibility in gene program

recruitment demonstrates a high level of modularly structured biological regulation within the broader context of embryonic development.

The concept of modularity plays a crucial role in the understanding of developmental mechanisms. A system is considered modular when it can be separated into multiple sets of parts that interact strongly with each other but are relatively independent. Modules can either refer to various parts of the individual that interact with each other, such as induction and morphogenesis, or sets of molecules that independently pattern multiple tissues (Wagner, Pavlicev, and Cheverud 2007; Melo et al. 2016). This modularity allows for flexibility and adaptability in developmental pathways at the tissue level, and it also facilitates the evolution of reproductive and regenerative strategies. By taking advantage of modularity, organisms can explore new developmental paths by reconfiguring or repurposing existing modules, facilitating the pace of evolution by which a function can be co-opted (Bolker 2000; Zelditch and Goswami 2021). Such a strategy results in a diverse range of reproductive and regenerative strategies that are unique to each species (Sood et al. 2022).

My transcriptomic comparisons between different NEDs and different species illustrate the complex interplay of genes and pathways that regulate developmental processes. The precision in the recruitment of genes specific to certain developmental mechanisms during embryogenesis, the co-option of pathways specific to certain tissues, and the modularity of developmental mechanisms collectively do not only contribute to the variety of reproductive and regenerative strategies observed but may also explain the high flexibility by which NEDs appear to emerge in evolution within colonial ascidians. Given the important role asexual reproduction modes play in the response of ascidians to dynamic environmental conditions, this research provides new insights into the basic principles underlying embryonic development and emphasizes the potential for dynamic evolution in response to environmental stressors.

This project has focused on *Styelidae*, as they provide a high diversity of different modes of NED, rendering them a model clade for questions regarding the evo-devo of reproductive strategies. One important question is whether the developmental mechanisms of *Styelidae* are unique, or if there are shared principles across diverse ascidian groups and beyond. Thus, future research on NEDs can help reveal the broader patterns and commonalities that underlie developmental mechanisms and provide important insights into the evolutionary

processes at play. Do dynamically evolving features share a propensity to modular and tissue-dependent co-option of gene networks central to embryogenesis or is this a specific feature of ascidians?

As we delve into the realm of evolutionary processes, it is fascinating to explore the parallels between Non-Embryonic Developmental processes (NEDs) and embryonic development. This exploration prompts us to inquire into the specific components of the underlying mechanisms that have been co-opted over time. It is important to understand what triggers the activation of these intricate pathways and what pivotal factors contribute to their divergence or convergence. Answering this question may also help explain why certain clades exhibit a diversity of different modes of asexual reproduction, while others lack this ability altogether. In addition, given the different responses of sexual and asexual reproduction strategies to environmental factors such as salinities, it is still unknown how, in the context of developmental regulation, the decision between sexual and asexual reproduction is elicited, and how environmental cues are integrated into this process.

As we continue our scientific exploration of NEDs, we are faced with another intriguing question: how do NEDs from different tissues converge towards a common stage of development? Is it possible that some specific attractors or chreodes (canalized developmental pathway, Waddington 2014; Levine and Davidson 2005; Ferrell 2012) guide this process with accuracy? Intriguingly, my results have shown that, in *P. zorritensis*, key changes in gene expression take place during the inception of budding. Does this imply that convergence is already reflected in the characteristic transcriptomic changes early on, or will the more subtle subsequent developmental dynamics guide the process into a common adult stage?

Considering the similarities in developmental processes across different organisms, I wonder at which level of organization the question of identifying homologies would be most informative. While many studies tend to focus on the level of genes, it is likely that modules integrating genes into pathways and networks, in concert with biomechanical mechanisms elicited by changes in structural proteins, cell shapes, and tissues, may represent that central and modular unit that can be most meaningfully compared between species and between different developmental processes (Newman and Bhat 2009). This might be exemplified in NEDs where tissue-specific genetic signatures are shared between diverse organisms in a

modular manner. In addition, finding homologue genes in different processes may be less meaningful, unless they are integrated in the same regulatory or tissue context. Thus, my studies in NEDs suggests that it would be meaningful to analyze when the concept of deep homology extends from the level of single genes to encompass the broader pathways that guide specific developmental processes and to the intricate level of network modules, where interconnected molecular players collaborate to shape the development of different organisms.

During the journey of my research, I have explored the complex interplay between environmental cues, evolutionary processes, and molecular players that drive the development of life. By focusing on NEDs in *Styelidae* ascidians and the homology of developmental mechanisms, I have encountered interesting questions at the crossroads of evolution, development and ecology that may instigate promising, and profound, insights into the intricate mechanisms of life that generate, reproduce, and adapt the complex shapes of organisms.

Appendices

Appendix 1

Number of bases of stolons, stolon tips, and buds (budding nests and zooids) per individual, per condition.

Experiment	Salinity value	Slide	Individual	Stolons bases	Nests and new zooids	Stolons tips
Autumn	40	3	1	6	6	7
Autumn	40	3	2	6	1	6
Autumn	40	3	3	2	1	3
Autumn	40	3	4	1	3	5
Autumn	40	3	5	4	2	6
Autumn	40	3	6	10	2	13
Autumn	40	3	7	3	1	3
Autumn	40	3	8	3	6	12
Autumn	40	3	9	2	1	2
Autumn	40	3	10	5	3	12
Autumn	40	2	1	5	4	6
Autumn	40	2	2	2	4	3
Autumn	40	2	3	3	1	3
Autumn	40	2	4	1	0	1
Autumn	40	2	5	11	5	15
Autumn	40	2	6	2	5	5
Autumn	40	2	7	2	0	3
Autumn	40	2	8	5	3	9
Autumn	40	2	9	1	0	1
Autumn	40	2	10	4	2	5
Autumn	40	2	11	5	4	9
Autumn	40	1	1	6	5	6
Autumn	40	1	2	7	4	8
Autumn	40	1	3	6	2	7
Autumn	40	1	4	6	4	7
Autumn	40	1	5	3	6	5
Autumn	40	1	6	6	0	6
Autumn	40	1	7	14	10	23
Autumn	40	1	8	12	9	21
Autumn	40	1	9	4	0	4
Autumn	40	1	10	4	4	8
Autumn	40	1	11	4	2	5
Autumn	40	1	12	0	0	0
Autumn	36	3	1	5	6	11
Autumn	36	3	2	4	2	4
Autumn	36	3	3	11	6	16
Autumn	36	3	4	9	7	12
Autumn	36	3	5	9	4	9
Autumn	36	3	6	15	5	6
Autumn	36	3	7	12	20	19

Autumn	36	3	8	4	2	4
Autumn	36	3	9	6	3	11
Autumn	36	2	1	5	6	7
Autumn	36	2	2	6	10	9
Autumn	36	2	3	9	7	11
Autumn	36	2	4	14	10	25
Autumn	36	2	5	22	14	37
Autumn	36	2	6	16	15	23
Autumn	36	2	7	7	4	7
Autumn	36	2	8	4	0	5
Autumn	36	2	9	2	1	3
Autumn	36	2	10	10	7	11
Autumn	36	2	11	11	11	18
Autumn	36	2	12	13	8	23
Autumn	36	1	1	14	15	23
Autumn	36	1	2	12	8	14
Autumn	36	1	3	11	6	18
Autumn	36	1	4	9	14	13
Autumn	36	1	5	5	10	9
Autumn	36	1	6	5	4	5
Autumn	36	1	7	10	9	12
Autumn	36	1	8	7	9	12
Autumn	36	1	9	8	6	12
Autumn	29	3	1	13	6	19
Autumn	29	3	2	8	0	10
Autumn	29	3	3	12	7	15
Autumn	29	3	4	6	5	8
Autumn	29	3	5	2	9	11
Autumn	29	3	6	12	9	19
Autumn	29	3	7	5	6	12
Autumn	29	3	8	3	5	7
Autumn	29	3	9	9	9	12
Autumn	29	3	10	3	0	3
Autumn	29	2	1	12	7	19
Autumn	29	2	2	8	10	15
Autumn	29	2	3	5	0	5
Autumn	29	2	4	13	9	24
Autumn	29	2	5	6	7	9
Autumn	29	2	6	12	18	25
Autumn	29	2	7	10	10	14
Autumn	29	2	8	10	9	13
Autumn	29	1	1	13	9	27
Autumn	29	1	2	9	8	11

Autumn	29	1	3	8	10	23
Autumn	29	1	4	3	1	4
Autumn	29	1	5	3	3	6
Autumn	29	1	6	4	3	4
Autumn	29	1	7	9	25	22
Autumn	29	1	8	16	12	23
Autumn	29	1	9	2	1	2
Autumn	29	1	10	5	2	5
Autumn	29	4	1	4	14	8
Autumn	29	4	2	8	20	16
Autumn	29	4	3	9	18	20
Autumn	29	4	4	4	11	6
Autumn	29	5	1	1	1	1
Autumn	29	5	2	10	11	13
Autumn	29	5	3	2	0	3
Autumn	29	5	4	2	4	2
Autumn	29	5	5	22	33	41
Autumn	29	5	6	13	23	23
Autumn	29	5	7	13	23	22
Autumn	29	6	1	12	17	18
Autumn	29	6	2	10	25	20
Autumn	29	6	3	4	28	19
Autumn	29	6	4	10	20	14
Autumn	29	6	5	8	23	18
Autumn	29	7	1	15	20	19
Autumn	29	7	2	5	5	6
Autumn	29	7	3	10	22	29
Autumn	29	7	4	14	23	24
Autumn	36	4	1	9	24	17
Autumn	36	4	2	4	24	13
Autumn	36	4	3	8	25	28
Autumn	36	4	4	7	36	26
Autumn	36	4	5	8	17	8
Autumn	36	4	6	10	18	15
Autumn	36	5	1	15	21	21
Autumn	36	5	2	16	25	18
Autumn	36	5	3	13	25	23
Autumn	36	5	4	11	16	13
Autumn	36	5	5	16	20	21
Autumn	36	6	1	8	21	31
Autumn	36	6	2	5	22	14
Autumn	36	6	3	7	10	13
Autumn	36	6	4	6	20	11

Autumn	36	6	5	5	12	12
Autumn	36	6	6	12	12	5
Autumn	36	7	1	4	23	24
Autumn	36	7	2	10	18	26
Autumn	36	7	3	15	22	17
Autumn	36	7	4	10	23	35
Autumn	36	7	5	12	11	16
Autumn	40	4	1	12	11	14
Autumn	40	4	2	12	7	15
Autumn	40	4	3	4	16	16
Autumn	40	4	4	6	2	8
Autumn	40	5	1	17	24	21
Autumn	40	5	2	15	14	24
Autumn	40	5	3	12	11	18
Autumn	40	5	4	12	21	20
Autumn	40	5	5	9	10	12
Autumn	40	6	1	13	24	29
Autumn	40	6	2	13	2	13
Autumn	40	6	3	13	15	14
Autumn	40	6	4	14	16	23
Autumn	40	6	5	9	19	19
Autumn	40	7	1	13	16	20
Autumn	40	7	2	9	17	13
Autumn	40	7	3	11	12	19
Autumn	40	7	4	10	21	25
Autumn	40	7	5	15	9	17
Winter	29	2	1	5	7	11
Winter	29	2	2	13	18	21
Winter	29	2	3	11	14	19
Winter	29	2	4	12	15	20
Winter	29	2	5	9	9	15
Winter	29	4	1	6	9	11
Winter	29	4	2	4	16	19
Winter	29	4	3	4	7	5
Winter	29	4	4	6	33	23
Winter	29	4	5	17	22	25
Winter	36	2	1	14	16	21
Winter	36	2	2	9	13	12
Winter	36	2	3	4	8	6
Winter	36	2	4	9	5	11
Winter	36	2	5	3	8	4
Winter	36	4	1	11	18	27
Winter	36	4	2	9	18	11

Winter	36	4	3	5	21	9
Winter	36	4	4	7	15	13
Winter	36	4	5	4	3	6
Winter	40	2	1	7	8	9
Winter	40	2	2	10	13	16
Winter	40	2	3	5	1	5
Winter	40	2	4	8	14	16
Winter	40	4	1	7	6	9
Winter	40	4	2	4	7	8
Winter	40	4	3	10	16	20
Winter	40	4	4	5	5	6
Winter	29	2	1	2	7	4
Winter	29	2	2	11	19	18
Winter	29	2	3	5	6	6
Winter	29	2	4	9	15	17
Winter	29	2	5	9	20	20
Winter	29	4	1	6	18	18
Winter	29	4	2	6	5	7
Winter	29	4	3	8	13	13
Winter	29	4	4	7	13	13
Winter	36	2	1	15	24	23
Winter	36	2	2	9	7	18
Winter	36	2	3	5	8	6
Winter	36	2	4	13	6	17
Winter	36	2	5	3	3	7
Winter	36	4	1	7	18	24
Winter	36	4	2	7	16	11
Winter	36	4	3	13	8	22
Winter	36	4	4	6	10	6
Winter	36	4	5	6	11	14
Winter	40	2	1	7	14	15
Winter	40	2	2	10	2	13
Winter	40	2	3	4	2	5
Winter	40	2	4	15	11	20
Winter	40	4	1	8	7	11
Winter	40	4	2	7	10	9
Winter	40	4	3	4	3	11
Winter	40	4	4	9	11	15
Winter	40	4	5	12	10	15
Spring	29	1	1	9	34	33
Spring	29	1	2	4	11	14
Spring	29	1	3	2	7	5
Spring	29	3	1	4	20	15

Spring	29	3	2	8	26	18
Spring	36	1	1	7	22	13
Spring	36	1	2	11	11	14
Spring	36	1	3	5	14	9
Spring	36	1	4	9	20	14
Spring	36	1	5	9	26	15
Spring	36	3	1	8	31	15
Spring	36	3	2	4	7	7
Spring	36	3	3	8	19	12
Spring	36	3	4	6	16	8
Spring	40	1	1	9	13	14
Spring	40	1	2	7	8	8
Spring	40	1	3	4	8	6
Spring	40	1	4	4	11	8
Spring	40	3	1	8	11	11
Spring	40	3	2	6	22	14
Spring	40	3	3	5	3	7
Spring	40	3	4	7	8	7
Spring	40	3	5	5	12	9

Appendix 2

Individuals on the Slide. A) First day of stolon shooting. B) Intermediate stage seven days after the stolons start to grow. C) Last day of image acquisition for counting the number of stolons bases, tips, and buds.

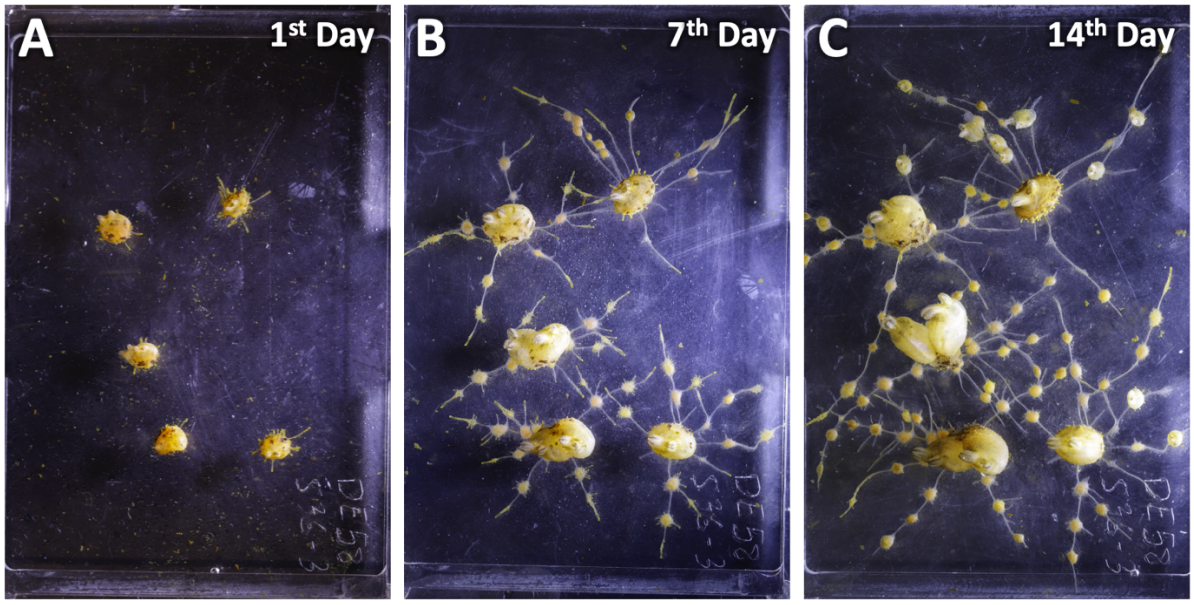

Appendix 3

Number of gonads and brooded embryos per individual, per condition.

Experiment	Salinity	Slide	Individual	Number of gonads	Number of embryos
Autumn	29	1	1	6	0
Autumn	29	1	2	6	2
Autumn	29	1	3	10	1
Autumn	29	1	4	7	0
Autumn	29	2	1	11	2
Autumn	29	2	2	8	0
Autumn	29	2	3	9	0
Autumn	29	2	4	8	0
Autumn	29	2	5	9	0
Autumn	29	2	6	7	0
Autumn	29	2	7	9	0
Autumn	29	3	1	13	2
Autumn	29	3	2	8	2
Autumn	29	3	3	0	0
Autumn	29	3	4	5	0
Autumn	29	3	5	9	1
Autumn	29	4	1	4	0
Autumn	29	4	2	2	0
Autumn	29	4	3	0	0
Autumn	29	4	4	4	0
Autumn	36	1	1	8	3
Autumn	36	1	2	11	2
Autumn	36	1	3	7	0
Autumn	36	1	4	8	0
Autumn	36	1	5	6	9
Autumn	36	1	6	7	5
Autumn	36	2	1	7	0
Autumn	36	2	2	5	4
Autumn	36	2	3	9	6
Autumn	36	2	4	3	3
Autumn	36	2	5	4	2
Autumn	36	3	1	8	1
Autumn	36	3	2	9	0
Autumn	36	3	3	6	0
Autumn	36	3	4	10	8
Autumn	36	3	5	11	0
Autumn	36	3	6	9	0

Autumn	36	4	1	7	0
Autumn	36	4	2	5	0
Autumn	36	4	3	7	2
Autumn	36	4	4	6	0
Autumn	36	4	5	4	0
Autumn	40	1	1	6	6
Autumn	40	1	2	6	10
Autumn	40	1	3	6	0
Autumn	40	1	4	5	0
Autumn	40	2	1	9	12
Autumn	40	2	2	5	0
Autumn	40	2	3	5	16
Autumn	40	2	4	11	0
Autumn	40	2	5	7	0
Autumn	40	3	1	9	0
Autumn	40	3	2	10	19
Autumn	40	3	3	6	6
Autumn	40	3	4	9	15
Autumn	40	3	5	6	0
Autumn	40	4	1	7	0
Autumn	40	4	2	8	0
Autumn	40	4	3	7	0
Autumn	40	4	4	7	0
Autumn	40	4	5	5	0

Appendix 4

Number of released larvae by day.

Experiment	Salinity	Day	Total of larvae released by day
Autumn	40	1	0
Autumn	40	2	0
Autumn	40	3	0
Autumn	40	4	0
Autumn	40	5	0
Autumn	40	6	1
Autumn	40	7	1
Autumn	40	8	15
Autumn	40	9	3
Autumn	36	1	0
Autumn	36	2	0
Autumn	36	3	1
Autumn	36	4	6
Autumn	36	5	20
Autumn	36	6	15
Autumn	36	7	9
Autumn	36	8	7
Autumn	36	9	11
Autumn	29	1	0
Autumn	29	2	0
Autumn	29	3	0
Autumn	29	4	0
Autumn	29	5	0
Autumn	29	6	0
Autumn	29	7	0
Autumn	29	8	1
Autumn	29	9	0

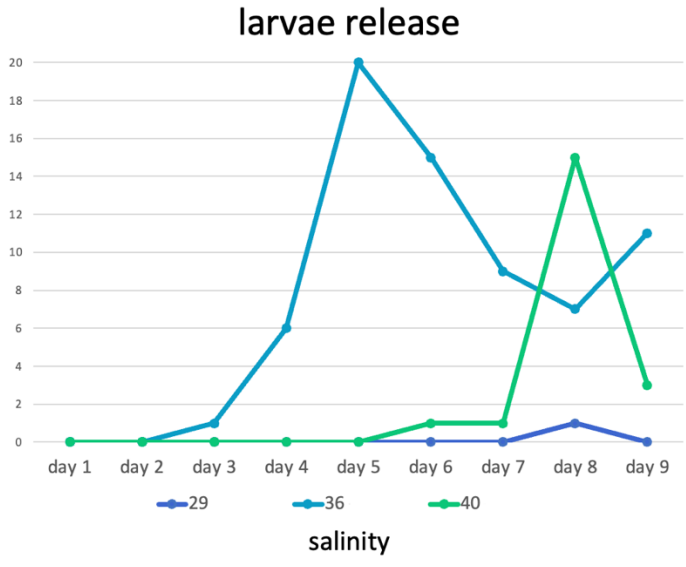

Appendix 5

Measuring parameters. A) A zooid is measured by summing the distance from the oral siphon (OS) opening to its base plus the distance from the base of the zooid to the middle of the two siphons. B) For gonads and brooded embryos counting, the zooids are dissected in the sense illustrated in this image. B') Indication of gonads location. AS: atrial siphon.

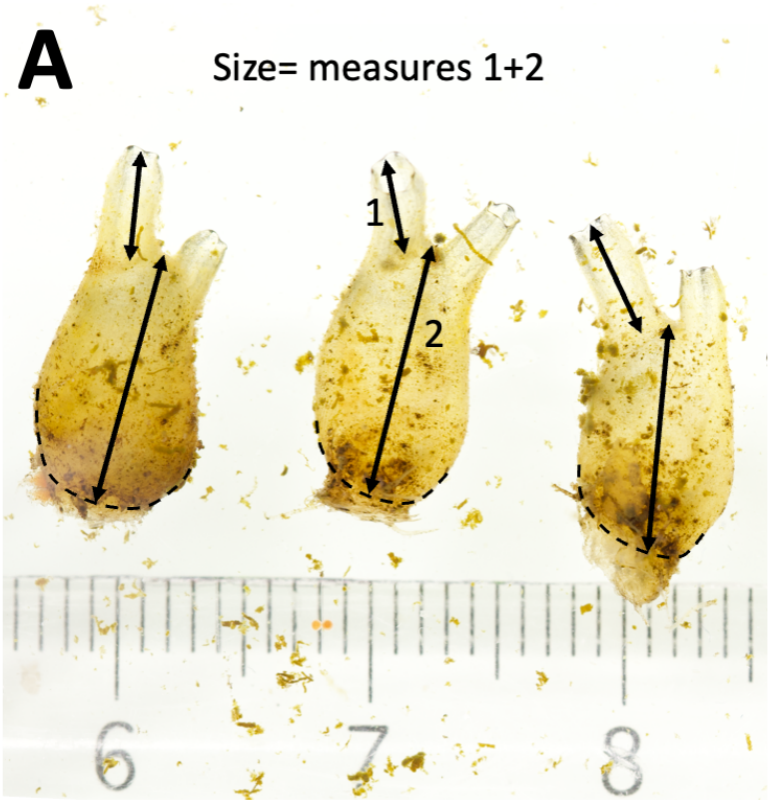

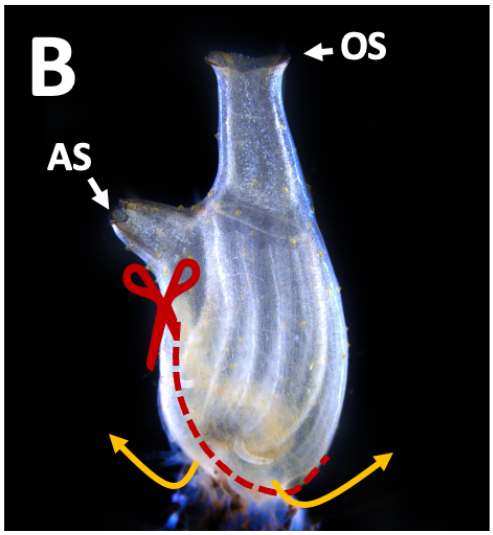

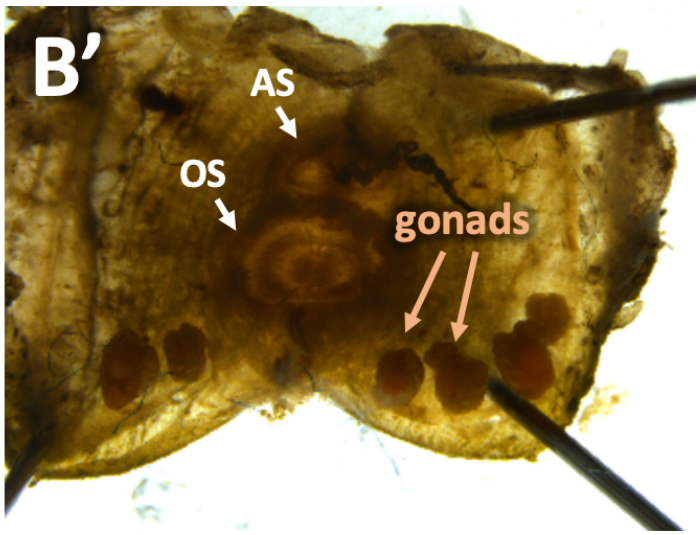

Zooid size measures:

Experiment	Slide	Salinity	Individual	Zooid size (cm)
Autumn	40	1	1	1,005
Autumn	40	1	2	0,867
Autumn	40	1	3	1,542
Autumn	40	1	4	1,041
Autumn	40	2	1	1,319
Autumn	40	2	2	1,499
Autumn	40	2	3	1,009
Autumn	40	2	4	1,214
Autumn	40	2	5	1,044
Autumn	40	3	1	1,467
Autumn	40	3	2	1,619
Autumn	40	3	3	0,885
Autumn	40	3	4	1,535
Autumn	40	3	5	1,657
Autumn	40	4	1	1,471
Autumn	40	4	2	1,667
Autumn	40	4	3	1,519
Autumn	40	4	4	1,534
Autumn	40	4	5	1,074
Autumn	36	1	1	1,467
Autumn	36	1	2	1,421
Autumn	36	1	3	1,348
Autumn	36	1	4	1,134
Autumn	36	1	5	1,103
Autumn	36	1	6	0,967
Autumn	36	2	1	0,908
Autumn	36	2	2	0,92
Autumn	36	2	3	1,216
Autumn	36	2	4	1,009
Autumn	36	2	5	0,976
Autumn	36	3	1	1,124
Autumn	36	3	2	1,291
Autumn	36	3	3	1,193
Autumn	36	3	4	1,434
Autumn	36	3	5	1,472
Autumn	36	3	6	1,817
Autumn	36	4	1	1,305

Autumn	36	4	2	1,721
Autumn	36	4	3	1,163
Autumn	36	4	4	1,26
Autumn	36	4	5	1,2
Autumn	29	1	1	1,249
Autumn	29	1	2	1,201
Autumn	29	1	3	1,311
Autumn	29	1	4	1,2
Autumn	29	2	1	1,61
Autumn	29	2	2	1,29
Autumn	29	2	3	1,019
Autumn	29	2	4	0,901
Autumn	29	2	5	1,201
Autumn	29	2	6	1,074
Autumn	29	2	7	1,182
Autumn	29	3	1	1,173
Autumn	29	3	2	1,03
Autumn	29	3	3	0,845
Autumn	29	3	4	0,979
Autumn	29	3	5	1,04
Autumn	29	4	1	1,113
Autumn	29	4	2	1,441
Autumn	29	4	3	0,943
Autumn	29	4	4	1,004

Appendix 6

Health measure parameters: Stolon pulsation and heart beating (number of beats per minute).

Experiment	Slide	Salinity	Individual	Stolon Pulsation (beats per min.)
Autumn	4	29	1	115
Autumn	4	29	2	115
Autumn	4	29	3	115
Autumn	4	29	4	115
Autumn	4	29	5	110
Autumn	4	29	6	105
Autumn	3	29	1	115
Autumn	3	29	2	110
Autumn	3	29	3	105
Autumn	3	29	4	105
Autumn	3	29	5	105
Autumn	2	36	1	110
Autumn	2	36	2	125
Autumn	2	36	3	120
Autumn	2	36	4	105
Autumn	2	36	5	100
Autumn	2	36	6	105
Autumn	2	36	7	105
Autumn	1	36	1	115
Autumn	1	36	2	120
Autumn	1	36	3	120
Autumn	1	40	1	115
Autumn	1	40	2	100
Autumn	1	40	3	105
Autumn	1	40	4	110
Autumn	1	40	5	115
Autumn	1	40	6	105
Autumn	2	40	1	110
Autumn	2	40	2	110
Autumn	2	40	3	100
Autumn	2	40	4	95
Autumn	2	40	5	100
Autumn	2	40	6	125
Autumn	2	40	7	105

Experiment	Salinity	Individual	Heart Beating (beats per min.)
Autumn	29	1	57
Autumn	29	2	55
Autumn	29	3	56
Autumn	29	4	56
Autumn	29	5	56
Autumn	36	1	60
Autumn	36	2	54
Autumn	36	3	64
Autumn	36	4	58
Autumn	36	5	64
Autumn	40	1	52
Autumn	40	2	62
Autumn	40	3	54
Autumn	40	4	60
Autumn	40	5	58

The videos can be found at this address:

https://drive.google.com/drive/folders/1Z522byRFvnHer677YMKoQZMvjaDs6fKX?usp=sharish

Appendix 7

The DNA sequences used for confectioning the *in situ* HCR probes for *Nk4* and *GataA*, together with the probes set of each can be found at this link:

https://drive.google.com/file/d/1xbo-DeFimoHIXzIQK7NnK0qRQgdo6H6d/view?usp=sharing

The sequences for the other species protein sequences can be retrieved at NCBI using the reference code present in the complete phylogenies in the appendices 8, 9, 10, 11, and 12.

Appendix 8

1- Simplified phylogenetic relationships among *BMP* (Bone Morphogenetic Protein) genes from *Homo sapiens* ('Hsap') and *Polyandrocarpa zorritensis* ('Pzor'). The tree reveals evolutionary groupings and divergence patterns, with branch lengths representing evolutionary change (blue) and numbers at nodes indicating support values for the respective branching (red).

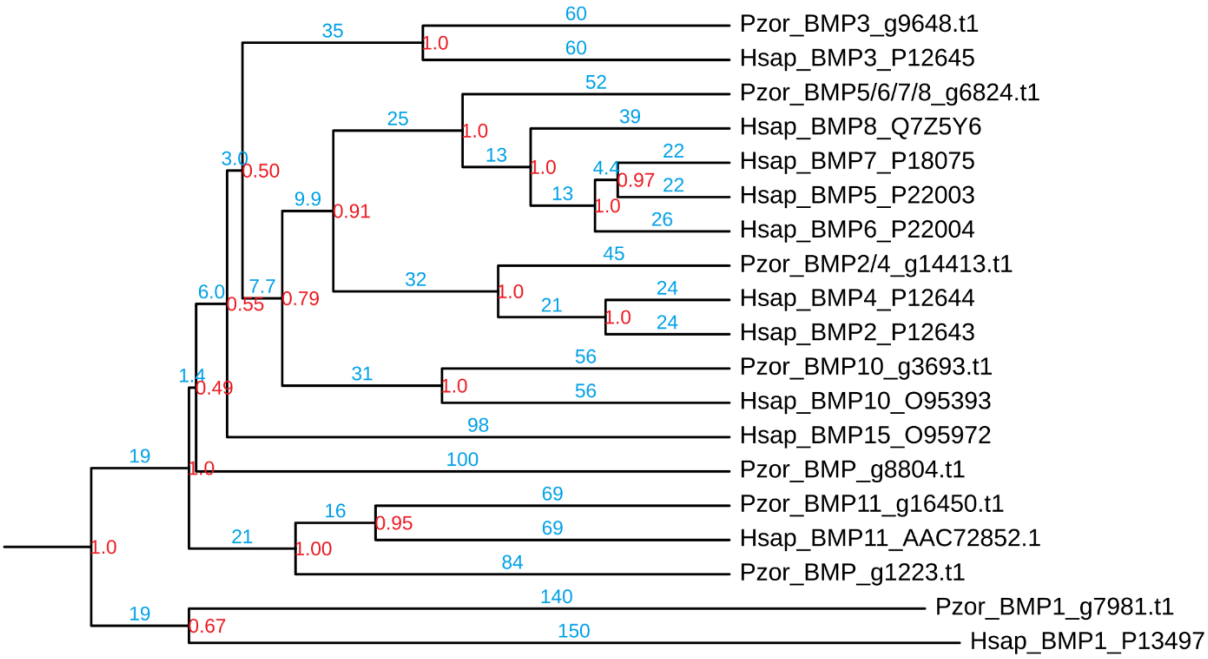

2 - Phylogenetic relationships among *BMP* (Bone Morphogenetic Protein) genes from Spur: *Strongylocentrotus purpuratus*, Drer: *Danio rerio*, Xtro: *Xenopus tropicalis*, Hsap: *Homo sapiens*, Dmel: *Drosophila melanogaster*, Skow: *Saccoglossus kowalevskii*, Cint: *Ciona intestinalis*, Scla: *Styela clava*, Pmis: *Polyandrocarpa misakiensis*, Blea: *Botrylloides leachii*, Pzor: *Polyandrocarpa zorritensis*, Bsch: *Botryllus schlosseri*. The tree illustrates the evolutionary relationships and divergence among the proteins, with branch lengths representing evolutionary distances (blue). Bootstrap values, given at the nodes, indicate the confidence of each branching event (red).

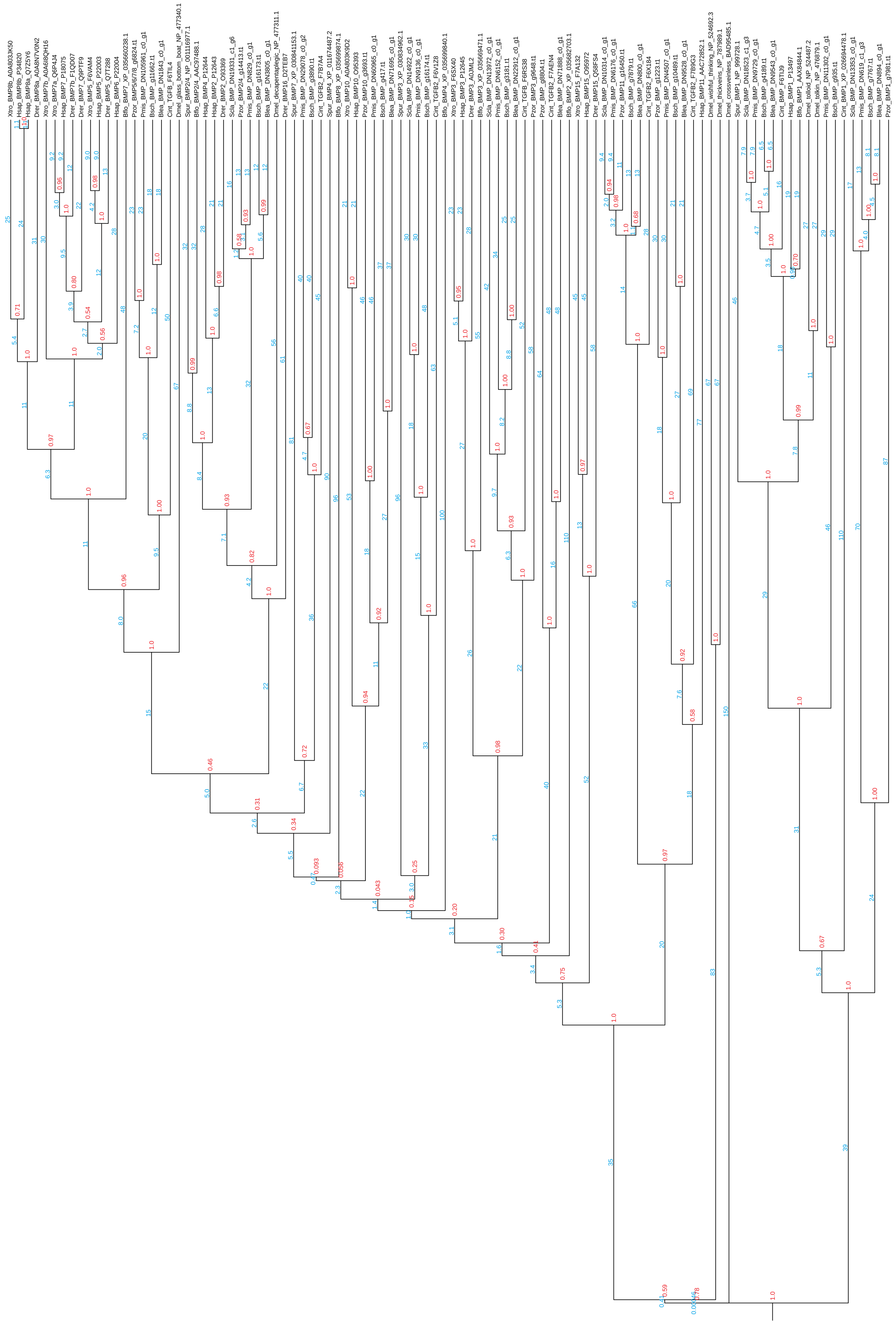

Appendix 9

Phylogenetic tree depicting relationships among *Hedgehog* (HH) gene sequences across diverse organisms, primarily vertebrates. Branch lengths indicate evolutionary distances. The tree showcases the evolutionary dynamics of HH genes, including SHH, IHH, and DHH, among species. Spur: *Strongylocentrotus purpuratus*, Drer: *Danio rerio*, Xtro: *Xenopus tropicalis*, Hsap: *Homo sapiens*, Dmel: *Drosophila melanogaster*, Skow: *Saccoglossus kowalevskii*, Cint: *Ciona intestinalis*, Scla: *Styela clava*, Pmis: *Polyandrocarpa misakiensis*, Blea: *Botrylloides leachii*, Pzor: *Polyandrocarpa zorritensis*, Bsch: *Botryllus schlosseri*. The tree illustrates the evolutionary relationships and divergence among the proteins, with branch lengths representing evolutionary distances (blue). Bootstrap values, given at the nodes, indicate the confidence of each branching event (red).

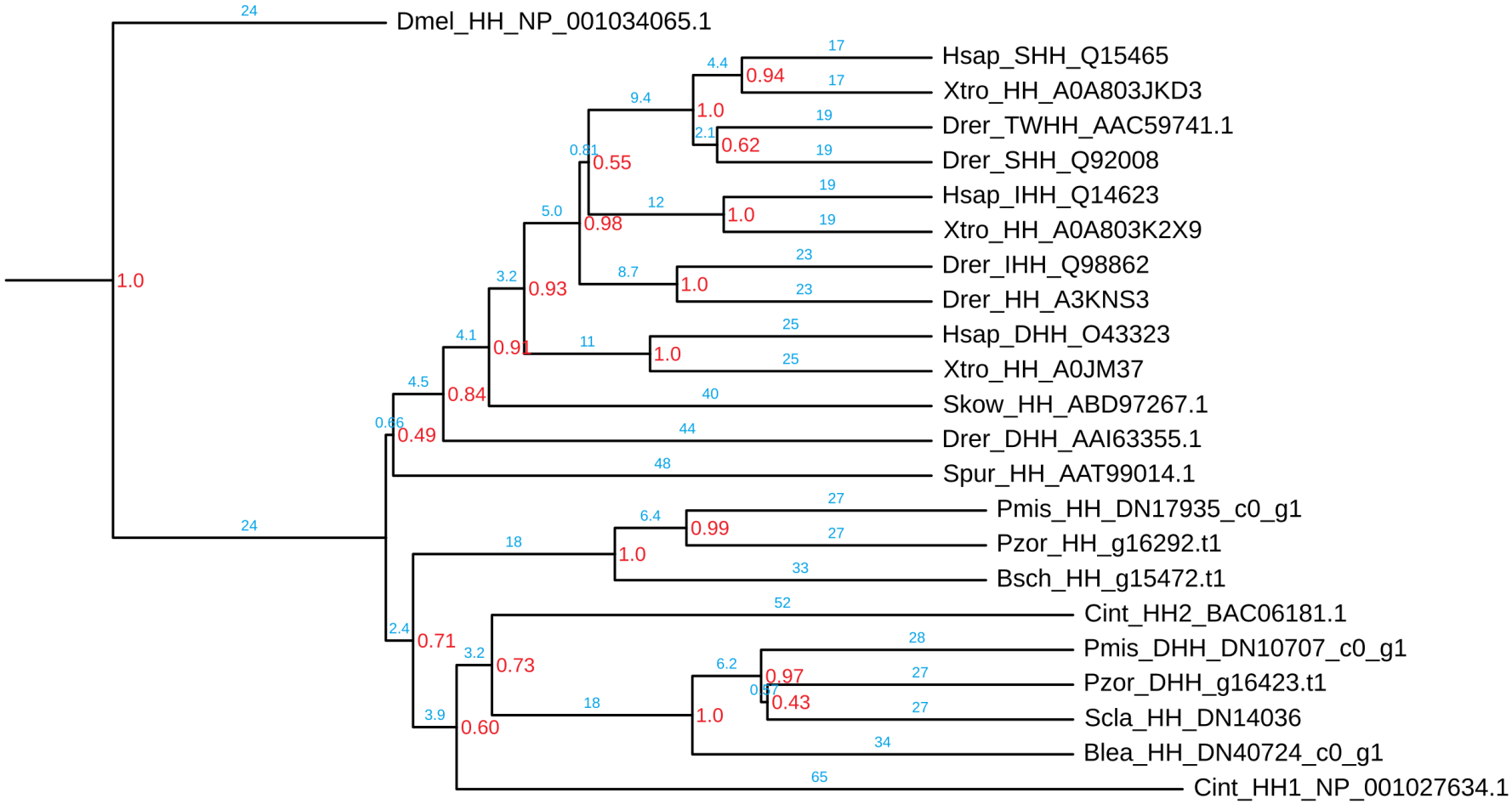
Dmel_HH_NP_001034065.1
Hsap_SHH_Q15465
Xtro_HH_A0A803JKD3
Drer_TWHH_AAC59741.1
Drer_SHH_Q92008
Hsap_IHH_Q14623
Xtro_HH_A0A803K2X9
Drer_IHH_Q98862
Drer_HH_A3KNS3
Hsap_DHH_O43323
Xtro_HH_A0JM37
Skow_HH_ABD97267.1
Drer_DHH_AAI63355.1
Spur_HH_AAT99014.1
Pmis_HH_DN17935_c0_g1
Pzor_HH_g16292.t1
Bsch_HH_g15472.t1
Cint_HH2_BAC06181.1
Pmis_DHH_DN10707_c0_g1
Pzor_DHH_g16423.t1
Scla_HH_DN14036
Blea_HH_DN40724_c0_g1
Cint_HH1_NP_001027634.1

Appendix 10

Phylogenetic tree representing evolutionary relationships among 'Runx/runt' genes across various species. Notably, genes from 'Xlae', 'Hsap', and 'Drer' species form distinct, closely related clades for Runx3, Runx2, and Runx1, highlighting their recent shared ancestry. Ascidians form another clade, a sister one, contain only one Runx. 'Dmel' serves as a more distantly related outgroup. Spur: *Strongylocentrotus purpuratus*, Drer: *Danio rerio*, Xlae: *Xenopus laevis*, Hsap: *Homo sapiens*, Dmel: *Drosophila melanogaster*, Skow: *Saccoglossus kowalevskii*, Cint: *Ciona intestinalis*, Scla: *Styela clava*, Pmis: *Polyandrocarpa misakiensis*, Blea: *Botrylloides leachii*, Pzor: *Polyandrocarpa zorritensis*, Bsch: *Botryllus schlosseri*. The tree illustrates the evolutionary relationships and divergence among the proteins, with branch lengths representing evolutionary distances (blue). Bootstrap values, given at the nodes, indicate the confidence of each branching event (red).

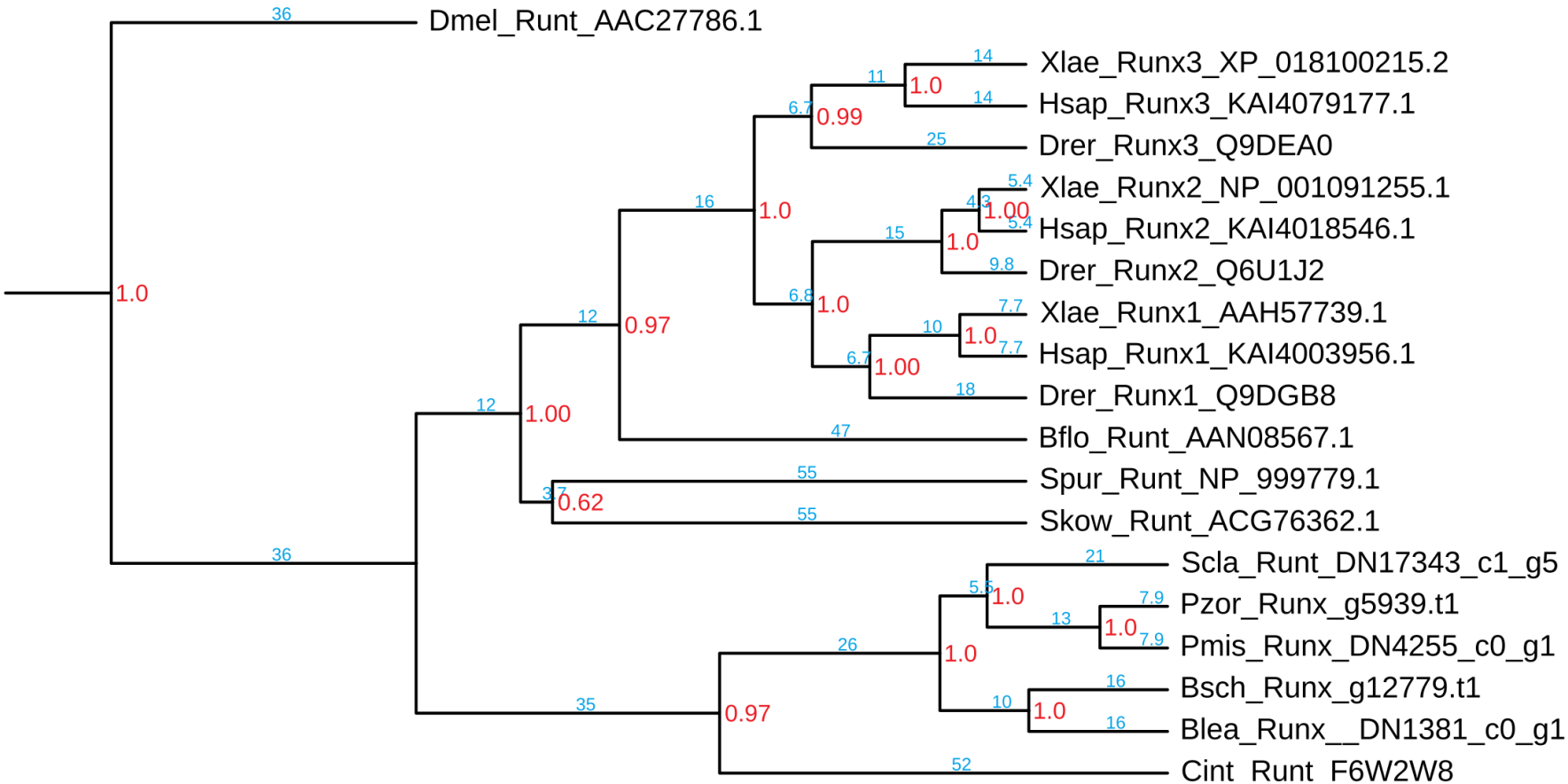
Dmel_Runt_AAC27786.1
Xlae_Runx3_XP_018100215.2
Hsap_Runx3_KAI4079177.1
Drer_Runx3_Q9DEA0
Xlae_Runx2_NP_001091255.1
Hsap_Runx2_KAI4018546.1
Drer_Runx2_Q6U1J2
Xlae_Runx1_AAH57739.1
Hsap_Runx1_KAI4003956.1
Drer_Runx1_Q9DGB8
Bflo_Runt_AAN08567.1
Spur_Runt_NP_999779.1
Skow_Runt_ACG76362.1
Scla_Runt_DN17343_c1_g5
Pzor_Runx_g5939.t1
Pmis_Runx_DN4255_c0_g1
Bsch_Runx_g12779.t1
Blea_Runx__DN1381_c0_g1
Cint_Runt_F6W2W8

Appendix 11

Phylogenetic tree of Argonaute (AGO) and Piwi-like (PIWL) proteins from various organisms. The tree illustrates the evolutionary relationships and divergence among the proteins, with branch lengths representing evolutionary distances (blue). Bootstrap values, given at the nodes, indicate the confidence of each branching event (red). Notably, Argonaute proteins and Piwi-like proteins form two distinct clades. Branch lengths represent evolutionary distances (blue), with closely related sequences clustered together. Bflo: *Branchiostoma floridanus*, Spur: *Strongylocentrotus purpuratus*, Drer: *Danio rerio*, Xlae: *Xenopus laevis*, Hsap: *Homo sapiens*, Dmel: *Drosophila melanogaster*, Skow: *Saccoglossus kowalevskii*, Cint: *Ciona intestinalis*, Scla: *Styela clava*, Pmis: *Polyandrocarpa misakiensis*, Blea: *Botrylloides leachii*, Pzor: *Polyandrocarpa zorritensis*, Bsch: *Botryllus schlosseri*.

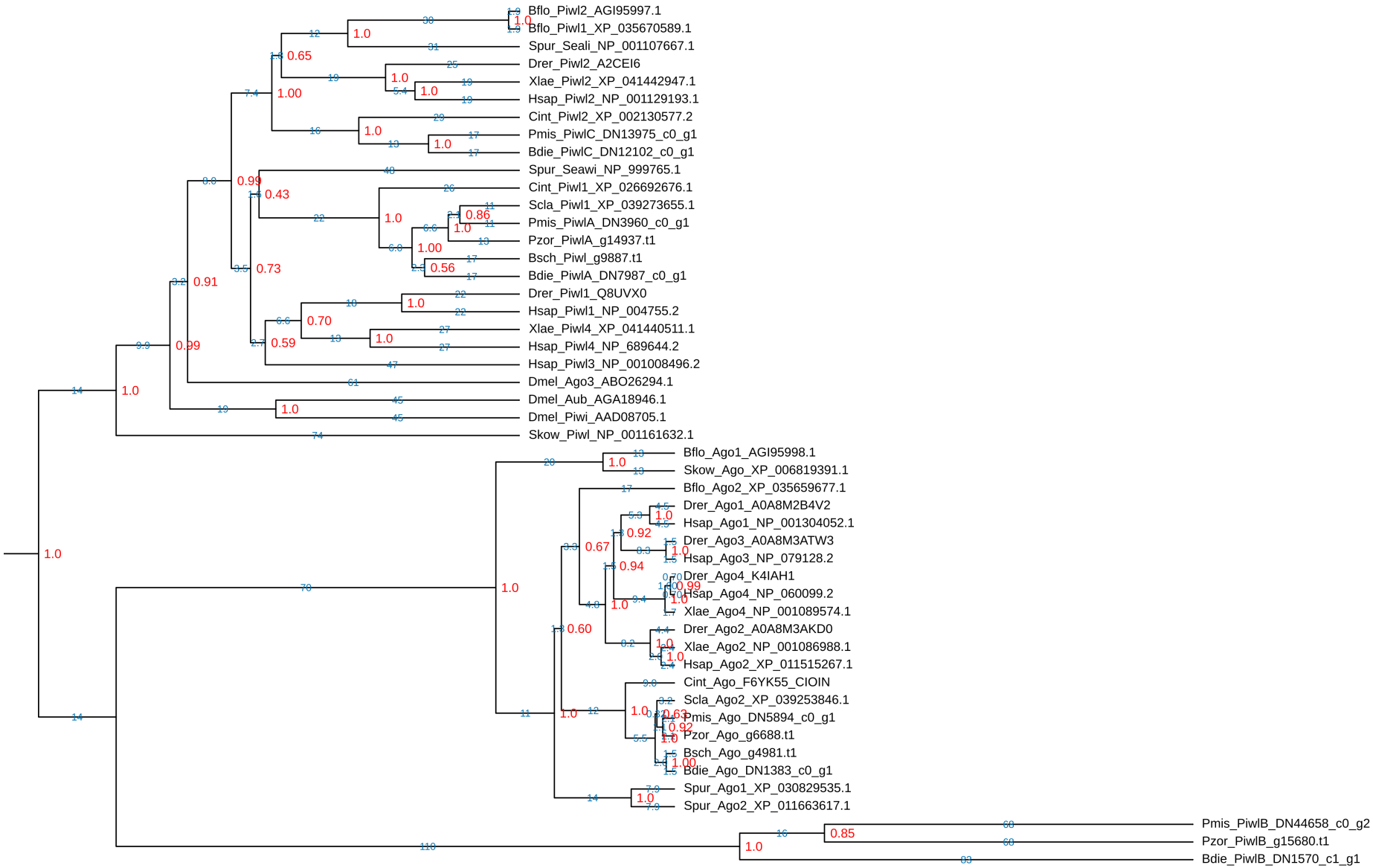
Bflo_Piwl2_AGI95997.1
Bflo_Piwl1_XP_035670589.1
Spur_Seali_NP_001107667.1
Drer_Piwl2_A2CEI6
Xlae_Piwl2_XP_041442947.1
Hsap_Piwl2_NP_001129193.1
Cint_Piwl2_XP_002130577.2
Pmis_PiwlC_DN13975_c0_g1
Bdie_PiwlC_DN12102_c0_g1
Spur_Seawi_NP_999765.1
Cint_Piwl1_XP_026692676.1
Scla_Piwl1_XP_039273655.1
Pmis_PiwlA_DN3960_c0_g1
Pzor_PiwlA_g14937.t1
Bsch_Piwl_g9887.t1
Bdie_PiwlA_DN7987_c0_g1
Drer_Piwl1_Q8UVX0
Hsap_Piwl1_NP_004755.2
Xlae_Piwl4_XP_041440511.1
Hsap_Piwl4_NP_689644.2
Hsap_Piwl3_NP_001008496.2
Dmel_Ago3_ABO26294.1
Dmel_Aub_AGA18946.1
Dmel_Piwi_AAD08705.1
Skow_Piwl_NP_001161632.1
Bflo_Ago1_AGI95998.1
Skow_Ago_XP_006819391.1
Bflo_Ago2_XP_035659677.1
Drer_Ago1_A0A8M2B4V2
Hsap_Ago1_NP_001304052.1
Drer_Ago3_A0A8M3ATW3
Hsap_Ago3_NP_079128.2
Drer_Ago4_K4IAH1
Hsap_Ago4_NP_060099.2
Xlae_Ago4_NP_001089574.1
Drer_Ago2_A0A8M3AKD0
Xlae_Ago2_NP_001086988.1
Hsap_Ago2_XP_011515267.1
Cint_Ago_F6YK55_CIOIN
Scla_Ago2_XP_039253846.1
Pmis_Ago_DN5894_c0_g1
Pzor_Ago_g6688.t1
Bsch_Ago_g4981.t1
Bdie_Ago_DN1383_c0_g1
Spur_Ago1_XP_030829535.1
Spur_Ago2_XP_011663617.1
Pmis_PiwlB_DN44658_c0_g2
Pzor_PiwlB_g15680.t1
Bdie_PiwlB_DN1570_c1_g1

Appendix 12

Phylogenetic relationships of GATA transcription factors across multiple species, including Ggal: *Gallus gallus*, Bflo: *Branchiostoma floridanus*, Spur: *Strongylocentrotus purpuratus*, Drer: *Danio rerio*, Xlae: *Xenopus laevis*, Hsap: *Homo sapiens*, Dmel: *Drosophila melanogaster*, Skow: *Saccoglossus kowalevskii*, Cint: *Ciona intestinalis*, Scla: *Styela clava*, Pmis: *Polyandrocarpa misakiensis*, Blea: *Botrylloides leachii*, Pzor: *Polyandrocarpa zorritensis*, Bsch: *Botryllus schlosseri*. The tree reveals evolutionary branching patterns of the GATA1 through GATA6 gene families, with bootstrap values given at the nodes, indicating the confidence of each branching event (red) and branch lengths representing evolutionary distances (blue).

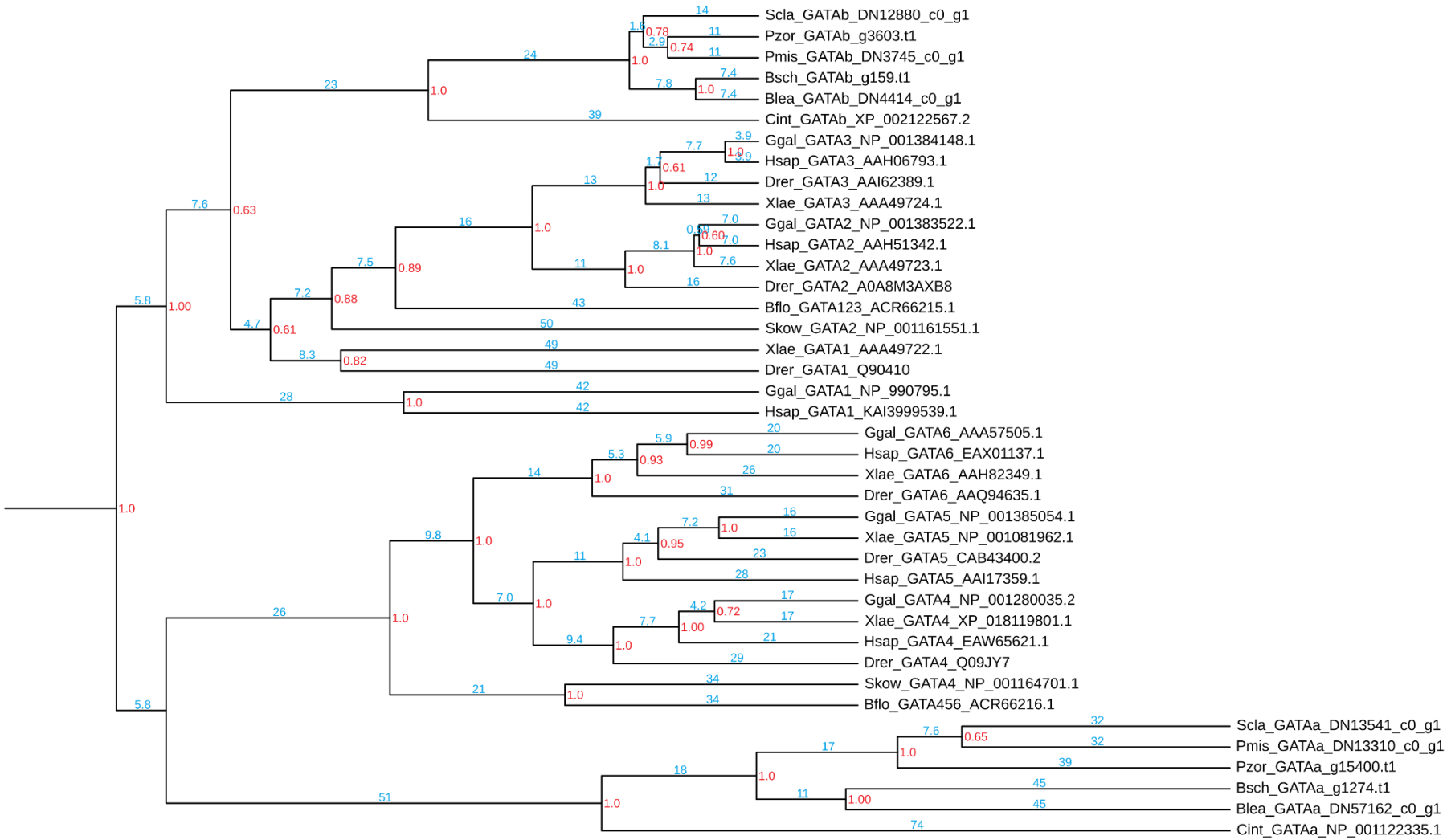
Scla_GATAb_DN12880_c0_g1
Pzor_GATAb_g3603.t1
Pmis_GATAb_DN3745_c0_g1
Bsch_GATAb_g159.t1
Blea_GATAb_DN4414_c0_g1
Cint_GATAb_XP_002122567.2
Ggal_GATA3_NP_001384148.1
Hsap_GATA3_AAH06793.1
Drer_GATA3_AAI62389.1
Xlae_GATA3_AAA49724.1
Ggal_GATA2_NP_001383522.1
Hsap_GATA2_AAH51342.1
Xlae_GATA2_AAA49723.1
Drer_GATA2_A0A8M3AXB8
Bflo_GATA123_ACR66215.1
Skow_GATA2_NP_001161551.1
Xlae_GATA1_AAA49722.1
Drer_GATA1_Q90410
Ggal_GATA1_NP_990795.1
Hsap_GATA1_KAI3999539.1
Ggal_GATA6_AAA57505.1
Hsap_GATA6_EAX01137.1
Xlae_GATA6_AAH82349.1
Drer_GATA6_AAQ94635.1
Ggal_GATA5_NP_001385054.1
Xlae_GATA5_NP_001081962.1
Drer_GATA5_CAB43400.2
Hsap_GATA5_AAI17359.1
Ggal_GATA4_NP_001280035.2
Xlae_GATA4_XP_018119801.1
Hsap_GATA4_EAW65621.1
Drer_GATA4_Q09JY7
Skow_GATA4_NP_001164701.1
Bflo_GATA456_ACR66216.1
Scla_GATAa_DN13541_c0_g1
Pmis_GATAa_DN13310_c0_g1
Pzor_GATAa_g15400.t1
Bsch_GATAa_g1274.t1
Blea_GATAa_DN57162_c0_g1
Cint_GATAa_NP_001122335.1

Appendix 13

Botryllus schlosseri genome assembly.

The genome assembly process was conducted by our collaborator, using a combination of HiFi reads and the Hifiasm algorithm. The initial assembly resulted in a genome size of 424,323,369 bp, with an N50 value of 1,657,153 bp, and a total of 829 contigs. The assembly completeness was evaluated using the Kat completeness metric, which yielded a score of 59.17%. Additionally, the BUSCO analysis indicated that 92.6% of the expected genes were found in the assembly, with 84.1% classified as complete single-copy genes, 8.5% as complete duplicated genes, 3.7% as fragmented genes, and 3.7% as missing genes.

To improve the assembly further, reads obtained using the Oxford Nanopore Technologies (ONT) were incorporated, and two different haplotype purging methods were applied. First, the "Purge_dups" step was performed to remove haplotigs and resolve contig overlaps. This process resulted in a reduced assembly size of 375,785,810 bp, an N50 value of 1,863,282 bp, and a total of 490 contigs. The Kat completeness score slightly decreased to 51.47%, and the BUSCO analysis indicated that 92.4% of the expected genes were present, with 90.6% complete single-copy genes, 1.8% complete duplicated genes, 3.7% fragmented genes, and 3.9% missing genes. The second haplotype purging step, "Purge_haplotigs," aimed to identify pairs of contigs that are syntenic. After this step, the assembly size was further reduced to 364,995,275 bp, with an N50 value of 1,913,193 bp and a total of 397 contigs. The Kat completeness score was similar to the previous step, at 50.54%, and the BUSCO analysis showed 92.4% of the expected genes present, with 90.7% complete single-copy genes, 1.7% complete duplicated genes, 3.7% fragmented genes, and 3.9% missing genes.

To scaffold the assembly, the ntLink method was employed, using both HiFi and ONT reads for lightweight mapping. The final scaffolded assembly had a size of 364,798,430 bp, an N50 value of 14,178,783 bp, and a total of 106 contigs. The Kat completeness score was 50.41%, and the BUSCO analysis yielded 92.4% of the expected genes, with 90.7% complete single-copy genes, 1.7% complete duplicated genes, 3.7% fragmented genes, and 3.9% missing genes. The assembled data was also polished using the HyPo method, which combined HiFi and Illumina reads. The polished assembly had a size of 364,761,307 bp, an N50 value of 14,177,737 bp, and a total of 106 contigs. However, the polishing process resulted in a slightly

decreased Kat completeness score of 49.61%. The BUSCO analysis showed 92.5% of the expected genes present, with 90.8% complete single-copy genes, 1.7% complete duplicated genes, 3.6% fragmented genes, and 3.9% missing genes.

The genome annotation process was conducted through a series of steps following genome assembly. Repeat identification was performed using Repeat Modeler2 and repeat annotation/masking was carried out using Repeat Masker. Transcripts alignment was performed using STAR, incorporating the HyPo output and RNAseq reads. Genome annotation was achieved using Braker 3, resulting in the identification of 17,126 genes and 21,451 transcripts.

Appendix 14

Botryllus schlosseri genome assembly pipeline and scores

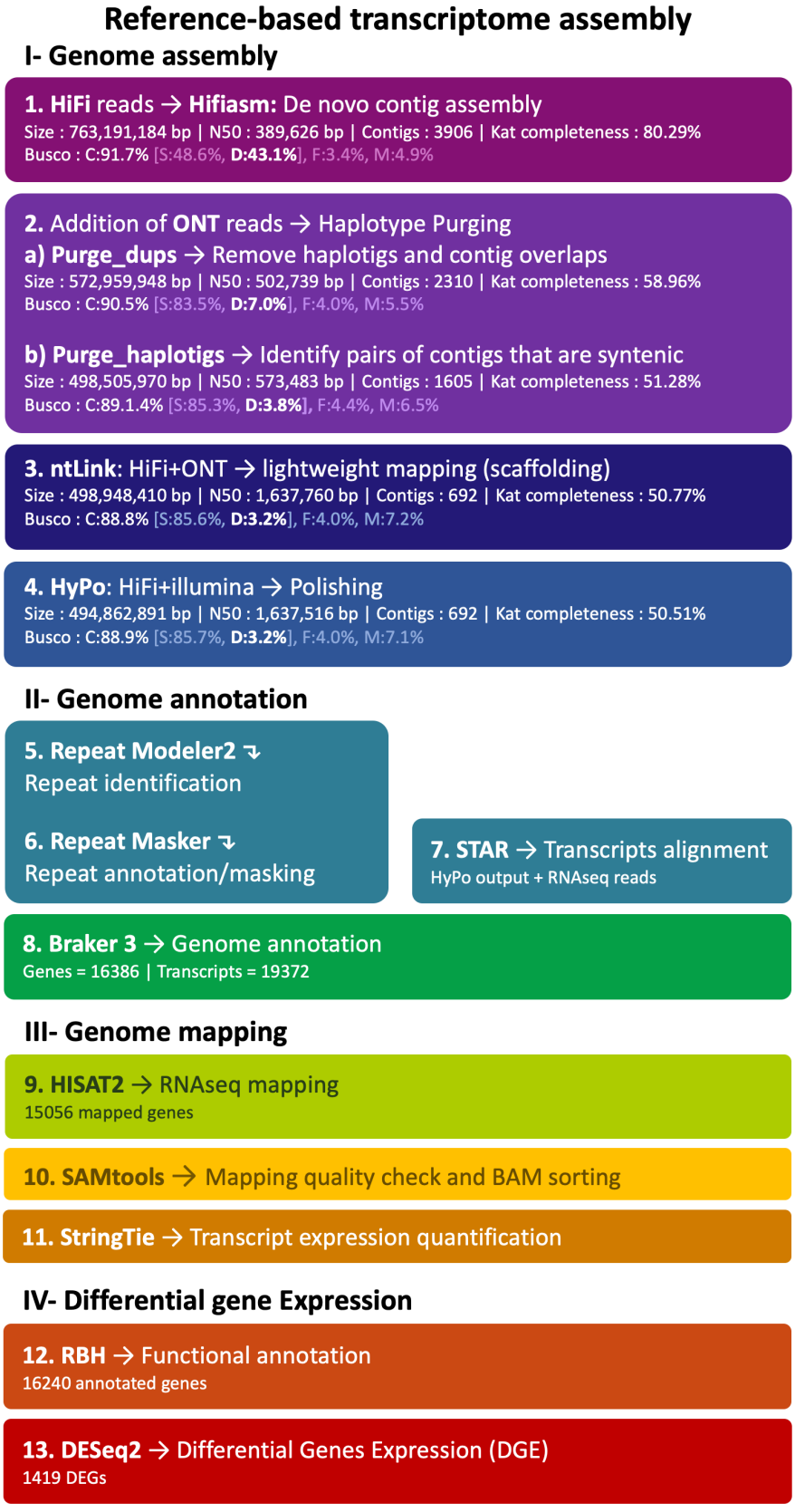

Images Index

References

Abbott, Donald P, A Todd Newberry, and Kendall M Morris. 1997. *Reef and Shore Fauna of Hawaii*. 6B ed.

Adell, Teresa, Francesc Cebrià, and Emili Saló. 2010. "Gradients in Planarian Regeneration and Homeostasis." *Cold Spring Harbor Perspectives in Biology* 2 (1): a000505.

Adler, Carolyn E., and Alejandro Sánchez Alvarado. 2015. "Types or States? Cellular Dynamics and Regenerative Potential." *Trends in Cell Biology* 25 (11): 687–96. https://doi.org/10.1016/j.tcb.2015.07.008.

Agata, Kiyokazu, Yumi Saito, and Elizabeth Nakajima. 2007. "Unifying Principles of Regeneration I: Epimorphosis versus Morphallaxis." *Development, Growth & Differentiation* 49 (2): 73–78. https://doi.org/10.1111/j.1440-169X.2007.00919.x.

Alié, Alexandre, Laurel S. Hiebert, Marta Scelzo, and Stefano Tiozzo. 2021. "The Eventful History of Nonembryonic Development in Tunicates." *Journal of Experimental Zoology Part B: Molecular and Developmental Evolution* 336 (3): 250–66. https://doi.org/10.1002/jez.b.22940.

Alié, Alexandre, Laurel Sky Hiebert, Paul Simion, Marta Scelzo, Maria Mandela Prünster, Sonia Lotito, Frédéric Delsuc, et al. 2018. "Convergent Acquisition of Nonembryonic Development in Styelid Ascidians." Edited by Nicole King. *Molecular Biology and Evolution* 35 (7): 1728–43. https://doi.org/10.1093/molbev/msy068.

Alvarado, A. 2003. "The Freshwater Planarian Schmidtea Mediterranea: Embryogenesis, Stem Cells and Regeneration." *Current Opinion in Genetics & Development* 13 (4): 438–44. https://doi.org/10.1016/S0959-437X(03)00082-0.

Alvarado, Alejandro Sánchez. 2000. "Regeneration in the Metazoans: Why Does It Happen?" *BioEssays* 22 (6): 578–90. https://doi.org/10.1002/(SICI)1521-1878(200006)22:6<578::AID-BIES11>3.0.CO;2-#.

Appel, Bruce, Lee Anne Givan, and Judith S. Eisen. 2001. "Delta-Notch Signaling and Lateral Inhibition in Zebrafish Spinal Cord Development." *BMC Developmental Biology* 1 (1): 13. https://doi.org/10.1186/1471-213X-1-13.

Audouin, Jacques. 1962. "Hydrologie de l'étang de Thau."

Ballarin, Loriano, and Kaz Kawamura. 2009. "The Hemocytes of Polyandrocarpa Mysakiensis: Morphology and Immune-Related Activities." *Invertebrate Survival Journal* 6 (November).

Barker, Nick. 2014. "Adult Intestinal Stem Cells: Critical Drivers of Epithelial Homeostasis and Regeneration." *Nature Reviews Molecular Cell Biology* 15 (1): 19–33. https://doi.org/10.1038/nrm3721.

Bast, Jens, Kamil S Jaron, Donovan Schuseil, Denis Roze, and Tanja Schwander. 2019. "Asexual Reproduction Reduces Transposable Element Load in

Experimental Yeast Populations." *eLife* 8 (September): e48548. https://doi.org/10.7554/eLife.48548.

Bely, Alexandra E., and Kevin G. Nyberg. 2010. "Evolution of Animal Regeneration: Re-Emergence of a Field." *Trends in Ecology & Evolution* 25 (3): 161–70. https://doi.org/10.1016/j.tree.2009.08.005.

Berrill, N. J. 1931. "Regeneration in Sabella Pavonina (Sav.) and Other Sabellid Worms." *Journal of Experimental Zoology* 58 (1): 495–523.

———. 1935. "Studies in Tunicate Development. Part IV. Asexual Reproduction." *Philosophical Transactions of the Royal Society of London. Series B, Biological Sciences* 225 (526): 327–79.

———. 1947. "The Development and Growth of *Ciona*." *Journal of the Marine Biological Association of the United Kingdom* 26 (4): 616–25. https://doi.org/10.1017/S0025315400013825.

———. 1951. "REGENERATION AND BUDDING IN TUNICATES." *Biological Reviews* 26 (4): 456–75. https://doi.org/10.1111/j.1469-185X.1951.tb01207.x.

Bertrand, Vincent, Clare Hudson, Danielle Caillol, Cornel POPOVICI, and Patrick Lemaire. 2003. "Neural Tissue in Ascidian Embryos Is Induced by FGF9/16/20, Acting via a Combination of Maternal GATA and Ets Transcription Factors." *Cell* 115 (December): 615–27. https://doi.org/10.1016/S0092-8674(03)00928-0.

Bielefeld, Kirsten A., Saeid Amini-Nik, and Benjamin A. Alman. 2013. "Cutaneous Wound Healing: Recruiting Developmental Pathways for Regeneration." *Cellular and Molecular Life Sciences* 70: 2059–81.

Blanchoud, Simon, Buki Rinkevich, and Megan J. Wilson. 2018. "Whole-Body Regeneration in the Colonial Tunicate Botrylloides Leachii." In *Marine Organisms as Model Systems in Biology and Medicine*, edited by Malgorzata Kloc and Jacek Z. Kubiak, 65:337–55. Results and Problems in Cell Differentiation. Cham: Springer International Publishing. https://doi.org/10.1007/978-3-319-92486-1_16.

Blanchoud, Simon, Lisa Zondag, Miles D. Lamare, and Megan J. Wilson. 2017. "Hematological Analysis of the Ascidian *Botrylloides Leachii* (Savigny, 1816) During Whole-Body Regeneration." *The Biological Bulletin* 232 (3): 143–57. https://doi.org/10.1086/692841.

Bolker, Jessica A. 2000. "Modularity in Development and Why It Matters to Evo-Devo1." *American Zoologist* 40 (5): 770–76. https://doi.org/10.1093/icb/40.5.770.

Borena, Bizunesh M., Ann Martens, Sarah Y. Broeckx, Evelyne Meyer, Koen Chiers, Luc Duchateau, and Jan H. Spaas. 2015. "Regenerative Skin Wound Healing in Mammals: State-of-the-Art on Growth Factor and Stem Cell Based Treatments." *Cellular Physiology and Biochemistry* 36 (1): 1–23.

Bosch, Thomas CG. 2007. "Why Polyps Regenerate and We Don't: Towards a Cellular and Molecular Framework for Hydra Regeneration." *Developmental Biology* 303 (2): 421–33.

Boyden, Alan. 1954. “The Significance of Asexual Reproduction.” *Systematic Zoology* 3 (1): 26. https://doi.org/10.2307/2411492.

Braconnot, Jean-Claude. 1970. “CONTRIBUTION A L’ÉTUDE BIOLOGIQUE ET ÉCOLOGIQUE DES TUNICIERS PÉLAGIQUES SALPIDES ET DOLIOLIDES II. _ ÉCOLOGIE DES DOLIOLIDES, BIOLOGIE DES DEUX GROUPES.”

Brewer, J., Andrei Molotkov, Pierre Mazot, Renée Hoch, and Philippe Soriano. 2015. “Fgfr1 Regulates Development through the Combinatorial Use of Signaling Proteins.” *Genes & Development* 29 (September). https://doi.org/10.1101/gad.264994.115.

Briscoe, James, and Pascal P. Thérond. 2013. “The Mechanisms of Hedgehog Signalling and Its Roles in Development and Disease.” *Nature Reviews Molecular Cell Biology* 14 (7): 416–29. https://doi.org/10.1038/nrm3598.

Brockes, Jeremy P., and Anoop Kumar. 2008. “Comparative Aspects of Animal Regeneration.” *Annual Review of Cell and Developmental Biology* 24 (1): 525–49. https://doi.org/10.1146/annurev.cellbio.24.110707.175336.

Brown, Federico D., Elena L. Keeling, Anna D. Le, and Billie J. Swalla. 2009. “Whole Body Regeneration in a Colonial Ascidian, *Botrylloides Violaceus*.” *Journal of Experimental Zoology Part B: Molecular and Developmental Evolution* 312B (8): 885–900. https://doi.org/10.1002/jez.b.21303.

Brown, Federico D., and Billie J. Swalla. 2012. “Evolution and Development of Budding by Stem Cells: Ascidian Coloniality as a Case Study.” *Developmental Biology* 369 (2): 151–62. https://doi.org/10.1016/j.ydbio.2012.05.038.

Brunetti, Riccardo. 1978. “Polyandrocarpa Zorritensis (Van Name, 1931) A Colonial Ascidian New to the Mediterranean Record.” *Vie Milieu* XXVIII–XXIX (AB): 647–52.

Brunetti, Riccardo, and Francesco Mastrototaro. 2004. “The Non-Indigenous Stolidobranch Ascidian Polyandrocarpa Zorritensis in the Mediterranean: Description, Larval Morphology and Pattern of Vascular Budding.” *Zootaxa* 528 (1): 1. https://doi.org/10.11646/zootaxa.528.1.1.

Bryant, Susan V., Tetsuya Endo, and David M. Gardiner. 2004. “Vertebrate Limb Regeneration and the Origin of Limb Stem Cells.” *International Journal of Developmental Biology* 46 (7): 887–96.

Bullard, S.G., G. Lambert, M.R. Carman, J. Byrnes, R.B. Whitlatch, G. Ruiz, R.J. Miller, et al. 2007. “The Colonial Ascidian Didemnum Sp. A: Current Distribution, Basic Biology and Potential Threat to Marine Communities of the Northeast and West Coasts of North America.” *Journal of Experimental Marine Biology and Ecology* 342 (1): 99–108. https://doi.org/10.1016/j.jembe.2006.10.020.

Buzgariu, Wanda, Yvan Wenger, Nina Tcaciuc, Ana-Paula Catunda-Lemos, and Brigitte Galliot. 2018. “Impact of Cycling Cells and Cell Cycle Regulation on Hydra Regeneration.” *Regeneration: From Cells to Tissues to Organisms* 433 (2): 240–53. https://doi.org/10.1016/j.ydbio.2017.11.003.

Cadigan, Ken M., and Roel Nusse. 1997. “Wnt Signaling: A Common Theme in Animal Development.” *Genes & Development* 11 (24): 3286–3305.

Cantalapiedra, Carlos P, Ana Hernández-Plaza, Ivica Letunic, Peer Bork, and Jaime Huerta-Cepas. 2021. “eggNOG-Mapper v2: Functional Annotation, Orthology Assignments, and Domain Prediction at the Metagenomic Scale.” *Molecular Biology and Evolution* 38 (12): 5825–29. https://doi.org/10.1093/molbev/msab293.

Capellini, Terence D., Giuseppina Di Giacomo, Valentina Salsi, Andrea Brendolan, Elisabetta Ferretti, Deepak Srivastava, Vincenzo Zappavigna, and Licia Selleri. 2006. “Pbx1/Pbx2 Requirement for Distal Limb Patterning Is Mediated by the Hierarchical Control of Hox Gene Spatial Distribution and Shh Expression.”

Carballo, Gabriela Basile, Jéssica Ribeiro Honorato, Giselle Pinto Farias de Lopes, and Tania Cristina Leite de Sampaio e Spohr. 2018. “A Highlight on Sonic Hedgehog Pathway.” *Cell Communication and Signaling* 16 (1): 11. https://doi.org/10.1186/s12964-018-0220-7.

Carballo, Jl. 2000. “Larval Ecology of an Ascidian Tropical Population in a Mediterranean Enclosed Ecosystem.” *Marine Ecology Progress Series* 195: 159–67. https://doi.org/10.3354/meps195159.

Cardeccia, Alice, Agnese Marchini, Anna Occhipinti-Ambrogi, Bella Galil, Stephan Gollasch, Dan Minchin, Aleksas Narščius, Sergej Olenin, and Henn Ojaveer. 2018. “Assessing Biological Invasions in European Seas: Biological Traits of the Most Widespread Non-Indigenous Species.” *Estuarine, Coastal and Shelf Science* 201 (February): 17–28. https://doi.org/10.1016/j.ecss.2016.02.014.

Carlson, Bruce M. 2011. *Principles of Regenerative Biology*. Elsevier.

Carman, Mary, Stephan Bullard, Rosana Rocha, Gretchen Lambert, Jennifer Dijkstra, James Roper, Anne Goodwin, Mimi Carman, and Elisabete Vail. 2011. “Ascidians at the Pacific and Atlantic Entrances to the Panama Canal.” *Aquatic Invasions* 6 (4): 371–80. https://doi.org/10.3391/ai.2011.6.4.02.

Cary, Gregory A., Andrew Wolff, Olga Zueva, Joseph Pattinato, and Veronica F. Hinman. 2019. “Analysis of Sea Star Larval Regeneration Reveals Conserved Processes of Whole-Body Regeneration across the Metazoa.” *BMC Biology* 17 (1): 16. https://doi.org/10.1186/s12915-019-0633-9.

Castilla, Juan Carlos, Ricardo Guiñez, Andrés U. Caro, and Verónica Ortiz. 2004. “Invasion of a Rocky Intertidal Shore by the Tunicate *Pyura Praeputialis* in the Bay of Antofagasta, Chile.” *Proceedings of the National Academy of Sciences* 101 (23): 8517–24. https://doi.org/10.1073/pnas.0401921101.

Cavodeassi, Florencia, Juan Modolell, and José Luis Gómez-Skarmeta. 2001. “The Iroquois Family of Genes: From Body Building to Neural Patterning.” *Development* 128 (15): 2847–55. https://doi.org/10.1242/dev.128.15.2847.

Chaigneau, Alexis, Noel Dominguez, Gérard Eldin, Luis Vasquez, Roberto Flores, Carmen Grados, and Vincent Echevin. 2013. “Near-Coastal Circulation in the Northern Humboldt Current System from Shipboard ADCP Data: CIRCULATION OF THE NHCS FROM SADCP DATA.” *Journal of Geophysical Research: Oceans* 118 (10): 5251–66. https://doi.org/10.1002/jgrc.20328.

Charlesworth, B. 1980. “The Cost of Sex in Relation to Mating System.” *Journal of Theoretical Biology* 84 (4): 655–71. https://doi.org/10.1016/S0022-5193(80)80026-9.

Chebbi, Nadia, Francesco Mastrototaro, and Hechmi Missaoui. 2010. “Spatial Distribution of Ascidians in Two Tunisian Lagoons of the Mediterranean Sea.”

Cho, Ken W.Y., Bruce Blumberg, Herbert Steinbeisser, and Eddy M. De Robertis. 1991. “Molecular Nature of Spemann’s Organizer: The Role of the Xenopus Homeobox Gene Goosecoid.” *Cell* 67 (6): 1111–20. https://doi.org/10.1016/0092-8674(91)90288-A.

Choi, Hyunwoo, Bo-Gyeong Kim, Yong Hwan Kim, Se-Jin Lee, Young Jae Lee, and S. Paul Oh. 2023. “BMP10 Functions Independently from BMP9 for the Development of a Proper Arteriovenous Network.” *Angiogenesis* 26 (1): 167–86. https://doi.org/10.1007/s10456-022-09859-0.

Choudhry, Zia, Azadeh Rikani, Adnan Choudhry, Sadaf Tariq, Fozia Zakaria, Waheed Asghar, Muhammad Sarfraz, Kamran Haider, Afia Shafiq, and Nusrat Mobassarah. 2014. “Sonic Hedgehog Signalling Pathway: A Complex Network.” *Annals of Neurosciences* 21 (January): 28–31. https://doi.org/10.5214/ans.0972.7531.210109.

Chuong, Cheng-Ming, Valerie A. Randall, Randall B. Widelitz, Ping Wu, and Ting-Xin Jiang. 2012. “Physiological Regeneration of Skin Appendages and Implications for Regenerative Medicine.” *Physiology* 27 (2): 61–72. https://doi.org/10.1152/physiol.00028.2011.

Cima, Francesca, Nicola Franchi, and Loriano Ballarin. 2016. “Chapter 2 - Origin and Functions of Tunicate Hemocytes.” In *The Evolution of the Immune System*, edited by Davide Malagoli, 29–49. Academic Press. https://doi.org/10.1016/B978-0-12-801975-7.00002-5.

Ciruna, Brian, and Janet Rossant. 2001. “FGF Signaling Regulates Mesoderm Cell Fate Specification and Morphogenetic Movement at the Primitive Streak.” *Developmental Cell* 1 (1): 37–49. https://doi.org/10.1016/S1534-5807(01)00017-X.

Clarke, Kaitlin, Yi Yang, Ronald Marsh, LingLin Xie, and Zhang Ke K. 2013. “Comparative Analysis of de Novo Transcriptome Assembly.” *Science China Life Sciences* 56 (2): 156–62. https://doi.org/10.1007/s11427-013-4444-x.

Clarke Murray, Cathryn, Heidi Gartner, Edward J. Gregr, Kai Chan, Evgeny Pakhomov, and Thomas W. Therriault. 2014. “Spatial Distribution of Marine Invasive Species: Environmental, Demographic and Vector Drivers.” Edited by Brian Leung. *Diversity and Distributions* 20 (7): 824–36. https://doi.org/10.1111/ddi.12215.

Clarke Murray, Cathryn, Evgeny A. Pakhomov, and Thomas W. Therriault. 2011. “Recreational Boating: A Large Unregulated Vector Transporting Marine Invasive Species: Transport of NIS by Recreational Boats.” *Diversity and Distributions* 17 (6): 1161–72. https://doi.org/10.1111/j.1472-4642.2011.00798.x.

Clevers, Hans, Kyle M. Loh, and Roel Nusse. 2014. “An Integral Program for Tissue Renewal and Regeneration: Wnt Signaling and Stem Cell Control.” *Science* 346 (6205): 1248012.

Cobaleda, César, Alexandra Schebesta, Alessio Delogu, and Meinrad Busslinger. 2007. “Pax5: The Guardian of B Cell Identity and Function.” *Nature Immunology* 8 (5): 463–70.

Cognetti, Giuseppe, and Ferruccio Maltagliati. 2000. “Biodiversity and Adaptive Mechanisms in Brackish Water Fauna.” *Marine Pollution Bulletin* 40 (1): 7–14. https://doi.org/10.1016/S0025-326X(99)00173-3.

Coll, Marta, Chiara Piroddi, Jeroen Steenbeek, Kristin Kaschner, Frida Ben Rais Lasram, Jacopo Aguzzi, Enric Ballesteros, et al. 2010. “The Biodiversity of the Mediterranean Sea: Estimates, Patterns, and Threats.” Edited by Steven J. Bograd. *PLoS ONE* 5 (8): e11842. https://doi.org/10.1371/journal.pone.0011842.

Collin, Matthew, Rachel Dickinson, and Venetia Bigley. 2015. “Haematopoietic and Immune Defects Associated with GATA2 Mutation.” *British Journal of Haematology* 169 (2): 173–87. https://doi.org/10.1111/bjh.13317.

Collu, Giovanna M., Ana Hidalgo-Sastre, and Keith Brennan. 2014. “Wnt–Notch Signalling Crosstalk in Development and Disease.” *Cellular and Molecular Life Sciences* 71 (18): 3553–67. https://doi.org/10.1007/s00018-014-1644-x.

Conesa, Ana, Stefan Götz, Juan Miguel García-Gómez, Javier Terol, Manuel Talón, and Montserrat Robles. 2005. “Blast2GO: A Universal Tool for Annotation, Visualization and Analysis in Functional Genomics Research.” *Bioinformatics* 21 (18): 3674–76. https://doi.org/10.1093/bioinformatics/bti610.

Crean, Angela J., and Dustin J. Marshall. 2015. “Eggs with Larger Accessory Structures Are More Likely to Be Fertilized in Both Low and High Sperm Concentrations in Styela Plicata (Ascidiaceae).” *Marine Biology* 162 (11): 2251–56. https://doi.org/10.1007/s00227-015-2755-0.

Crow, James F. 1994. “Advantages of Sexual Reproduction.” *Developmental Genetics* 15 (3): 205–13. https://doi.org/10.1002/dvg.1020150303.

Cummings, Susan G., and Hans R. Bode. 1984. “Head Regeneration and Polarity Reversal in Hydra Attenuata Can Occur in the Absence of DNA Synthesis.” *Wilhelm Roux’s Archives of Developmental Biology* 194: 79–86.

Darras, Sébastien, and Hiroki Nishida. 2001. “The BMP/CHORDIN Antagonism Controls Sensory Pigment Cell Specification and Differentiation in the Ascidian Embryo.” *Developmental Biology* 236 (2): 271–88. https://doi.org/10.1006/dbio.2001.0339.

Darricarrère, Nicole, Na Liu, Toshiaki Watanabe, and Haifan Lin. 2013. “Function of Piwi, a Nuclear Piwi/Argonaute Protein, Is Independent of Its Slicer Activity.” *Proceedings of the National Academy of Sciences* 110 (4): 1297–1302. https://doi.org/10.1073/pnas.1213283110.

De Meeûs, T., F. Prugnolle, and P. Agnew. 2007. “Asexual Reproduction: Genetics and Evolutionary Aspects.” *Cellular and Molecular Life Sciences* 64 (11): 1355–72. https://doi.org/10.1007/s00018-007-6515-2.

De Robertis, Eddy M., Martin Blum, Christof Niehrs, and Herbert Steinbeisser. 1992. “Goosecoid and the Organizer.” *Development* 116 (Supplement): 167–71. https://doi.org/10.1242/dev.116.Supplement.167.

De Robertis, Edward M., and Hiroki Kuroda. 2004. “DORSAL-VENTRAL PATTERNING AND NEURAL INDUCTION IN XENOPUS EMBRYOS.” *Annual Review of Cell and Developmental Biology* 20 (1): 285–308. https://doi.org/10.1146/annurev.cellbio.20.011403.154124.

Dechaud, Corentin, Jean-Nicolas Volff, Manfred Schartl, and Magali Naville. 2019. “Sex and the TEs: Transposable Elements in Sexual Development and Function in Animals.” *Mobile DNA* 10 (1): 42. https://doi.org/10.1186/s13100-019-0185-0.

Deibel, Don, and Ben Lowen. 2012. “A Review of the Life Cycles and Life-History Adaptations of Pelagic Tunicates to Environmental Conditions.” *ICES Journal of Marine Science* 69 (3): 358–69. https://doi.org/10.1093/icesjms/fsr159.

DeLaForest, Ann, Masato Nagaoka, Karim Si-Tayeb, Fallon K. Noto, Genevieve Konopka, Michele A. Battle, and Stephen A. Duncan. 2011. “HNF4A Is Essential for Specification of Hepatic Progenitors from Human Pluripotent Stem Cells.” *Development* 138 (19): 4143–53.

Delsuc, Frédéric, Henner Brinkmann, Daniel Chourrout, and Hervé Philippe. 2006. “Tunicates and Not Cephalochordates Are the Closest Living Relatives of Vertebrates.” *Nature* 439 (7079): 965–68. https://doi.org/10.1038/nature04336.

Delsuc, Frédéric, Georgia Tsagkogeorga, Nicolas Lartillot, and Hervé Philippe. 2008. “Additional Molecular Support for the New Chordate Phylogeny.” *Genesis* 46 (11): 592–604. https://doi.org/10.1002/dvg.20450.

Di Maio, Alessandro, Leah Setar, Stefano Tiozzo, and Anthony W. De Tomaso. 2015. “Wnt Affects Symmetry and Morphogenesis during Post-Embryonic Development in Colonial Chordates.” *EvoDevo* 6 (1): 17. https://doi.org/10.1186/s13227-015-0009-3.

Dias, Gm, Cgm Delboni, and Lfl Duarte. 2008. “Effects of Competition on Sexual and Clonal Reproduction of a Tunicate: The Importance of Competitor Identity.” *Marine Ecology Progress Series* 362 (June): 149–56. https://doi.org/10.3354/meps07447.

Dijkstra, Jennifer, Anthony Dutton, Erica Westerman, and Larry Harris. 2008. “Heart Rate Reflects Osmostic Stress Levels in Two Introduced Colonial Ascidians Botryllus Schlosseri and Botrylloidesviolaceus.” *Marine Biology* 154 (5): 805–11. https://doi.org/10.1007/s00227-008-0973-4.

Duncan, Andrew W, Frédérique M Rattis, Leah N DiMascio, Kendra L Congdon, Gregory Pazianos, Chen Zhao, Keejung Yoon, et al. 2005. “Integration of Notch and Wnt Signaling in Hematopoietic Stem Cell Maintenance.” *Nature Immunology* 6 (3): 314–22. https://doi.org/10.1038/ni1164.

Durante, Kathleen M. 1991. “Larval Behavior, Settlement Preference, and Induction of Metamorphosis in the Temperate Solitary Ascidian Molgula Citrina Alder & Hancock.” *Journal of Experimental Marine Biology and Ecology* 145 (2): 175–87. https://doi.org/10.1016/0022-0981(91)90174-U.

Dybern, Bernt I. 1967. “The Distribution and Salinity Tolerance of *Ciona Intestinalis* (L.) F. *Typica* with Special Reference to the Waters around Southern Scandinavia.” *Ophelia* 4 (2): 207–26. https://doi.org/10.1080/00785326.1967.10409621.

———. 1969. “Distribution and Ecology of Ascidians in Kviturdvikpollen and Vågsböpollen on the West Coast of Norway.” *Sarsia* 37 (1): 21–40. https://doi.org/10.1080/00364827.1969.10411143.

Engelstädter, Jan. 2008. “Constraints on the Evolution of Asexual Reproduction.” *BioEssays* 30 (11–12): 1138–50. https://doi.org/10.1002/bies.20833.

Epelbaum, A., L.M. Herborg, T.W. Therriault, and C.M. Pearce. 2009. “Temperature and Salinity Effects on Growth, Survival, Reproduction, and Potential Distribution of Two Non-Indigenous Botryllid Ascidians in British Columbia.” *Journal of Experimental Marine Biology and Ecology* 369 (1): 43–52. https://doi.org/10.1016/j.jembe.2008.10.028.

Esposito, Maurizio. 2013. “Weismann versus Morgan Revisited: Clashing Interpretations on Animal Regeneration.” *Journal of the History of Biology* 46: 511–41.

Falvo, James V., Alla V. Tsytsykova, and Anne E. Goldfeld. 2010. “Transcriptional Control of the TNF Gene.” *TNF Pathophysiology* 11: 27–60.

Fernandes-Silva, Hugo, Jorge Correia-Pinto, and Rute S. Moura. 2017. “Canonical Sonic Hedgehog Signaling in Early Lung Development.” *Journal of Developmental Biology* 5 (1). https://doi.org/10.3390/jdb5010003.

Ferrario, Jasmine, Sarah Caronni, Anna Occhipinti-Ambrogi, and Agnese Marchini. 2017. “Role of Commercial Harbours and Recreational Marinas in the Spread of Non-Indigenous Fouling Species.” *Biofouling* 33 (8): 651–60. https://doi.org/10.1080/08927014.2017.1351958.

Ferrell, James E. 2012. “Bistability, Bifurcations, and Waddington’s Epigenetic Landscape.” *Current Biology* 22 (11): R458–66.

Fialka, I, H Schwarz, E Reichmann, M Oft, M Busslinger, and H Beug. 1996. “The Estrogen-Dependent c-JunER Protein Causes a Reversible Loss of Mammary Epithelial Cell Polarity Involving a Destabilization of Adherens Junctions.” *The Journal of Cell Biology* 132 (6): 1115–32. https://doi.org/10.1083/jcb.132.6.1115.

Fiuza, Ulla-Maj, Takefumi Negishi, Alice Rouan, Hitoyoshi Yasuo, and Patrick Lemaire. 2020. “A Nodal/Eph Signalling Relay Drives the Transition from Apical Constriction to Apico-Basal Shortening in Ascidian Endoderm Invagination.” *Development* 147 (15): dev186965. https://doi.org/10.1242/dev.186965.

Flood, P. R., and A. Fiala-Medioni. 1981. “Ultrastructure and Histochemistry of the Food Trapping Mucous Film in Benthic Filter-Feeders (Ascidians).” *Acta Zoologica* 62 (1): 53–65. https://doi.org/10.1111/j.1463-6395.1981.tb00616.x.

Fodor, Alexander C A, Megan M Powers, Kristin Andrykovich, Jiatai Liu, Elijah K Lowe, C Titus Brown, Anna Di Gregorio, Alberto Stolfi, and Billie J Swalla. 2021. “The Degenerate Tale of Ascidian Tails.” *Integrative and Comparative Biology* 61 (2): 358–69. https://doi.org/10.1093/icb/icab022.

Fujita, Hisao, and Hisaka Nanba. 1971. “Fine Structure and Its Functional Properties of the Endostyle of Ascidians,Ciona Intestinalis: A Part of Phylogenetic Studies of the Thyroid Gland.” *Zeitschrift F□r Zellforschung Und Mikroskopische Anatomie* 121 (4): 455–69. https://doi.org/10.1007/BF00560154.

Fujiwara, Shigeki, and Kazuo Kawamura. 1992. “Ascidian Budding as a Transdifferentiation-Like System: Multipotent Epithelium Is Not Undifferentiated.”

Furtado, Milena B., Mark J. Solloway, Vanessa J. Jones, Mauro W. Costa, Christine Biben, Orit Wolstein, Jost I. Preis, Duncan B. Sparrow, Yumiko Saga, and Sally L. Dunwoodie. 2008. “BMP/SMAD1 Signaling Sets a Threshold for the Left/Right Pathway in Lateral Plate Mesoderm and Limits Availability of SMAD4.” *Genes & Development* 22 (21): 3037–49.

Gamse, Joshua, and Hazel Sive. 2000. “Vertebrate Anteroposterior Patterning: The Xenopus Neurectoderm as a Paradigm.” *BioEssays* 22 (11): 976–86.

Gao, Junying, Lixia Fan, Long Zhao, and Ying Su. 2021. “The Interaction of Notch and Wnt Signaling Pathways in Vertebrate Regeneration.” *Cell Regeneration* 10 (1): 11. https://doi.org/10.1186/s13619-020-00072-2.

Garg, Vidu, Irfan S. Kathiriya, Robert Barnes, Marie K. Schluterman, Isabelle N. King, Cheryl A. Butler, Caryn R. Rothrock, et al. 2003. “GATA4 Mutations Cause Human Congenital Heart Defects and Reveal an Interaction with TBX5.” *Nature* 424 (6947): 443–47. https://doi.org/10.1038/nature01827.

Gasparini, Fabio, and Loriano Ballarin. 2018. “Reproduction in Tunicates.” In *Encyclopedia of Reproduction*, 546–53. Elsevier. https://doi.org/10.1016/B978-0-12-809633-8.20601-8.

Gasparini, Fabio, Fabrizio Longo, Lucia Manni, Paolo Burighel, and Giovanna Zaniolo. 2007. “Tubular Sprouting as a Mode of Vascular Formation in a Colonial Ascidian (Tunicata).” *Developmental Dynamics* 236 (3): 719–31. https://doi.org/10.1002/dvdy.21073.

Ge, Gaoxiang, and Daniel S. Greenspan. 2006. “Developmental Roles of the BMP1/TLD Metalloproteinases.” *Birth Defects Research Part C: Embryo Today: Reviews* 78 (1): 47–68. https://doi.org/10.1002/bdrc.20060.

Gehrke, Andrew R., and Mansi Srivastava. 2016. “Neoblasts and the Evolution of Whole-Body Regeneration.” *Current Opinion in Genetics & Development* 40: 131–37.

Gewing, Mey-Tal, Eyal Goldstein, Yehezkel Buba, and Noa Shenkar. 2019. “Temperature Resilience Facilitates Invasion Success of the Solitary Ascidian

Herdmania Momus." *Biological Invasions* 21 (2): 349–61. https://doi.org/10.1007/s10530-018-1827-8.

Gewing, Mey-Tal, Susanna López-Legentil, and Noa Shenkar. 2017. "Anthropogenic Factors Influencing Invasive Ascidian Establishment in Natural Environments." *Marine Environmental Research* 131 (October): 236–42. https://doi.org/10.1016/j.marenvres.2017.10.001.

Gewing, Mey-Tal, and Noa Shenkar. 2017. "Monitoring the Magnitude of Marine Vessel Infestation by Non-Indigenous Ascidians in the Mediterranean." *Marine Pollution Bulletin* 121 (1–2): 52–59. https://doi.org/10.1016/j.marpolbul.2017.05.041.

Giese, Arthur C., John S. Pearse, and Vicki Pearse. 1974. *Reproduction of Marine Invertebrates*. New York: Academic Press.

Gómez-Skarmeta, José Luis, and Juan Modolell. 2002. "Iroquois Genes: Genomic Organization and Function in Vertebrate Neural Development." *Current Opinion in Genetics & Development* 12 (4): 403–8. https://doi.org/10.1016/S0959-437X(02)00317-9.

Goodbody, Ivan. 1975. "The Physiology of Ascidians." In *Advances in Marine Biology*, edited by Frederick S. Russell and Maurice Yonge, 12:1–149. Academic Press. https://doi.org/10.1016/S0065-2881(08)60457-5.

Gordon, Tal, Lachan Roth, Federico Caicci, Lucia Manni, and Noa Shenkar. 2020. "Spawning Induction, Development and Culturing of the Solitary Ascidian Polycarpa Mytiligera, an Emerging Model for Regeneration Studies." *Frontiers in Zoology* 17 (1): 19. https://doi.org/10.1186/s12983-020-00365-x.

Goss, Richard J. 1992. "The Evolution of Regeneration: Adaptive or Inherent?" *Journal of Theoretical Biology* 159 (2): 241–60.

Granot, Itai, Noa Shenkar, and Jonathan Belmaker. 2017. "Habitat Niche Breadth Predicts Invasiveness in Solitary Ascidians." *Ecology and Evolution* 7 (19): 7838–47. https://doi.org/10.1002/ece3.3351.

Gröner, Frederike, Mark Lenz, Martin Wahl, and Stuart R. Jenkins. 2011. "Stress Resistance in Two Colonial Ascidians from the Irish Sea: The Recent Invader Didemnum Vexillum Is More Tolerant to Low Salinity than the Cosmopolitan Diplosoma Listerianum." *Journal of Experimental Marine Biology and Ecology* 409 (1–2): 48–52. https://doi.org/10.1016/j.jembe.2011.08.002.

Grosberg, Richard K. 1992. "Asexual Obsessions." Edited by Roger N. Hughes. *Evolution* 46 (6): 1976–79. https://doi.org/10.2307/2410050.

Guaiquil, Victor H., Yun-Cin Luo, Joy Sarkar, and Mark Rosenblatt. 2016. "Mechanistic Studies for Vascular Endothelial Growth Factor-A and-B Induced Neuronal and Endothelial Cell Growth." *Investigative Ophthalmology & Visual Science* 57 (12): 3524–3524.

Hamada, Mayuko, Spela Goricki, Mardi S. Byerly, Noriyuki Satoh, and William R. Jeffery. 2015. "Evolution of the Chordate Regeneration Blastema: Differential Gene Expression and Conserved Role of Notch Signaling during Siphon

Regeneration in the Ascidian Ciona." *Developmental Biology* 405 (2): 304–15. https://doi.org/10.1016/j.ydbio.2015.07.017.

Han, Gangwen, Allen Li, Yao-Yun Liang, Philip Owens, Wei He, Shi-Long Lu, Yasuhiro Yoshimatsu, et al. 2006. "Smad7-Induced β-Catenin Degradation Alters Epidermal Appendage Development." *Developmental Cell* 11 (October): 301–12. https://doi.org/10.1016/j.devcel.2006.06.014.

Hanashima, Carina, Suzanne C. Li, Lijian Shen, Eseng Lai, and Gord Fishell. 2004. "Foxg1 Suppresses Early Cortical Cell Fate." *Science* 303 (5654): 56–59. https://doi.org/10.1126/science.1090674.

Haque, T., S. Nakada, and Reggie C. Hamdy. 2007. "A Review of FGF18: Its Expression, Signaling Pathways and Possible Functions during Embryogenesis and Post-Natal Development." *Histology and Histopathology*.

Havenhand, Jon. N. 1991. "Fertilisation and the Potential for Dispersal of Gametes and Larvae in the Solitary Ascidian *Ascidia Mentula* Müller." *Ophelia* 33 (1): 01–15. https://doi.org/10.1080/00785326.1991.10429738.

Haworth, Kim E., Surendra Kotecha, Timothy J. Mohun, and Branko V. Latinkic. 2008. "GATA4 and GATA5 Are Essential for Heart and Liver Development in Xenopusembryos." *BMC Developmental Biology* 8 (1): 74. https://doi.org/10.1186/1471-213X-8-74.

Heisenberg, Carl-Philipp, and Lilianna Solnica-Krezel. 2008. "Back and Forth between Cell Fate Specification and Movement during Vertebrate Gastrulation." *Pattern Formation and Developmental Mechanisms* 18 (4): 311–16. https://doi.org/10.1016/j.gde.2008.07.011.

Hendin, Noam, Tal Gordon, Noa Shenkar, and Omri Wurtzel. 2022. "Molecular Characterization of the Immediate Wound Response of the Solitary Ascidian *POLYCARPA MYTILIGERA* ." *Developmental Dynamics* 251 (12): 1968–81. https://doi.org/10.1002/dvdy.526.

Henry, Lea-Anne, and Michael Hart. 2005. "Regeneration from Injury and Resource Allocation in Sponges and Corals–a Review." *International Review of Hydrobiology: A Journal Covering All Aspects of Limnology and Marine Biology* 90 (2): 125–58.

Hiebert, Laurel S., Marta Scelzo, Alexandre Alié, Anthony W. De Tomaso, Federico D. Brown, and Stefano Tiozzo. 2022. "Comparing Dormancy in Two Distantly Related Tunicates Reveals Morphological, Molecular, and Ecological Convergences and Repeated Co-Option." *Scientific Reports* 12 (1): 12620. https://doi.org/10.1038/s41598-022-16656-8.

Hiebert, Laurel S., Carl Simpson, and Stefano Tiozzo. 2021. "Coloniality, Clonality, and Modularity in Animals: The Elephant in the Room." *Journal of Experimental Zoology Part B: Molecular and Developmental Evolution* 336 (3): 198–211. https://doi.org/10.1002/jez.b.22944.

Hiebert, Laurel Sky, Edson A Vieira, Gustavo M Dias, Stefano Tiozzo, and Federico D Brown. 2019. "Colonial Ascidians Strongly Preyed upon, yet Dominate the Substrate in a Subtropical Fouling Community."

Hill, Susan Douglas. 1970. “Origin of the Regeneration Blastema in Polychaete Annelids.” *American Zoologist* 10 (2): 101–12. https://doi.org/10.1093/icb/10.2.101.

Hirokawa, Nobutaka, Yosuke Tanaka, Yasushi Okada, and Sen Takeda. 2006. “Nodal Flow and the Generation of Left-Right Asymmetry.” *Cell* 125 (1): 33–45. https://doi.org/10.1016/j.cell.2006.03.002.

Hisata, Kanako, S. Fujiwara, Yuko Tsuchida, M. Ohashi, and Kazuo Kawamura. 1998. “Expression and Function of a Retinoic Acid Receptor in Budding Ascidians.” *Development Genes and Evolution* 208 (10): 537–46. https://doi.org/10.1007/s004270050213.

Höck, Julia, and Gunter Meister. 2008. “The Argonaute Protein Family.” *Genome Biology* 9 (2): 210. https://doi.org/10.1186/gb-2008-9-2-210.

Holland, Linda Z. 2007. “A Chordate with a Difference.” *Nature* 447 (7141): 153–54. https://doi.org/10.1038/447153a.

———. 2016. “Tunicates.” *Current Biology* 26 (4): R146–52. https://doi.org/10.1016/j.cub.2015.12.024.

Holstein, T.W., E. Hobmayer, and U. Technau. 2003. “Cnidarians: An Evolutionarily Conserved Model System for Regeneration?” *Developmental Dynamics* 226 (2): 257–67. https://doi.org/10.1002/dvdy.10227.

Hosseini-Alghaderi, Samira, and Martin Baron. 2020. “Notch3 in Development, Health and Disease.” *Biomolecules* 10 (March): 485. https://doi.org/10.3390/biom10030485.

Hubert, Katharine A., and Deneen M. Wellik. 2023. “Hox Genes in Development and Beyond.” *Development* 150 (1): dev192476. https://doi.org/10.1242/dev.192476.

Hudson, Clare, Sonia Lotito, and Hitoyoshi Yasuo. 2007. “Sequential and Combinatorial Inputs from Nodal, Delta2/Notch and FGF/MEK/ERK Signalling Pathways Establish a Grid-like Organisation of Distinct Cell Identities in the Ascidian Neural Plate.”

Hudson, Clare, and Hitoyoshi Yasuo. 2005. “Patterning across the Ascidian Neural Plate by Lateral Nodal Signaling Sources.” *Development (Cambridge, England)* 132 (April): 1199–1210. https://doi.org/10.1242/dev.01688.

Huebner, Eric A., and Stephen M. Strittmatter. 2009. “Axon Regeneration in the Peripheral and Central Nervous Systems.” *Cell Biology of the Axon*, 305–60.

Hughes, R. N. 1987. “The Functional Ecology of Clonal Animals.” *Functional Ecology* 1 (1): 63–69. https://doi.org/10.2307/2389359.

———. 1989. *A Functional Biology of Clonal Animals*. Functional Biology Series. London ; New York: Chapman and Hall.

Hughes, S., and A. Woollard. 2017. “RUNX in Invertebrates.” In *RUNX Proteins in Development and Cancer*, edited by Yoram Groner, Yoshiaki Ito, Paul Liu, James C. Neil, Nancy A. Speck, and Andre van Wijnen, 3–18. Singapore: Springer Singapore. https://doi.org/10.1007/978-981-10-3233-2_1.

Hyams, Yosef, Julia Panov, Amalia Rosner, Leonid Brodsky, Yuval Rinkevich, and Baruch Rinkevich. 2022. “Transcriptome Landscapes That Signify Botrylloides Leachi (Ascidiacea) Torpor States.” *Developmental Biology* 490 (October): 22–36. https://doi.org/10.1016/j.ydbio.2022.06.005.

Hyams, Yosef, Guy Paz, Claudette Rabinowitz, and Baruch Rinkevich. 2017. “Insights into the Unique Torpor of Botrylloides Leachi, a Colonial Urochordate.” *Developmental Biology* 428 (1): 101–17. https://doi.org/10.1016/j.ydbio.2017.05.020.

Imai, Kaoru S., Kyosuke Hino, Kasumi Yagi, Nori Satoh, and Yutaka Satou. 2004. “Gene Expression Profiles of Transcription Factors and Signaling Molecules in the Ascidian Embryo: Towards a Comprehensive Understanding of Gene Networks.”

Ingham, Philip W., and Marysia Placzek. 2006. “Orchestrating Ontogenesis: Variations on a Theme by Sonic Hedgehog.” *Nature Reviews Genetics* 7 (11): 841–50. https://doi.org/10.1038/nrg1969.

Iwasaki, Keiji, Taeko Kimura, Kyoko Kinoshita, Toshiyuki Yamaguchi, Teruaki Nishikawa, Eijiroh Nishi, Ryohei Yamanishi, et al. 2004. “Human-Mediated Introduction and Dispersal of Marine Organisms in Japan: Results of a Questionnaire Survey by the Committee for the Preservation of the Natural Environment, the Japanese Association of Benthology.” *Japanese Journal of Benthology* 59 (January): 22–44. https://doi.org/10.5179/benthos.59.22.

Izquierdo-Muñoz, Andrés. 2009. “Recent Non-Indigenous Ascidians in the Mediterranean Sea.” *Aquatic Invasions* 4 (1): 59–64. https://doi.org/10.3391/ai.2009.4.1.5.

Jackson, Jeremy, and Terence Hughes. 1985. “Adaptive Strategies of Coral-Reef Invertebrates.” *American Scientist - AMER SCI* 73 (January): 265–73.

Jeays-Ward, Katherine, Christine Hoyle, Jennifer Brennan, Mathieu Dandonneau, Graham Alldus, Blanche Capel, and Amanda Swain. 2003. “Endothelial and Steroidogenic Cell Migration Are Regulated by WNT4 in the Developing Mammalian Gonad.” *Development* 130 (16): 3663–70. https://doi.org/10.1242/dev.00591.

Jeffery, William R., and Billie J. Swalla. 1992. “Evolution of Alternate Modes of Development in Ascidians.” *BioEssays* 14 (4): 219–26. https://doi.org/10.1002/bies.950140404.

Jenner, Ronald A., and Matthew A. Wills. 2007. “The Choice of Model Organisms in Evo–Devo.” *Nature Reviews Genetics* 8 (4): 311–14. https://doi.org/10.1038/nrg2062.

Jiang, Di, and William C. Smith. 2005. “Self- and Cross-Fertilization in the Solitary Ascidian *Ciona Savignyi*.” *The Biological Bulletin* 209 (2): 107–12. https://doi.org/10.2307/3593128.

Jopling, Chris, Stephanie Boue, and Juan Carlos Izpisua Belmonte. 2011. “Dedifferentiation, Transdifferentiation and Reprogramming: Three Routes to

Regeneration." *Nature Reviews Molecular Cell Biology* 12 (2): 79–89. https://doi.org/10.1038/nrm3043.

Jopling, Chris, Eduard Sleep, Marina Raya, Mercè Martí, Angel Raya, and Juan Carlos Izpisúa Belmonte. 2010. "Zebrafish Heart Regeneration Occurs by Cardiomyocyte Dedifferentiation and Proliferation." *Nature* 464 (7288): 606–9. https://doi.org/10.1038/nature08899.

Joukov, Vladimir, Arja Kaipainen, Michael Jeltsch, Katri Pajusola, Birgitta Olofsson, Vijay Kumar, Ulf Eriksson, and Kari Alitalo. 1997. "Vascular Endothelial Growth Factors VEGF-B and VEGF-C." *Journal of Cellular Physiology* 173 (2): 211–15.

Kamachi, Yusuke, Masanori Uchikawa, Aki Tanouchi, Ryohei Sekido, and Hisato Kondoh. 2001. "Pax6 and SOX2 Form a Co-DNA-Binding Partner Complex That Regulates Initiation of Lens Development." *Genes & Development* 15 (10): 1272–86. https://doi.org/10.1101/gad.887101.

Kaneko, Nagamoto, You Katsuyama, Kazuo Kawamura, and Shigeki Fujiwara. 2010. "Regeneration of the Gut Requires Retinoic Acid in the Budding Ascidian Polyandrocarpa Misakiensis: Regeneration of Ascidians." *Development, Growth & Differentiation* 52 (5): 457–68. https://doi.org/10.1111/j.1440-169X.2010.01184.x.

Kang, HyunJun, Walatta-Tseyon Mesquitta, Ho Sun Jung, Oleg V. Moskvin, James A. Thomson, and Igor I. Slukvin. 2018. "GATA2 Is Dispensable for Specification of Hemogenic Endothelium but Promotes Endothelial-to-Hematopoietic Transition." *Stem Cell Reports* 11 (1): 197–211. https://doi.org/10.1016/j.stemcr.2018.05.002.

Kardong, Kenneth V. 2019. *Vertebrates: Comparative Anatomy, Function, Evolution*. Eighth edition. New York, NY: McGraw-Hill Education.

Kassmer, Susannah H., Adam D. Langenbacher, and Anthony W. De Tomaso. 2020. "Integrin-Alpha-6+ Candidate Stem Cells Are Responsible for Whole Body Regeneration in the Invertebrate Chordate Botrylloides Diegensis." *Nature Communications* 11 (1): 4435. https://doi.org/10.1038/s41467-020-18288-w.

Kassmer, Susannah H., Adam Langenbacher, and Anthony W. De Tomaso. 2019. "Integrin-Alpha-6+ Stem Cells (ISCs) Are Responsible for Whole Body Regeneration in an Invertebrate Chordate." Preprint. Developmental Biology. https://doi.org/10.1101/647578.

Katsumura, Koichi R., Charu Mehta, Kyle J. Hewitt, Alexandra A. Soukup, Isabela Fraga de Andrade, Erik A. Ranheim, Kirby D. Johnson, and Emery H. Bresnick. 2018. "Human Leukemia Mutations Corrupt but Do Not Abrogate GATA-2 Function." *Proceedings of the National Academy of Sciences* 115 (43): E10109–18. https://doi.org/10.1073/pnas.1813015115.

Kawamura, Kaz, and Takeshi Sunanaga. 2009. "Hemoblasts in Colonial Tunicates: Are They Stem Cells or Tissue-Restricted Progenitor Cells?: Hemoblasts in Colonial Tunicates." *Development, Growth & Differentiation* 52 (1): 69–76. https://doi.org/10.1111/j.1440-169X.2009.01142.x.

———. 2011. “Role of Vasa, Piwi, and Myc-Expressing Coelomic Cells in Gonad Regeneration of the Colonial Tunicate, Botryllus Primigenus.” *Mechanisms of Development* 128 (7): 457–70. https://doi.org/10.1016/j.mod.2011.09.001.

Kawamura, Kazuo, Yasuo Sugino, Takeshi Sunanaga, and Shigeki Fujiwara. 2007. “Multipotent Epithelial Cells in the Process of Regeneration and Asexual Reproduction in Colonial Tunicates: Multipotent Cells in Colonial Tunicates.” *Development, Growth & Differentiation* 50 (1): 1–11. https://doi.org/10.1111/j.1440-169X.2007.00972.x.

Kimelman, David, and Benjamin L. Martin. 2012. “Anterior-Posterior Patterning in Early Development: Three Strategies: Anterior-Posterior Patterning in Early Development.” *Wiley Interdisciplinary Reviews: Developmental Biology* 1 (2): 253–66. https://doi.org/10.1002/wdev.25.

Kostyuchenko, R. P., V. V. Kozin, and E. E. Kupriashova. 2016. “Regeneration and Asexual Reproduction in Annelids: Cells, Genes, and Evolution.” *Biology Bulletin* 43 (3): 185–94. https://doi.org/10.1134/S1062359016030067.

Kott, Patricia. 1989. “Form and Function in the Ascidiacea.” *BULLETIN OF MARINE SCIENCE* 45.

Kowarsky, Mark, Chiara Anselmi, Kohji Hotta, Paolo Burighel, Giovanna Zaniolo, Federico Caicci, Benyamin Rosental, et al. 2021. “Sexual and Asexual Development: Two Distinct Programs Producing the Same Tunicate.” *Cell Reports* 34 (4): 108681. https://doi.org/10.1016/j.celrep.2020.108681.

Kragl, Martin, Dunja Knapp, Eugen Nacu, Shahryar Khattak, Malcolm Maden, Hans Henning Epperlein, and Elly M. Tanaka. 2009. “Cells Keep a Memory of Their Tissue Origin during Axolotl Limb Regeneration.” *Nature* 460 (7251): 60–65.

Kramer, Ina, Markus Sigrist, Joriene C. de Nooij, Ichiro Taniuchi, Thomas M. Jessell, and Silvia Arber. 2006. “A Role for Runx Transcription Factor Signaling in Dorsal Root Ganglion Sensory Neuron Diversification.” *Neuron* 49 (3): 379–93. https://doi.org/10.1016/j.neuron.2006.01.008.

Kucerova, Romana, Natalie Dorà, Richard L Mort, Karen Wallace, Lucy J Leiper, Christina Lowes, Carlos Neves, et al. 2012. “Interaction between Hedgehog Signalling and PAX6 Dosage Mediates Maintenance and Regeneration of the Corneal Epithelium.” *Molecular Vision*.

Kühl, Michael, Laird C Sheldahl, Maiyon Park, Jeffrey R Miller, and Randall T Moon. 2000. “The Wnt/Ca2+ Pathway: A New Vertebrate Wnt Signaling Pathway Takes Shape.” *Trends in Genetics* 16 (7): 279–83. https://doi.org/10.1016/S0168-9525(00)02028-X.

Kumar, M P Santhosh, and T. Nandhini. 2018. “Mechanism of Action of Bone Morphogenic Protein 3 in the Maintenance of Tissue Homeostasis.” *Research Journal of Pharmacy and Technology* 11 (January): 1270. https://doi.org/10.5958/0974-360X.2018.00236.6.

Kumar, V., S. A. Bustin, and I. A. McKay. 1995. “Transforming Growth Factor Alpha.” *Cell Biology International* 19 (5): 373–88.

Laflamme, Michael A., and Charles E. Murry. 2011. “Heart Regeneration.” *Nature* 473 (7347): 326–35.

Laird, Diana J., Anthony W. De Tomaso, and Irving L. Weissman. 2005. “Stem Cells Are Units of Natural Selection in a Colonial Ascidian.” *Cell* 123 (7): 1351–60. https://doi.org/10.1016/j.cell.2005.10.026.

Lambert, C. C., and G. Lambert. 1998. “Non-Indigenous Ascidians in Southern California Harbors and Marinas.” *Marine Biology* 130 (4): 675–88. https://doi.org/10.1007/s002270050289.

Lambert, Cc, and G Lambert. 2003. “Persistence and Differential Distribution of Nonindigenous Ascidians in Harbors of the Southern California Bight.” *Marine Ecology Progress Series* 259: 145–61. https://doi.org/10.3354/meps259145.

Lambert, Gretchen. 2002. “Nonindigenous Ascidians in Tropical Waters.” *Pacific Science* 56 (3): 291–98. https://doi.org/10.1353/psc.2002.0026.

———. 2019. “Fouling Ascidians (Chordata: Ascidiacea) of the Galápagos: Santa Cruz and Baltra Islands.” *Aquatic Invasions* 14 (1): 132–49. https://doi.org/10.3391/ai.2019.14.1.05.

Lambert, Gretchen, Zen Faulkes, Charles C Lambert, and Virginia L Scofield. 2005. “Ascidians of South Padre Island, Texas, with a Key to Species.” *THE TEXAS JOURNAL OF SCIENCE* 57 (3).

Langenbacher, Adam D., Delany Rodriguez, Alessandro Di Maio, and Anthony W. De Tomaso. 2015. “Whole-Mount Fluorescent in Situ Hybridization Staining of the Colonial Tunicate Botryllus Schlosseri.” *Genesis* 53 (1): 194–201. https://doi.org/10.1002/dvg.22820.

Laron, Z. 2001. “Insulin-like Growth Factor 1 (IGF-1): A Growth Hormone.” *Molecular Pathology* 54 (5): 311. https://doi.org/10.1136/mp.54.5.311.

Lee, Jae Ho, Dorothea Schütte, Gerald Wulf, Laszlo Füzesi, Heinz-Joachim Radzun, Stephan Schweyer, Wolfgang Engel, and Karim Nayernia. 2006. “Stem-Cell Protein Piwil2 Is Widely Expressed in Tumors and Inhibits Apoptosis through Activation of Stat3/Bcl-XL Pathway.” *Human Molecular Genetics* 15 (2): 201–11.

Lee, Sung-Gwon, Dokyun Na, and Chungoo Park. 2021. “Comparability of Reference-Based and Reference-Free Transcriptome Analysis Approaches at the Gene Expression Level.” *BMC Bioinformatics* 22 (11): 310. https://doi.org/10.1186/s12859-021-04226-0.

Lemaire, Patrick. 2009. “Unfolding a Chordate Developmental Program, One Cell at a Time: Invariant Cell Lineages, Short-Range Inductions and Evolutionary Plasticity in Ascidians.” *Developmental Biology* 332 (1): 48–60. https://doi.org/10.1016/j.ydbio.2009.05.540.

Lemos, Manuel C., and Rajesh V. Thakker. 2020. “Hypoparathyroidism, Deafness, and Renal Dysplasia Syndrome: 20 Years after the Identification of the First GATA3 Mutations.” *Human Mutation* 41 (8): 1341–50. https://doi.org/10.1002/humu.24052.

Levine, Michael, and Eric H. Davidson. 2005. “Gene Regulatory Networks for Development.” *Proceedings of the National Academy of Sciences* 102 (14): 4936–42.

Li, Hanbo, Xiaoyu Wei, Li Zhou, Weiqi Zhang, Chen Wang, Yang Guo, Denghui Li, et al. 2021. “Dynamic Cell Transition and Immune Response Landscapes of Axolotl Limb Regeneration Revealed by Single-Cell Analysis.” *Protein & Cell* 12 (1): 57–66. https://doi.org/10.1007/s13238-020-00763-1.

Lim, Shu Ly, Enkhjargal Tsend-Ayush, R. Daniel Kortschak, Reuben Jacob, Carmela Ricciardelli, Martin K. Oehler, and Frank Grützner. 2013. “Conservation and Expression of PIWI-Interacting RNA Pathway Genes in Male and Female Adult Gonad of Amniotes1.” *Biology of Reproduction* 89 (6): 136, 1–13. https://doi.org/10.1095/biolreprod.113.111211.

Lindeyer, Frederike, and Adriaan Gittenberger. 2011. “Ascidians in the Succession of Marine Fouling Communities.” *Aquatic Invasions* 6 (4): 421–34. https://doi.org/10.3391/ai.2011.6.4.07.

Lins, Daniel M., Paulo De Marco, Andre F. A. Andrade, and Rosana M. Rocha. 2018. “Predicting Global Ascidian Invasions.” Edited by Hugh MacIsaac. *Diversity and Distributions* 24 (5): 692–704. https://doi.org/10.1111/ddi.12711.

Liu, Ting, Lingyun Zhang, Donghyun Joo, and Shao-Cong Sun. 2017. “NF-κB Signaling in Inflammation.” *Signal Transduction and Targeted Therapy* 2 (1): 17023. https://doi.org/10.1038/sigtrans.2017.23.

Lloyd, David G. 1980. “Benefits and Handicaps of Sexual Reproduction.” In *Evolutionary Biology: Volume 13*, edited by Max K. Hecht, William C. Steere, and Bruce Wallace, 69–111. Boston, MA: Springer US. https://doi.org/10.1007/978-1-4615-6962-6_2.

Locke, Andrea. 2009. “A Screening Procedure for Potential Tunicate Invaders of Atlantic Canada.” *Aquatic Invasions* 4 (1): 71–79. https://doi.org/10.3391/ai.2009.4.1.7.

López-Legentil, Susanna, Miquel L. Legentil, Patrick M. Erwin, and Xavier Turon. 2015. “Harbor Networks as Introduction Gateways: Contrasting Distribution Patterns of Native and Introduced Ascidians.” *Biological Invasions* 17 (6): 1623–38. https://doi.org/10.1007/s10530-014-0821-z.

Louvi, Angeliki, and Spyros Artavanis-Tsakonas. 2006. “Notch Signalling in Vertebrate Neural Development.” *Nature Reviews Neuroscience* 7 (2): 93–102. https://doi.org/10.1038/nrn1847.

Lowe, Andrew. 2002. “Microcosmus Squamiger, a Solitary Ascidian Introduced to Southern California Harbors and Marinas : Salinity Tolerance and Phylogenetic Analysis /,” January.

Luxardi, Guillaume, Leslie Marchal, Virginie Thomé, and Laurent Kodjabachian. 2010. “Distinct Xenopus Nodal Ligands Sequentially Induce Mesendoderm and Control Gastrulation Movements in Parallel to the Wnt/PCP Pathway.” *Development* 137 (3): 417–26. https://doi.org/10.1242/dev.039735.

Mace, Kimberly A., Scott L. Hansen, Connie Myers, David M. Young, and Nancy Boudreau. 2005. “HOXA3 Induces Cell Migration in Endothelial and Epithelial Cells Promoting Angiogenesis and Wound Repair.” *Journal of Cell Science* 118 (12): 2567–77.

Mackie, G. O. 1986. “From Aggregates to Integrates: Physiological Aspects of Modularity in Colonial Animals.” *Philosophical Transactions of the Royal Society of London. Series B, Biological Sciences* 313 (1159): 175–96.

Manni, Lucia, Chiara Anselmi, Francesca Cima, Fabio Gasparini, Ayelet Voskoboynik, Margherita Martini, Anna Peronato, Paolo Burighel, Giovanna Zaniolo, and Loriano Ballarin. 2019. “Sixty Years of Experimental Studies on the Blastogenesis of the Colonial Tunicate Botryllus Schlosseri.” *Developmental Biology* 448 (2): 293–308. https://doi.org/10.1016/j.ydbio.2018.09.009.

Manni, Lucia, Fabio Gasparini, Kohji Hotta, Katherine J. Ishizuka, Lorenzo Ricci, Stefano Tiozzo, Ayelet Voskoboynik, and Delphine Dauga. 2014. “Ontology for the Asexual Development and Anatomy of the Colonial Chordate Botryllus Schlosseri.” Edited by Hector Escriva. *PLoS ONE* 9 (5): e96434. https://doi.org/10.1371/journal.pone.0096434.

Marshall, Owen J., and Vincent R. Harley. 2000. “Molecular Mechanisms of SOX9 Action.” *Molecular Genetics and Metabolism* 71 (3): 455–62.

Martinez, Veronica G, Gus J Menger, and Mark J Zoran. 2005. “Regeneration and Asexual Reproduction Share Common Molecular Changes: Upregulation of a Neural Glycoepitope during Morphallaxis in Lumbriculus.” *Mech Dev* 122 (5): 721–32. https://doi.org/10.1016/j.mod.2004.12.003.

Matos, Irina, Amma Asare, John Levorse, Tamara Ouspenskaia, June Dela Cruz-Racelis, Laura-Nadine Schuhmacher, and Elaine Fuchs. 2020. “Progenitors Oppositely Polarize WNT Activators and Inhibitors to Orchestrate Tissue Development,” April. https://doi.org/10.7554/elife.54304.sa2.

Matsubara, Shin, Tomohiro Osugi, Akira Shiraishi, Azumi Wada, and Honoo Satake. 2021. “Comparative Analysis of Transcriptomic Profiles among Ascidians, Zebrafish, and Mice: Insights from Tissue-Specific Gene Expression.” *PLOS ONE* 16 (9): e0254308. https://doi.org/10.1371/journal.pone.0254308.

Melo, Diogo, Arthur Porto, James M. Cheverud, and Gabriel Marroig. 2016. “Modularity: Genes, Development, and Evolution.” *Annual Review of Ecology, Evolution, and Systematics* 47: 463–86.

Melo, Jimmy de, Xiangguo Qiu, Guoyan Du, Leah Cristante, and David D. Eisenstat. 2003. “Dlx1, Dlx2, Pax6, Brn3b, and Chx10 Homeobox Gene Expression Defines the Retinal Ganglion and Inner Nuclear Layers of the Developing and Adult Mouse Retina.” *Journal of Comparative Neurology* 461 (2): 187–204. https://doi.org/10.1002/cne.10674.

Mevel, Renaud, Julia E. Draper, Michael Lie-a-Ling, Valerie Kouskoff, and Georges Lacaud. 2019. “RUNX Transcription Factors: Orchestrators of Development.” *Development* 146 (17): dev148296. https://doi.org/10.1242/dev.148296.

Mieko Mizutani, Claudia, and Ethan Bier. 2008. “EvoD/Vo: The Origins of BMP Signalling in the Neuroectoderm.” *Nature Reviews Genetics* 9 (9): 663–77. https://doi.org/10.1038/nrg2417.

Millar, R.H. 1958. “Some Ascidians from Brazil.” *Annals and Magazine of Natural History* 1 (8): 497–514. https://doi.org/10.1080/00222935808650975.

Millar, Sarah E., Karl Willert, Patricia C. Salinas, Henk Roelink, Roel Nusse, Daniel J. Sussman, and Gregory S. Barsh. 1999. “WNT Signaling in the Control of Hair Growth and Structure.” *Developmental Biology* 207 (1): 133–49. https://doi.org/10.1006/dbio.1998.9140.

Miyazono, Kohei. 2000. “Positive and Negative Regulation of TGF-Beta Signaling.” *Journal of Cell Science* 113 (7): 1101–9.

Monniot, Françoise. 2016. “A New Species of Polyandrocarpa (Ascidiacea, Styelidae) in the Mediterranean Sea.” *Zootaxa* 4132 (1): 87. https://doi.org/10.11646/zootaxa.4132.1.7.

———. 2018. “Ascidians Collected during the Madibenthos Expedition in Martinique: 2. Stolidobranchia, Styelidae.” *Zootaxa* 4410 (2): 291. https://doi.org/10.11646/zootaxa.4410.2.3.

Monsoro-Burq, Anne H. 2015. “PAX Transcription Factors in Neural Crest Development.” In *Seminars in Cell & Developmental Biology*, 44:87–96. Elsevier.

Morgan, T. H. 1898. “REGENERATION AND LIABILITY TO INJURY.” *Zoological Bulletin* 1 (6): 287–300. https://doi.org/10.2307/1535478.

Morgan, Thomas Hunt. 1901. *Regeneration*. New York: The Macmillan Company. https://www.biodiversitylibrary.org/bibliography/87895.

Morrisey, Edward E., Zhihua Tang, Kirsten Sigrist, Min Min Lu, Fang Jiang, Hon S. Ip, and Michael S. Parmacek. 1998. “GATA6 Regulates HNF4 and Is Required for Differentiation of Visceral Endoderm in the Mouse Embryo.” *Genes & Development* 12 (22): 3579–90. https://doi.org/10.1101/gad.12.22.3579.

Müller, Thomas, Henning Brohmann, Alessandra Pierani, Paul A. Heppenstall, Gary R. Lewin, Thomas M. Jessell, and Carmen Birchmeier. 2002. “The Homeodomain Factor Lbx1 Distinguishes Two Major Programs of Neuronal Differentiation in the Dorsal Spinal Cord.” *Neuron* 34 (4): 551–62.

Muraoka, Osamu, Takashi Shimizu, Taijiro Yabe, Hideaki Nojima, Young-Ki Bae, Hisashi Hashimoto, and Masahiko Hibi. 2006. “Sizzled Controls Dorso-Ventral Polarity by Repressing Cleavage of the Chordin Protein.” *Nature Cell Biology* 8 (4): 329–40.

Murawala, Prayag, Elly M Tanaka, and Joshua D Currie. 2012. “Regeneration: The Ultimate Example of Wound Healing.” *Semin Cell Dev Biol* 23 (9): 954–62. https://doi.org/10.1016/j.semcdb.2012.09.013.

Nagar, Lilach, and Noa Shenkar. 2016. “Temperature and Salinity Sensitivity of the Invasive Ascidian Microcosmus Exasperatus Heller, 1878.” *Aquatic Invasions* 11 (1): 33–43. https://doi.org/10.3391/ai.2016.11.1.04.

Nagarajan, Rakesh, John Svaren, Nam Le, Toshiyuki Araki, Mark Watson, and Jeffrey Milbrandt. 2001. “EGR2 Mutations in Inherited Neuropathies Dominant-Negatively Inhibit Myelin Gene Expression.” *Neuron* 30 (June): 355–68. https://doi.org/10.1016/S0896-6273(01)00282-3.

Nakashima, Keisuke, Lixy Yamada, Yutaka Satou, Jun-ichi Azuma, and Nori Satoh. 2004. “The Evolutionary Origin of Animal Cellulose Synthase.” *Development Genes and Evolution* 214 (2): 81–88. https://doi.org/10.1007/s00427-003-0379-8.

Nakauchi, MITSUAKI. 1982. “Asexual Development of Ascidians: Its Biological Significance, Diversity, and Morphogenesis.” *American Zoologist* 22 (4): 753–63. https://doi.org/10.1093/icb/22.4.753.

Newman, Stuart A., and Ramray Bhat. 2009. “Dynamical Patterning Modules: A" Pattern Language" for Development and Evolution of Multicellular Form.” *International Journal of Developmental Biology* 53 (5–6): 693–705.

Nichols, Claire L., Gretchen Lambert, and Marie L. Nydam. 2023. “Continued Persistence of Non-Native Ascidians in Southern California Harbors and Marinas.” *Aquatic Invasions* 18 (1): 1–22. https://doi.org/10.3391/ai.2023.18.1.101962.

Nijjar, Sarbjit S., Lorraine Wallace, Heather A. Crosby, Stefan G. Hubscher, and Alastair J. Strain. 2002. “Altered Notch Ligand Expression in Human Liver Disease: Further Evidence for a Role of the Notch Signaling Pathway in Hepatic Neovascularization and Biliary Ductular Defects.” *The American Journal of Pathology* 160 (5): 1695–1703. https://doi.org/10.1016/S0002-9440(10)61116-9.

Nourizadeh, Shane, Susannah Kassmer, Delany Rodriguez, Laurel S. Hiebert, and Anthony W. De Tomaso. 2021. “Whole Body Regeneration and Developmental Competition in Two Botryllid Ascidians.” *EvoDevo* 12 (1): 15. https://doi.org/10.1186/s13227-021-00185-y.

Nusse, Roel. 2005. “Wnt Signaling in Disease and in Development.” *Cell Research* 15 (1): 28–32. https://doi.org/10.1038/sj.cr.7290260.

Odland, George, and Russell Ross. 1968. “Human Wound Repair: I. Epidermal Regeneration.” *The Journal of Cell Biology* 39 (1): 135–51.

Ogasawara, Michio, Roberto Di Lauro, and Nori Satoh. 1999. “Ascidian Homologs of Mammalian Thyroid Peroxidase Genes Are Expressed in the Thyroid-Equivalent Region of the Endostyle.” *Journal of Experimental Zoology* 285 (2): 158–69. https://doi.org/10.1002/(SICI)1097-010X(19990815)285:2<158::AID-JEZ8>3.0.CO;2-0.

Oomen, Rebekah A., Halvor Knutsen, Esben M. Olsen, Sissel Jentoft, Nils Chr. Stenseth, and Jeffrey A. Hutchings. 2022. “Comparison of de Novo</Em> and Reference Genome-Based Transcriptome Assembly Pipelines for Differential Expression Analysis of RNA Sequencing Data.” *bioRxiv*, January, 2022.08.20.504634. https://doi.org/10.1101/2022.08.20.504634.

Otani, Michio. 2002. “Appearance and Latest Trends of Introduced Marine Sessile Animals in Japanese Waters.” *Sessile Org* 19 (January): 69–92. https://doi.org/10.4282/sosj.19.69.

Otto, Joann J., and Richard D. Campbell. 1977. “Budding inHydra Attenuata: Bud Stages and Fate Map.” *Journal of Experimental Zoology* 200 (3): 417–28. https://doi.org/10.1002/jez.1402000311.

Otto, Sarah P., and Thomas Lenormand. 2002. “Resolving the Paradox of Sex and Recombination.” *Nature Reviews Genetics* 3 (4): 252–61. https://doi.org/10.1038/nrg761.

Pan, Yong, Chunyang Brian Bai, Alexandra L. Joyner, and Baolin Wang. 2006. “Sonic Hedgehog Signaling Regulates Gli2 Transcriptional Activity by Suppressing Its Processing and Degradation.” *Molecular and Cellular Biology* 26 (9): 3365–77.

Parks, Annette L., Kristin M. Klueg, Jane R. Stout, and Marc AT Muskavitch. 2000. “Ligand Endocytosis Drives Receptor Dissociation and Activation in the Notch Pathway.” *Development* 127 (7): 1373–85.

Pasini, Andrea, Aldine Amiel, Ute Rothbächer, Agnès Roure, Patrick Lemaire, and Sébastien Darras. 2006. “Formation of the Ascidian Epidermal Sensory Neurons: Insights into the Origin of the Chordate Peripheral Nervous System.” *PLOS Biology* 4 (7): e225. https://doi.org/10.1371/journal.pbio.0040225.

Patient, Roger K, and James D McGhee. 2002. “The GATA Family (Vertebrates and Invertebrates).” *Current Opinion in Genetics & Development* 12 (4): 416–22. https://doi.org/10.1016/S0959-437X(02)00319-2.

Pellegrinet, Luca, Veronica Rodilla Benito, Zhenyi Liu, Shuang Chen, Ute Koch, Lluis Espinosa, Klaus Kaestner, Raphael Kopan, Julian Lewis, and Freddy Radtke. 2011. “Dll1- and Dll4-Mediated Notch Signaling Are Required for Homeostasis of Intestinal Stem Cells.” *Gastroenterology* 140 (April): 1230-1240.e1. https://doi.org/10.1053/j.gastro.2011.01.005.

Pellettieri, Jason. 2019. “Regenerative Tissue Remodeling in Planarians – The Mysteries of Morphallaxis.” *Seminars in Cell & Developmental Biology* 87 (March): 13–21. https://doi.org/10.1016/j.semcdb.2018.04.004.

Perkins, Rachel S., Sarocha Suthon, Gustavo A. Miranda-Carboni, and Susan A. Krum. 2022. “WNT5B in Cellular Signaling Pathways.” *Special Issue: Interplay between Non-Canonical and Canonical Wnt Signalling by Terry Van Raay/ Special Issue: The Making of Memories by Patricio Opazo and Victor Anggono* 125 (May): 11–16. https://doi.org/10.1016/j.semcdb.2021.09.019.

Petersen, J., and I. Svane. 2002. “Filtration Rate in Seven Scandinavian Ascidians: Implications of the Morphology of the Gill Sac.” *Marine Biology* 140 (2): 397–402. https://doi.org/10.1007/s002270100706.

Petersen, Jens Kjerulf. 2007. “Ascidian Suspension Feeding.” *Journal of Experimental Marine Biology and Ecology* 342 (1): 127–37. https://doi.org/10.1016/j.jembe.2006.10.023.

Pineda, Mari Carmen, Xavier Turon, and Susanna López-Legentil. 2012. “Stress Levels over Time in the Introduced Ascidian Styela Plicata: The Effects of

Temperature and Salinity Variations on Hsp70 Gene Expression." *Cell Stress and Chaperones* 17 (4): 435–44. https://doi.org/10.1007/s12192-012-0321-y.

Platin, Raz, and Noa Shenkar. 2023. "Can Stand the Heat – Ecology of the Potentially Invasive Ascidian Styela Plicata along the Mediterranean Coast of Israel." *Frontiers in Marine Science* 10 (April): 1159231. https://doi.org/10.3389/fmars.2023.1159231.

Pogoda, Hans-Martin, Lilianna Solnica-Krezel, Wolfgang Driever, and Dirk Meyer. 2000. "The Zebrafish Forkhead Transcription Factor FoxH1/Fast1 Is a Modulator of Nodal Signaling Required for Organizer Formation." *Current Biology* 10 (17): 1041–49. https://doi.org/10.1016/S0960-9822(00)00669-2.

Poss, Kenneth D. 2010. "Advances in Understanding Tissue Regenerative Capacity and Mechanisms in Animals." *Nature Reviews Genetics* 11 (10): 710–22. https://doi.org/10.1038/nrg2879.

Powers, Shannon E., Kenichiro Taniguchi, Weiwei Yen, Tiffany A. Melhuish, Jun Shen, Christopher A. Walsh, Ann E. Sutherland, and David Wotton. 2010. "Tgif1 and Tgif2 Regulate Nodal Signaling and Are Required for Gastrulation." *Development* 137 (2): 249–59.

Price, J., and S. Allen. 2004. "Exploring the Mechanisms Regulating Regeneration of Deer Antlers." Edited by J. P. Brockes and P. Martin. *Philosophical Transactions of the Royal Society of London. Series B: Biological Sciences* 359 (1445): 809–22. https://doi.org/10.1098/rstb.2004.1471.

Prünster, Maria Mandela, Lorenzo Ricci, Federico D Brown, and Stefano Tiozzo. 2019a. "De Novo Neurogenesis in a Budding Chordate: Co-Option of Larval Anteroposterior Patterning Genes in a Transitory Neurogenic Organ." *Current Directions in Tunicate Development* 448 (2): 342–52. https://doi.org/10.1016/j.ydbio.2018.10.009.

Prünster, Maria Mandela, Lorenzo Ricci, Federico D. Brown, and Stefano Tiozzo. 2019b. "Modular Co-Option of Cardiopharyngeal Genes during Non-Embryonic Myogenesis." *EvoDevo* 10 (1): 3. https://doi.org/10.1186/s13227-019-0116-7.

Ragkousi, Katerina, Jeni Beh, Sarah Sweeney, Ella Starobinska, and Brad Davidson. 2011. "A Single GATA Factor Plays Discrete, Lineage Specific Roles in Ascidian Heart Development." *Developmental Biology* 352 (1): 154–63. https://doi.org/10.1016/j.ydbio.2011.01.007.

Ramalhosa, Patrício, Ignacio Gestoso, Rosana M. Rocha, Gretchen Lambert, and João Canning-Clode. 2021. "Ascidian Biodiversity in the Shallow Waters of the Madeira Archipelago: Fouling Studies on Artificial Substrates and New Records." *Regional Studies in Marine Science* 43 (March): 101672. https://doi.org/10.1016/j.rsma.2021.101672.

Ramsdell, Fred, and Steven F. Ziegler. 2014. "FOXP3 and Scurfy: How It All Began." *Nature Reviews Immunology* 14 (5): 343–49.

Reya, Tannishtha, and Hans Clevers. 2005. "Wnt Signalling in Stem Cells and Cancer." *Nature* 434 (7035): 843–50. https://doi.org/10.1038/nature03319.

Ricci, Lorenzo, Fabien Cabrera, Sonia Lotito, and Stefano Tiozzo. 2016. “Redeployment of Germ Layers Related TFs Shows Regionalized Expression during Two Non-Embryonic Developments.” *Developmental Biology* 416 (1): 235–48. https://doi.org/10.1016/j.ydbio.2016.05.016.

Ricci, Lorenzo, Ankita Chaurasia, Pascal Lapébie, Philippe Dru, Rebecca R. Helm, Richard R. Copley, and Stefano Tiozzo. 2016. “Identification of Differentially Expressed Genes from Multipotent Epithelia at the Onset of an Asexual Development.” *Scientific Reports* 6 (1): 27357. https://doi.org/10.1038/srep27357.

Ricci, Lorenzo, Bastien Salmon, Caroline Olivier, Rita Andreoni-Pham, Ankita Chaurasia, Alexandre Alié, and Stefano Tiozzo. 2022. “The Onset of Whole-Body Regeneration in Botryllus Schlosseri: Morphological and Molecular Characterization.” *Frontiers in Cell and Developmental Biology* 10 (February): 843775. https://doi.org/10.3389/fcell.2022.843775.

Rinkevich, Yuval, Baruch Rinkevich, and Ram Reshef. 2008. “Cell Signaling and Transcription Factor Genes Expressed during Whole Body Regeneration in a Colonial Chordate.” *BMC Developmental Biology* 8 (1): 100. https://doi.org/10.1186/1471-213X-8-100.

Rinkevich, Yuval, Amalia Rosner, Claudette Rabinowitz, Ziva Lapidot, Elithabeth Moiseeva, and Buki Rinkevich. 2010. “Piwi Positive Cells That Line the Vasculature Epithelium, Underlie Whole Body Regeneration in a Basal Chordate.” *Developmental Biology* 345 (1): 94–104. https://doi.org/10.1016/j.ydbio.2010.05.500.

Rocha, Rm, Gc Castellano, and Ca Freire. 2017. “Physiological Tolerance as a Tool to Support Invasion Risk Assessment of Tropical Ascidians.” *Marine Ecology Progress Series* 577 (August): 105–19. https://doi.org/10.3354/meps12225.

Rodriguez, Delany, Erin N. Sanders, Kelsea Farell, Adam D. Langenbacher, Daryl A. Taketa, Michelle Rae Hopper, Morgan Kennedy, Andrew Gracey, and Anthony W. De Tomaso. 2014. “Analysis of the Basal Chordate Botryllus Schlosseri Reveals a Set of Genes Associated with Fertility.” *BMC Genomics* 15 (1): 1183. https://doi.org/10.1186/1471-2164-15-1183.

Rosner, Amalia, Elizabeth Moiseeva, Claudette Rabinowitz, and Baruch Rinkevich. 2013. “Germ Lineage Properties in the Urochordate Botryllus Schlosseri – From Markers to Temporal Niches.” *Developmental Biology* 384 (2): 356–74. https://doi.org/10.1016/j.ydbio.2013.10.002.

Rothbächer, Ute, Vincent Bertrand, Clement Lamy, and Patrick Lemaire. 2007. “A Combinatorial Code of Maternal GATA, Ets and β-Catenin-TCF Transcription Factors Specifies and Patterns the Early Ascidian Ectoderm.” *Development* 134 (22): 4023–32. https://doi.org/10.1242/dev.010850.

Salazar-ciudad, Isaac, and Jukka Jernvall. 2004. “How Different Types of Pattern Formation Mechanisms Affect the Evolution of Form and Development.” *Evolution & Development* 6 (1): 6–16. https://doi.org/10.1111/j.1525-142X.2004.04002.x.

Salvador-Martínez, Irepan, and Isaac Salazar-Ciudad. 2015. “How Complexity Increases in Development: An Analysis of the Spatial–Temporal Dynamics of 1218 Genes in Drosophila Melanogaster.” *Developmental Biology* 405 (2): 328–39. https://doi.org/10.1016/j.ydbio.2015.07.003.

Sánchez-Duffhues, Gonzalo, Christian Hiepen, Petra Knaus, and Peter Dijke. 2015. “Bone Morphogenetic Protein Signaling in Bone Homeostasis.” *Bone* 80 (June). https://doi.org/10.1016/j.bone.2015.05.025.

Sasakura, Yasunori, and Akiko Hozumi. 2018. “Formation of Adult Organs through Metamorphosis in Ascidians.” *WIREs Developmental Biology* 7 (2). https://doi.org/10.1002/wdev.304.

Scelzo, Marta, Alexandre Alié, Sophie Pagnotta, Camille Lejeune, Pauline Henry, Laurent Gilletta, Laurel S. Hiebert, Francesco Mastrototaro, and Stefano Tiozzo. 2019. “Novel Budding Mode in Polyandrocarpa Zorritensis: A Model for Comparative Studies on Asexual Development and Whole Body Regeneration.” *EvoDevo* 10 (1): 7. https://doi.org/10.1186/s13227-019-0121-x.

Schubert, Frank R., Roy C. Mootoosamy, Esther H. Walters, Anthony Graham, Loretta Tumiotto, Andrea E. Münsterberg, Andrew Lumsden, and Susanne Dietrich. 2002. “Wnt6 Marks Sites of Epithelial Transformations in the Chick Embryo.” *Mechanisms of Development* 114 (1–2): 143–48.

Shackelford, Todd K, and Viviana A Weekes-Shackelford, eds. 2021. *Encyclopedia of Evolutionary Psychological Science*. Cham: Springer International Publishing. https://doi.org/10.1007/978-3-319-19650-3.

Sharma, Garima, Ashish Ranjan Sharma, Eun-Min Seo, and Ju-Suk Nam. 2015. “Genetic Polymorphism in Extracellular Regulators of Wnt Signaling Pathway.” Edited by Andrei Surguchov. *BioMed Research International* 2015 (April): 847529. https://doi.org/10.1155/2015/847529.

Shenkar, N., and Y. Loya. 2008. “The Solitary Ascidian Herdmania Momus: Native (Red Sea) versus Non-Indigenous (Mediterranean) Populations.” *Biological Invasions* 10 (8): 1431–39. https://doi.org/10.1007/s10530-008-9217-2.

Shenkar, Noa, and Billie J. Swalla. 2011. “Global Diversity of Ascidiacea.” Edited by Howard Browman. *PLoS ONE* 6 (6): e20657. https://doi.org/10.1371/journal.pone.0020657.

Shimeld, Sebastian M., Bernard Degnan, and Graham N. Luke. 2010. “Evolutionary Genomics of the Fox Genes: Origin of Gene Families and the Ancestry of Gene Clusters.” *Genomics* 95 (5): 256–60.

Sibly, Richard, and Peter Calow. 1982. “Asexual Reproduction in Protozoa and Invertebrates.” *Journal of Theoretical Biology* 96 (3): 401–24. https://doi.org/10.1016/0022-5193(82)90118-7.

Simeone, Antonio, Dario Acampora, Antonio Mallamaci, Anna Stornaiuolo, M. Rosaria D’Apice, Vincenzo Nigro, and E. Boncinelli. 1993. “A Vertebrate Gene Related to Orthodenticle Contains a Homeodomain of the Bicoid Class and Demarcates Anterior Neuroectoderm in the Gastrulating Mouse Embryo.” *The EMBO Journal* 12 (7): 2735–47.

Sims, Linda L. 1984. “OSMOREGULATORY CAPABILITIES OF THREE MACROSYMPATRIC.”

Sinigaglia, Chiara, Alexandre Alié, and Stefano Tiozzo. 2022. “The Hazards of Regeneration: From Morgan’s Legacy to Evo-Devo.” In *Whole-Body Regeneration*, edited by Simon Blanchoud and Brigitte Galliot, 2450:3–25. Methods in Molecular Biology. New York, NY: Springer US. https://doi.org/10.1007/978-1-0716-2172-1_1.

Sinigaglia, Chiara, Alba Almazán, Marie Lebel, Marie Sémon, Benjamin Gillet, Sandrine Hughes, Eric Edsinger, Michalis Averof, and Mathilde Paris. 2022. “Distinct Gene Expression Dynamics in Developing and Regenerating Crustacean Limbs.” *Proceedings of the National Academy of Sciences* 119 (27): e2119297119. https://doi.org/10.1073/pnas.2119297119.

Slack, Jonathan Mw. 2017. “Animal Regeneration: Ancestral Character or Evolutionary Novelty?” *EMBO Reports* 18 (9): 1497–1508. https://doi.org/10.15252/embr.201643795.

Smidt, Marten P., Simone M. Smits, and J. Peter H. Burbach. 2004. “Homeobox Gene Pitx3 and Its Role in the Development of Dopamine Neurons of the Substantia Nigra.” *Cell and Tissue Research* 318 (1): 35–43.

Sommer, Ralf J. 2009. “The Future of Evo–Devo: Model Systems and Evolutionary Theory.” *Nature Reviews Genetics* 10 (6): 416–22. https://doi.org/10.1038/nrg2567.

Song, Yixian, Stefan Scheu, and Barbara Drossel. 2011. “Geographic Parthenogenesis in a Consumer-Resource Model for Sexual Reproduction.” *Journal of Theoretical Biology* 273 (1): 55–62. https://doi.org/10.1016/j.jtbi.2010.12.020.

Sood, Pranidhi, Athena Lin, Connie Yan, Rebecca McGillivary, Ulises Diaz, Tatyana Makushok, Ambika V Nadkarni, Sindy Ky Tang, and Wallace F Marshall. 2022. “Modular, Cascade-like Transcriptional Program of Regeneration in Stentor.” *eLife* 11 (August): e80778. https://doi.org/10.7554/eLife.80778.

Srivastava, Mansi. 2021. “Beyond Casual Resemblances: Rigorous Frameworks for Comparing Regeneration Across Species.”

Steventon, Ben, Claudio Araya, Claudia Linker, Sei Kuriyama, and Roberto Mayor. 2009. “Differential Requirements of BMP and Wnt Signalling during Gastrulation and Neurulation Define Two Steps in Neural Crest Induction.” *Development* 136 (5): 771–79. https://doi.org/10.1242/dev.029017.

Stolfi, Alberto, and Federico D. Brown. 2015. “Tunicata.” In *Evolutionary Developmental Biology of Invertebrates 6*, edited by Andreas Wanninger, 135–204. Vienna: Springer Vienna. https://doi.org/10.1007/978-3-7091-1856-6_4.

Streit, Olivia T., Gretchen Lambert, Patrick M. Erwin, and Susanna López-Legentil. 2021. “Diversity and Abundance of Native and Non-Native Ascidians in Puerto Rican Harbors and Marinas.” *Marine Pollution Bulletin* 167 (June): 112262. https://doi.org/10.1016/j.marpolbul.2021.112262.

Stuhlmiller, Timothy J., and Martín I. García-Castro. 2012. “Current Perspectives of the Signaling Pathways Directing Neural Crest Induction.” *Cellular and Molecular Life Sciences* 69 (22): 3715–37. https://doi.org/10.1007/s00018-012-0991-8.

Subramoniam, Thanumalaya. 2018. “Mode of Reproduction: Invertebrate Animals.” In *Encyclopedia of Reproduction*, 32–40. Elsevier. https://doi.org/10.1016/B978-0-12-809633-8.20533-5.

Sullivan, James C., Daniel Sher, Miriam Eisenstein, Katsuya Shigesada, Adam M. Reitzel, Heather Marlow, Ditsa Levanon, Yoram Groner, John R. Finnerty, and Uri Gat. 2008. “The Evolutionary Origin of the Runx/CBFbeta Transcription Factors – Studies of the Most Basal Metazoans.” *BMC Evolutionary Biology* 8 (1): 228. https://doi.org/10.1186/1471-2148-8-228.

Sun, Jiahe, Fang Lu, Yongjiang Luo, Lingzi Bie, Ling Xu, and Yi Wang. 2023. “OrthoVenn3: An Integrated Platform for Exploring and Visualizing Orthologous Data across Genomes.” *Nucleic Acids Research* 51 (W1): W397–403. https://doi.org/10.1093/nar/gkad313.

Sunanaga, Takeshi, Hironori Inubushi, and Kazuo Kawamura. 2010. “Piwi-Expressing Hemoblasts Serve as Germline Stem Cells during Postembryonic Germ Cell Specification in Colonial Ascidian, Botryllus Primigenus.” *Development, Growth & Differentiation* 52 (7): 603–14. https://doi.org/10.1111/j.1440-169X.2010.01196.x.

Suzuki, Makoto, Nayuta Yakushiji, Yasuaki Nakada, Akira Satoh, Hiroyuki Ide, and Koji Tamura. 2006. “Limb Regeneration in Xenopus Laevis Froglet.” *The Scientific World Journal* 6: 26–37.

Svane, Ib, and Craig M. Young. 1989. “The Ecology and Behaviour of Ascidian Larvae.” *Oceanography and Marine Biology* 27: 45–90.

Swanson, David, Boris Sabirzhanov, Amanda Vandezande, and Timothy Clark. 2009. “Seasonal Variation of Myostatin Gene Expression in Pectoralis Muscle of House Sparrows (Passer Domesticus) Is Consistent with a Role in Regulating Thermogenic Capacity and Cold Tolerance.” *Physiological and Biochemical Zoology : PBZ* 82 (February): 121–28. https://doi.org/10.1086/591099.

Takatori, Naohito, Yutaka Satou, and Nori Satoh. 2002. “Expression of Hedgehog Genes in Ciona Intestinalis Embryos.” *Mechanisms of Development* 116 (1): 235–38. https://doi.org/10.1016/S0925-4773(02)00150-8.

Tanaka, Elly M., and Peter W. Reddien. 2011. “The Cellular Basis for Animal Regeneration.” *Developmental Cell* 21 (1): 172–85. https://doi.org/10.1016/j.devcel.2011.06.016.

Tariqul Islam, A. F. M., Pricila Khan Moly, Yuki Miyamoto, and Takehiro G. Kusakabe. 2010. “Distinctive Expression Patterns of Hedgehog Pathway Genes in the Ciona Intestinalis Larva: Implications for a Role of Hedgehog Signaling in Postembryonic Development and Chordate Evolution.” *Zoological Science* 27 (2): 84–90. https://doi.org/10.2108/zsj.27.84.

Tempesti, Jonathan, Joachim Langeneck, Luigi Romani, Marie Garrido, Claudio Lardicci, Ferruccio Maltagliati, and Alberto Castelli. 2022. “Harbour Type and Use Destination Shape Fouling Community and Non-Indigenous Species Assemblage: A Study of Three Northern Tyrrhenian Port Systems (Mediterranean Sea).” *Marine Pollution Bulletin* 174 (January): 113191. https://doi.org/10.1016/j.marpolbul.2021.113191.

Thorndyke, M. C. 1977. “Observations on the Gastric Epithelium of Ascidians with Special Reference to Styela Clava.” *Cell and Tissue Research* 184 (4): 539–50. https://doi.org/10.1007/BF00220977.

Tiozzo, Stefano, Loriano Ballarin, P Burighel, and G Zaniolo. 2006. “Programmed Cell Death in Vegetative Development: Apoptosis during the Colonial Life Cycle of the Ascidian Botryllus Schlosseri.” *Tissue & Cell* 38 (July): 193–201. https://doi.org/10.1016/j.tice.2006.02.003.

Tiozzo, Stefano, and Richard R. Copley. 2015. “Reconsidering Regeneration in Metazoans: An Evo-Devo Approach.” *Frontiers in Ecology and Evolution* 3 (June). https://doi.org/10.3389/fevo.2015.00067.

Tiozzo, Stefano, and Anthony W. De Tomaso. 2009. “Functional Analysis of Pitx during Asexual Regeneration in a Basal Chordate.” *Evolution & Development* 11 (2): 152–62. https://doi.org/10.1111/j.1525-142X.2009.00316.x.

Tokuoka, Miki, Gaku Kumano, and Hiroki Nishida. 2007. “FGF9/16/20 and Wnt-5α Signals Are Involved in Specification of Secondary Muscle Fate in Embryos of the Ascidian, Halocynthia Roretzi.” *Development Genes and Evolution* 217: 515–27.

Tomizawa, Kazuhito, Hideki Matsui, Eisaku Kondo, Kazuhiro Miyamoto, Masaaki Tokuda, Toshifumi Itano, Shunichiro Nagahata, Tadaatsu Akagi, and Osamu Hatase. 1995. “Developmental Alteration and Neuron-Specific Expression of Bone Morphogenetic Protein-6 (BMP-6) mRNA in Rodent Brain.” *Brain Research. Molecular Brain Research* 28 (February): 122–28. https://doi.org/10.1016/0169-328X(94)00199-O.

Torok, Maureen A., David M. Gardiner, Juan-Carlos Izpisúa-Belmonte, and Susan V. Bryant. 1999. “Sonic Hedgehog (Shh) Expression in Developing and Regenerating Axolotl Limbs.” *Journal of Experimental Zoology* 284 (2): 197–206. https://doi.org/10.1002/(SICI)1097-010X(19990701)284:2<197::AID-JEZ9>3.0.CO;2-F.

Troilo, Helen, Anne L. Barrett, Alexander P. Wohl, Thomas A. Jowitt, Richard F. Collins, Christopher P. Bayley, Alexandra V. Zuk, Gerhard Sengle, and Clair Baldock. 2015. “The Role of Chordin Fragments Generated by Partial Tolloid Cleavage in Regulating BMP Activity.” *Biochemical Society Transactions* 43 (5): 795–800.

Tyrrell, Megan C., and James E. Byers. 2007. “Do Artificial Substrates Favor Nonindigenous Fouling Species over Native Species?” *Journal of Experimental Marine Biology and Ecology* 342 (1): 54–60. https://doi.org/10.1016/j.jembe.2006.10.014.

Ulman, Aylin, Jasmine Ferrario, Aitor Forcada, Christos Arvanitidis, Anna Occhipinti-Ambrogi, and Agnese Marchini. 2019. “A Hitchhiker’s Guide to Mediterranean Marina Travel for Alien Species.” *Journal of Environmental Management* 241 (July): 328–39. https://doi.org/10.1016/j.jenvman.2019.04.011.

Ulman, Aylin, Jasmine Ferrario, Aitor Forcada, Hanno Seebens, Christos Arvanitidis, Anna Occhipinti-Ambrogi, and Agnese Marchini. 2019. “Alien Species Spreading via Biofouling on Recreational Vessels in the Mediterranean Sea.” Edited by Nessa O’Connor. *Journal of Applied Ecology* 56 (12): 2620–29. https://doi.org/10.1111/1365-2664.13502.

Ulman, Aylin, Jasmine Ferrario, Anna Occhpinti-Ambrogi, Christos Arvanitidis, Ada Bandi, Marco Bertolino, Cesare Bogi, et al. 2017. “A Massive Update of Non-Indigenous Species Records in Mediterranean Marinas.” *PeerJ* 5 (October): e3954. https://doi.org/10.7717/peerj.3954.

Ulmer, Bärbel, Melanie Tingler, Sabrina Kurz, Markus Maerker, Philipp Andre, Dina Mönch, Marina Campione, et al. 2017. “A Novel Role of the Organizer Gene Goosecoid as an Inhibitor of Wnt/PCP-Mediated Convergent Extension in Xenopus and Mouse.” *Scientific Reports* 7 (1): 43010. https://doi.org/10.1038/srep43010.

Vadon-Le Goff, Sandrine, David J.S. Hulmes, and Catherine Moali. 2015. “BMP-1/Tolloid-like Proteinases Synchronize Matrix Assembly with Growth Factor Activation to Promote Morphogenesis and Tissue Remodeling.” *Metalloproteinases in Extracellular Matrix Biology* 44–46 (May): 14–23. https://doi.org/10.1016/j.matbio.2015.02.006.

Van Name, Willard Gibb. 1931. *The North and South American Ascidians.* Vol. 61. Bulletin of the Amer. Mus. Nat. Hist.

Vazquez, E., A. A. Ramos-Espla, and X. Turon. 1995. “The Genus *Polycarpa* (Ascidiacea, Styelidae) on the Atlantic and Mediterranean Coasts of the Iberian Peninsula.” *Journal of Zoology* 237 (4): 593–614. https://doi.org/10.1111/j.1469-7998.1995.tb05017.x.

Vázquez, E, and Cm Young. 1996. “Responses of Compound Ascidian Larvae to Haloclines.” *Marine Ecology Progress Series* 133: 179–90. https://doi.org/10.3354/meps133179.

Vazquez, Elsa, and Craig M Young. 1998. “Ontogenetic Changes in Phototaxis during Larval Life of the Ascidian Polyandrocarpa Zorritensis (Van Name, 1931).” *J. Exp. Mar. Biol. Ecol.*

Vázquez, Elsa, and Craig M. Young. 2005. “Effects of Low Salinity on Metamorphosis in Estuarine Colonial Ascidians.” *Invertebrate Biology* 119 (4): 433–44. https://doi.org/10.1111/j.1744-7410.2000.tb00113.x.

Villa, Luisa Anna, and Eleonora Patricolo. 2000. “The Follicle Cells of Styela Plicata (Ascidiacea, Tunicata): A Sem Study.” *Zoological Science* 17 (8): 1115–21. https://doi.org/10.2108/zsj.17.1115.

Villalobos, Stephanie, Gretchen Lambert, Noa Shenkar, and Susanna López-Legentil. 2017. “Distribution and Population Dynamics of Key Ascidians in North Carolina

Harbors and Marinas." *Aquatic Invasions* 12 (4): 447–58. https://doi.org/10.3391/ai.2017.12.4.03.

Von Der Hardt, Sophia, Jeroen Bakkers, Adi Inbal, Lara Carvalho, Lilianna Solnica-Krezel, Carl-Philipp Heisenberg, and Matthias Hammerschmidt. 2007. "The Bmp Gradient of the Zebrafish Gastrula Guides Migrating Lateral Cells by Regulating Cell-Cell Adhesion." *Current Biology* 17 (6): 475–87.

Voskoboynik, Ayelet, Noa Simon-Blecher, Yoav Soen, Baruch Rinkevich, Anthony W. De Tomaso, Katherine J. Ishizuka, and Irving L. Weissman. 2007. "Striving for Normality: Whole Body Regeneration through a Series of Abnormal Generations." *The FASEB Journal* 21 (7): 1335–44. https://doi.org/10.1096/fj.06-7337com.

Vukicevic, Slobodan, and Lovorka Grgurevic. 2009. "BMP-6 and Mesenchymal Stem Cell Differentiation." *Cytokine & Growth Factor Reviews* 20 (November): 441–48. https://doi.org/10.1016/j.cytogfr.2009.10.020.

Wada, H. 1998. "Evolutionary History of Free-Swimming and Sessile Lifestyles in Urochordates as Deduced from 18S rDNA Molecular Phylogeny." *Molecular Biology and Evolution* 15 (9): 1189–94. https://doi.org/10.1093/oxfordjournals.molbev.a026026.

Waddington, Conrad Hal. 2014. *The Strategy of the Genes*. Routledge.

Wagner, Günter P., Mihaela Pavlicev, and James M. Cheverud. 2007. "The Road to Modularity." *Nature Reviews Genetics* 8 (12): 921–31. https://doi.org/10.1038/nrg2267.

Wang, Jianbo, Leah Etheridge, and Anthony Wynshaw-Boris. 2007. "The Wnt-signaling Pathways in Mammalian Patterning and Morphogenesis." In *Advances in Developmental Biology*, 17:111–58. Elsevier. https://doi.org/10.1016/S1574-3349(06)17004-0.

Wang, Wei, Florian Razy-Krajka, Eric Siu, Alexandra Ketcham, and Lionel Christiaen. 2013. "NK4 Antagonizes Tbx1/10 to Promote Cardiac versus Pharyngeal Muscle Fate in the Ascidian Second Heart Field." *PLOS Biology* 11 (12): e1001725. https://doi.org/10.1371/journal.pbio.1001725.

Warzecha, Jörg, Stephan Göttig, Christian Brüning, Elmar Lindhorst, Mohammad Arabmothlagh, and Andreas Kurth. 2006. "Sonic Hedgehog Protein Promotes Proliferation and Chondrogenic Differentiation of Bone Marrow-Derived Mesenchymal Stem Cells in Vitro." *Journal of Orthopaedic Science* 11: 491–96.

Weismann, A. 1889. *The Significance of Sexual Reproduction in the Theory of Natural Selection In: Poulton EB, Schönland S, Shipley AE, Editors. Essays upon Heredity and Kindred Biological Problems*. Oxford: Clarendon Press.[Google Scholar].

Weismann, August. 1892. "Amphimixis or the Essential Meaning of Conjugation and Sexual Reproduction." *Essays upon Heredity and Kindred Biological Problems* 2: 101–222.

Weiße, Andrea Y., Diego A. Oyarzún, Vincent Danos, and Peter S. Swain. 2015. “Mechanistic Links between Cellular Trade-Offs, Gene Expression, and Growth.” *Proceedings of the National Academy of Sciences* 112 (9). https://doi.org/10.1073/pnas.1416533112.

Wenemoser, Danielle, Sylvain Lapan, Alex Wilkinson, George Bell, and Peter Reddien. 2012. “A Molecular Wound Response Program Associated with Regeneration Initiation in Planarians.” *Genes & Development* 26 (May): 988–1002. https://doi.org/10.1101/gad.187377.112.

Whyte, Jemima, Andrew Smith, and Jill Helms. 2012. “Wnt Signaling and Injury Repair.” In *Cold Spring Harbor Perspectives in Biology*, 4:409–22. https://doi.org/10.1101/cshperspect.a008078.

Winklbauer, Rudolf, Araceli Medina, Rajeeb K. Swain, and Herbert Steinbeisser. 2001. “Frizzled-7 Signalling Controls Tissue Separation during Xenopus Gastrulation.” *Nature* 413 (6858): 856–60.

Wodarz, Andreas, and Roel Nusse. 1998. “MECHANISMS OF WNT SIGNALING IN DEVELOPMENT.” *Annual Review of Cell and Developmental Biology* 14 (1): 59–88. https://doi.org/10.1146/annurev.cellbio.14.1.59.

Yamada, Gen, Ahmed Mansouri, Miguel Torres, Edward T. Stuart, Martin Blum, M. Schultz, Eddy M. De Robertis, and Peter Gruss. 1995. “Targeted Mutation of the Murine Goosecoid Gene Results in Craniofacial Defects and Neonatal Death.” *Development* 121 (9): 2917–22. https://doi.org/10.1242/dev.121.9.2917.

Yamaguchi, M. 1975. “Growth and Reproductive Cycles of the Marine Fouling Ascidians Ciona Intestinalis, Styela Plicata, Botrylloides Violaceus, and Leptoclinum Mitsukurii at Aburatsubo-Moroiso Inlet (Central Japan).” *Marine Biology* 29 (3): 253–59. https://doi.org/10.1007/BF00391851.

Yamamoto, M, Chikara Meno, Y Sakai, Hidetaka Shiratori, K Mochida, Y Ikawa, Yukio Saijoh, and Hiroshi Hamada. 2001. “The Transcription Factor FoxH1 (FAST) Mediates Nodal Signaling during Anterior-Posterior Patterning and Node Formation in the Mouse.” *Genes & Development* 15 (June): 1242–56. https://doi.org/10.1101/gad.

Yan, Xiaohua, Ziying Liu, and Yeguang Chen. 2009. “Regulation of TGF-β Signaling by Smad7.” *Acta Biochimica et Biophysica Sinica* 41 (May): 263–72.

Yang, Liang-Tung, and Vesa Kaartinen. 2007. “Tgfb1 Expressed in the Tgfb3 Locus Partially Rescues the Cleft Palate Phenotype of Tgfb3 Null Mutants.” *Developmental Biology* 312 (1): 384–95.

Yao, Jie, and Daniel S. Kessler. 2001. “Goosecoid Promotes Head Organizer Activity by Direct Repression of Xwnt8 in Spemann’s Organizer.” *Development* 128 (15): 2975–87. https://doi.org/10.1242/dev.128.15.2975.

Yasuhiko, Yukuto, Seiki Haraguchi, Satoshi Kitajima, Yu Takahashi, Jun Kanno, and Yumiko Saga. 2006. “Tbx6-Mediated Notch Signaling Controls Somite-Specific Mesp2 Expression.” *Proceedings of the National Academy of Sciences* 103 (10): 3651–56.

Yu, Channing, Kathy K. Niakan, Mark Matsushita, George Stamatoyannopoulos, Stuart H. Orkin, and Wendy H. Raskind. 2002. “X-Linked Thrombocytopenia with Thalassemia from a Mutation in the Amino Finger of GATA-1 Affecting DNA Binding Rather than FOG-1 Interaction.” *Blood* 100 (6): 2040–45. https://doi.org/10.1182/blood-2002-02-0387.

Zega, Giuliana, Michael C. Thorndyke, and Euan R. Brown. 2006. “Development of Swimming Behaviour in the Larva of the Ascidian *Ciona Intestinalis*.” *Journal of Experimental Biology* 209 (17): 3405–12. https://doi.org/10.1242/jeb.02421.

Zelditch, Miriam L., and Anjali Goswami. 2021. “What Does Modularity Mean?” *Evolution & Development* 23 (5): 377–403. https://doi.org/10.1111/ede.12390.

Zha, Jun-pu, Xiao-qing Wang, and Jun Di. 2020. “MiR-920 Promotes Osteogenic Differentiation of Human Bone Mesenchymal Stem Cells by Targeting HOXA7.” *Journal of Orthopaedic Surgery and Research* 15 (July). https://doi.org/10.1186/s13018-020-01775-7.

Zhang, Zhen, Fabiana Cerrato, Huansheng Xu, Francesca Vitelli, Masae Morishima, Joshua Vincentz, Yasuhide Furuta, Lijiang Ma, James F. Martin, and Antonio Baldini. 2005. “Tbx1 Expression in Pharyngeal Epithelia Is Necessary for Pharyngeal Arch Artery Development.”

Zondag, Lisa E, Kim Rutherford, Neil J. Gemmell, and Megan J. Wilson. 2016. “Uncovering the Pathways Underlying Whole Body Regeneration in a Chordate Model, Botrylloides Leachi Using de Novo Transcriptome Analysis.” *BMC Genomics* 17 (1): 114. https://doi.org/10.1186/s12864-016-2435-6.